STRUCTURAL AND MATERIAL PERFORMANCE OF RUBBERIZED AND HYBRID CONCRETE PIPES

by

MOHAMMAD MOHAMMADAGHA

Presented to the Faculty of the Graduate School of

The University of Texas at Arlington in Partial Fulfillment

of the Requirements

for the Degree of

MASTER OF SCIENCE IN CIVIL ENGINEERING

THE UNIVERSITY OF TEXAS AT ARLINGTON

August 2013

Acknowledgements

I would like to express my sincere gratitude to Dr. Ali Abolmaali, supervising professor, for his support and mentoring with love and care throughout the course of this research. Appreciations are also extended to Dr. Shih-Ho Chao and Dr. Sahadat Hossain for serving on my committee.

I would also like to express my gratitude to Hanson Pipe & Precast for donating materials required for this study.

In addition, I would like to express my appreciation to my colleagues, Mojtaba Salehi Dezfooli and special thanks to Dr. Mohammad Razavi for his unconditional support who dedicated his time and energy throughout my Master's degree.

Finally, I would like to give my heartfelt thanks to my parents for their support and encouragement.

July 18, 2013

Abstract

STRUCTURAL AND MATERIAL PERFORMANCE OF RUBBERIZED AND HYBRID CONCRETE PIPES

Mohammad Mohammadagha, M.S.

The University of Texas at Arlington, 2013

Supervising Professor: Ali Abolmaali

This study investigates how the combination of steel fiber, crumb rubber, synthetic fiber, and conventional steel cage will improve the ductility of regular concrete pipes and thin-walled semi-rigid concrete pipes. In this study, pipes with four different concrete mixtures were produced and tested: (1) Steel Bar Reinforced Concrete Pipe (SBRCP), (2) Crumb Rubber Reinforced Concrete Pipe (CRRCP), (3) Steel Fiber Reinforced Concrete Pipe (SFRCP), and (4) Synthetic Fiber Reinforced Concrete Pipe (SNFRCP). This study investigates how the variation of the fiber volume fraction and crumb rubber content in concrete mix affects the behavior of pipes with diameters ranging from 24in. (610 mm) to 60in. (1524 mm).

In this research, the crumb rubber particles were replaced from 3% to 20% (by volume) of sand in the mixture of concrete pipes. Steel fibers (RC-65/35-BN, Bekaert) used in this study have a hooked end shape with a length of 1.38 in. (35 mm), a diameter of 0.022in (0.55 mm) and an aspect ratio of 65 with dosages of 10 (Volume fraction of 0.08%), 11 (V_f of 0.08%), 22 (V_f of 0.17%), 44 (V_f of 0.33%), 66 (V_f, of 0.5%) and 88 lb/yd^3 (V_f of 0.67%). Macrosynthetic fibers were from BASF MasterFiber™ MAC Matrix with dosages of 2, 4, 5, and 8 lb/yd3.

A total of 86 pipes were produced and tested in accordance with ASTM C 497 three-edged bearing at Hanson Precast Plant in Grand Prairie, TX. In addition, a total of 233 cylindrical specimens, 4in. (101.6mm) in diameter and 8in. (203mm) in height, were tested in 1, 3, 7 and 28 days. Moreover, a total of 57 beam specimens, 20in. (508mm) in length, 6in. (152mm) in width and height were produced and tested at the Civil Engineering Lab Building (CELB) at the University of Texas at Arlington. Test results revealed that as the crumb rubber content increased the compressive strength of pipes decreased; however, ductility and energy absorption enhanced over pconventional concrete.

Table of Contents

Acknowledgements iii

Abstract iv

List of Illustrations viii

List of Tables xxi

Chapter 1 Introduction 1

Pipe Production Methods and Equipment 2

Pipe Design Methods 7

Objectives of The Study 12

Chapter 2 Literature Review 14

Introduction 14

History and Application of Crumb Rubber 14

Previous Research on Crumb Rubber Concrete 15

Steel Fiber Reinforcement Concrete 17

History and Application of Steel Fiber 17

Mechanical Properties of Steel Fiber Reinforced Concrete 17

Previous Research On Steel Fiber Reinforcement Concrete 18

History and Application of Synthetic Fiber 19

Chapter 3 Structural Pipe Test 21

Introduction 21

Three-edged Bearing Test D-load Test 24

Test Set Up and Procedure 24

Test Results 27

Chapter 4 Material Tests 43

Introduction 43
Flexural Beam Test 45
Test Set Up and Procedure 45
Test Results 47
Compressive Cylinder Tests 48
Test Set Up and Procedure 48
Test Results 49
Chapter 5 Summary, Conclusions And Recommendations 51
Summary 51
Conclusions 52
Recommendations for Future Work 53
Appendix A Test results 55
Appendix B PIPE GRAPHS 74
Appendix C Flexural Beam Test Results 156
References 212
Biographical Information 215

List of Illustrations

Figure 1-1 Photograph of Steel cage machine at Hanson facility in Grand prairie, TX 3

Figure 1-2 Photograph of Packerhead Machine 5

Figure 1-3 Photograph of Roller heads in Packerhead Machine 5

Figure 1-4 Photograph of a Curing Chamber 6

Figure 1-5 Vertical Arching factor 10

Figure 1-6 Controlling Criteria (ASCE 15-98) 12

Figure 1-7 Outline of this study 13

Figure 2-1 Photograph of Typical Crumb Rubber Used 15

Figure 2-2 Photograph of Typical Steel Fibers (RC-65/35-BN) used 18

Figure 2-3 Photograph of Macrosynthetic fibers used in this study 19

Figure 3-1 Photograph of D-Load rack at Hanson facility 25

Figure 3-2 Data acquisition unit (Vishay scanner) 25

Figure 3-3 Photograph of CDS for measuring deflection 26

Figure 3-4 Photograph of load cell at Hanson facility 26

Figure 3-5 36in load-deflection graphs 27

Figure 3-6 24in load-deflection graphs 28

Figure 3-7 Load-Deflection Plot for RCP-24-6-B, HYCP-24-6-B-44lbs steel-6% rubber and CRCP-24-6-B-6% rubber 29

Figure 3-8 Load-Deflection Plot for HYCP-24-6-B-44lbs steel-8%rubber, CRCP-24-6-B-8%rubber and HYCP-24-6-B-44lbs steel-8% rubber 30

Figure 3-9 Load-Deflection Plot for RCP-24-6-B, HYCP-24-6-B-44lbs steel-10%rubber and CRCP-24-6-B-10%rubber 31

Figure 3-10 SFCP-24-6-B-10lbs steel, RCP-24-6-B 32

Figure 3-11 Load-Deflection Plot for HYCP-36-6-B-22lbs steel-8% rubber, CRCP-36-6-8% rubber and RCP-36-6-B 33
Figure 3-12 Load-Deflection Plot for HYCP-36-6-B-44lbs steel-12%rubber, CRCP-36-6-12%rubber and RCP-36-6-B 34
Figure 3-13 Load-Deflection Plot for HYCP-36-6-B-22lbs steel-10%rubber, CRCP-36-6-B10%rubber, RCP-36-6-B 35
Figure 3-14 Load-Deflection Plot for HYCP-24-6-B-44lbs steel-10%rubber, CRCP-24-6-B-10% rubber and RCP-24-6-B 36
Figure 3-15 Load-Deflection Plot for HYCP-36-6-B-44-10%rubber, CRCP-36-6-B-10%rubber, RCP-36-6-B. 37
Figure 3-16 Load-Deflection Plot for CRCP-24-6-B-10%rubber, SFCP-24-6-B-44lbs steel fiber, HYCP-24-6-B-44lbs steel, and HYCP-24-6-B-10%rubber-8lbs synth. 38
Figure 3-17 Load-Deflection Plot for Thin wall-60-8, Thin wall-60-8-13%rubber, Thin wall-12lbs synth, Thin wall-66lbs steel fiber and RCP. 39
Figure 3-18 Load-Deflection Plot for Thin wall-60in-20%rubber, Thin wall-60in-4pcy synth-20%rubber, Thin wall-60in-11pcy synth-20%rubber, and RCP. 40
Figure 3-19 Photograph of crack failure mode in 24 and 36 in. pipes 41
Figure 3-20 Photograph of crack failure mode in 54 and 60 in. pipes 41
Figure 4-1Typical ASTM C1609 Test Fixtures 46
Figure 4-2 Experimental set up for Flexural beam test 46
Figure 4-3 Flexural Test Toughness for beam specimens 47
Figure 4-4 The photograph of most frequent failure type for Flexural Beam Specimens 48
Figure 4-5 Photograph of Compressive Cylinder Testing Machine at CELB 49
Figure 4-6 Failure types of cylindrical specimens 50
Figure 5-1 Photograph of opening of the crack and the pull-out of the steel fibers 54

Figure B-1 Load-Deflection Plot for HYCP-24-6-B-22lbs steel-5% rubber-2%synth 75
Figure B-2 Crack propagation for HYCP-24-6-B-22lbs steel-5% rubber-2%synth 75
Figure B-3 Load-Deflection Plot for HYCP-24-6-B-44lbs steel-3% rubber-5lbs synth 76
Figure B-4 Crack propagation for HYCP-24-6-B-44lbs steel-3% rubber-5lbs synth 76
Figure B-5 Load-Deflection Plot for HYCP-36-6-B-44lbs steel-3% rubber-5lbs synth 77
Figure B-6 Crack propagation for HYCP-36-6-B-44lbs steel-3% rubber-5lbs synth 77
Figure B-7 Load-Deflection Plot for HYCP-24-6-B-44lbs steel-8% rubber 78
Figure B-8 Crack propagation for HYCP-24-6-B-44lbs steel-8% rubber 78
Figure B-9 Load-Deflection Plot for CRCP-24-6-B-8%rubber 79
Figure B-10 Crack propagation for CRCP-24-6-B-8%rubber 79
Figure B-11 Load-Deflection Plot for CRCP-24-6-B-8%rubber 80
Figure B-12 Crack propagation for CRCP-24-6-B-8%rubber 80
Figure B-13 Load-Deflection Plot for CRCP-24-6-B-6%rubber 81
Figure B-14 Crack propagation for CRCP-24-6-B-6%rubber 81
Figure B-15 Load-Deflection Plot for CRCP-24-6-B-6%rubber 82
Figure B-16 Crack propagation for CRCP-24-6-B-6%rubber 82
Figure B-17 Load-Deflection Plot for HYCP-24-6-B-44lbs steel-6%rubber 83
Figure B-18 Crack propagation for HYCP-24-6-B-44lbs steel-6%rubber 83
Figure B-19 Load-Deflection Plot for HYCP-24-6-B-44lbs steel-6%rubber 84
Figure B-20 Crack propagation for HYCP-24-6-B-44lbs steel-6%rubber 84
Figure B-21 Load-Deflection Plot for RCP-24-6-B 85
Figure B-22 Crack propagation for RCP-24-6-B 85
Figure B-23 Load-Deflection Plot for RCP-24-6-B 86
Figure B-24 Crack propagation for RCP-24-6-B 86
Figure B-25 Load-Deflection Plot for RCP-24-6-B 87

Figure B-26 Crack propagation for RCP-24-6-B 87
Figure B-27 Load-Deflection Plot for RCP-24-6-B 88
Figure B-28 Crack propagation for RCP-24-6-B 88
Figure B-29 Load-Deflection Plot for CRCP-24-6-10%rubber 89
Figure B-30 Crack propagation for CRCP-24-6-10%rubber 89
Figure B-31 Load-Deflection Plot for CRCP-24-6-10%rubber 90
Figure B-32 Crack propagation for CRCP-24-6-10%rubber 90
Figure B-33 Load-Deflection Plot for HYCP-24-6-B-44lbs steel-10%rubber 91
Figure B-34 Crack propagation for HYCP-24-6-B-44lbs steel-10%rubber 91
Figure B-35 Load-Deflection Plot for HYCP-24-6-B-44lbs steel-10%rubber 92
Figure B-36 Crack propagation for HYCP-24-6-B-44lbs steel-10%rubber 92
Figure B-37 Load-Deflection Plot for RCP-24-6-B 93
Figure B-38 Crack propagation for RCP-24-6-B 93
Figure B-39 Load-Deflection Plot for SFCP-24-6-B-10lbs steel 94
Figure B-40 Crack propagation for SFCP-24-6-B-10lbs steel 94
Figure B-41 Load-Deflection Plot for SFCP-24-6-B-10lbs steel 95
Figure B-42 Crack propagation for SFCP-24-6-B-10lbs steel 95
Figure B-43 Load-Deflection Plot for HYRCP-24-6-B-10lbs steel-8% rubber 96
Figure B-44 Crack propagation for HYRCP-24-6-B-10lbs steel-8% rubber 96
Figure B-45 Load-Deflection Plot for RCP-24-6-B 97
Figure B-46 Crack propagation for RCP-24-6-B 97
Figure B-47 Load-Deflection Plot for CRCP-36-6-8%rubber 98
Figure B-48 Crack propagation for CRCP-36-6-8%rubber 98
Figure B-49 Load-Deflection Plot for HYCP-36-6-22lbs steel-8%rubber 99
Figure B-50 Crack propagation for HYCP-36-6-22lbs steel-8%rubber 99

Figure B-51 Load-Deflection Plot for CRCP-36-6-8%rubber 100
Figure B-52 Crack propagation for CRCP-36-6-8%rubber 100
Figure B-53 Load-Deflection Plot for RCP-36-6-B 101
Figure B-54 Crack propagation for RCP-36-6-B 101
Figure B-55 Load-Deflection Plot for RCP-36-6-B 102
Figure B-56 Crack propagation for RCP-36-6-B 102
Figure B-57 Load-Deflection Plot for HYCP-36-6-22-8% rubber 103
Figure B-58 Crack propagation for HYCP-36-6-22-8% rubber 103
Figure B-59 Load-Deflection Plot for CRCP-36-6-B-10%rubber 104
Figure B-60 Crack propagation for CRCP-36-6-B-10%rubber 104
Figure B-61 Load-Deflection Plot for HYCP-36-6-B-22-10%rubber 105
Figure B-62 Crack propagation for HYCP-36-6-B-22-10%rubber 105
Figure B-63 Load-Deflection Plot for RCP-36-6-B 106
Figure B-64 Crack propagation for RCP-36-6-B 106
Figure B-65 Load-Deflection Plot for CRCP-36-6-B-10%rubber 107
Figure B-66 Crack propagation for CRCP-36-6-B-10%rubber 107
Figure B-67 Load-Deflection Plot for RCP-36-6-B 108
Figure B-68 Crack propagation for RCP-36-6-B 108
Figure B-69 Load-Deflection Plot for HYCP-36-6-B-22-10%rubber 109
Figure B-70 Crack propagation for HYCP-36-6-B-22-10%rubber 109
Figure B-71 Load-Deflection Plot for RCP-36-6-B 110
Figure B-72 Crack propagation for RCP-36-6-B 110
Figure B-73 Load-Deflection Plot for HYCP-36-6-B-44lbs steel-12%rubber 111
Figure B-74 Crack propagation for HYCP-36-6-B-44lbs steel-12%rubber 111
Figure B-75 Load-Deflection Plot for RCP-36-6-B 112

Figure B-76 Crack propagation for RCP-36-6-B 112
Figure B-77 Load-Deflection Plot for CRCP-36-6-B-12%rubber 113
Figure B-78 Crack propagation for CRCP-36-6-B-12%rubber 113
Figure B-79 Load-Deflection Plot for CRCP-36-6-B-12%rubber 114
Figure B-80 Crack propagation for CRCP-36-6-B-12%rubber 114
Figure B-81 Load-Deflection Plot for HYCP-24-6-B-44lbs steel-10%rubber 115
Figure B-82 Crack propagation for HYCP-24-6-B-44lbs steel-10%rubber 115
Figure B-83 Load-Deflection Plot for CRCP-24-6-B-10%rubber 116
Figure B-84 Crack propagation for CRCP-24-6-B-10%rubber 116
Figure B-85 Load-Deflection Plot for RCP-24-6-B 117
Figure B-86 Crack propagation for RCP-24-6-B 117
Figure B-87 Load-Deflection Plot for CRCP-24-6-B-10%rubber 118
Figure B-88 Crack propagation for CRCP-24-6-B-10%rubber 118
Figure B-89 Load-Deflection Plot for CRCP-24-6-B-10%rubber 119
Figure B-90 Crack propagation for CRCP-24-6-B-10%rubber 119
Figure B-91 Load-Deflection Plot for HYCP-36-6-B-44lbs steel-10%rubber 120
Figure B-92 Load-Deflection Plot for RCP-36-6-B 120
Figure B-93 Load-Deflection Plot for CRCP-36-6-B-10%rubber 121
Figure B-94 Load-Deflection Plot for CRCP-24-6-B-15%rubber 122
Figure B-95 Crack propagation for CRCP-24-6-B-15%rubber 122
Figure B-96 Load-Deflection Plot for RCP-24-6-B 123
Figure B-97 Crack propagation for RCP-24-6-B 123
Figure B-98 Load-Deflection Plot for HYCP-24-6-B-44lbs steel-15%rubber 124
Figure B-99 Crack propagation for HYCP-24-6-B-44lbs steel-15%rubber 124
Figure B-100 Load-Deflection Plot for HYCP-24-6-B-44lbs steel-15%rubber 125

Figure B-101 Crack propagation for HYCP-24-6-B-44lbs steel-15%rubber 125
Figure B-102 Load-Deflection Plot for RCP-24-6-B 126
Figure B-103 Crack propagation for RCP-24-6-B 126
Figure B-104 Load-Deflection Plot for CRCP-24-6-B-15%rubber 127
Figure B-105 Crack propagation for CRCP-24-6-B-15%rubber 127
Figure B-106 Load-Deflection Plot for HYCP-24-6-B-44lbs steel-15%rubber, CRCP-24-6-15%rubber and RCP-24-6-B 128
Figure B-107 Load-Deflection Plot for RCP-24-6-B-20%rubber 129
Figure B-108 Load-Deflection Plot for HYCP-24-6-B-44lbs steel-20%rubber 129
Figure B-109 Load-Deflection Plot for CRCP-24-6-B-20%rubber 130
Figure B-110 Crack propagation for CRCP-24-6-B-20%rubber 130
Figure B-111 Load-Deflection Plot for CRCP-24-6-B-20%rubber 131
Figure B-112 Crack propagation for CRCP-24-6-B-20%rubber 131
Figure B-113 Load-Deflection Plot for RCP-24-6-B 132
Figure B-114 Crack propagation for RCP-24-6-B 132
Figure B-115 Load-Deflection Plot for RCP-36-6-B 133
Figure B-116 Crack propagation for RCP-36-6-B 133
Figure B-117 Load-Deflection Plot for RCP-36-6-B 134
Figure B-118 Crack propagation for RCP-36-6-B 134
Figure B-119 Load-Deflection Plot for SNFCP-24-6-B-10%rubber-8lbs synth 135
Figure B-120 Crack propagation for SNFCP-24-6-B-10%rubber-8lbs synth 135
Figure B-121 Load-Deflection Plot for HYCP-24-6-B-44lbs steel-10%rubber 136
Figure B-122 Crack propagation for HYCP-24-6-B-44lbs steel-10%rubber 136
Figure B-123 Load-Deflection Plot for HYCP-24-6-B-44lbs steel-10%rubber 137
Figure B-124 Crack propagation for HYCP-24-6-B-44lbs steel-10%rubber 137

Figure B-125 Load-Deflection Plot for SNFCP-24-6-B-10%rubber-8lbs synth 138
Figure B-126 Crack propagation for SNFCP-24-6-B-10%rubber-8lbs synth 138
Figure B-127 Load-Deflection Plot for RCP-24-6-B 139
Figure B-128 Crack propagation for RCP-24-6-B 139
Figure B-129 Load-Deflection Plot for CRCP-24-6-10%rubber 140
Figure B-130 Crack propagation for CRCP-24-6-10%rubber 140
Figure B-131 Load-Deflection Plot for RCP-24-6-B 141
Figure B-132 Crack propagation for RCP-24-6-B 141
Figure B-133 Load-Deflection Plot for CRCP-24-6-10%rubber 142
Figure B-134 Crack propagation for CRCP-24-6-10%rubber 142
Figure B-135 Load-Deflection Plot for RCP-24-6-B 143
Figure B-136 Crack propagation for RCP-24-6-B 143
Figure B-137 Load-Deflection Plot for CRCP-24-6-B-20%rubber 144
Figure B-138 Crack propagation for CRCP-24-6-B-20%rubber 144
Figure B-139 Load-Deflection Plot for CRCP-24-6-B-20%rubber 145
Figure B-140 Load-Deflection Plot for RCP-24-6-B 146
Figure B-141 Crack propagation for RCP-24-6-B 146
Figure B-142 Load-Deflection Plot for Thin wall- CR-60in-8ft-13% 147
Figure B-143 Crack propagation for Thin wall-60-8-13%rubber 148
Figure B-144 Load-Deflection Plot for Thin wall-60"-20% rubber-8ft 149
Figure B-145 Crack propagation for Thin wall-60"-20% rubber-8ft 149
Figure B-146 Load-Deflection Plot for Thin wall-60"-20% rubber-8ft 150
Figure B-147 Crack propagation for Thin wall-60"-20% rubber-8ft 151
Figure B-148 Load-Deflection Plot for Thin wall-60"-11PCY SF-20% rubber-8ft 152
Figure B-149 Crack propagation for Thin wall-60"-11PCY SF-20% rubber-8ft 153

Figure B-150 Load-Deflection Plot for Thin wall-60"-4PCY Synth-20% rubber-8ft..... 154
Figure B-151 Crack propagation for Thin wall-60"-4PCY Synth-20% rubber-8ft..... 155
Figure C-1 Load-Deflection Plot for HY-24-6-BM-44lbs-8%..... 157
Figure C-2 Photograph of Crack for HY-24-6-BM-44lbs-8% 157
Figure C-3 Load-Deflection Plot for HY-24-6-BM-44lbs-10%..... 158
Figure C-4 Load-Deflection Plot for HY-24-6-BM-44lbs-8%..... 158
Figure C-5 Load-Deflection Plot for CR-24-6-BM-8%..... 159
Figure C-6 Photograph of Crack for HY-24-6-BM-44lbs-8% 159
Figure C-7 Load-Deflection Plot for HY-24-6-BM-44lbs-6%..... 160
Figure C-8 Photograph of Crack for HY-24-6-BM-44lbs-6% 160
Figure C-9 Load-Deflection Plot for CR-24-6-BM-6%..... 161
Figure C-10 Photograph of Crack for CR-24-6-BM-6%..... 161
Figure C-11 Load-Deflection Plot for HY-24-6-BM-44-6%..... 162
Figure C-12 Photograph of Crack for HY-24-6-BM-44lbs-6% 162
Figure C-13 Load-Deflection Plot for HY-24-6 -BM-44lbs-10%..... 163
Figure C-14 Photograph of HY-24-6-BM-44lbs-10%..... 163
Figure C-15 Load-Deflection Plot for HY-24-6-BM-44lbs-10%..... 164
Figure C-16 Photograph of HY-24-6-BM-44lbs-10%..... 164
Figure C-17 Load-Deflection Plot for CR-24-6-BM-10%..... 165
Figure C-18 Photograph of CR-24-6-BM-10%..... 165
Figure C-19 Load-Deflection Plot for HY-24-6-BM-10lbs-8%..... 166
Figure C-20 Photograph of HY-24-6-BM-10lbs-8%..... 166
Figure C-21 Load-Deflection Plot for HY-24-6-BM-10lbs-8%..... 167
Figure C-22 Photograph of HY-24-6-BM-10lbs-8%..... 167
Figure C-23 Load-Deflection Plot for CR-24-6-BM-8%..... 168

Figure C-24 Photograph of CR-24-6-BM-8%.....168
Figure C-25 Load-Deflection Plot for CR-36-6-BM-8%.....169
Figure C-26 Photograph of CR-36-6-BM-8%.....169
Figure C-27 Load-Deflection Plot for HY-36-6-BM-22lbs-8%.....170
Figure C-28 Photograph of HY-36-6-BM-22lbs-8%.....170
Figure C-29 Load-Deflection Plot for HY-36-6-BM-22lbs-8%.....171
Figure C-30 Photograph of HY-36-6-BM-22lbs-8%.....171
Figure C-31 Load-Deflection Plot for HY-36-6-BM-22lbs-10%.....172
Figure C-32 Photograph of HY-36-6-BM-22lbs-10%.....172
Figure C-33 Load-Deflection Plot for CR-36-6-BM-10%.....173
Figure C-34 Photograph of CR-36-6-BM-10%.....173
Figure C-35 Load-Deflection Plot for HY-36-6-BM-22lbs-10%.....174
Figure C-36 Photograph of HY-36-6- BM-22lbs-10%.....174
Figure C-37 Load-Deflection Plot for CR-36-6-BM-10%.....175
Figure C-38 Photograph of CR-36-6-BM-10%.....175
Figure C-39 Load-Deflection Plot for HY-36-6-BM-44lbs-12%.....176
Figure C-40 Photograph of HY-36-6-BM-44lbs-12%.....176
Figure C-41 Load-Deflection Plot for HY-36-6-BM-44lbs-12%.....177
Figure C-42 Photograph of HY-36-6-BM-44lbs-12%.....177
Figure C-43 Load-Deflection Plot for CR-36-6-BM-10%.....178
Figure C-44 Photograph of CR-36-6-BM-10%.....178
Figure C-45 Load-Deflection Plot for HY-24-6-BM-44lbs-10%.....179
Figure C-46 Photograph of HY-24-6-BM-44lbs-10%.....179
Figure C-47 Load-Deflection Plot for CR-36-6-BM-10%.....180
Figure C-48 Photograph of CR-36-6-BM-10%.....180

Figure C-49 Load-Deflection Plot for HY-24-6-BM-44lbs-10% 181
Figure C-50 Photograph of HY-24-6-BM-44lbs-10% 181
Figure C-51 Load-Deflection Plot for HY-36-44lbs-10% 182
Figure C-52 Photograph of HY-36-BM-44lbs-10% 182
Figure C-53 Load-Deflection Plot for CR-36-6-B-BM-10% 183
Figure C-54 Photograph of CR-36-6-BM-10% 183
Figure C-55 Load-Deflection Plot for HY-24-6-B-BM-44lbs-15% 184
Figure C-56 Photograph of HY-24-6-BM-44lbs-15% 184
Figure C-57 Load-Deflection Plot for CR-24-6-B-BM-20% 185
Figure C-58 Photograph of CR-24-6-BM-20% 185
Figure C-59 Load-Deflection Plot for CR-24-6-B-BM-20% 186
Figure C-60 Photograph of CR-24-6-BM-20% 186
Figure C-61 Load-Deflection Plot for HY-24-6-BM-44lbs-20% 187
Figure C-62 Photograph of HY-24-6-BM-44lbs-20% 187
Figure C-63 Load-Deflection Plot for HY-44lbs steel-5lbs synth-3% 188
Figure C-64 Photograph of HY-44lbs steel-5lbs synth-3% 188
Figure C-65 Load-Deflection Plot for HY-24-6-B-BM-22lbs-5lbs-2% 189
Figure C-66 Photograph of HY-24-6-B-BM-22lbs-5lbs-2% 189
Figure C-67 Load-Deflection Plot for Control-36-6-B-BM 190
Figure C-68 Photograph of Control-36-6-B-BM 190
Figure C-69 HY-36-6-B-BM-44-10 191
Figure C-70 Photograph of HY-36-6-B-BM-44-10 191
Figure C-71 Load-Deflection Plot for CR-36-6-B-BM-20% 192
Figure C-72 Photograph of CR-36-6-B-BM-20% 192
Figure C-73 Load-Deflection Plot for CR-36-6-B-BM-20% 193

Figure C-74 Photograph of for CR-36-6-B-BM-20%.....193
Figure C-75 Load-Deflection Plot for CR-36-6-B-BM-10%.....194
Figure C-76 Photograph of CR-36-6-B-BM-10%.....194
Figure C-77 Load-Deflection Plot for HY-36-6-B-BM-8% synth-20% rubber.....195
Figure C-78 Photograph of HY-36-6-B-BM-8% synth-20% rubber.....195
Figure C-79 Load-Deflection Plot for HY-36-6-B-BM-44lbs-20% 196
Figure C-80 Photograph of HY-36-6-B-BM-44lbs-20% 196
Figure C-81 Load-Deflection Plot for CR-36-6-B-BM-10%.....197
Figure C-82 Photograph of CR-36-6-B-BM-10%.....197
Figure C-83 Load-Deflection Plot for Control-36-6-B-BM.....198
Figure C-84 Photograph of Control-36-6-B-BM.....198
Figure C-85 Load-Deflection Plot for HY-36-6-B-BM-44lbs-10% 199
Figure C-86 Photograph of HY-36-6-B-BM-44lbs-10% 199
Figure C-87 Load-Deflection Plot for HY-36-6-B-BM-44-10%-8lbs Synth.....200
Figure C-88 Photograph of HY-36-6-B-BM-44-10%-8lbs Synth.....200
Figure C-89 Load-Deflection Plot for HY-44lbs steel-5lbs synth-3%.....201
Figure C-90 Photograph of HY-44lbs steel-5lbs synth-3%.....201
Figure C-91 Load-Deflection Plot for HY-36-6-B-BM-44lbs-20% 202
Figure C-92 Photograph of HY-36-6-B-BM-44lbs-20% 202
Figure C-93 Load-Deflection Plot for HY-36-6-B-BM-20%-8lbs synth.....203
Figure C-94 Photograph of HY-36-6-B-BM-20%-8lbs synth.....203
Figure C-95 Load-Deflection Plot for HY-36-6-B-BM-44lbs-5lbs synth-3%rubber 204
Figure C-96 Photograph of HY-36-6-B-BM-44lbs-5lbs synth-3%rubber 204
Figure C-97 Load-Deflection Plot for HY-36-6-B-BM-44lbs-8lbs synth-3%rubber 205
Figure C-98 Photograph of HY-36-6-B-BM-44lbs-8lbs synth-3%rubber 205

Figure C-99 Thin wall-60in-20% rubber-8ft..... 206
Figure C-100 Photograph of Thin wall-60in-20% rubber-8ft..... 206
Figure C-101 Thin wall-60in-20% rubber-8ft..... 207
Figure C-102 Photograph of Thin wall-60in-20% rubber-8ft..... 207
Figure C-103 Thin wall-60in-11PCY SF-20% rubber-8ft 208
Figure C-104 Photograph of Thin wall-60in-11PCY SF-20% rubber-8ft..... 208
Figure C-105 Thin wall-60in-11PCY SF-20% rubber-8ft 209
Figure C-106 Photograph of Thin wall-60in-11PCY SF-20% rubber-8ft..... 209
Figure C-107 Thin wall-60in-4PCY Synth-20% rubber-8ft..... 210
Figure C-108 Photograph of Thin wall-60in-4PCY Synth-20% rubber-8ft..... 210
Figure C-109 Thin wall-60in-4PCY Synth-20% rubber-8ft..... 211
Figure C-110 Photograph of Thin wall-60in-4PCY Synth-20% rubber-8ft..... 211

List of Tables

Table 1-1 Coefficients for Analysis of Pipe in Standard Installation type 1 and in crown location (Direct design method) 8

Table 1-2 Vertical and Horizontal arching factor 11

Table 2-1 Performance Characteristics of MasterFiber™ MAC Matrix used in this study 20

Table 3-1 Details of Mix Design 1 22

Table 3-2 Details of Mix Design 2 22

Table 3-3 Various fiber dosages for 24in. Pipe, 6ft long and B wall-thickness 23

Table 3-4 Various fiber dosages for 36in. Pipe, 6ft long and B wall-thickness 23

Table 3-5 Various fiber dosages for 60in. Pipe, 8ft long and Thin-walled 24

Table 4-1 Test Specimen Matrix 43

Table A-1 Concrete pipe specimens production and tested 56

Table A-2 Cylinder Specimen Test Results 61

Chapter 1

Introduction

The construction of pipes dates back to thousands of years ago. Throughout history, the early water carrying structures were open channels. In roman times, the pipes could not carry water under pressure due to weak tensile capacity of materials that were used. Tensile strength, weight, and cost are the fundamental factors for designing pipes. Fibers have been used to reinforce brittle material since ancient times (Doyle, Fang 1999). Brittle materials are considered to have no significant impact on post-cracking ductility. Also, fibers improve the long-term serviceability of the structure such as the control of cracking.

The concrete pipe installation was a sanitary sewer constructed in 1842 in Mohawk, New York, USA. It remained in operation for over 100 years. After that, the French were the first to engage steel reinforcement in concrete pipes in 1896. The concept was brought to America in 1905 and to Australia in 1910.

Concrete pipes have an excellent performance and durability for storm water drainage and sewer applications. Also, concrete pipes consists relies mostly on the strength of the pipe itself and slightly dependent on the strength derived from the adjacent soil. Moreover, the concrete pipes are less susceptible to damage during construction and maintaining its shape, by not showing deflection. Engaging steel reinforcement cage in concrete pipes significantly increases its strength.

Ductility is the ability of material to deform under the tensile force without the material breaking. Since the final goal of the structure is safety, ductility is vital for the structure to provide warnings well before the collapse occurs. Due to a low ductility of concrete, replacing a portion of the sand with crumb rubber particles can enhance the

ductile property of concrete. Concrete with crumb rubber has higher durability, energy absorption, and is more environmental friendly than regular concrete.

This thesis consists of five chapters: Chapter 1 is an introduction which addresses the scope and objectives of the study. Chapter 2 is a literature review for the current design methods of reinforced concrete pipes and a review on the history and application of the steel fiber and crumb rubber. Chapter 3 is a structural test on pipes under the three-edged bearing test at Hanson Pipe and Precast Plant in Grand Prairie, Texas. Chapter 4 consists of the material tests such as flexural beam test and compressive cylinder test to find the concrete properties. Summary, conclusions, and recommendations of this study are mentioned in Chapter 5.

Pipe Production Methods and Equipment

All the pipe specimens were produced and tested at Hanson Pipe and Precast Plant in Grand Prairie, Texas. Batching is preceded by the design of the mix which provides the proportions of cement, fine and coarse aggregates, water, and any admixtures used. Steel cage machines form steel wire into circular or elliptical shapes as shown in Figure 1-1 Photograph of Steel cage machine.

Figure 1-1 Photograph of Steel cage machine at Hanson facility in Grand prairie, TX

Reinforced Concrete Pipe is designed for sanitary sewers, storm drain culverts, jacked or tunneled systems, and treatment plant piping. Reinforced Concrete Pipe is normally available in diameters from 12 inches (300mm) to 144 inches (3600mm). The Circular Reinforced Concrete Pipe is used when: larger size than available unreinforced pipe is required; Low, moderate or severe cover and/or live load conditions exist in Structural failure that might endanger life or property; Internal hydrostatic pressures (up to 65 psi) are expected; trenchless installation is required. Non-Reinforced Concrete Pipe

is normally available in diameters of 10 inches (250mm) to 36 inches (900mm). Circular Non-Reinforced Concrete Pipe is used for the Storm drains and Culverts.

There are several methods for pipe production: Packerhead, Dry Cast, Centrifugal, Tamp, and Wet cast.

Dry Cast uses zero slump concrete mix. Since there is very little moisture in the dry cast mix, the mix sets up in a matter of minutes and forms which can be stripped off and reused multiple times during the production cycle. Concrete pipes and manholes are produced using the dry cast method. In this method, low frequency and high amplitude vibration are used to produce a dense and durable concrete. When the consolidation is complete, the forms are stripped immediately as the newly formed pipe can stand and support itself.

Wet cast process as the name implies, uses a concrete mix that is wet relative to the mixes used in the other process. Wet casting is mostly used for production of very large pipe diameters, manholes, end sections, and top and base sections. In a wet cast production, an inner and outer form is required and a higher slump wet mix is placed in the form and cannot be removed until the wet mix concrete gains enough strength and is safe to handle.

The process used to produce reinforced concrete pipe at the Grand Prairie Plant is called Packerhead as shown in Figure 1-2 Photograph of Packerhead Machine. In this method, concrete is deposited onto the conveyors and then is delivered to the forms which are set up under the discharge end of the conveyor. Metal pipe forms or three-piece jackets are placed by a forklift onto the openings in a circular casting floor. The floor then rotates slowly to put the pipe under the concrete chute. The operator on the platform controls the speed of the rollers as shown in Figure 1-3 Photograph of Roller heads in Packerhead Machine . The mechanism of rapidly up-and-down motion of the

packerhead is called a rollerhead which compacts radially the interior of the pipe. When compaction is complete, the floor rotates on an empty jacket under the concrete chute and the forklift removes the cast pipe and mold to a curing area where the exterior form is immediately removed and the form is transported back to the production station.

Figure 1-2 Photograph of Packerhead Machine

Figure 1-3 Photograph of Roller heads in Packerhead Machine

As soon as the concrete pipe is formed, the curing process begins. During the curing process, durability and strength of the concrete pipes are increased. Time, moisture, and temperature are the three fundamantal factors for the curing of the concrete pipes. As the temperature is increased, the curing of the concrete will increase. In a curing chamber, (as shown in Figure 1-4 Photograph of a Curing Chamber) the curtains are dropped to provide an enclosed area for a couple of hours. A low-pressure steam with high humidity, and high temperature is introduced into a chamber which allows circulation of steam around the entire pipe.

Figure 1-4 Photograph of a Curing Chamber

Pipe Design Methods

There are two methods for the design of reinforcement concrete pipe: the indirect design method and the direct design method.

Currently, the indirect or direct design method is used for the design of the reinforcement concrete pipe. In the 1970's, American Concrete Pipe Association (ACPA) used the finite element computer program, Soil-Pipe Interaction Design and Analysis program (SPIDA) to develop the direct design method. In this procedure, strength and serviceability limits are considered. Direct design method is the design of the pipe in the installed condition. In this method after finding the magnitude and distribution of the loads, the physical properties necessary to support these loads are calculated. In this approach, the supporting strength is determined by the effect of pressure distribution around the pipe defined in terms of moment, thrust, and shear which are calculated using Equations:

$$\text{Moment} \qquad M_i = C_{mi} \times W_i \times \frac{D_m}{2} \qquad (1),$$

$$\text{Thrust} \qquad N_i = C_{ni} \times W_i \qquad (2),$$

$$\text{Shear} \qquad V_i = C_{vi} \times W_i \qquad (3),$$

The factors for pipe crown and installation type 1 is shown In Table 1-1 Coefficients for Analysis of Pipe in Standard Installation type 1 and in crown location (Direct design method)

Table 1-1 Coefficients for Analysis of Pipe in Standard Installation type 1 and in crown location (Direct design method)

Installation Type 1				
Location	Load Type	Coefficients		
		C_{mi}	C_{ni}	C_{vi}
Crown	W_p	0.079	-0.077	
	W_e	0.083	0.157	
	W_f	0.057	-0.187	
	W_{L1}	0.068	0.2	
	W_{L2}	0.236	0.046	

It is noted that for the pipes larger than 72in and the D-Load greater than 2000 lb/ft/ft, the direct design methods should be considered. Large diameter pipes should be designed by direct design methods to minimize reinforcement costs due to the fact that the equations were originally formulated for the larger diameter pipes; otherwise, the design is very conservative.

Indirect design or traditional design method is the comparison between the structural strength of the pipe found in the Three-Edged Bearing Test and the field supporting strength of a buried pipe. This method is a simplified method for the direct design method. Marston and Spangler's research was the basis of this method and it was developed by ASCE 15-93.

The indirect design procedure for the selection of pipe strength includes: determination of earth load and live load, selection of bedding, determination of the bedding factor, factor of safety, and the selection of pipe strengths (concrete pipe design manual).

Trench, positive projecting embankment, negative projecting embankment, and trench are the three common types of installation.

Typical loads that should be considered for a buried pipe includes: pipe weight, earth load, fluid weight and internal pressure, surface concentrated loads, and surface surcharge loads.

In some cases, the weight of the pipe (W_p) is insignificant compared to the other loads and can be calculated by using equations (4) and (5):

$W_p = 3.3 \times h \times (D_i + t)$ (4) for circular pipes (Di: inside pipe diameter, t pipe wall thickness)

$W_p = a \times h \times (S_i + t)$ (5) for elliptical pipes (a=2.8 for horizontal elliptical and a = 4.2 for Vertical elliptical and S_i: inside Horizontal span)

The relationship between wall thickness, wall thickness type, and inside diameter is governed by the following expressions:

Wall A $t = \frac{D_i\ (in)}{12}$ (6)

Wall B $t = \frac{D_i\ (in)}{12} + 1$ (7)

Wall C $t = \frac{D_i\ (in)}{12} + 1.75$ (8)

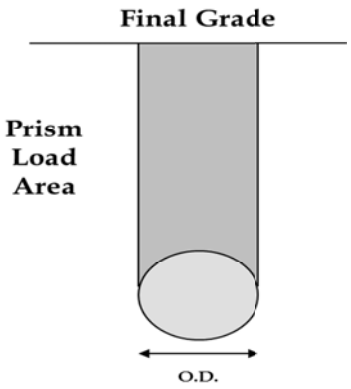

Figure 1-5 Vertical Arching factor

The AASHTO Standard Specifications for Highway Bridges states that a pipe design should use a fluid weight of 62.4 lbs/ft^3

(1) W_e = prism load x VAF (AASHTO Equation 12.10.2.1-1) (Where: VAF is vertical arching factor as per Heger distribution)

Table 1-2 Vertical and Horizontal arching factor

Standard Installation Type	VAF	HAF
Type 1	1.35	0.45
Type 2	1.4	0.4
Type 3	1.4	0.37
Type 4	1.45	0.3

$$PL = w \times \left(H + \frac{D_0 \times (4-\pi)}{8}\right) \times D_0 \qquad (9)$$

w = soil unit weight, (lb/ft^3)

H = height of fill, (ft)

Do= outside diameter, (ft)

$$D = \left(\frac{12}{S_i}\right) \times \left(\frac{W_E + W_F}{B_{FE}} + \frac{W_L}{B_{FLL}}\right) \qquad (10)$$

In which:

B_{FE} = Earth load bedding factor specified in Article 12.10.4.3.2a or Article 12.10.4.3.2b

B_{FLL} = Live load bedding factor specified in Article 12.10.4.3.2c

S_i = Internal diameter of pipe (in.)

W_E = Total unfactored earth load specified in Article 12.10.2.1 (kip/ft)

W_F = Total unfactored fluid load in the pipe as specified in Article 12.10.2.2 (kip/ft)

W_L = Total unfactored live load on unit length pipe specified in Article 12.10.2.3 (kip/ft)

Figure 1-6 Controlling Criteria (ASCE 15-98) illustrates a non-dimensional graph for the strength of the pipe depending on the circumferential reinforcement and the height of the earth cover. As the fill heights increase the circumferential steel is required more. Also, as the height of the earth cover increases, the failure modes of the pipe changes from flexural control to crack control and then to shear controlled design.

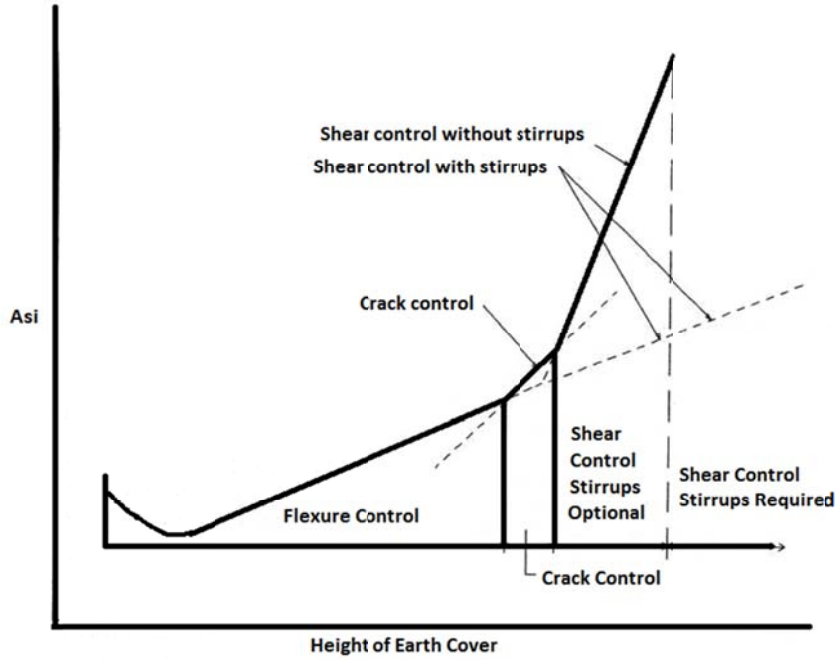

Figure 1-6 Controlling Criteria (ASCE 15-98)

Objectives of The Study

The objectives of this study was to develop highly ductile concrete pipes by using a combination of Steel Fiber, Crumb Rubber, Synthetic Fiber and Conventional Cage and also to develop thin wall semi-rigid concrete pipes by using the above combinations.

The outline of this research Is shown in

Figure 1-7 Outline of this study

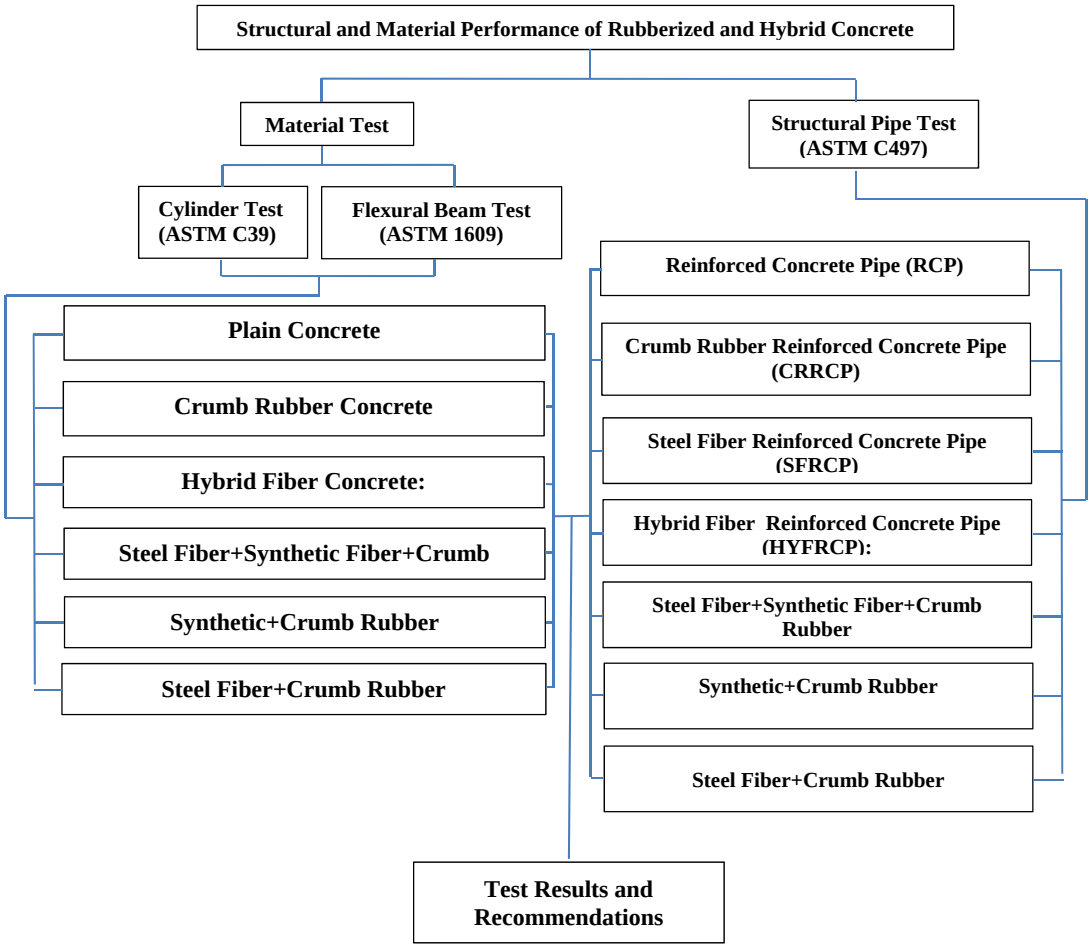

Figure 1-7 Outline of this study

Chapter 2

Literature Review

Introduction

There has been no previous research study on the dry cast crumb rubber concrete pipe before and this research has been conducted for the first time in the United States. In this chapter, history and application of crumb rubber, steel fiber, and synthetic fiber in concrete pipes are reviewed.

History and Application of Crumb Rubber

Crumb rubber is produced from used vehicle tires. Crumb rubber particles range from 4.75mm (No. 4 Sieve) to 0.075 mm (No. 200 Sieve). Addition of the crumb rubber reduce the unit weight of mixture because the mineral aggregates have the higher unit weight than the crumb rubber particles.

. The photograph of Crumb rubber which was used in Hanson facility is shown in Figure 2-1 Photograph of Typical Crumb Rubber Used

Each year in the United States, millions of scrap tires are produced which is a serious threat to the environment. (Atahan, Yücel, 2012). Tires take up large space of landfills and there is a fire risk involved as well. In addition, tire piles create ideal breeding sites for mosquitos. Many states in the U.S. are working on recycling the tires from going to landfills so that a lot of money can be saved by using cheaper ingredients in concrete. According to the Environmental Protection Agency (EPA), thirty-eight states banned whole tires from going to landfills. By recycling, scrap tires in stockpiles have been reduced by over 87 percent since the year 1990. Statistics show that there are at least 275 million scrap tires in stockpiles in the U.S. In addition, approximately 290 million scrap tires were generated in 2003.

Figure 2-1 Photograph of Typical Crumb Rubber Used

Previous Research on Crumb Rubber Concrete

Several studies have been carried out to evaluate the effects of rubber in concrete; Gideon Momanyi (2012) investigated the effects of Crumb rubber, or Tire Derivative Aggregate (TDA) in unreinforced concrete. He observed that compressive strength of up to 4000 psi (27.5 MPa) can be reached by replacing the coarse aggregates in concrete with small amounts of TDA ranging from 7.5% to 10% with top size of 2in (50.8 mm) by using enhanced materials such as silica fume. He found that the replacement of mineral aggregate with TDA will decrease the compressive strength of concrete but it will increase the ductility of concrete. It was determined that the addition of Crumb Rubber into the concrete will increase the toughness and impact resistance as well but on the other hand, it will decrease the modulus of elasticity, splitting tensile strength and the modulus of rupture. He recommended that post cracking behavior of concrete improves by adding crumb rubber to the concrete mix.

Ilker Bekir Topçu (1995) investigated the influence of fine and coarse rubber particles on physical and mechanical properties of concrete. He observed that 50% decreases by using fine rubber and 60% decreases by using coarse rubber particles in compression strength of cylindrical specimens. His results showed that using coarse rubber aggregates affects properties of concrete more than fine rubber aggregates. He found that with the addition of rubber, concrete shows more elastic behavior and becomes more ductile.

A study by H.A. Toutanji (1996) evaluated the effects of the replacement of coarse aggregates by volume contents of 25%, 50%, 75% and 100% rubber tire. The results showed that using rubber in concrete reduces both the compressive and flexural strength of concrete however increases the ductility of the specimens. He also found that the compressive strength was decreased twice of the reduction of the flexural strength.

Another study by Khaloo, Ali R., M. Dehestani, and P. Rahmatabadi (2008) investigated the mechanical and physical properties of tire-rubber concrete. They found that rubberized concrete with fine rubber particles exhibits an acceptable workability and more ductility with respect to plain concrete. The replacement of mineral aggregates with tire–rubber particles reduce the ultimate strength of concrete significantly. They recommended to use less than 25% rubber replacement to have less reduction in ultimate strength.

Steel Fiber Reinforcement Concrete

History and Application of Steel Fiber

The use of steel fibers as the main reinforcement of concrete is an alternative to the traditional steel bar concrete pipes. Steel fibers are randomly distributed to the batch to provide post cracking control, ductility, or toughness (defined as some function of the area under the load vs. deflection curve) after the initial crack occurs. The concept of using steel fiber reinforced concrete dates back to the 1960s. Steel fibers have been used in pavements, tunnel lining, bridge deck slab repairs, spillways, and dams over the past forty years (Chanh, Nguyen, 2004). In 1874, the first patent was developed by A. Berard in California, in which he added irregular scrap material (Maidl 1995). In August 1971, the first commercial SFRC pavement was placed at a truck weighing station near Ashland, Ohio (Hoff, 1986).

Mechanical Properties of Steel Fiber Reinforced Concrete

The steel fibers used in this study were Dramix®, RC-65/35-BN steel fibers from Bekaert global company with headquarters in Belgium. Dramix® Steel Fiber is a cold drawn steel wire fiber glued into bundles, with hooked ends as shown in Figure 2-2 Photograph of Typical Steel Fibers (RC-65/35-BN) used. The fibers are 1.38in (35mm) in length, 0.022in (0.55mm) in diameter, the young modulus of 30458 lb/in^2(210 N/mm^2), the relative density of 7.85 (13226 lb/yd^3 or 7847 kg/m^3), tensile strength of 195 lb/in^2 (1.345 N/mm2).

The bond between steel fibers and concrete is very critical for the concrete pipes. Strong bonds after the occurrence of the first crack causes the steel fibers to not pull out, showing a significant effect on the tensile strength of the pipe. In addition, the number of

steel fibers in the direction of the tensile force yields after the occurrence of the crack, without significantly pulling out, will increase the strength of the pipe.

Figure 2-2 Photograph of Typical Steel Fibers (RC-65/35-BN) used

Previous Research On Steel Fiber Reinforcement Concrete

Nguyen Van Chanh in (2004) investigated the mechanic properties and applications of steel fiber reinforced concrete. He found that steel fibers have little effect on compressive strength, however, it can improve the resistance of conventionally reinforced structural members to cracking, deflection and post-cracking ductility. After the occurrence of the crack, the steel fibers hold the matrix even after the ultimate crack. His results showed that using 5% of smooth, straight steel fibers aligned in the direction of the tension, can increase the direct tensile strength by 33%.

M.N. Soutsos, T.T. Le, A.P. Lampropoulos, investigated the flexural strength and mechanical properties of shape, length and dosage of steel fibers. They concluded that the presence of 50 and 84 lb/ft^3 steel fibers increase by about 580psi and 725psi and

observed that the steel fibers significantly increase with the flexural toughness of concrete, however, fibers didn't improve the flexural strength.

History and Application of Synthetic Fiber

Macrosynthetic fibers used in this study were MasterFiber™ MAC Matrix as shown in Figure 2-3 Photograph of Macrosynthetic fibers used in this study from BASF chemical company, manufactured from polypropylene resins. These fibers are used as reinforcement to control shrinkage, temperature cracking, settlement cracking, and used as a replacement of steel fibers, in some cases. These fibers were recommended to be used in shotcrete, composite metal decks, pavements, precast concrete, tunnel lining which provide increased flexural toughness and increased impact and shatter resistance to help improve the long-term durability and integrity of concrete. The Performance Characteristics of MasterFiber™ MAC Matrix is shown in Table 2-1 Performance Characteristics of MasterFiber™ MAC Matrix used in this study.

Figure 2-3 Photograph of Macrosynthetic fibers used in this study

Table 2-1 Performance Characteristics of MasterFiber™ MAC Matrix used in this study

Physical Properties	
Configuration	Stick-like fiber
Fiber Type	Embossed
Material	100% virgin polypropylene
Specific Gravity	0.91
Melting Point	320 °F (160 °C)
Ignition Point	1094 °F (590 °C)
Available Lengths	1.9 in. and 2.1 in. (48 mm and 54 mm)
Water Absorption	Nil
Tensile Strength	85 ksi (585 MPa) min
Alkali Resistance	Excellent
Chemical Resistance	Excellent
Color	White, translucent
Electrical Conductivity	Low

Cominoli, L., C. Failla, and G. A. Plizzari (2007) investigated the toughness and shrinkage behavior of reinforcement concrete by using different types of hooked end steel and synthetic fibers . He found that steel fibers increase the toughness of the concrete reinforced. Also, he observed that the synthetic fibers reduce the shrinkage crack.

Chapter 3

Structural Pipe Test

Introduction

A total of 86 pipes were produced and tested in accordance with ASTM C 497 three-edged bearing at Hanson Precast Plant in Grand Prairie, TX. The pipe designation used in this study is as follows: pipe type-diameter of pipe-length of pipe-thickness type-dosage of steel fiber (lb/yd^3)-percentage of replacement of sand with crumb rubber-dosage of synthetic fiber (lb/yd^3) in the mixture. For example, CRRCP-24-6-B-44-3-5 represents a Crumb Rubber Reinforced Concrete Pipe with 24in. (609mm) diameter of pipe, 6ft (1828mm) length of pipe, B wall thickness, 44 lb/yd^3 (26 kg/m^3) of steel fiber, 3% replacement of sand with crumb rubber and 5 lb/yd^3 (3 kg/m^3) of Macrosynthetic fibers.

The pipes were tested on the 7^{th} day of production according to the ASTM C 497 Standard Test Methods for Concrete Pipe, Manhole Sections, or Tile at Hanson Precast Plant in Grand Prairie, TX.

Two different mix designs were used for the production of all the pipes as shown in Table 3-1 and Table 3-2 .

For each batch, six cylindrical specimens of size 4×8 inch. (100×200 mm) and two beam specimens of size 6×6×20 in. (152×152×508 mm) were casted. Further details of casting and curing of the specimens have been mentioned in Chapter 4.

Table 3-1 Details of Mix Design 1

Pipe class	Ash Groves Type I/II cement (lbs)	Fly Ash (lbs)	Crushed Limestone 3/8 (in)	Crushed Limestone 5/8 (in)	Sand (lbs)	Water (lbs)	Admix Silica Fl. Oz./(100lb)	W/C	Total (lbs per one cuy ssd)
III	380	125	1450	N/A	1917	217	5.5	0.43	4089
IV	424	140	1450	N/A	1824	233	5.5	0.41	4069
IV	424	140	1300	370	1605	233	5.5	0.41	4070
V	461	150	1450	N/A	1746	242	5.5	0.40	4057

Table 3-2 Details of Mix Design 2

Ash Groves Type I/II cement (lbs)	Fly Ash (lbs)	Crushed Limestone 3/8 (in)	Crushed Limestone 5/8 (in)	Sand (lbs)	Water (lbs)	Admix Silica Fl. Oz./(100lb)	W/C	Total (lbs per one cuy ssd)
569	139	1957	N/A	1368	242	5.5	0.34	4275

The variation of the fiber volume fraction and crumb rubber content for the 24 and 36 inches, 6 ft long and B wall thickness of pipes are shown in Table 3-3 Various fiber dosages for 24in. Pipe, 6ft long and B wall-thickness and Table 3-4 , subsequently.

Table 3-3 Various fiber dosages for 24in. Pipe, 6ft long and B wall-thickness

Mix class	Steel Fiber (lbs)	Rubber (%)	Synthetic Fiber (lbs)	Cage
III	44 (Vf, of 0.33%)	3	5	N/A
	22 (Vf, of 0.17%)	5	2	
IV	44 (Vf, of 0.33%)	20	N/A	N/A
		15		N/A
		10		×
		10		N/A
		8		N/A
		6		N/A
	10 (Vf, of 0.08%)	8	N/A	×
		N/A		N/A
	N/A	20	N/A	×
		15		
		10		
		6		
		N/A		
V	44 (Vf, of 0.33%)	8	N/A	N/A
	N/A	8		×

Table 3-4 Various fiber dosages for 36in. Pipe, 6ft long and B wall-thickness

Mix class	Steel Fiber (lbs)	Rubber (%)	Synthetic Fiber (lbs)	Cage
III	44 (Vf, of 0.33%)	3	5	N/A
IV	44 (Vf, of 0.33%)	12	N/A	N/A
		10		
	22 (Vf, of 0.17%)	10	N/A	N/A
		8		
	N/A	8	N/A	×
		12		
		10	8	N/A
		10	N/A	×
		N/A		

The variation of the fiber volume fraction and crumb rubber content for the 60 inches, 8 ft long, single layer of reinforcement, class III and Thin-walled thickness of pipes are shown in Table 3-5 .

Table 3-5 Various fiber dosages for 60in. Pipe, 8ft long and Thin-walled

Steel Fiber (lbs)	Rubber (%)	Synthetic Fiber (lbs)
66 (Vf, of 0.5%)	N/A	N/A
88 (Vf, of 0.67%)		
11 (Vf, of 0.08%)	20	N/A
N/A	20	N/A
	20	4
	13	N/A
	N/A	12
	N/A	N/A

Three-edged Bearing Test D-load Test

Test Set Up and Procedure

The three-edge-bearing method of loading were used for the crushing test. According to ASTM C497, the pipe specimen were supported on a lower bearing of two longitudinal rubber strips and the load applied through a hydraulic cylinder. After placing of the pipe, the Cable extension Displacement Sensors (CDS) as shown in Figure 3-3 Photograph of CDS for measuring deflection were installed inside, and 6in. from the edge of the pipe and then were connected to the Vishay Scanner. System 5000's Model 5100B Vishay Scanner as shown in Figure 3-2 Data acquisition unit (Vishay scanner) was used to record intervals as short as 0.02 seconds. Strain Smart Software on Windows-based computer acquired data from Vishay scanner. The load cell as shown in

Figure 3-4 Photograph of load cell at Hanson facility controlled the load of hydraulic cylinder which applied to the pipe up to 5% deflection of the inside diameter of the pipe.

Figure 3-1 Photograph of D-Load rack at Hanson facility

Figure 3-2 Data acquisition unit (Vishay scanner)

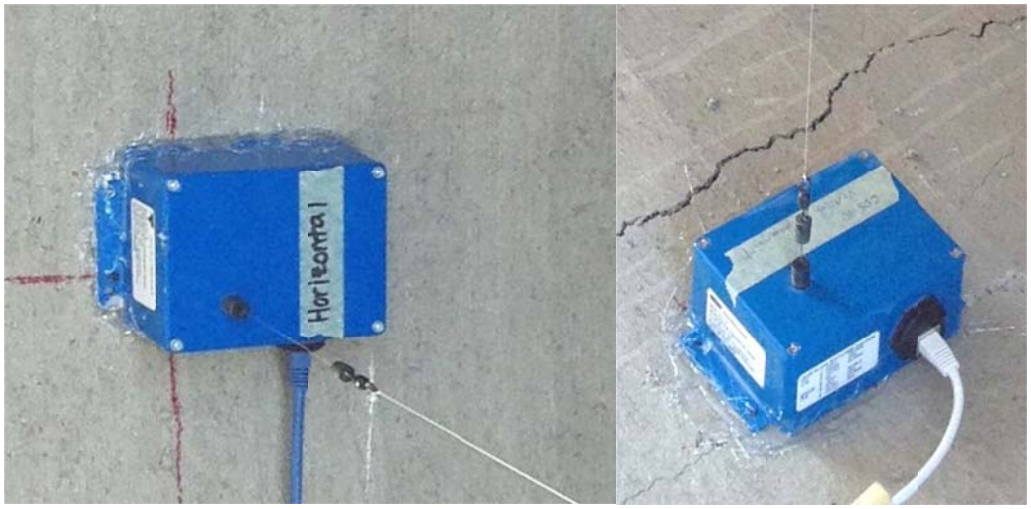

Figure 3-3 Photograph of CDS for measuring deflection


Figure 3-4 Photograph of load cell at Hanson facility

Test Results

The D-load strength in pounds per linear foot per foot versus deflection of all of the 86 pipes which were tested in accordance with ASTM C 497 three-edged bearing at Hanson Precast Plant in Grand Prairie, TX, in detail are in appendix B. The comparison of all the pipes are shown in the graphs below:

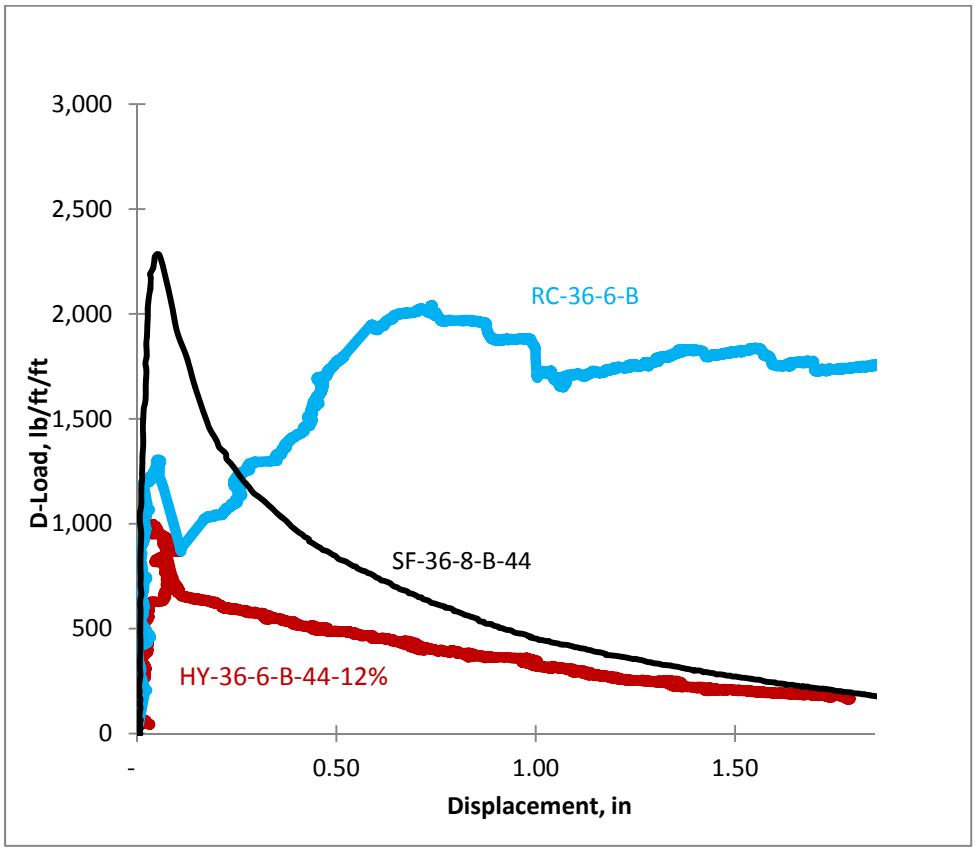

Figure 3-5 36in load-deflection graphs

From Figure 3-5 36in load-deflection graphs it was found that steel-fiber concrete pipe had a higher initial strength than the conventional strength but, the steel fiber pipe was not produced on the same day as the other pipes.

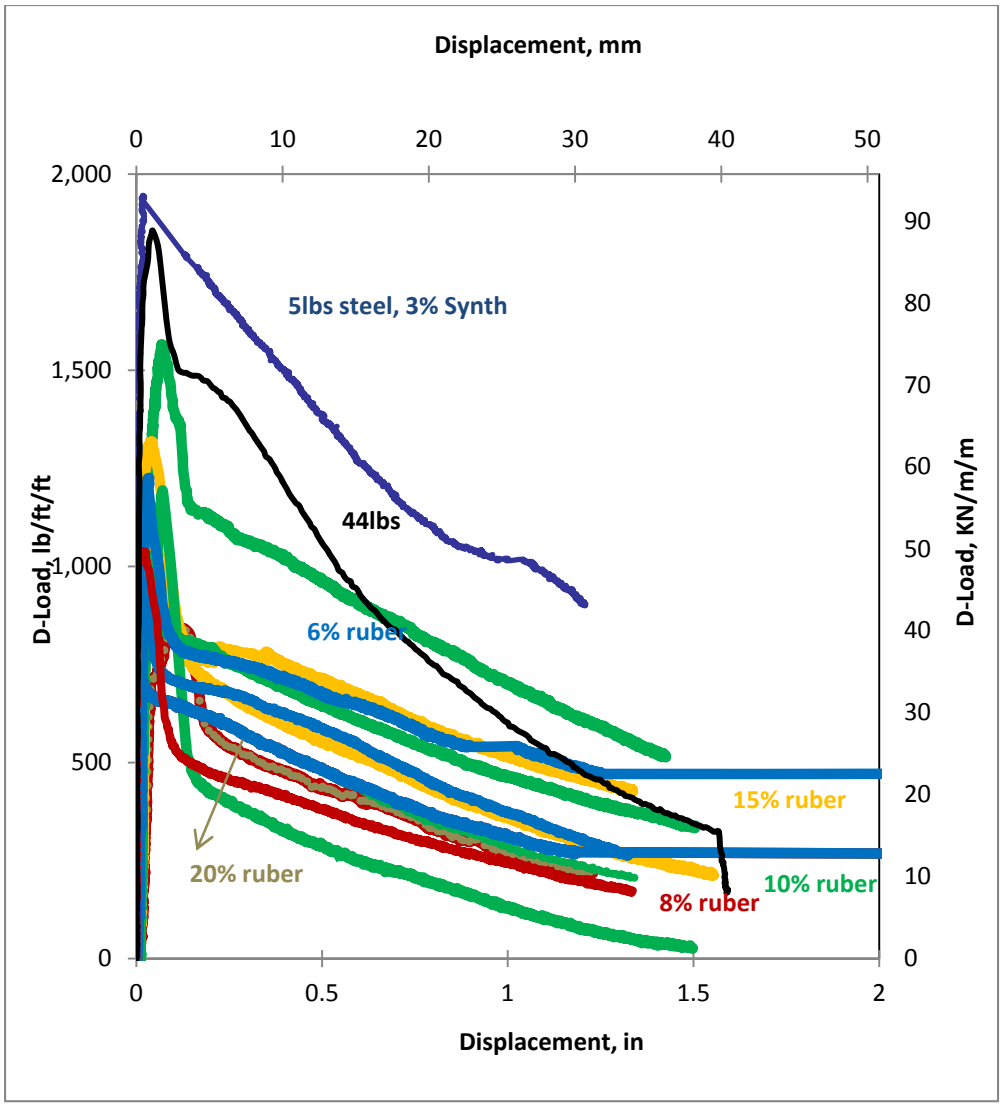

Figure 3-6 24in load-deflection graphs

Different crumb rubber content for 24in. pipes are shown in Figure 3-6 24in load-deflection graphs. It was observed that as crumb rubber increased, the initial crack strength reduced.

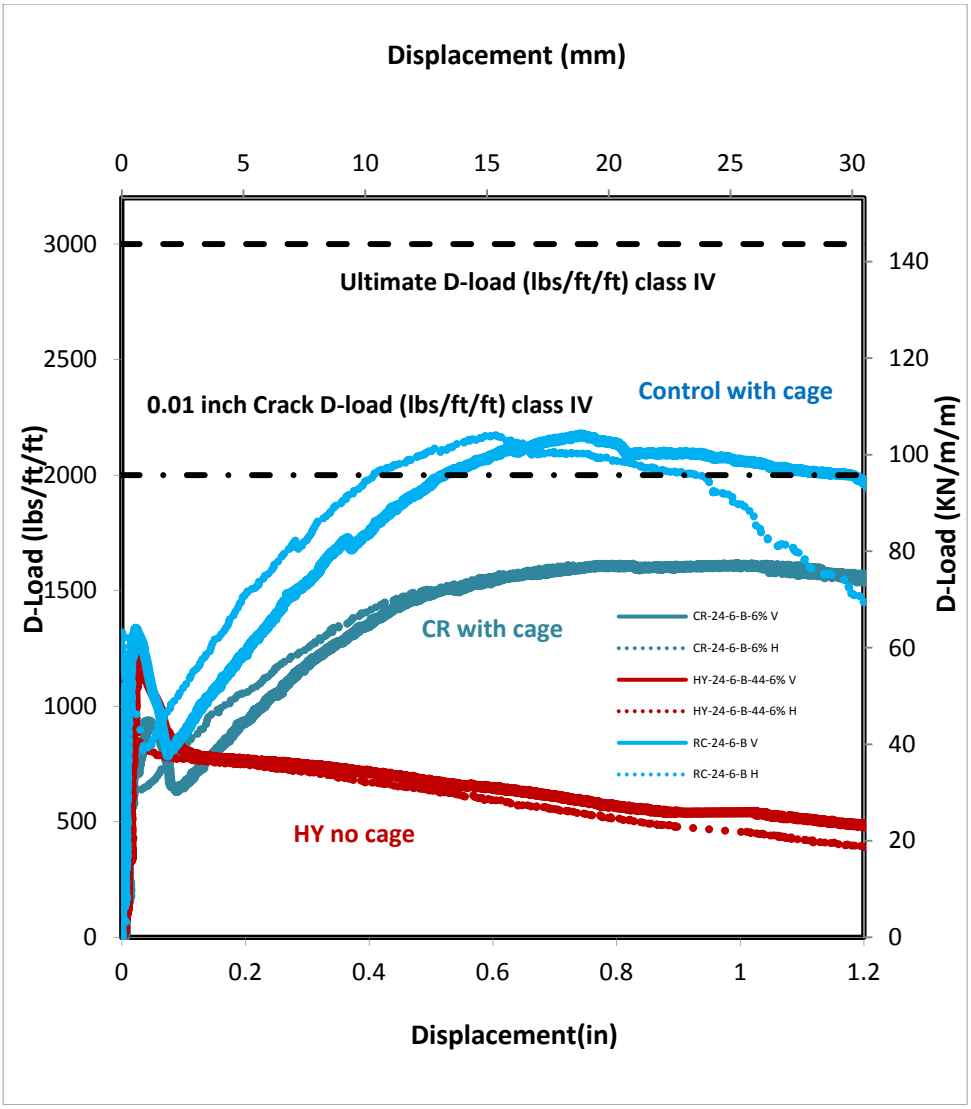

Figure 3-7 Load-Deflection Plot for RCP-24-6-B, HYCP-24-6-B-44lbs steel-6% rubber and CRCP-24-6-B-6% rubber

The results of the 24in. with 6% crumb rubber showed that the initial crack strength was reduced by 25% compared to the reinforced concrete pipe(RCP), however, the ultimate strength of the CRCP was gradually in the rightward direction of the graph, resulting in more ductility as shown in Figure 3-7 Load-Deflection Plot for RCP-24-6-B, HYCP-24-6-B-44lbs steel-6% rubber and CRCP-24-6-B-6% rubber.

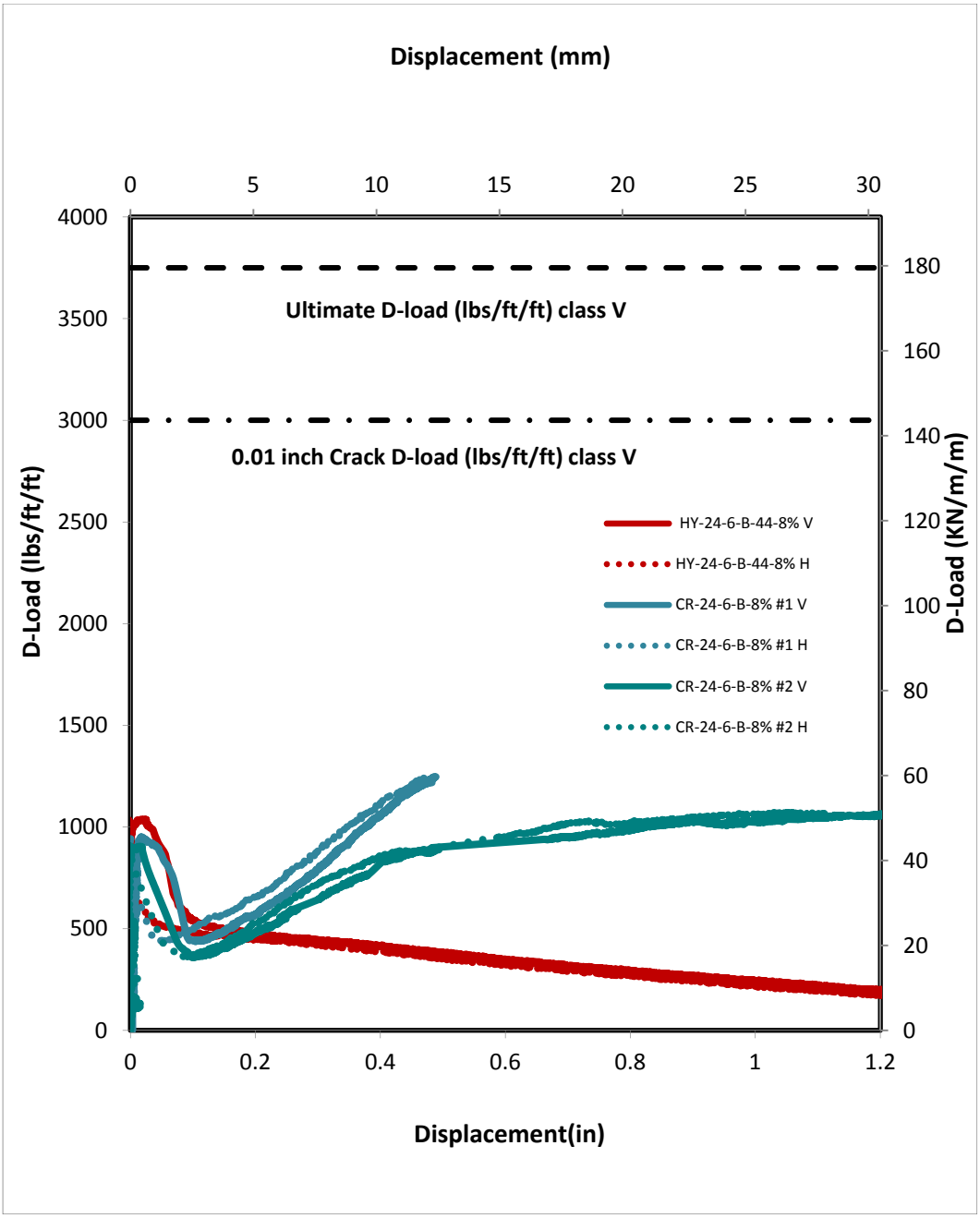

Figure 3-8 Load-Deflection Plot for HYCP-24-6-B-44lbs steel-8%rubber, CRCP-24-6-B-8%rubber and HYCP-24-6-B-44lbs steel-8% rubber

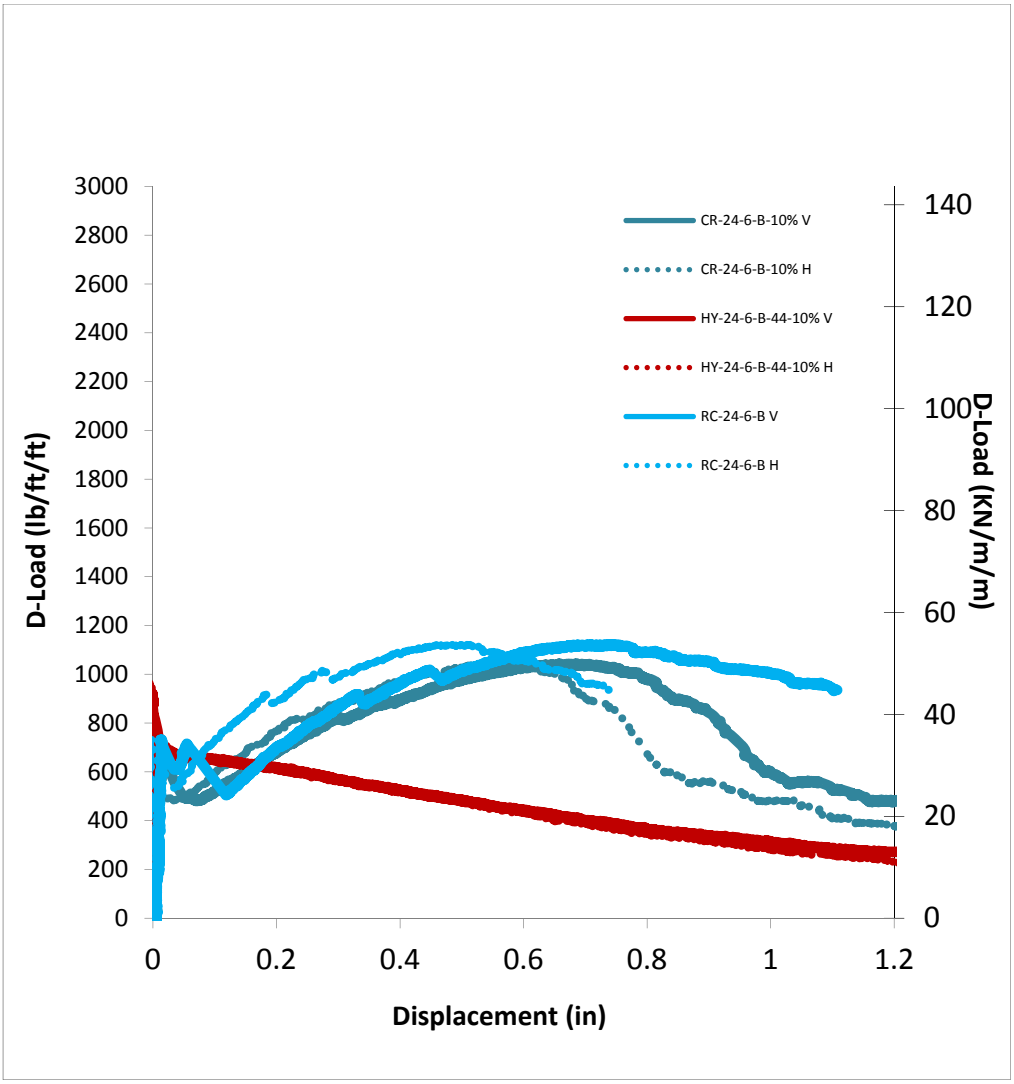

Figure 3-9 Load-Deflection Plot for RCP-24-6-B, HYCP-24-6-B-44lbs steel-10%rubber and CRCP-24-6-B-10%rubber

From Figure 3-9 Load-Deflection Plot for RCP-24-6-B, HYCP-24-6-B-44lbs steel-10%rubber and CRCP-24-6-B-10%rubber, the Hybrid Concrete Pipe with 44lbs of steel and 10% rubber showed that the initial strength was 30% higher than conventional concrete pipe. The crumb rubber graph showed that as it moves in the rightward direction, more ductility is present.

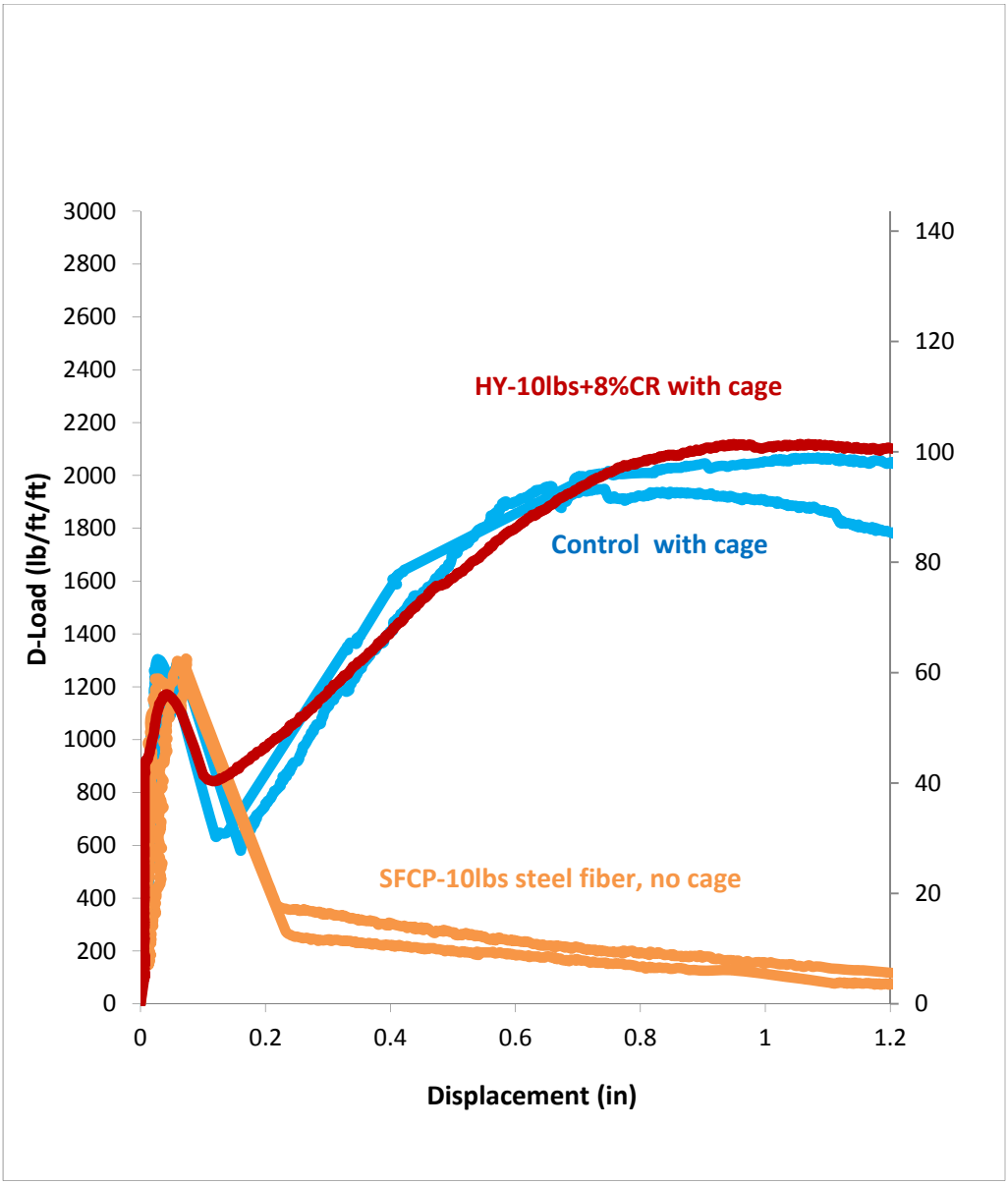

Figure 3-10 SFCP-24-6-B-10lbs steel, RCP-24-6-B

Shown in Figure 3-10 SFCP-24-6-B-10lbs steel, RCP-24-6-B 10lbs steel fiber without crumb rubber concrete pipe, the strength significantly decreased after the initial crack occurred, due to the fact that the steel fibers were pulled out of the rather than yielded.

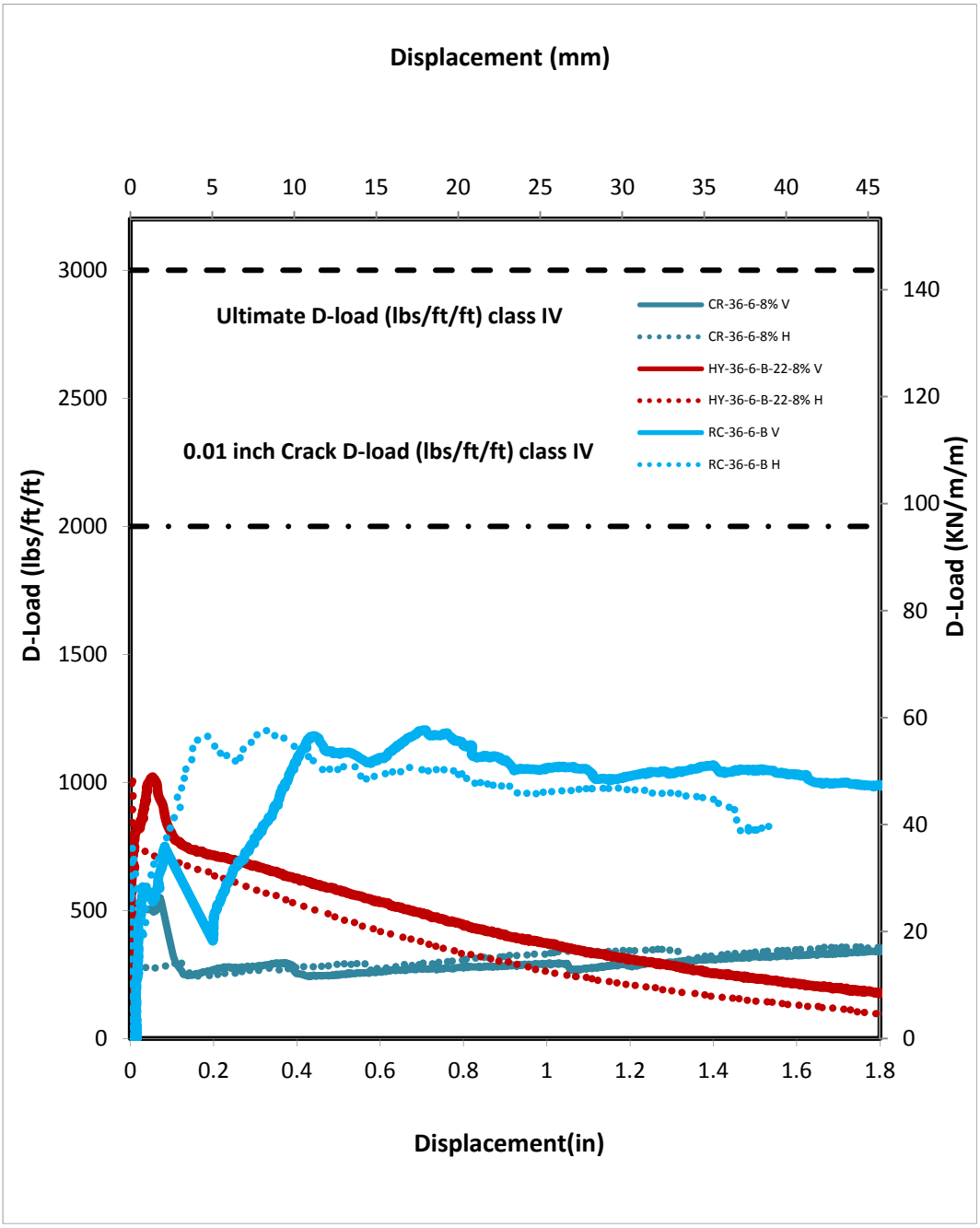

Figure 3-11 Load-Deflection Plot for HYCP-36-6-B-22lbs steel-8% rubber, CRCP-36-6-8% rubber and RCP-36-6-B

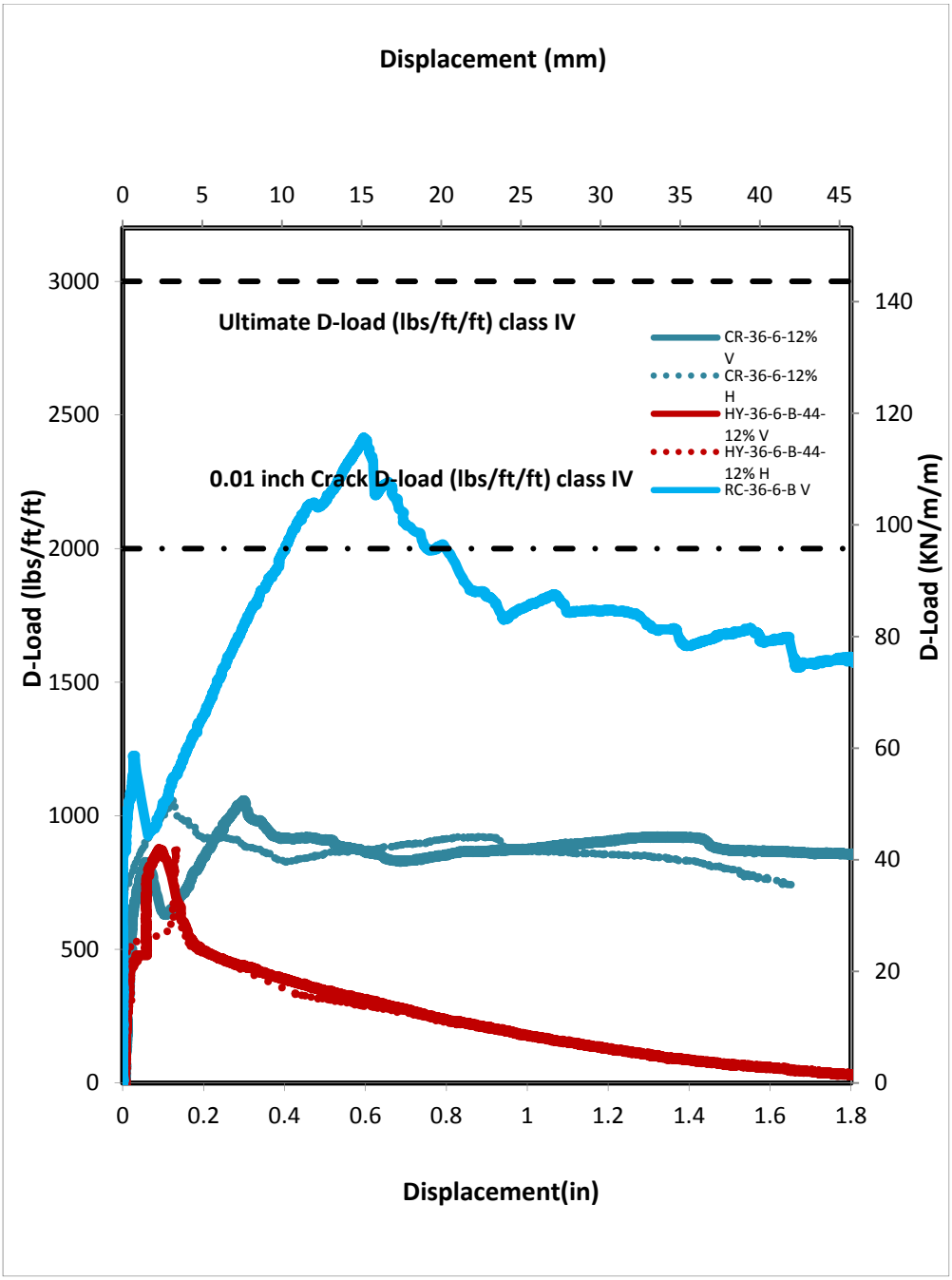

Figure 3-12 Load-Deflection Plot for HYCP-36-6-B-44lbs steel-12%rubber, CRCP-36-6-12%rubber and RCP-36-6-B

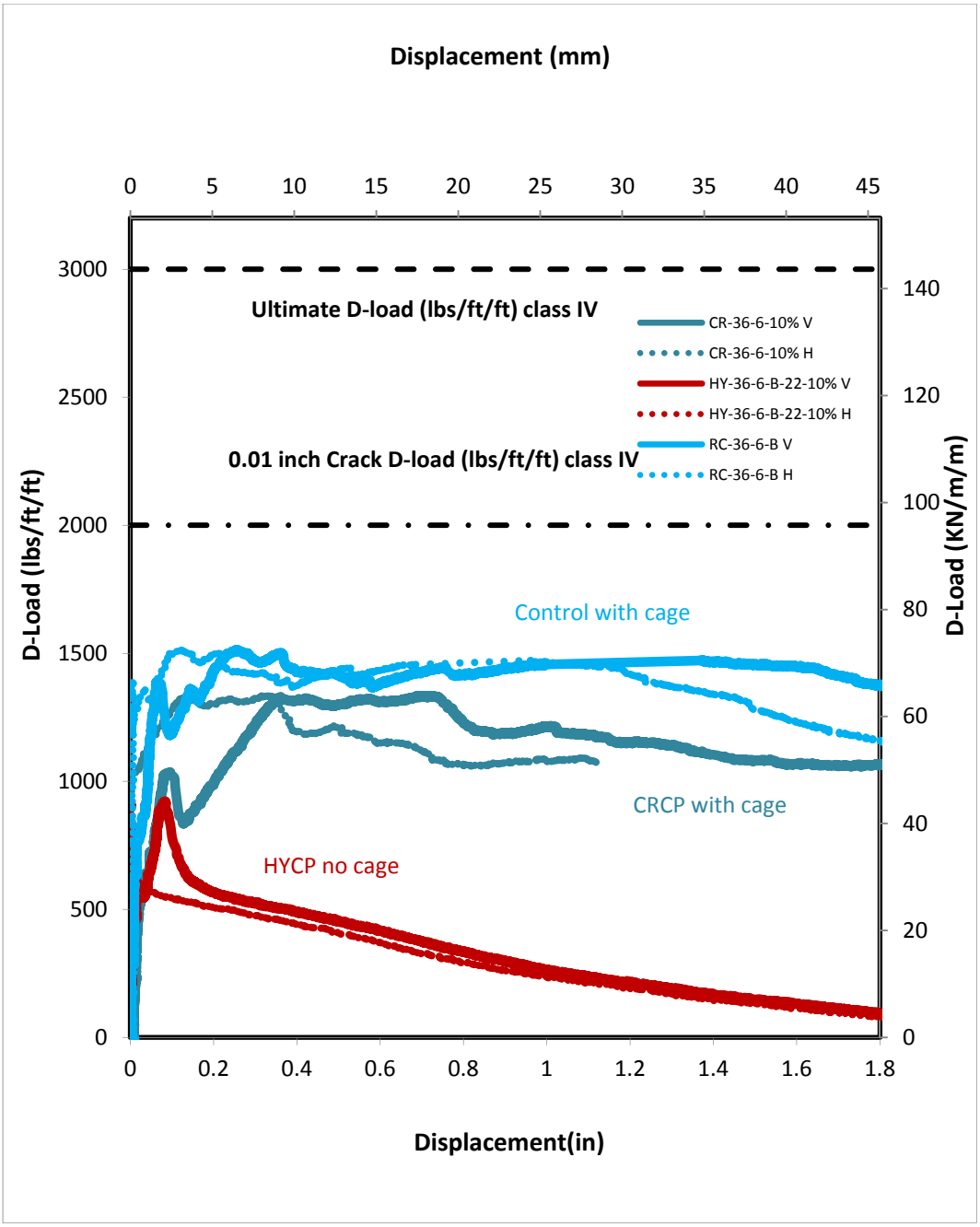

Figure 3-13 Load-Deflection Plot for HYCP-36-6-B-22lbs steel-10%rubber, CRCP-36-6-B10%rubber, RCP-36-6-B

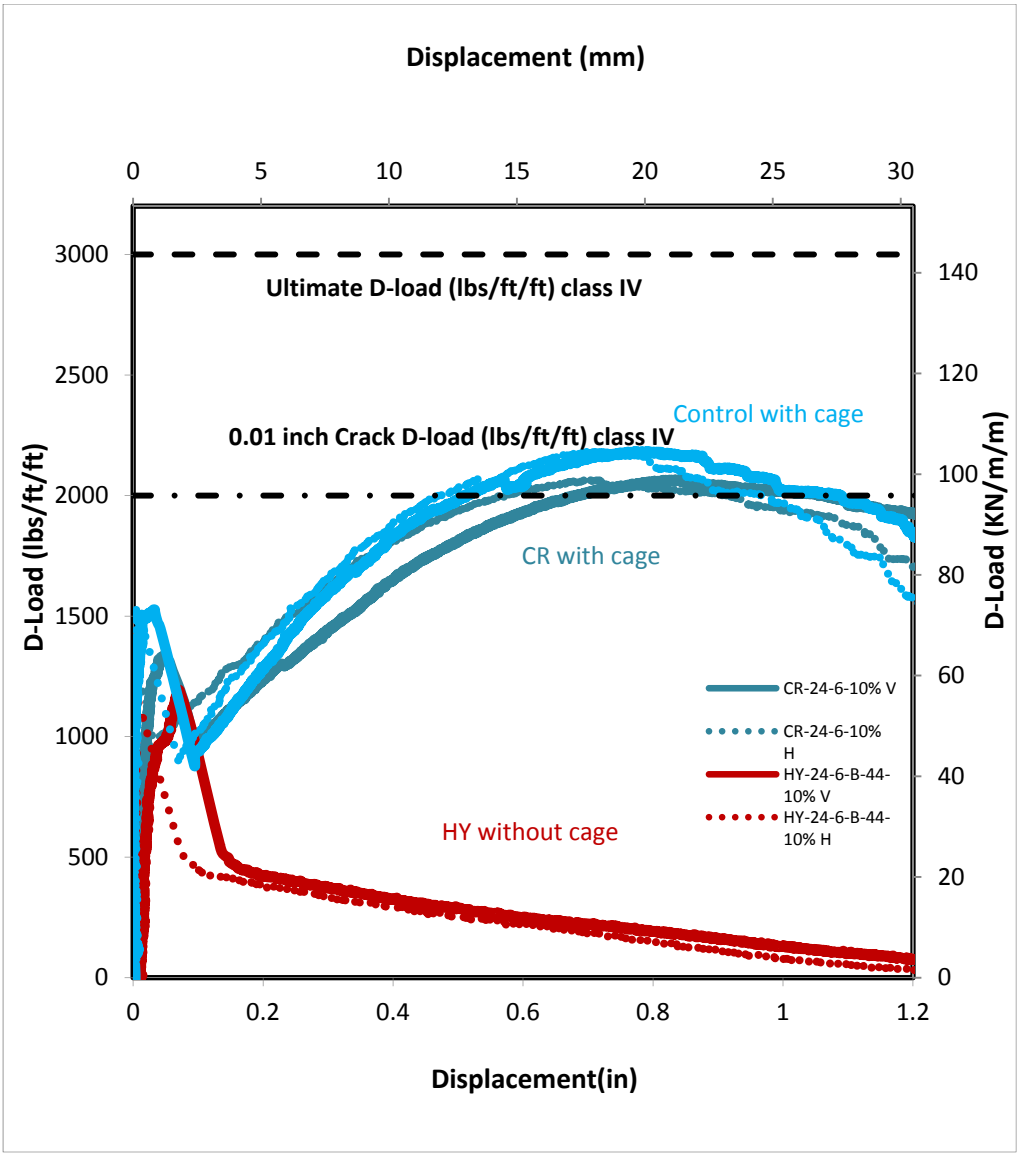

Figure 3-14 Load-Deflection Plot for HYCP-24-6-B-44lbs steel-10%rubber, CRCP-24-6-B-10% rubber and RCP-24-6-B

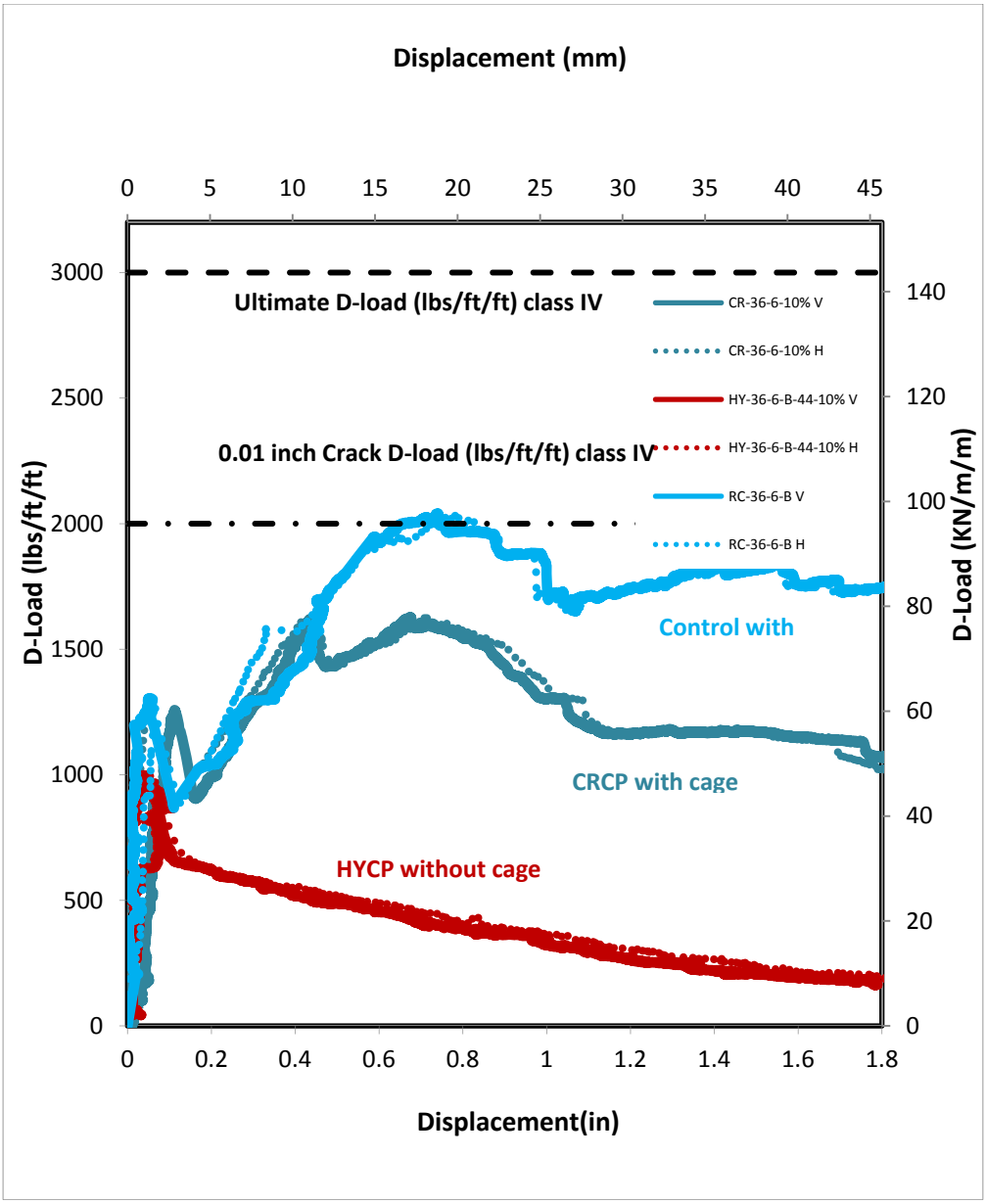

Figure 3-15 Load-Deflection Plot for HYCP-36-6-B-44-10%rubber, CRCP-36-6-B-10%rubber, RCP-36-6-B.

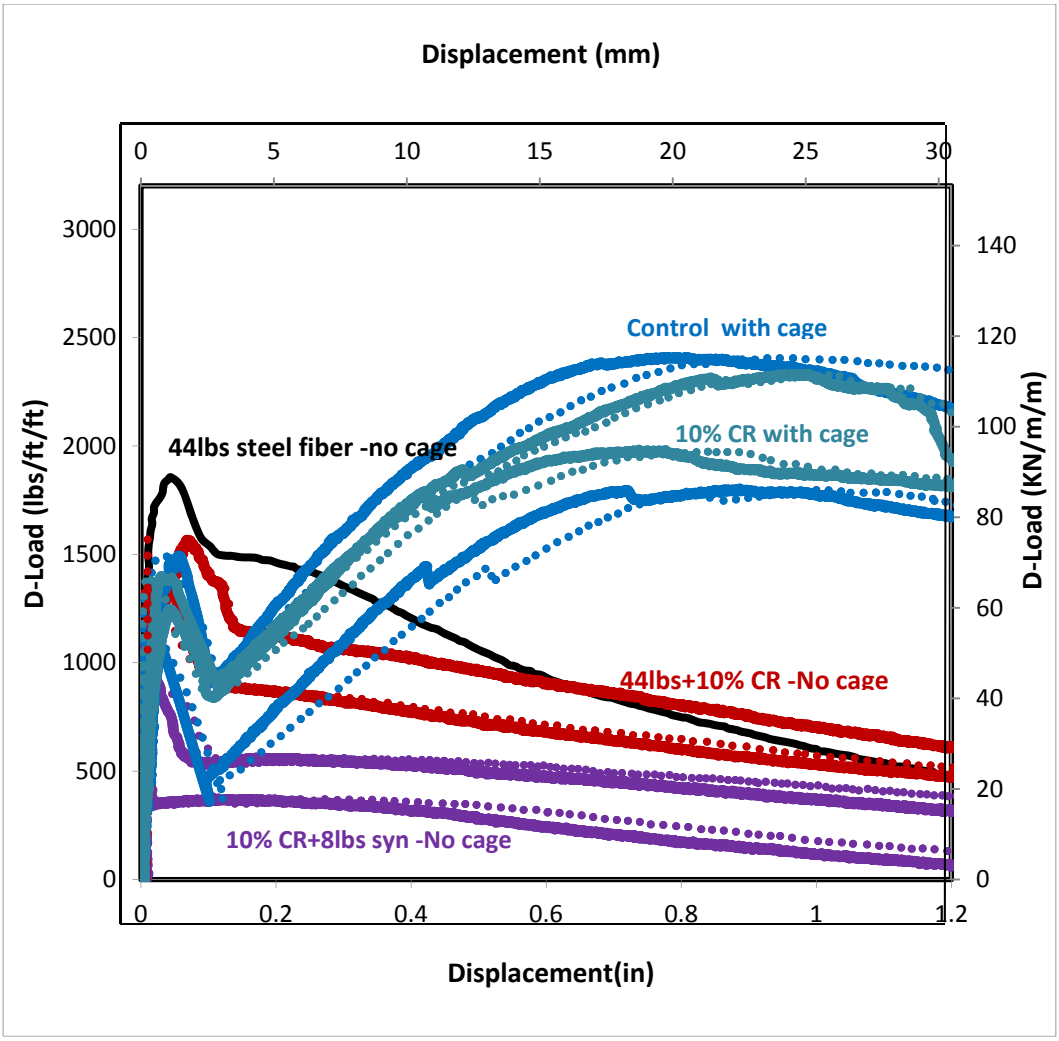

Figure 3-16 Load-Deflection Plot for CRCP-24-6-B-10%rubber, SFCP-24-6-B-44lbs steel fiber, HYCP-24-6-B-44lbs steel, and HYCP-24-6-B-10%rubber-8lbs synth.

For the 44lbs steel fiber, the initial crack was found to be 20% more than the conventional concrete pipe. The ultimate strength and hardening of the crumb rubber concrete pipe was longer than the RCP, resulting in more ductility.

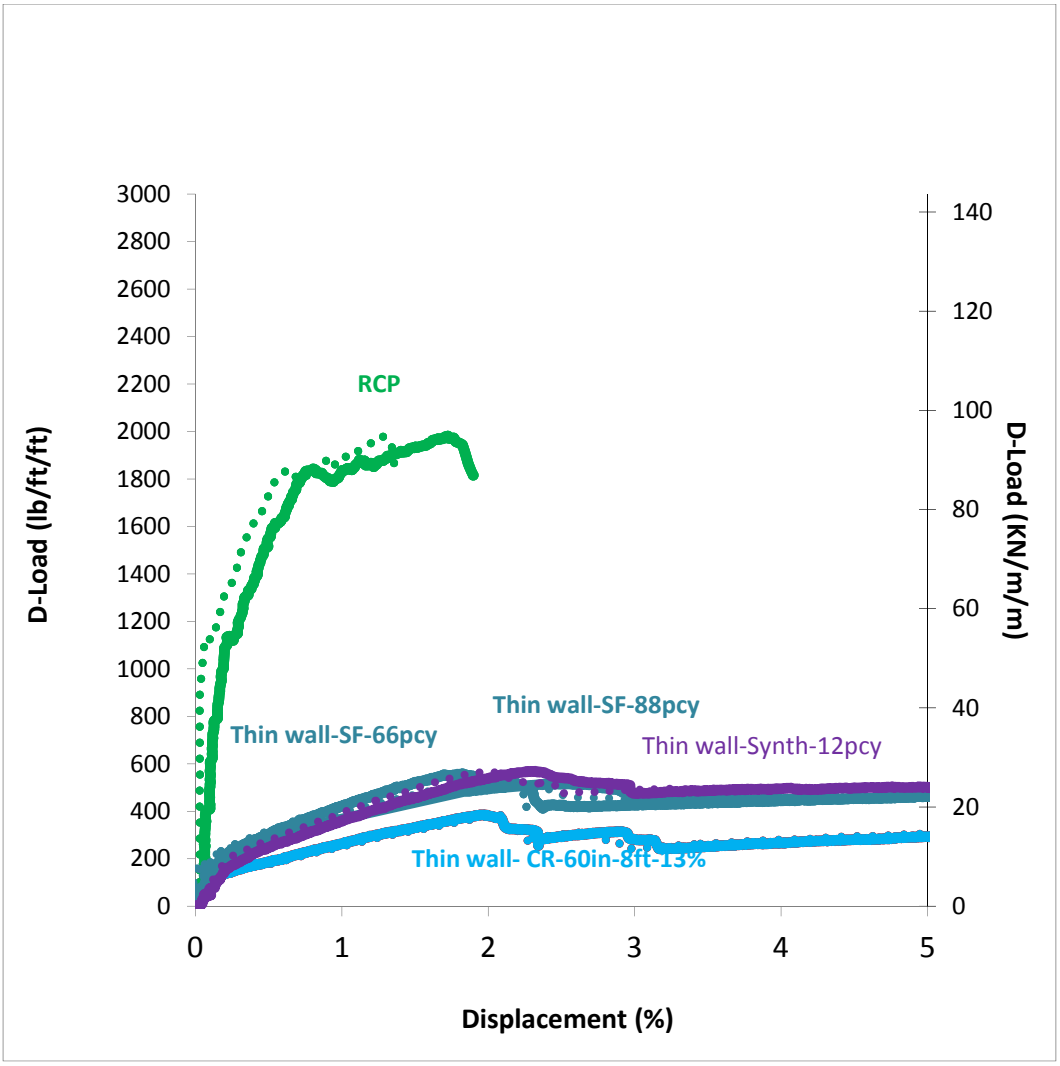

Figure 3-17 Load-Deflection Plot for Thin wall-60-8, Thin wall-60-8-13%rubber, Thin wall-12lbs synth, Thin wall-66lbs steel fiber and RCP.

The 60in RCP with a single layer of reinforcement versus thin-walled concrete pipes: Thin wall-60-8, Thin wall-60-8-13%rubber, Thin wall-12lbs synth, Thin wall-66lbs steel fiber with a double layer of reinforcement are plotted in Figure 3-17 Load-Deflection Plot for Thin wall-60-8, Thin wall-60-8-13%rubber, Thin wall-12lbs synth, Thin wall-66lbs steel fiber and RCP.

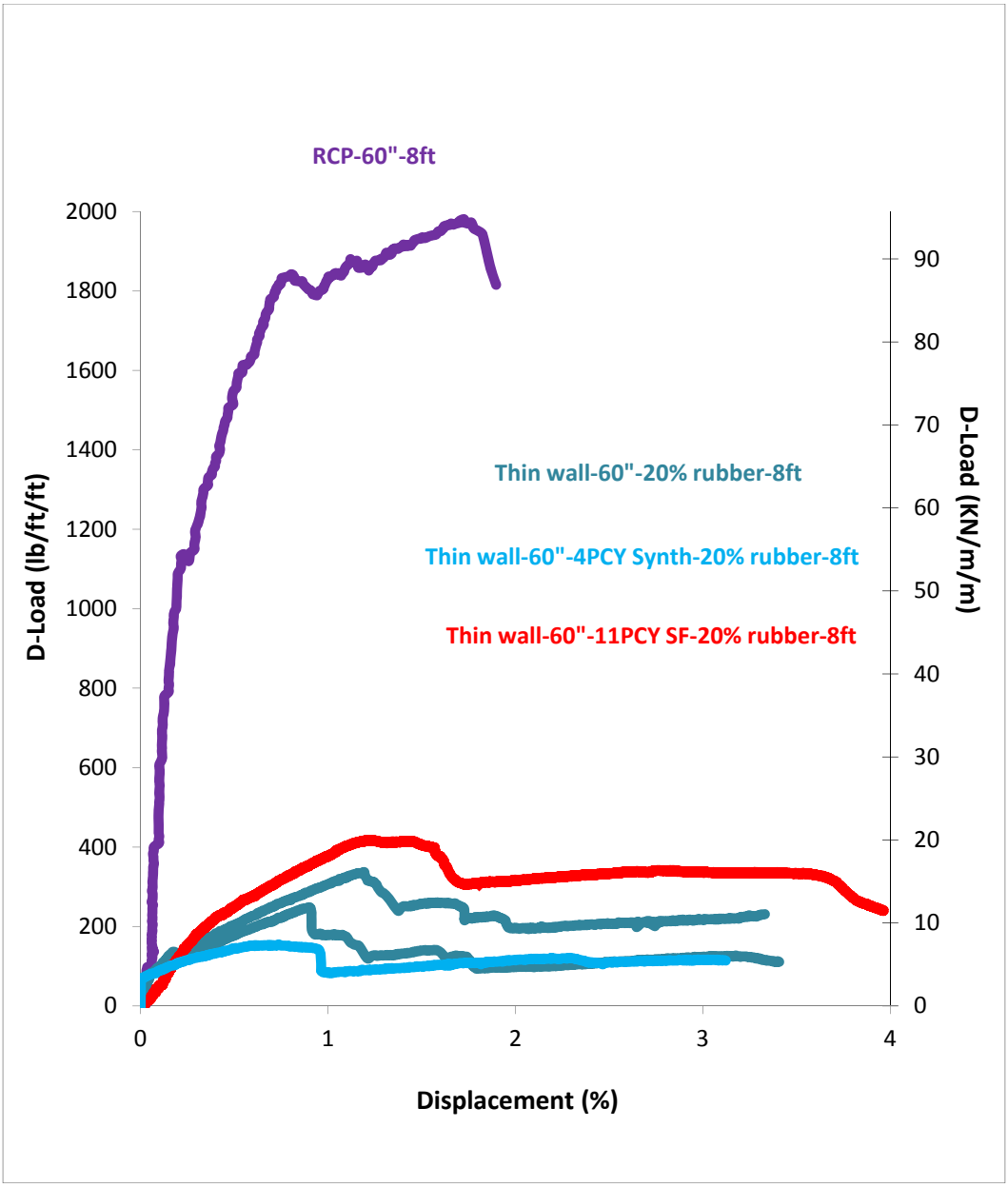

Figure 3-18 Load-Deflection Plot for Thin wall-60in-20%rubber, Thin wall-60in-4pcy synth-20%rubber, Thin wall-60in-11pcy synth-20%rubber, and RCP.

This graph shows that the Thin wall-60in-11pcy synth-20%rubber has more ductility and strength compared to the other thin wall pipe graphs.

Figure 3-19 Photograph of crack failure mode in 24 and 36 in. pipes

The most frequent failure mode for the concrete pipes for the 24 and 36 in. was a shear crack which occurred vertically in crown and invert of the pipe,occurring in the spring line. However, for the larger diameter pipes such as 54 and 60 in. pipes, it is essential to note that the failure mode crack was circumferential and subsequently; the failure mode changed from a shear to a flexural failure as the diameter of the pipe increased.

Figure 3-20 Photograph of crack failure mode in 54 and 60 in. pipes

After the initial crack of the steel fiber specimens, the slope of the load-deformation decreased gradually, but, after the initial crack of the RCP and CRRCP, the strength was increased, after reaching an ultimate strength, the slope progressively decreased.

For 24in pipe with 10pcy steel fiber and 8% crumb rubber the steel fibers were yielded and were not pulled out of the concrete and after the initial crack the decline of stiffness was significantly less than the conventional concrete pipes.

The incorporation of 5pcy steel fiber and 3% Macrosynthetic synthetic fibers became efficient for 24in. pipes. It has been observed that the addition of 44pcy of steel fiber and 10% of crumb rubber in the mixture of the concrete increased the initial crack strength of the 24 in. pipe. The results show that for the thin-walled concrete pipes, the addition of 11pcy of steel fiber and the replacement of 20% of sand with crumb rubber was efficient, resulting in more ductility.

Chapter 4

Material Tests

Introduction

There are two methods of measuring the compressive strength of concrete specimens: cube test and cylindrical test. In this study, Compressive cylinder test was used to measure the compressive strength of the samples. A total of 233 cylindrical specimens, 4in. (101.6mm) in diameter and 8in. (203mm) in height, were casted onto a vibrating table at Hanson facility in accordance with the requirements of ASTM C31, “Standard Practice for Making and Curing Concrete Test Specimens in the Field”. All the specimens were tested at the Civil Engineering Lab Building (CELB).

Also, a total of 57 beam specimens, 20in. (508mm) in length, 6in. (152mm) in width and height were produced and tested at CELB at the University of Texas at Arlington in accordance with the requirements of ASTM C1609, “Standard Test Method for Flexural Performance of Fiber-Reinforced Concrete (Using Beam With Third-Point Loading”. All the specimen matrix are shown in Table 4-1 Test Specimen Matrix

Table 4-1 Test Specimen Matrix

Production Date	Mix Designation	Steel Fiber (pcy)	Rubber (%)	Synthetic Fiber (pcy)
1) 05-30-12	HY-24-6-B-22-02-0.05	22	5	2
2) 06-26-12	HY-24-6-B-44-05-0.03	44	3	5
3) 07-03-12	HY-36-6-B-44-05-0.03	44	3	5
4) 07-17-12	HY-24-6-B-44-0.08	44	8	N/A
5) 07-26-12	HY-24-6-B-44-0.08	44	8	N/A
	CR-24-6-B-0.08	N/A	8	N/A
6) 08-02-12	HY-24-6-B-44-0.06	44	6	N/A

Table 4-1—Continued

Production Date	Mix Designation	Steel Fiber (pcy)	Rubber (%)	Synthetic Fiber (pcy)
7) 08-07-12	HY-24-6-B-44-10%	44	10	N/A
	CR-24-6-B-10%	N/A	10	N/A
8) 08-16-12	HY-24-6-B-10-8%	10	8	N/A
	SFRC-24-6-B-10	10	N/A	N/A
9) 08-30-12	HY-36-6-B-22-8%	22	8	N/A
	CR-36-6-B-8%	N/A	8	N/A
10) 09-04-12	HY-36-6-B-22-10%	22	10	N/A
	CR-36-6-B-10%	N/A	10	N/A
11) 09-12-12	HY-36-6-B-44-12%	44	12	N/A
	CR-36-6-B-12%	N/A	12	N/A
12) 10-01-12	HY-24-6-B-44-10%	44	10	N/A
	CR-24-6-B-10%	N/A	10	N/A
13) 10-04-12	HY-36-6-B-44-10%	44	10	N/A
	CR-36-6-B-10%	N/A	10	N/A
14) 10-11-12	HY-24-6-B-44-15%	44	15	N/A
	CR-24-6-B-15%	N/A	15	N/A
15) 10-24-12	HY-24-6-B-44-20% CR	44	20	N/A
	CR-24-6-B-20% CR	N/A	20	N/A
16) 11-19-12	CR-36-6-B-10%	N/A	10	N/A
	Control-36-6-B	N/A	N/A	N/A
17) 01-29-13	HY-24-6-B-44-10%	44	10	N/A
	CR-24-6-B-10%	N/A	10	N/A
	Synth-24-6-B-10%-8%	N/A	10	8
	Control-24-6-B	N/A		N/A
18) 01-30-13	HY-24-6-B-44-20%	44	20	N/A
	CR-24-6-B-20%	N/A	20	N/A
	Synth-24-6-B-20%-8%	N/A	20	8
	Control-24-6-B	N/A	N/A	N/A
19) 03-07-13	Thin wall- CR-60-6-B-13%	N/A	13	N/A
20) 4/24/2013	Thin wall-60in-20% rubber-8ft	N/A	20	N/A
21) 04-25-13	Thin wall-60in-11PCY SF-20% rubber-8ft	11	20	N/A
22) 04-25-13	Thin wall-60in-4PCY Synth-20% rubber-8ft	N/A	20	4

Flexural Beam Test

Test Set Up and Procedure

The Flexural Beam Test evaluates the flexural performance of fiber reinforced concrete based on the parameters form the load-deflection curve. The specimens were tested by using the Material testing system (MTS) machine in accordance with ASTM C1609, “Standard Test Method for Flexural Performance of Fiber-Reinforced Concrete using Beam With Third-Point Loading”. The initial-crack strength, ultimate strength were determined by this test. Two Linear Variable Displacement Transducers (LVDTs) were installed on the sides and in the middle of the beam specimen to measure the deflection of the beam under the constant-displacement load rate. Strain Smart Software on Windows-based computer acquired data from Vishay scanner. The two LVDTs, displacement and load channel were connected to the high-voltage Vishay scanner. All the load-deflection graphs are based on the average value from two LVDTs up to a deflection of 1/150 of the span. The MTS machine and experimental set up for Flexural beam test are shown in Figure 4-1Typical ASTM C1609 Test Fixtures and Figure 0-2 Experimental set up for Flexural beam test subsequently. All the test results are shown in appendix B.

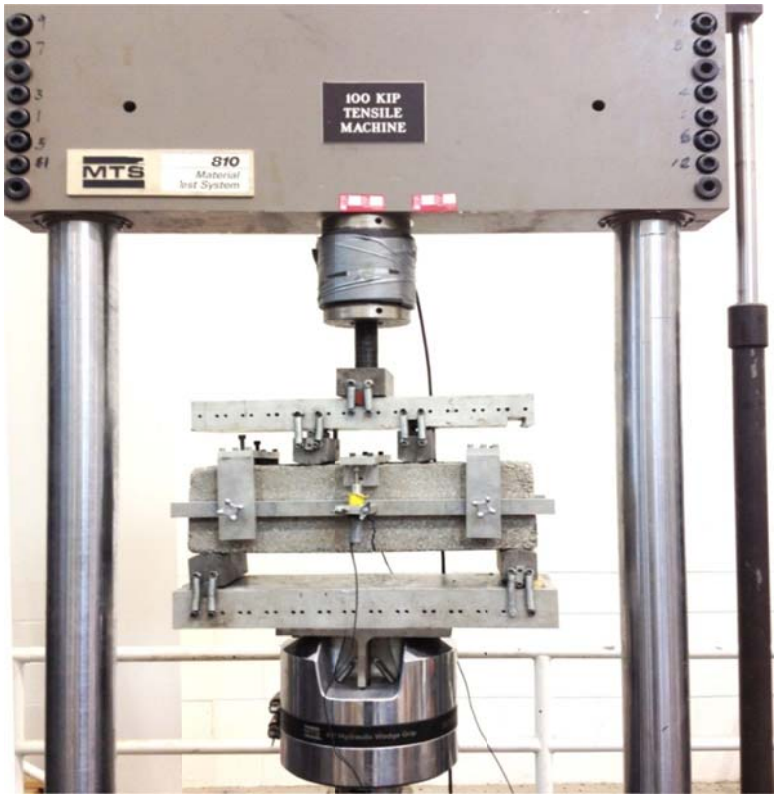

Figure 4-1Typical ASTM C1609 Test Fixtures

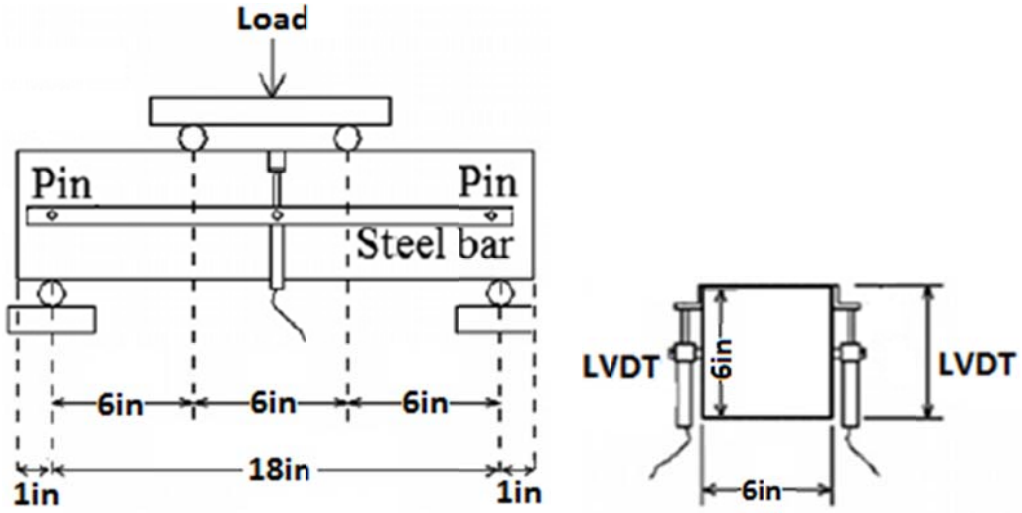

Figure 4-2 Experimental set up for **F**lexural beam test

Test Results

The following formula was used for the modulus of rupture of the specimens.

$$f = \frac{P \times L}{b \times d^2} \qquad (11)$$

Where:

f= the strength, psi (MPa),

P= the load, lbf (N),

L= the span length, in. (mm),

b= the average width of the specimen, in. (mm),

d= the average depth of the specimen, in. (mm).

The area under the load-deflection curve up to a deflection of 1/150 of the span (1.2in.) is shown in Figure 4-3 Flexural Test Toughness for beam specimens.

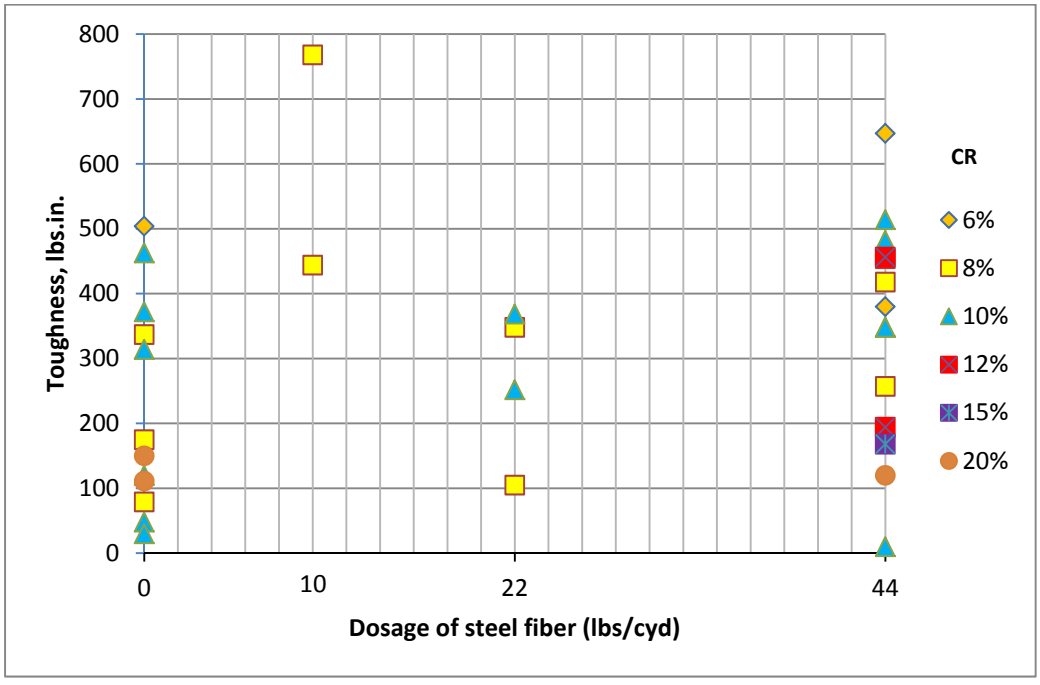

Figure 4-3 Flexural Test Toughness for beam specimens

From the Flexural Test Toughness for beam specimens, it can be found that the specimens with 44lbs steel fiber (lbs/cy^3) and 6% crumb rubber showed better toughness.

The most frequent failure type for Flexural Beam Test was a vertical crack in the center of the specimens as shown in Figure 4-4 The photograph of most frequent failure type for Flexural Beam Specimens.

Figure 4-4 The photograph of most frequent failure type for Flexural Beam Specimens

All of the flexural beam test results are attached in Appendix C.

Compressive Cylinder Tests

Test Set Up and Procedure

After casting the cylindrical specimens, the specimens were immediately moved to the curing chamber to be steam cured for one day. Finally, after a day of curing, the samples were transported and demolded at the Civil Engineering Lab Building (CELB) at the University of Texas at Arlington. The bottom and top of all the cylindrical concrete specimens were capped prior to the test for compressive strength to provide a smoother, parallel, and uniform bearing ends. The Flake capping sulfur compound was used as a capping compound material. All the specimens were tested after about 1, 3, 7 and 28 days of curing according to the . The load cell applied a vertical load with a load rate of 420lbs/sec. according to the ASTM C39, "Standard Test Method for Compressive

Strength of Cylindrical Concrete Specimens," onto the specimens. The compressive strengths of the specimens were calculated by dividing the ultimate load by the cross sectional area of the cylinder and all the results are shown in Appendix A.

Figure 4-5 Photograph of Compressive Cylinder Testing Machine at CELB

Test Results

The replacement of coarse aggregate by crumb rubber reduced the compression strength of the specimens which ranges up to 30% depending on the fiber dosage and crumb rubber content.

Plain concrete cylinders showed a brittle failure mode which was sudden and explosive, however, the specimens with fibers or, crumb rubber were more ductile,

causing the failure to occur gradually. Most of the failures were inclined at an angle of approximately 45degrees in the direction of applied compression load as shown in Figure 4-6 Failure types of cylindrical specimens.

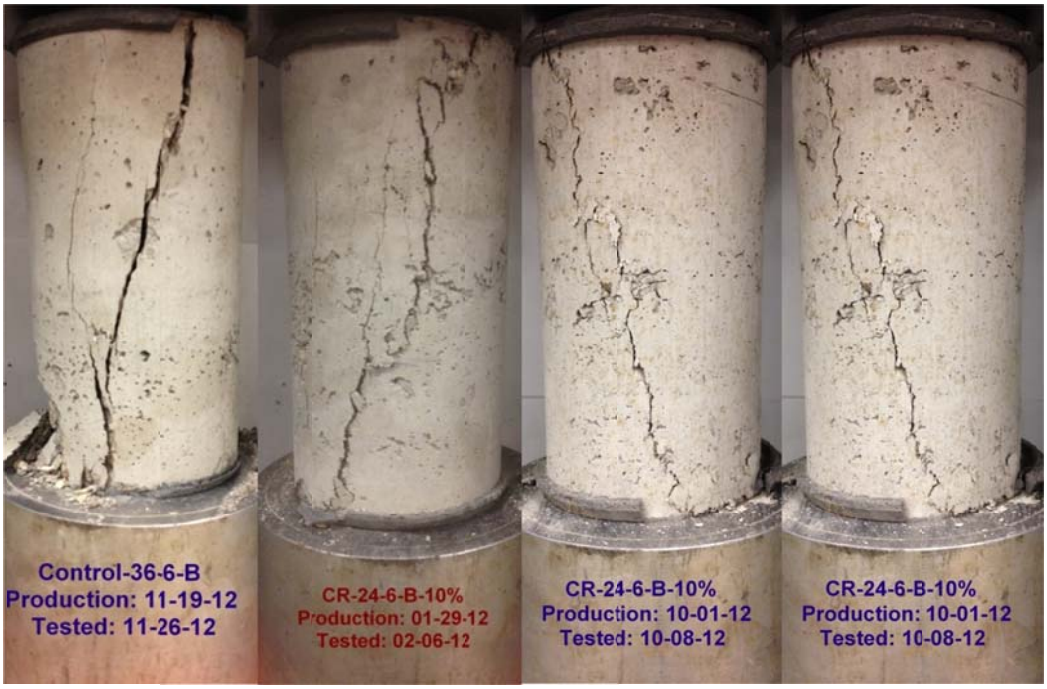

Figure 4-6 Failure types of cylindrical specimens

Chapter 5

Summary, Conclusions And Recommendations

Summary

There has been no previous research study on the dry cast crumb rubber concrete pipe before and this research has been conducted for the first time in the United States. This study investigates how the variation of the fiber volume fraction and crumb rubber content in concrete mix affects the behavior of pipes with diameters ranging from 24in. (610 mm) to 60in. (1524 mm). Also it has been investigated that the combination of steel fiber, crumb rubber, synthetic fiber, and conventional steel cage improved the ductility of regular concrete pipes and thin-walled semi-rigid concrete pipes. Different concrete mixtures were produced and tested: (1) Steel Bar Reinforced Concrete Pipe (SBRCP), (2) Crumb Rubber Reinforced Concrete Pipe (CRRCP), (3) Steel Fiber Reinforced Concrete Pipe (SFRCP), and (4) Synthetic Fiber Reinforced Concrete Pipe (SNFRCP).

In this research, the crumb rubber particles were replaced from 3% to 20% (by volume) of sand in the mixture of concrete pipes. Steel fibers (RC-65/35-BN, Bekaert) used in this study have a hooked end shape with a length of 1.38 in. (35 mm), a diameter of 0.022in (0.55 mm) and an aspect ratio of 65 with dosages of 10 (Volume fraction of 0.08%), 11 (V_f of 0.08%), 22 (V_f of 0.17%), 44 (V_f of 0.33%), 66 (V_f, of 0.5%) and 88 lb/yd^3 (V_f of 0.67%). Macrosynthetic fibers were from BASF MasterFiber™ MAC Matrix with dosages of 2, 4, 5, and 8 lb/yd3.

A total of 86 pipes were produced and tested in accordance with ASTM C 497 three-edged bearing at Hanson Precast Plant in Grand Prairie, TX. In addition, a total of 57 beam specimens, 20in. (508mm) in length, 6in. (152mm) in width and height were produced and tested at 7days. Also, a total of 233 cylindrical specimens, 4in. (101.6mm)

in diameter and 8in. (203mm) in height, were tested in 1, 3, 7 and 28 days at the Civil Engineering Lab Building (CELB) at the University of Texas at Arlington. All the results are shown in Appendix A, B and C.

Conclusions

This study shows that for the thin-walled concrete pipes, the incorporation of 11pcy of steel fiber and the replacement of 20% of sand with crumb rubber was efficient, resulting in more ductility. Also, for 24in pipe with 10pcy steel fiber and 8% crumb rubber, the steel fibers were yielded and were not pulled out of the concrete and after the initial crack, the decline of stiffness was significantly less than the conventional concrete pipes.

It has also been found that the addition of 5pcy steel fiber and 3% macrosynthetic fibers became efficient for 24in and the stiffness decreased very slowly which showed more ductility. It has been observed that the addition of 44pcy of steel fiber and 10% of crumb rubber in the mixture of the concrete increased the initial crack strength of the 24 in. pipe by 25%.

The results of this study showed that the replacement of the crumb rubber with sand in the concrete pipe causes the compressive strength of concrete to decrease depending on the content of the crumb rubber, however on the other hand, the ductility of the concrete increased.

The comparison of crack pattern between thin-walled, CR pipe and SF pipe indicated that the cracks in CR pipes are less severe and therefore more ductile. Also, comparison of crack pattern between CR, TW and Synthetic fiber pipe showed similarities between the behavior. The behavior of thin-walled with rubber is similar to the behavior of the thin-wall with steel or synthetic fiber. In addition, the comparison between thin-wall and RCP showed that thin-wall with any type of fiber or CR requires soil support and needs to be designed as semi-rigid.

The most frequent failure mode for the concrete pipes for the 24 and 36 in. was a shear crack which occurred vertically in crown and invert of the pipe, occurring in the spring line. However, for the larger diameter pipes such as 54 and 60 in. pipes, it was observed that the failure mode crack was circumferential and subsequently; the failure mode changed from a shear to a flexural failure.

The results of this research showed that for the TW pipes, the CR is as effective as steel and synthetic fiber with regard to ductile behavior. Also, the concrete pipes without cage, need to be designed as a semi-rigid pipe to include the effects of soil support.

Recommendations for Future Work

It was observed, in some cases, the steel fibers were not yielded and were pulled out of the concrete during the flexural beam and three-edged bearing test as shown in Figure 5-1 Photograph of opening of the crack and the pull-out of the steel fibers due to the lack of anchorage between the hooked end steel fibers and the concrete.

It is recommended that by changing the geometry of the hooked end steel fibers to a rectangular shape will provide more anchorage between the steel fibers and the concrete. Two sides of the rectangular shape will act as a tension and the other two sides will provide anchorage. There is a need for future studies to investigate the bond between the fiber and matrix of the dry cast concrete pipes.

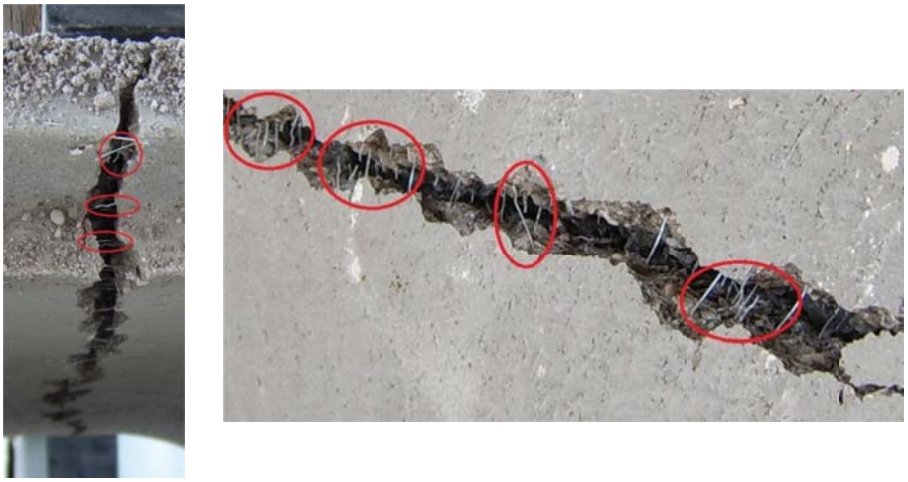

Figure 5-1 Photograph of opening of the crack and the pull-out of the steel fibers

Appendix A

Test results

Table A-1 Concrete pipe specimens production and tested

Test No	Production Date	Mix class	Length(ft)	Pipe Diameter(in)	Wall thickness type	Steel Fiber (pcy)	Rubber (%)	Synthetic Fiber (pcy)	Cage	First crack load(lbs)	First crack load(lbs/ft/ft)	Ultimate load(lbs)	Ultimate load(lbs/ft/ft)	Test Date
1	5/30/2012	III	6	24	B	22	5	2	N/A	18529	1544	18529	1544	6/7/2012
										17063	1422	17063	1422	
2	6/26/2012	III	6	24	B	44	3	5	N/A	23421	1951	23421	1951	7/3/2012
3	7/3/2012	III	6	36	B	44	3	5	N/A	23492	1305	23492	1305	7/10/2012
										23894	1327	23894	1327	
4	7/17/2012	IV	6	24	B	44	8	N/A	N/A	12455	1038	12455	1038	7/24/2012
5	7/26/2012	V	6	24	B	44	8	N/A	N/A	13282	1107	13282	1107	8/2/2012
						N/A	8	N/A	×	11415	951	12880	1073	
						N/A	8	N/A	×	10919	910	13282	1107	
6	8/2/2012	IV	6	24	B	44	6	N/A	N/A	13589	1132	13589	1132	8/10/2012
										14700	1225	14700	1225	8/15/2012
						N/A	6	N/A	×	10375	865	20254	1688	8/10/2012
										11202	933	19356	1613	
						N/A	N/A	N/A	×	15811	1318	26683	2224	8/15/2012
										16000	1333	26092	2174	
7	8/7/2012	IV	6	24	B	44	10	N/A	N/A	11510	959	11510	959	8/21/2012
						44	10	N/A	N/A	11439	922	11439	922	
						N/A	10	N/A	×	7917	660	12526	1044	
						N/A	10	N/A	×	7090	591	12479	1040	
						N/A	N/A	N/A	×	8792	733	13471	1123	
						N/A	N/A	N/A	×	11013	918	12928	1077	

Table A-1 —*Continued*

Test No	Production Date	Mix class	Length(ft)	Pipe Diameter(in)	Wall thickness type	Steel Fiber (pcy)	Rubber (%)	Synthetic Fiber (pcy)	Cage	First crack load(lbs)	First crack load(lbs/ft/ft)	Ultimate load(lbs)	Ultimate load(lbs/ft/ft)	Test Date
8	8/16/2012	IV	6	24	B	10	8	N/A	×	14064	1172	25440	2120	2/25/2013
						10	N/A	N/A	N/A	15669	1306	15669	1306	
						10	N/A	N/A	N/A	15575	1298	15575	1298	
						N/A	N/A	N/A	×	15648	1304	24816	2068	
						N/A	N/A	N/A	×	15408	1284	23520	1960	
9	8/30/2012	IV	6	36	B	22	8	N/A	N/A	18363	1020	18363	1020	9/13/2012
						22	8	N/A	N/A	15102	839	15102	839	
						N/A	8	N/A	×	9903	550	9903	550	
						N/A	8	N/A	×	14417	801	14417	801	
						N/A	N/A	N/A	×	13495	750	21672	1204	
						N/A	N/A	N/A	×	12833	713	18363	1020	
10	9/4/2012	IV	6	36	B	22	10	N/A	N/A	16591	922	16591	922	9/18/2012
						22	10	N/A	N/A	22523	1251	22523	1251	
						N/A	10	N/A	×	18647	1036	24012	1334	
						N/A	10	N/A	×	18647	1036	25926	1440	
						N/A	N/A	N/A	×	24957	1386	27226	1513	
						N/A	N/A	N/A	×	13117	729	30535	1696	
11	9/12/2012	IV	6	36	B	44	12	N/A	_	15764	876	15764	876	9/25/2012
						N/A	12	N/A	×	15173	842.9	15173	842.9	
						N/A	12	N/A	×	14889	827	19049	1058	
						N/A	N/A	N/A	×	22901	1272	38523	2140	
						N/A	N/A	N/A	×	22050	1225	43486	2416	

Table A-1 —*Continued*

Test No	Production Date	Mix class	Length(ft)	Pipe Diameter(in)	Wall thickness type	Steel Fiber (pcy)	Rubber (%)	Synthetic Fiber (pcy)	Cage	First crack load(lbs)	First crack load(lbs/ft/ft)	Ultimate load(lbs)	Ultimate load(lbs/ft/ft)	Test Date
12	10/1/2012	IV	6	24	B	44	10	N/A	×	14322	1193	14322	1193	10/31/2012
						N/A	10	N/A	×	16709	1392	24957	2080	11/7/2012
						N/A	10	N/A	×	15480	1290	24367	2030	
						N/A	10	N/A	×	8792	1335	13471	2064	
						N/A	N/A	N/A	×	18316	1526	26186	2182	
13	10/4/2012	IV	6	36	B	44	10	N/A	N/A	17962	998	17962	998	12/13/2012
						N/A	10	N/A	×	22641	1258	29306	1628	
						N/A	N/A	N/A	×	23492	1305	36727	2040	
14	10/11/2012	IV	6	24	B	44	15	N/A	N/A	13377	1115	13377	1115	11/8/2012
						44	15	N/A	N/A	15811	1318	15811	1318	
						N/A	15	N/A	×	10824	902	18789	1566	
						N/A	15	N/A	×	10635	886	21578	1798	
						N/A	N/A	N/A	×	16142	1345	24414	2035	
						N/A	N/A	N/A	×	14535	1211	21720	1810	
15	10/24/2012	IV	6	24	B	44	20	N/A	N/A	10233	853	10233	853	12/13/2012
						N/A	20	N/A	×	4272	356	11510	959	2/7/2013
						N/A	20	N/A	×	11959	997	11959	997	2/7/2013
						N/A	N/A	N/A	×	17394	1450	24485	2040	12/13/2012
						N/A	N/A	N/A	×	11533	961	20040	1670	2/7/2013
16	11/19/2012 NCP	IV	6	36	B	N/A	10	N/A	×	22239	1854	34104	1895	12/13/2012
						N/A	N/A	N/A	×	21105	1172	32780	1821	
						N/A	N/A	N/A	×	19191	1066	34080	1893	

Table A-1 —*Continued*

Test No	Production Date	Mix class	Length(ft)	Pipe Diameter(in)	Wall thickness type	Steel Fiber (pcy)	Rubber (%)	Synthetic Fiber (pcy)	Cage	First crack load(lbs)	First crack load(lbs/ft/ft)	Ultimate load(lbs)	Ultimate load(lbs/ft/ft)	Test Date
17	1/29/2013 NCP	IV	6	36	B	44	10	N/A	N/A	18789	1566	18789	1566	2/8/2013
						44	10	N/A	N/A	16615	1385	16615	1385	
						N/A	10	8	N/A	13046	1087	13046	1087	
						N/A	10	8	×	10464	872	10464	872	
						N/A	10	N/A	×	16776	1398	27984	2332	
						N/A	10	N/A	×	14964	1247	23772	1981	
						N/A	N/A	N/A	×	13560	1130	21624	1802	
						N/A	N/A	N/A	×	17916	1493	28908	2409	
18	1/30/2013 NCP	IV	6	24	B	N/A	20	N/A	×	10824	902	18792	1566	02/07/2013
						N/A	20	N/A	×	7704	642	16092	1341	
						N/A	N/A	N/A	×	2788	232	2788	232	
						N/A	N/A	N/A	×	11412	951	12528	1044	

Table A-1 —*Continued*

Test No	Production Date	Mix class	Length(ft)	Pipe Diameter(in)	Wall thickness type	Steel Fiber (pcy)	Rubber (%)	Synthetic Fiber (pcy)	Cage	First crack load(lbs)	First crack load(lbs/ft/ft)	Ultimate load(lbs)	Ultimate load(lbs/ft/ft)	Test Date
19	03/07/2013 NCP	III	8	60	Thin-walled	N/A	N/A	N/A	×	79200	1980	79200	1980	3/8/2013
						N/A	13	N/A	×	15409	385	15409	385	3/14/2013
						88	N/A	N/A	×	20600	515	20600	515	3/8/2013
						66	N/A	N/A	×	22308	558	22308	558	3/8/2013
						N/A	N/A	12	×	22747	569	22747	569	3/8/2013
20	04/24/2013 NCP	III	8	60	Thin-walled	N/A	20	N/A	×	13471	336.8	13471	337	2/5/2013
						N/A	20	N/A	×	9926	248	9926	248	
21	04/25/2013 NCP	III	8	60	Thin-walled	11	20	N/A	×	16709	417.7	16709	418	2/5/2013
22	04/25/2013 NCP	III	8	60	Thin-walled	N/A	20	4	×	6191	154.8	6191	155	2/5/2013

Table A-2 Cylinder Specimen Test Results

Production Date	Mix Designation	Steel Fiber (pcy)	Rubber (%)	Synthetic Fiber (pcy)	Days	Stress (psi)	Average Stress (psi)
1) 05-30-12	HY-24-6-B-22-02-0.05	22	5	2	1	2099	2618
						3137	
					3	2748	2929
						3111	
					7	4620	5026
						5432	
2) 06-26-12	HY-24-6-B-44-05-0.03	44	3	5	1	2843	2859
						2875	
					3	4124	4189
						4255	
					7	4873	4540
						4207	
3) 07-03-12	HY-36-6-B-44-05-0.03	44	3	5	3	2979	2915
						3352	
						2415	
4) 07-17-12	HY-24-6-B-44-0.08	44	8	N/A	1	1467	1590
						1713	
5) 07-26-12	HY-24-6-B-44-0.08	44	8	N/A	1	3145	3133
						3120	
					3	3126	3495
						3863	
					7	3636	3634
						3632	
	CR-24-6-B-0.08	N/A	8	N/A	1	1841	1841
					3	2718	1904
						1090	
					7	1280	2185
						3091	

Table A-2 —*Continued*

Production Date	Mix Designation	Steel Fiber (lbs)	Rubber (%)	Synthetic Fiber (lbs)	Days	Stress (psi)	Average Stress (psi)
6) 08-02-12	HY-24-6-B-44-0.06	44	6	N/A	1	3002	2985
						2968	
					3	3076	3127
						3178	
					7	2792	3616
						4440	
	CR-24-6-B-0.06	N/A	6	N/A	1	1917	2285
						2653	
					3	1578	1691
						1803	
					7	1474	2534
						3595	
7) 08-07-12	HY-24-6-B-44-10%	44	10	N/A	1	2477	2209
						1941	
					3	2628	2821
						3014	
					7	3373	3475
						3577	
	CR-24-6-B-10%	N/A	10	N/A	1	336	356
						376	
					3	2196	1816
						1436	
					7	1432	1432

Table A-2 —*Continued*

Production Date	Mix Designation	Steel Fiber (lbs)	Rubber (%)	Synthetic Fiber (lbs)	Days	Stress (psi)	Average Stress (psi)
8) 08-16-12	HY-24-6-B-10-8%	10	8	N/A	1	1786	2034
						2282	
					3	2589	3133
						3676	
					7	3096	3087
						3078	
	SFRC-24-6-B-10	10	N/A	N/A	1	2593	2601
						2609	
					3	2858	2574
						2289	
					7	2341	3393
						4445	
9) 08-30-12	HY-36-6-B-22-8%	22	8	N/A	1	1965	1934
						1903	
					3	2493	2107
						1721	
					7	1458	1383
						1309	
	CR-36-6-B-8%	N/A	8	N/A	1	670	758
						845	
					3	1453	1611
						1770	
					7	2089	1777
						1465	

Table A-2 —*Continued*

Production Date	Mix Designation	Steel Fiber (lbs)	Rubber (%)	Synthetic Fiber (lbs)	Days	Stress (psi)	Average Stress (psi)
10) 09-04-12	HY-36-6-B-22-10%	22	10	N/A	1	2588	2306
						2024	
					3	2414	2631
						2848	
					7	3538	3347
						3157	
	CR-36-6-B-10%	N/A	10	N/A	1	1621	1464
						1307	
					3	1869	1743
						1617	
					7	3067	2889
						2711	
11) 09-12-12	HY-36-6-B-44-12%	44	12	N/A	1	1939	1822
						1705	
					3	2800	2644
						2488	
					7	2919	3126
						3334	
	CR-36-6-B-12%	N/A	12	N/A	1	673	765
						857	
					3	1131	1425
						1720	
					7	1191	1738
						2285	

Table A-2 —*Continued*

Production Date	Mix Designation	Steel Fiber (lbs)	Rubber (%)	Synthetic Fiber (lbs)	Days	Stress (psi)	Average Stress (psi)
12) 10-01-12	HY-24-6-B-44-10%	44	10	N/A	3	2628	2804
						3050	
						2733	
					7	3614	3132
						2888	
						2895	
	CR-24-6-B-10%	N/A	10	N/A	3	3233	2714
						3718	
						1191	
					7	3805	3142
						1805	
						3816	
13) 10-04-12	HY-36-6-B-44-10%	44	10	N/A	1	1305	995
						685	
					3	756	1082
						1409	
					7	1445	1445
	CR-36-6-B-10%	N/A	10	N/A	1	213	213
					3	256	256
					7	214	214

Table A-2 —*Continued*

Production Date	Mix Designation	Steel Fiber (lbs)	Rubber (%)	Synthetic Fiber (lbs)	Days	Stress (psi)	Average Stress (psi)
14) 10-11-12	HY-24-6-B-44-15%	44	15	N/A	1	1122	1356
						1591	
					3	2291	1655
						1019	
					7	2282	2189
						2096	
	CR-24-6-B-15%	N/A	15	N/A	1	1240	1175
						1110	
					3	2005	1754
						1504	
					7	2710	2591
						2471	
15) 10-24-12	HY-24-6-B-44-20% CR	44	20	N/A	1	1288	1321
						1354	
					3	2035	1952
						1869	
					28	1959	2334
						2708	
	CR-24-6-B-20% CR	N/A	20	N/A	1	452	600
						749	
					3	1265	1291
						1317	
					28	1592	1481
						1371	

Table A-2 —*Continued*

Production Date	Mix Designation	Steel Fiber (lbs)	Rubber (%)	Synthetic Fiber (lbs)	Days	Stress (psi)	Average Stress (psi)
16) 11-19-12	CR-36-6-B-10%	N/A	10	N/A	3	1997	2663
						3088	
						2923	
					7	3505	3350
						3196	
	Control-36-6-B	N/A	N/A	N/A	3	4888	4922
						3913	
						5966	
					7	4120	4737
						5347	
						4743	

Table A-2 —*Continued*

Production Date	Mix Designation	Steel Fiber (lbs)	Rubber (%)	Synthetic Fiber (lbs)	Days	Stress (psi)	Average Stress (psi)
17) 01-29-13	HY-24-6-B-44-10%	44	10	N/A	1	2563	1906
						1249	
					3	4327	3642
						2957	
					7	1794	3271
						4747	
					45	3239	3540
						3840	
	CR-24-6-B-10%	N/A	10	N/A	1	2002	1826
						1650	
					3	3244	2992
						2741	
					7	3214	3465
						3715	
					45	4459	4511
						4562	
	Synth-24-6-B-10%-8%	N/A	10	8	1	1940	2264
						2588	
					3	1902	2319
						2736	
					7	2803	3391
						3980	
					45	3290	2987
						2683	
	Control-24-6-B	N/A	N/A	N/A	1	2617	2603
						2588	
					3	2998	3204
						3410	
					7	3824	3129
						2435	
					45	4000	3711
						3422	

Table A-2 —*Continued*

Production Date	Mix Designation	Steel Fiber (lbs)	Rubber (%)	Synthetic Fiber (lbs)	Days	Stress (psi)	Average Stress (psi)
18) 01-30-13	HY-24-6-B-44-20%	44	20	N/A	1	1174	1214
						1255	
					3	1742	1889
						2036	
					7	2442	2442
					44	2529	2370
						2211	
	CR-24-6-B-20%	N/A	20	N/A	1	755	927
						1098	
					3	1663	1748
						1832	
					7	2881	2881
					44	2803	2667
						2530	
	Synth-24-6-B-20%-8%	N/A	20	8	1	813	1109
						1404	
					3	1296	1194
						1093	
					7	1439	1439
					45	1006	613
						219	
	Control-24-6-B	N/A	N/A	N/A	1	1713	2104
						2496	
					3	3998	4942
						5886	
					7	3218	3081
						2944	
					44	5118	5928
						6737	

Table A-2 —*Continued*

Production Date	Mix Designation	Steel Fiber (lbs)	Rubber (%)	Synthetic Fiber (lbs)	Days	Stress (psi)	Average Stress (psi)
19) 03-07-13	Thin wall- CR-60-6-B-13%	N/A	13	N/A	7	1192	1062
						735	
						1260	
20) 4/24/2013	Thin wall-60in-20% rubber-8ft	N/A	20	N/A	1	607	516
						426	
					7	1490	1203
						1256	
						908	
						1159	
21) 04-25-13	Thin wall-60in-11PCY SF-20% rubber-8ft	11	20	N/A	1	939	931
						923	
					7	1225	1343
						1449	
						1514	
						1185	
22) 04-25-13	Thin wall-60in-4PCY Synth-20% rubber-8ft	N/A	20	4	1	812	674
						536	
					8	1132	1232
						1216	
						1361	
						1222	

Table A-3 Beam Specimen Test Results

Production Date	Mix Designation	Steel Fiber (lbs)	Rubber (%)	Synthetic Fiber (lbs)	Test Date	Peak Load (lbs)	Strength (psi)
1) 05-30-12	HY-24-6-B-22-02-0.05	22	5	2	2/12/2013	9892	824.3
2) 06-26-12	HY-24-6-B-44-05-0.03	44	3	5	2/13/2013	9318	776.5
					2/13/2013	10688	890.7
3) 07-03-12	HY-36-6-B-44-05-0.03	44	3	5	2/13/2013	7578	631.5
					2/12/2013	5097	424.8
4) 07-17-12	HY-24-6-B-44-0.08	44	8	N/A	12/21/2012	5625	468.8
					12/21/2012	8421	701.8
5) 07-26-12	HY-24-6-B-44-0.08	44	8	N/A	12/20/2012	8296	691.3
	CR-24-6-B-0.08	N/A	8	N/A	12/21/2012	5012	417.7
6) 08-02-12	HY-24-6-B-44-0.06	44	6	N/A	12/20/2012	9895	824.6
					12/21/2012	6638	553.2
	CR-24-6-B-0.06	N/A	6	N/A	12/20/2012	6983	581.9
7) 08-07-12	HY-24-6-B-44-10%	44	10	N/A	12/21/2012	7533	627.8
					12/21/2012	5198	433.2
	CR-24-6-B-10%	N/A	10	N/A	12/22/2012	1618	134.8
8) 08-16-12	HY-24-6-B-10-8%	10	8	N/A	12/20/2012	7789	649.1
					12/20/2012	9236	769.7
	CR-24-6-B-8%	N/A	8	N/A	12/21/2012	7197	599.8
9) 08-30-12	HY-36-6-B-22-8%	22	8	N/A	12/20/2012	2078	173.2
					12/20/2012	6727	560.6
	CR-36-6-B-8%	N/A	8	N/A	12/19/2012	3724	310.3

Table A-3 —*Continued*

Production Date	Mix Designation	Steel Fiber (lbs)	Rubber (%)	Synthetic Fiber (lbs)	Test Date	Peak Load (lbs)	Strength (psi)
10) 09-04-12	HY-36-6-B-22-10%	22	10	N/A	12/20/2012	4130	344.2
					12/21/2012	5674	472.8
	CR-36-6-B-10%	N/A	10	N/A	12/21/2012	6275	522.9
					12/21/2012	4355	362.9
11) 09-12-12	HY-36-6-B-44-12%	44	12	N/A	12/19/2012	3455	287.9
					12/19/2012	6315	526.3
12) 10-01-12	HY-24-6-B-44-10%	44	10	N/A	12/19/2012	6324	527.0
					12/19/2012	6739	561.6
	CR-24-6-B-10%	N/A	10	N/A	12/19/2012	7804	650.3
					12/19/2012	6287	523.9
13) 10-04-12	HY-36-6-B-44-10%	44	10	N/A	11/28/2012	1551	129.3
	CR-36-6-B-10%	N/A	10	N/A	12/19/2012	1728	144.0
14) 10-11-12	HY-24-6-B-44-15%	44	15	N/A	11/28/2012	3113	259.4
15) 10-24-12	HY-24-6-B-44-20% CR	44	20	N/A	11/28/2012	1258	104.8
	CR-24-6-B-20% CR	N/A	20	N/A	11/28/2012	4224	352.0
					11/28/2012	4609	384.1
17) 01-29-13	HY-24-6-B-44-10%	44	10	N/A	12/2/2013	3458	288.2
				N/A	2/13/2013	4594	382.8
	CR-24-6-B-10%	N/A	10	N/A	2/12/2013	5665	472.1
					2/13/2013	5744	478.7
	Synth-24-6-B-10%-8%	N/A	10	8	2/13/2013	2970	247.5
	Control-24-6-B	N/A	N/A	N/A	2/13/2013	3629	302.4
		N/A	N/A	N/A	2/12/2013	4212	351.0
18) 01-30-13	HY-24-6-B-44-20%	44	20	N/A	2/13/2013	4300	358.3
					2/13/2013	4972	414.3
	CR-24-6-B-20%	N/A	20	N/A	2/12/2013	4542	378.5
					2/12/2013	5024	418.7
	Synth-24-6-B-20%-8%	N/A	20	8	2/13/2013	3904	325.3
					2/13/2013	4456	371.3
	Control-24-6-B	N/A	N/A	N/A	2/12/2013	4542	378.5

Table A-3 —*Continued*

Production Date	Mix Designation	Steel Fiber (lbs)	Rubber (%)	Synthetic Fiber (lbs)	Test Date	Peak Load (lbs)	Strength (psi)
20) 4/24/2013	Thin wall-60in-20% rubber-8ft	N/A	20	N/A	5/3/2013	3525	293.8
						4718	393.2
21) 04-25-13	Thin wall-60in-11PCY SF-20% rubber-8ft	11	20	N/A	5/3/2013	5182	431.8
						5378	448.2
22) 04-25-13	Thin wall-60in-4PCY Synth-20% rubber-8ft	N/A	20	4	5/3/2013	5094	424.5
						5811	484.3

Appendix B

PIPE GRAPHS

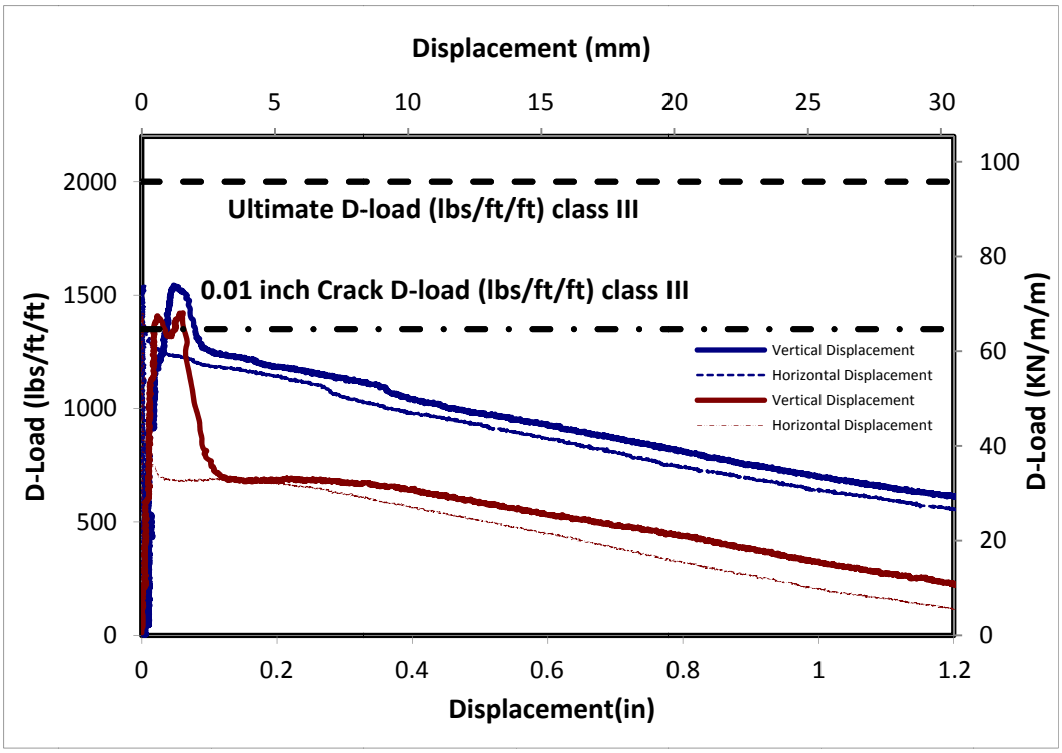

Figure B-1 Load-Deflection Plot for HYCP-24-6-B-22lbs steel-5% rubber-2%synth

Figure B-2 Crack propagation for HYCP-24-6-B-22lbs steel-5% rubber-2%synth

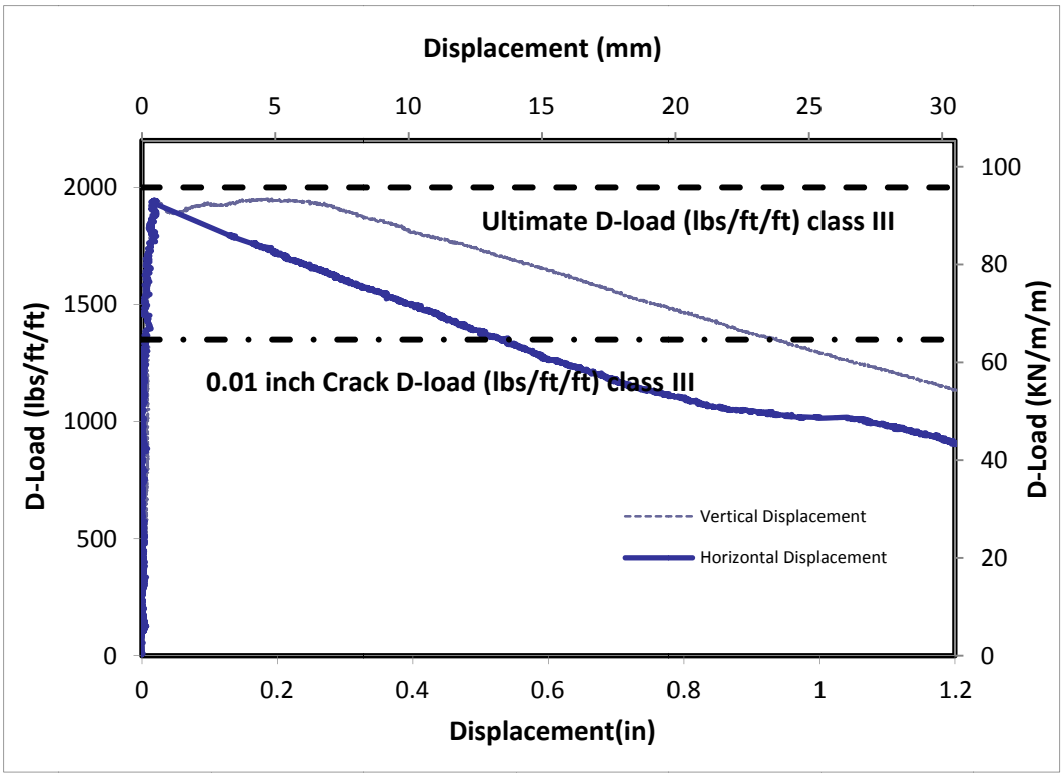

Figure B-3 Load-Deflection Plot for HYCP-24-6-B-44lbs steel-3% rubber-5lbs synth

Figure B-4 Crack propagation for HYCP-24-6-B-44lbs steel-3% rubber-5lbs synth

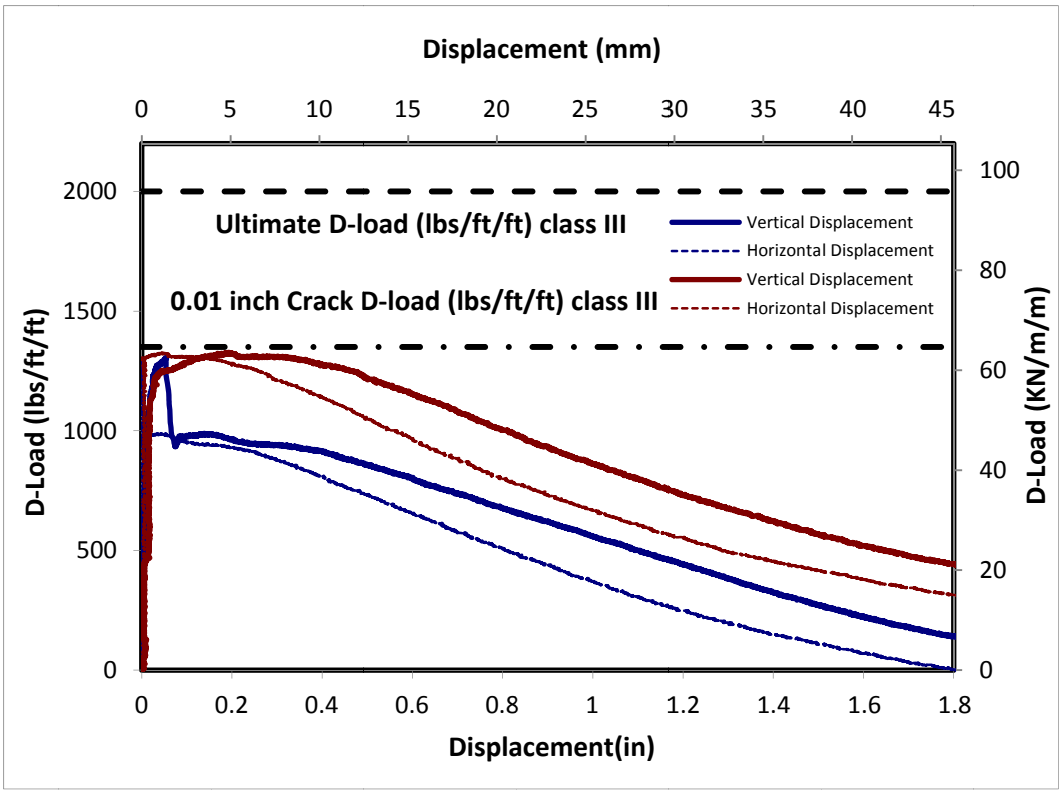

Figure B-5 Load-Deflection Plot for HYCP-36-6-B-44lbs steel-3% rubber-5lbs synth

Figure B-6 Crack propagation for HYCP-36-6-B-44lbs steel-3% rubber-5lbs synth

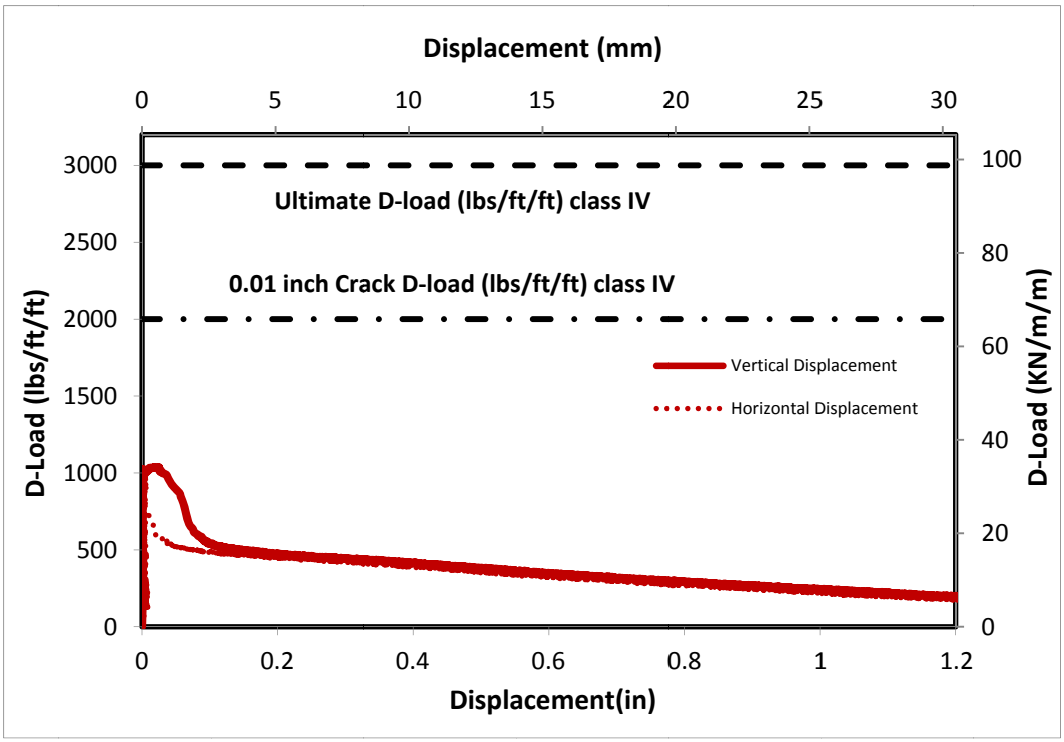

Figure B-7 Load-Deflection Plot for HYCP-24-6-B-44lbs steel-8% rubber

Figure B-8 Crack propagation for HYCP-24-6-B-44lbs steel-8% rubber

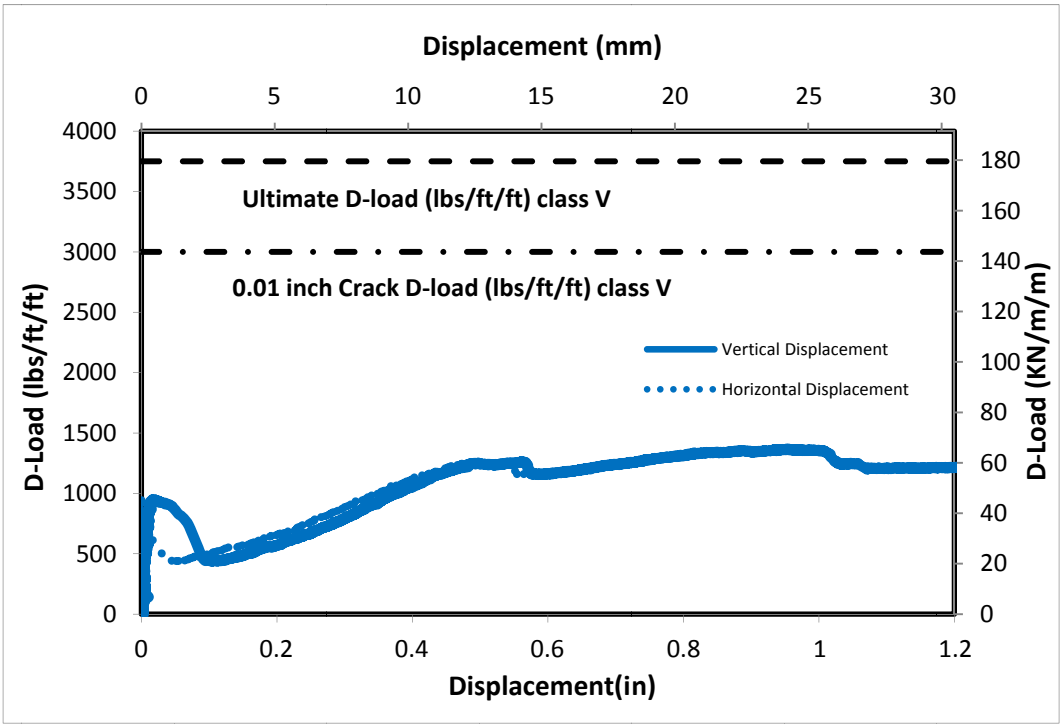

Figure B-9 Load-Deflection Plot for CRCP-24-6-B-8%rubber

Figure B-10 Crack propagation for CRCP-24-6-B-8%rubber

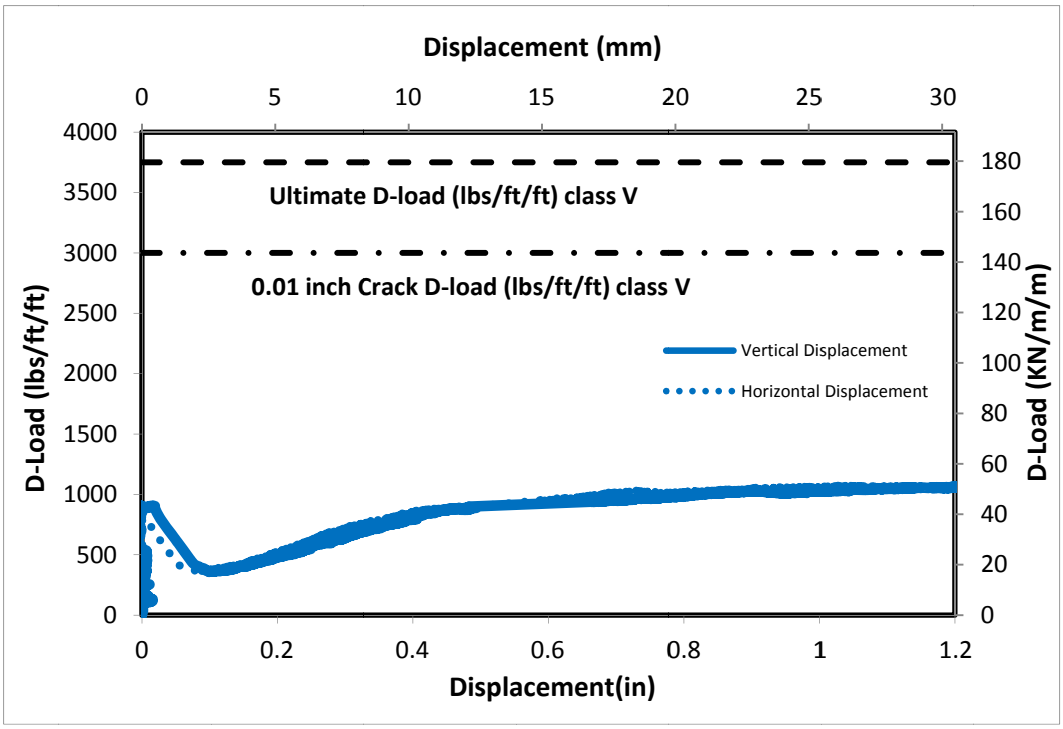

Figure B-11 Load-Deflection Plot for CRCP-24-6-B-8%rubber

Figure B-12 Crack propagation for CRCP-24-6-B-8%rubber

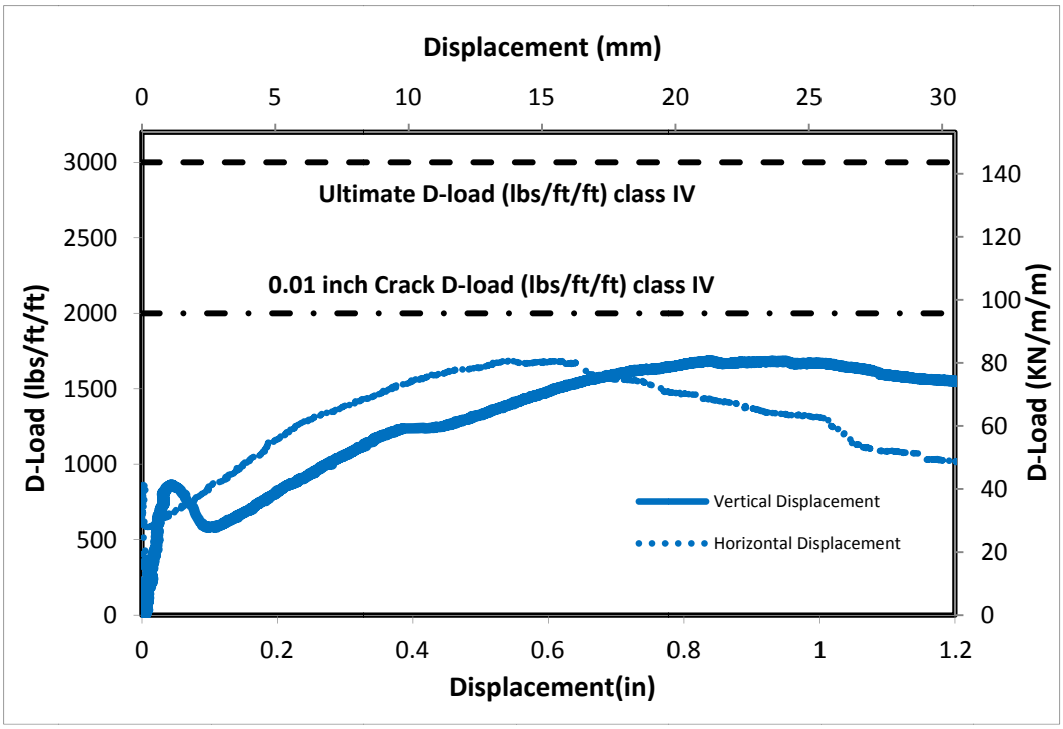

Figure B-13 Load-Deflection Plot for CRCP-24-6-B-6%rubber

Figure B-14 Crack propagation for CRCP-24-6-B-6%rubber

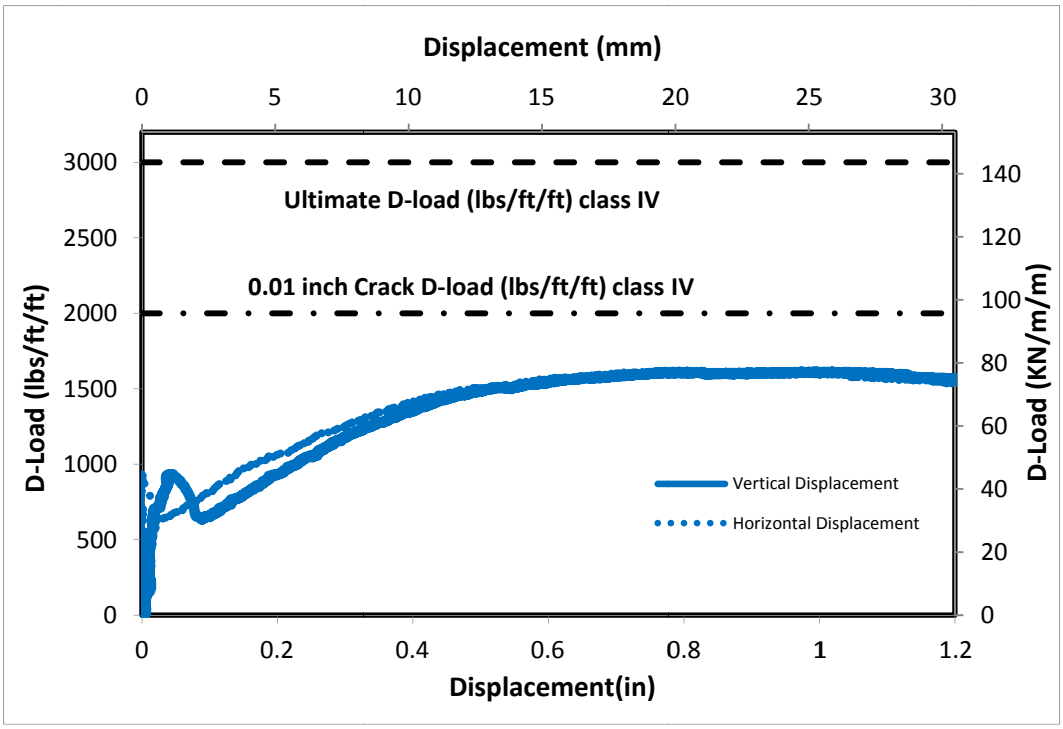

Figure B-15 Load-Deflection Plot for CRCP-24-6-B-6%rubber

Figure B-16 Crack propagation for CRCP-24-6-B-6%rubber

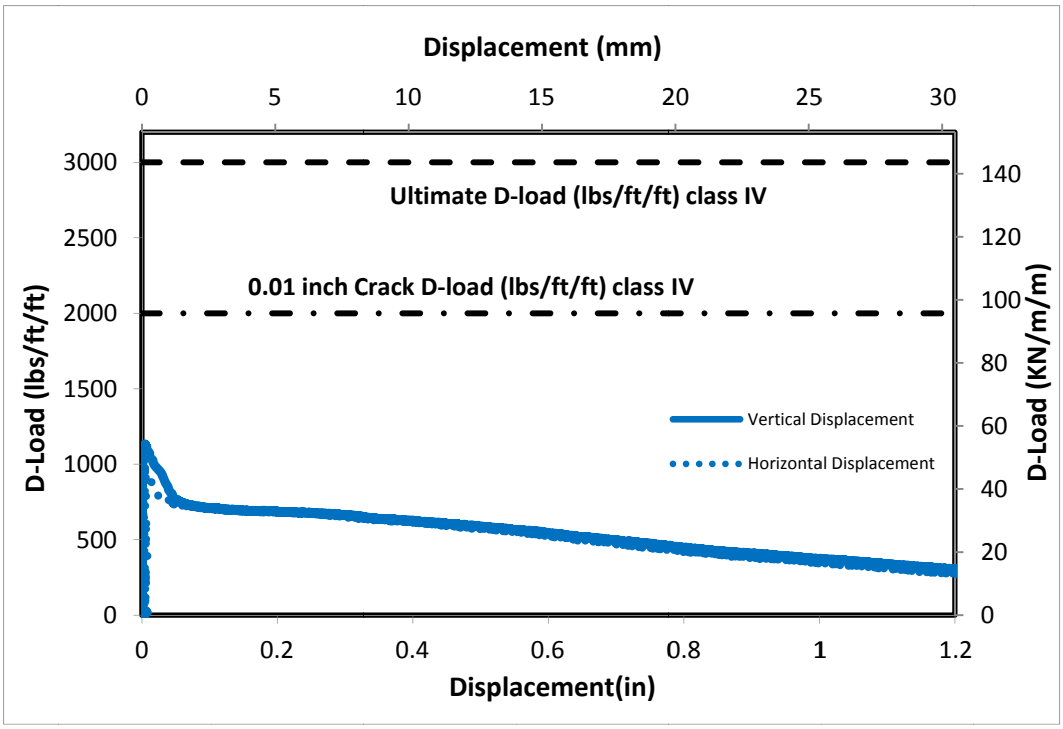

Figure B-17 Load-Deflection Plot for HYCP-24-6-B-44lbs steel-6%rubber

Figure B-18 Crack propagation for HYCP-24-6-B-44lbs steel-6%rubber

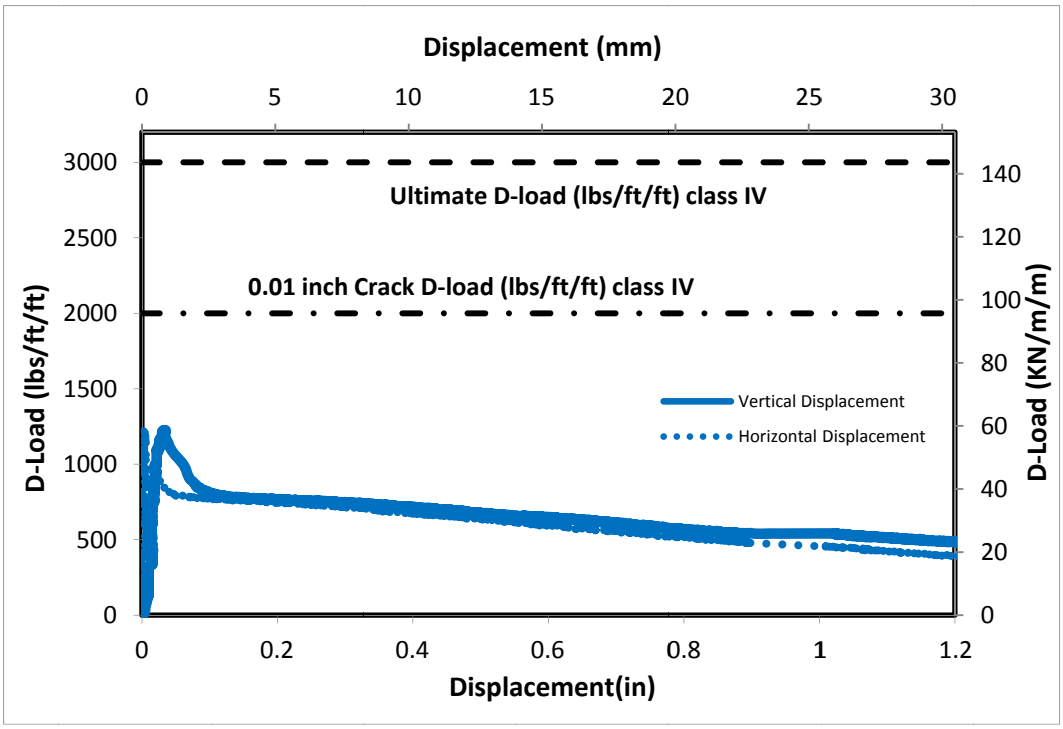

Figure B-19 Load-Deflection Plot for HYCP-24-6-B-44lbs steel-6%rubber

Figure B-20 Crack propagation for HYCP-24-6-B-44lbs steel-6%rubber

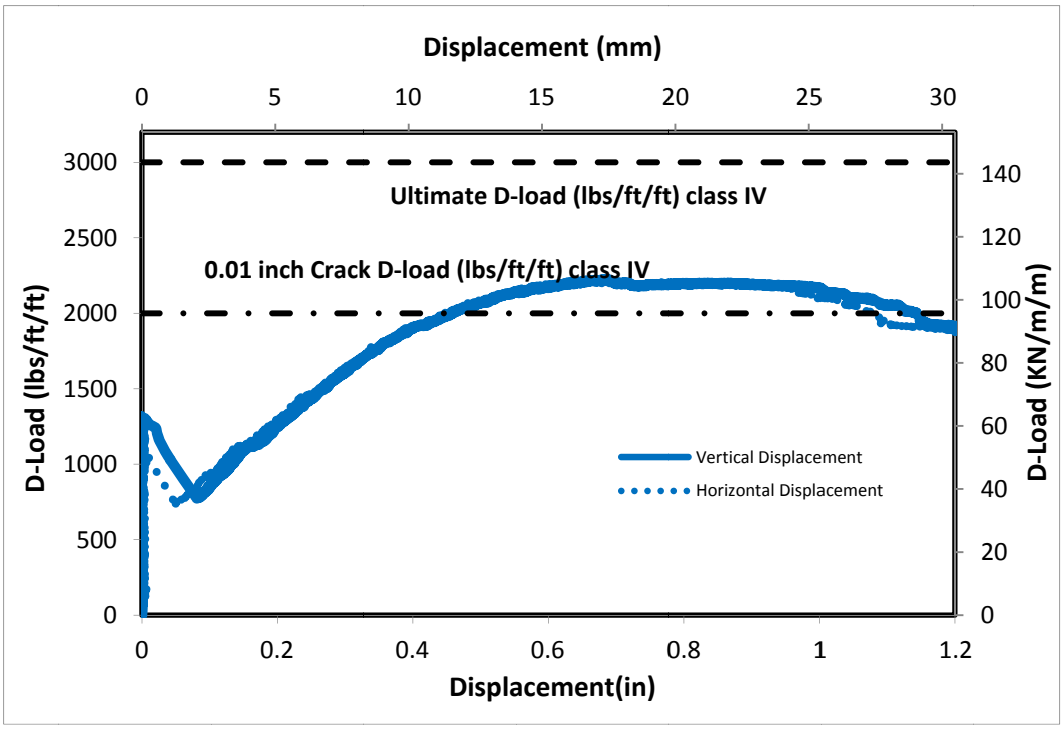

Figure B-21 Load-Deflection Plot for RCP-24-6-B

Figure B-22 Crack propagation for RCP-24-6-B

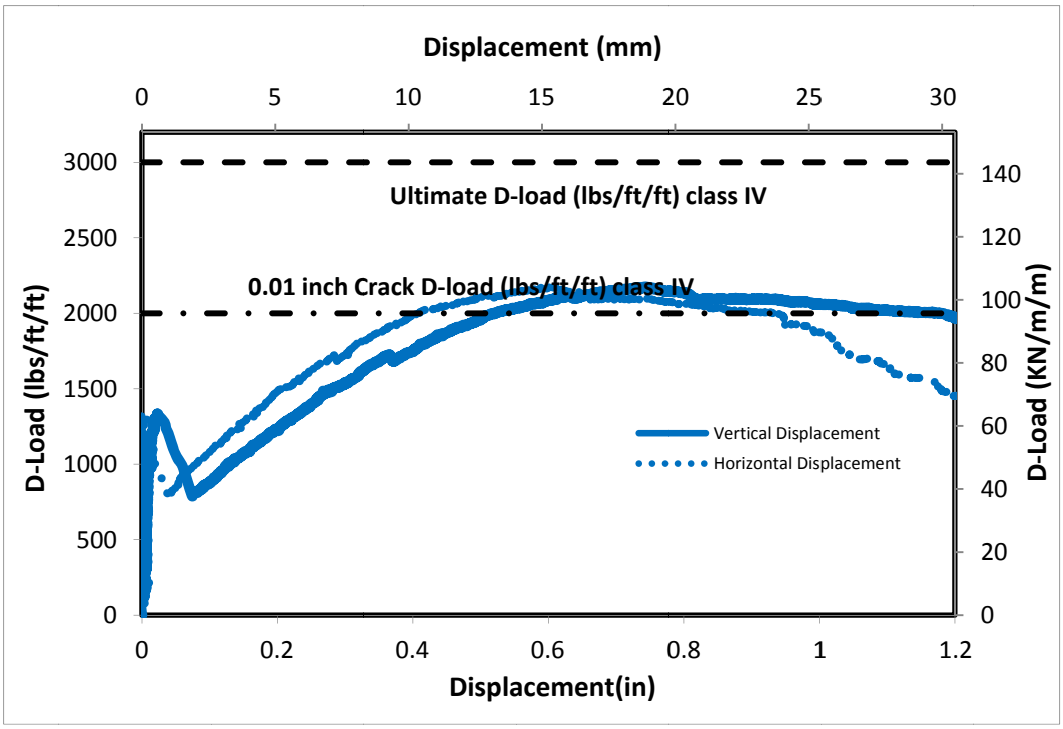

Figure B-23 Load-Deflection Plot for RCP-24-6-B

Figure B-24 Crack propagation for RCP-24-6-B

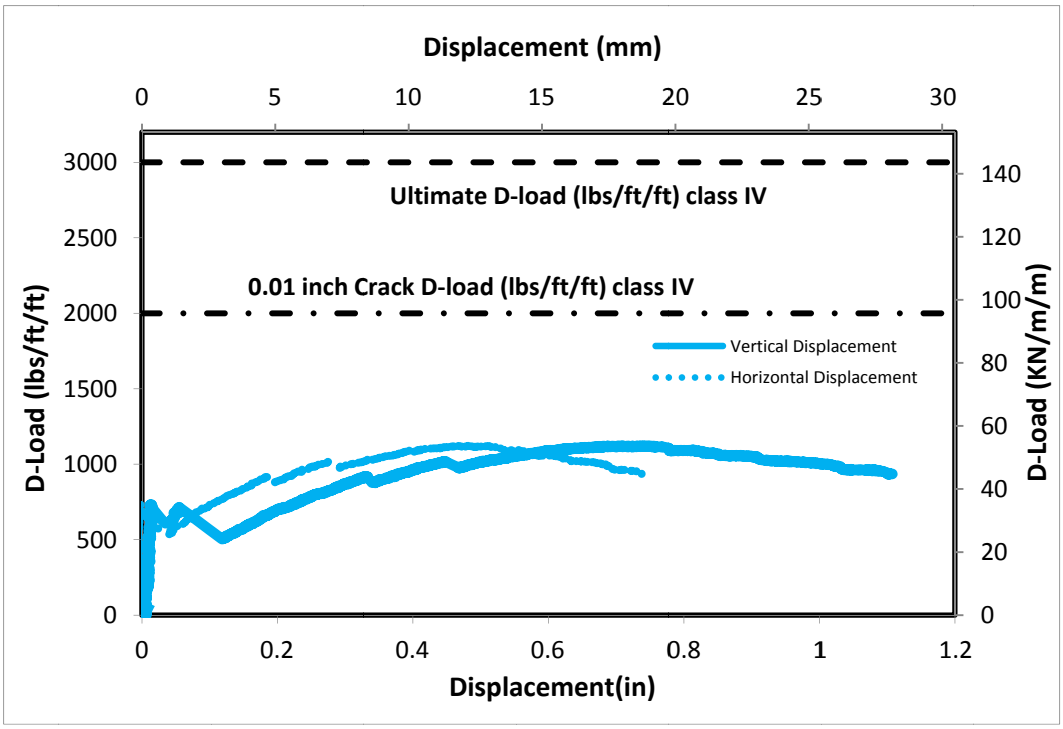

Figure B-25 Load-Deflection Plot for RCP-24-6-B

Figure B-26 Crack propagation for RCP-24-6-B

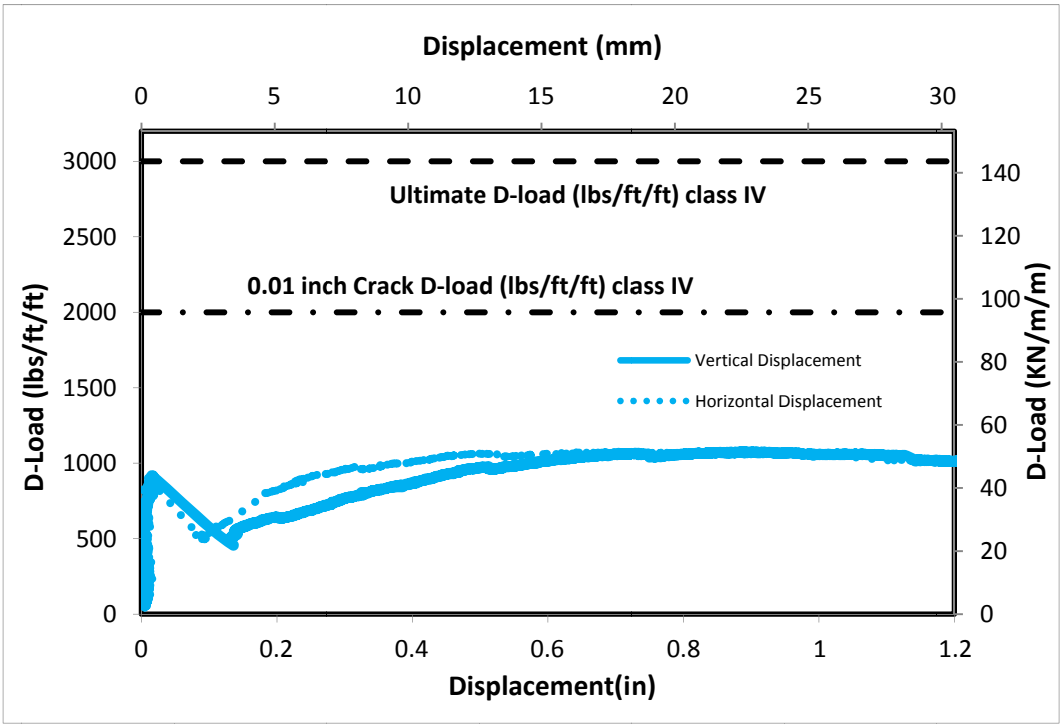

Figure B-27 Load-Deflection Plot for RCP-24-6-B

Figure B-28 Crack propagation for RCP-24-6-B

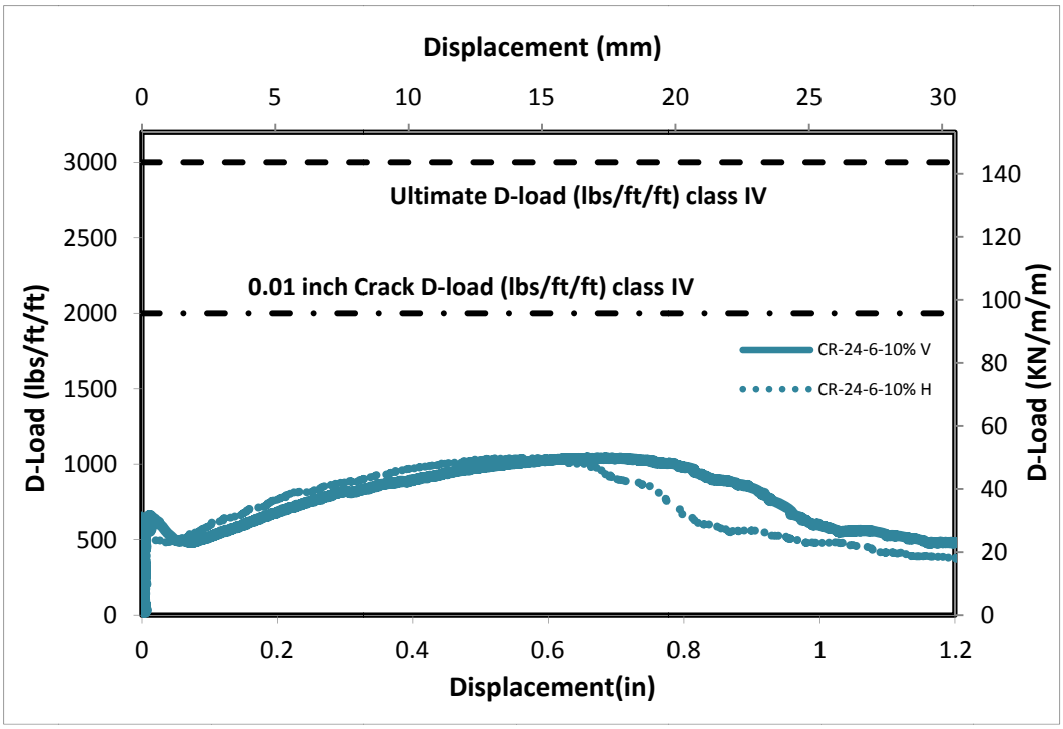

Figure B-29 Load-Deflection Plot for CRCP-24-6-10%rubber

Figure B-30 Crack propagation for CRCP-24-6-10%rubber

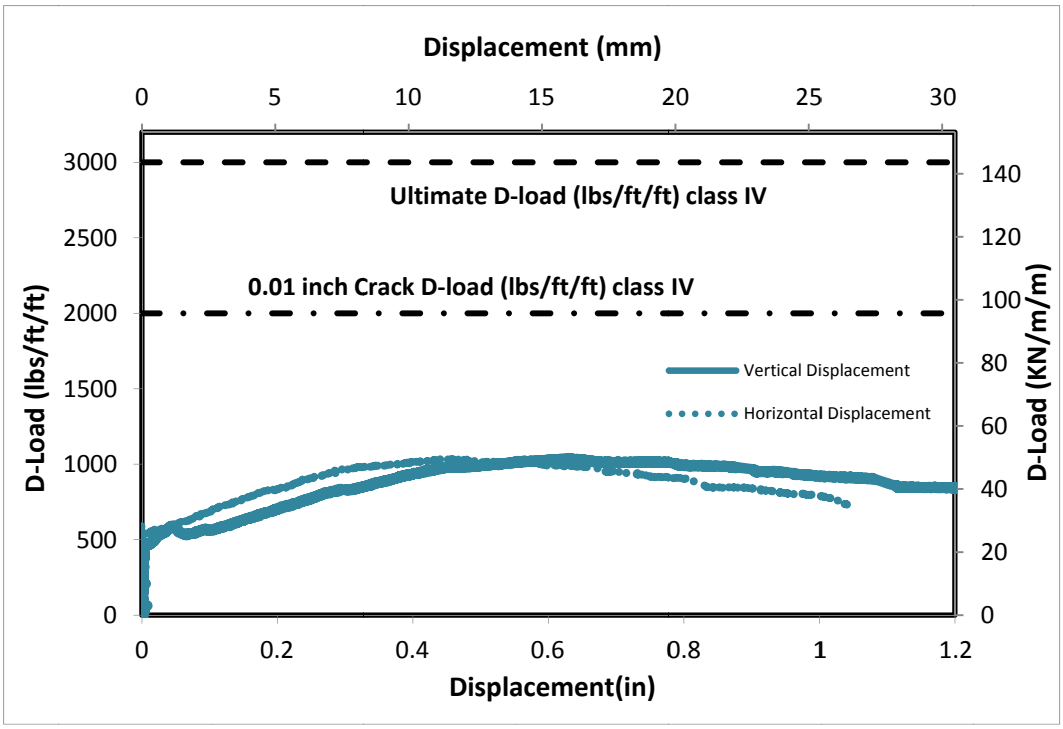

Figure B-31 Load-Deflection Plot for CRCP-24-6-10%rubber

Figure B-32 Crack propagation for CRCP-24-6-10%rubber

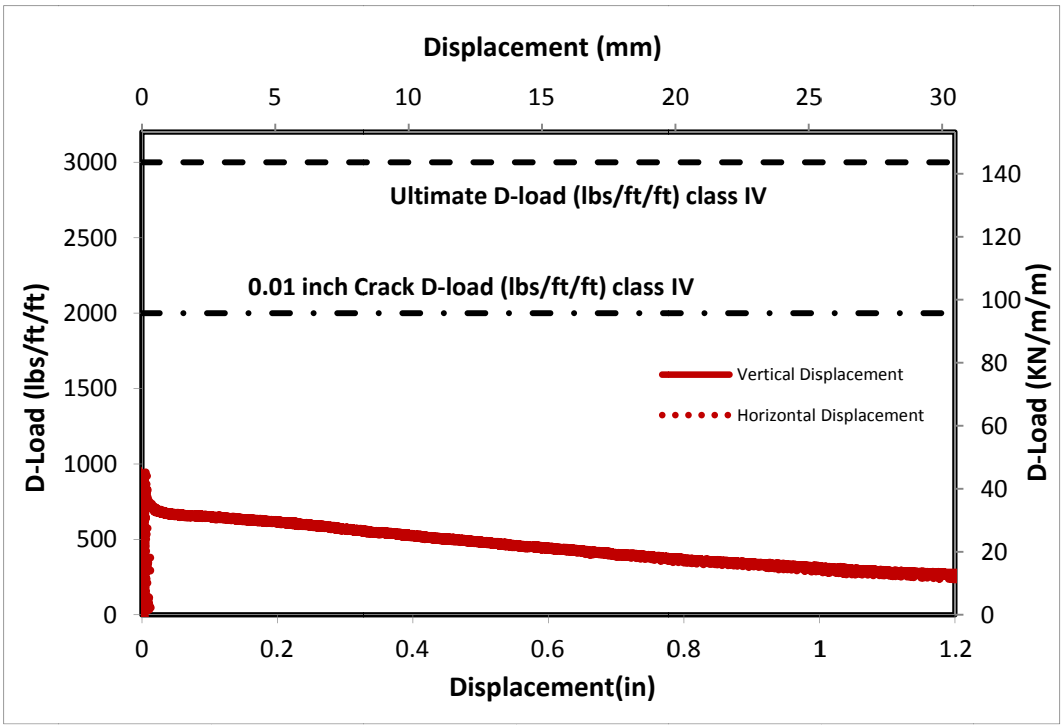

Figure B-33 Load-Deflection Plot for HYCP-24-6-B-44lbs steel-10%rubber

Figure B-34 Crack propagation for HYCP-24-6-B-44lbs steel-10%rubber

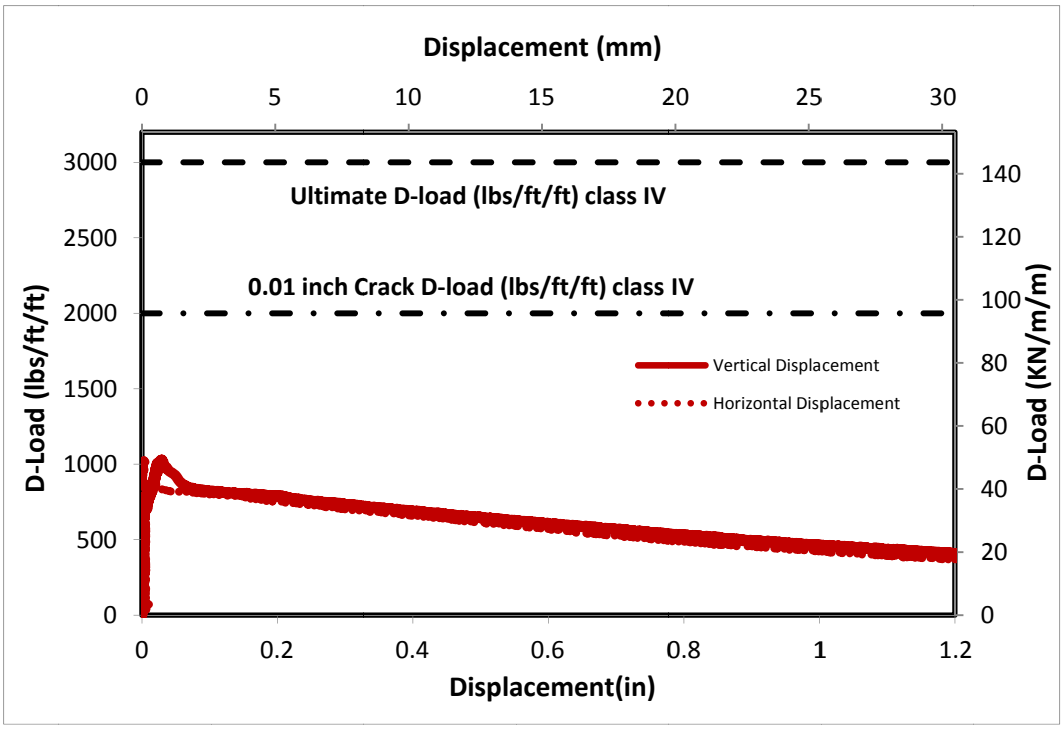

Figure B-35 Load-Deflection Plot for HYCP-24-6-B-44lbs steel-10%rubber

Figure B-36 Crack propagation for HYCP-24-6-B-44lbs steel-10%rubber

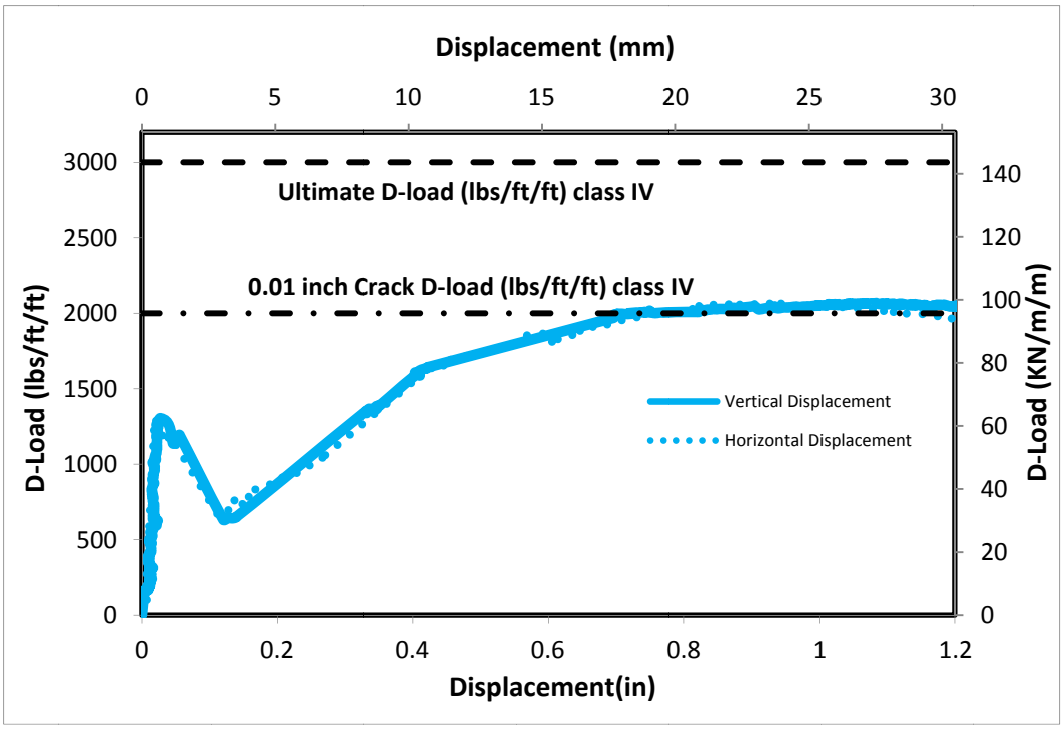

Figure B-37 Load-Deflection Plot for RCP-24-6-B

Figure B-38 Crack propagation for RCP-24-6-B

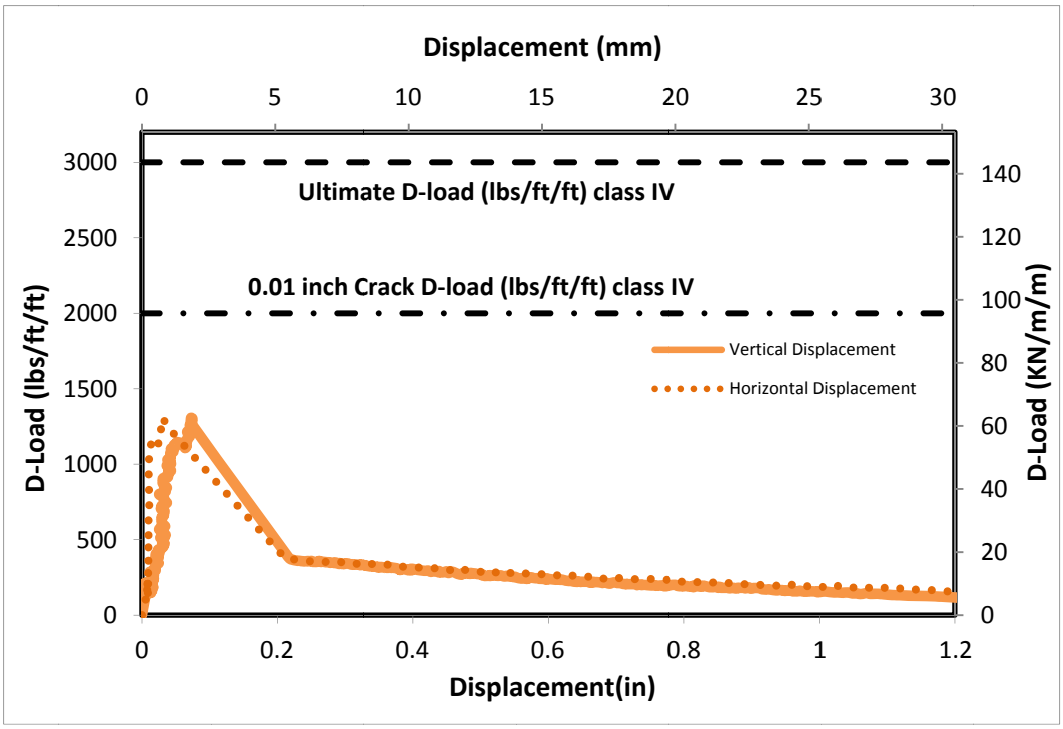

Figure B-39 Load-Deflection Plot for SFCP-24-6-B-10lbs steel

Figure B-40 Crack propagation for SFCP-24-6-B-10lbs steel

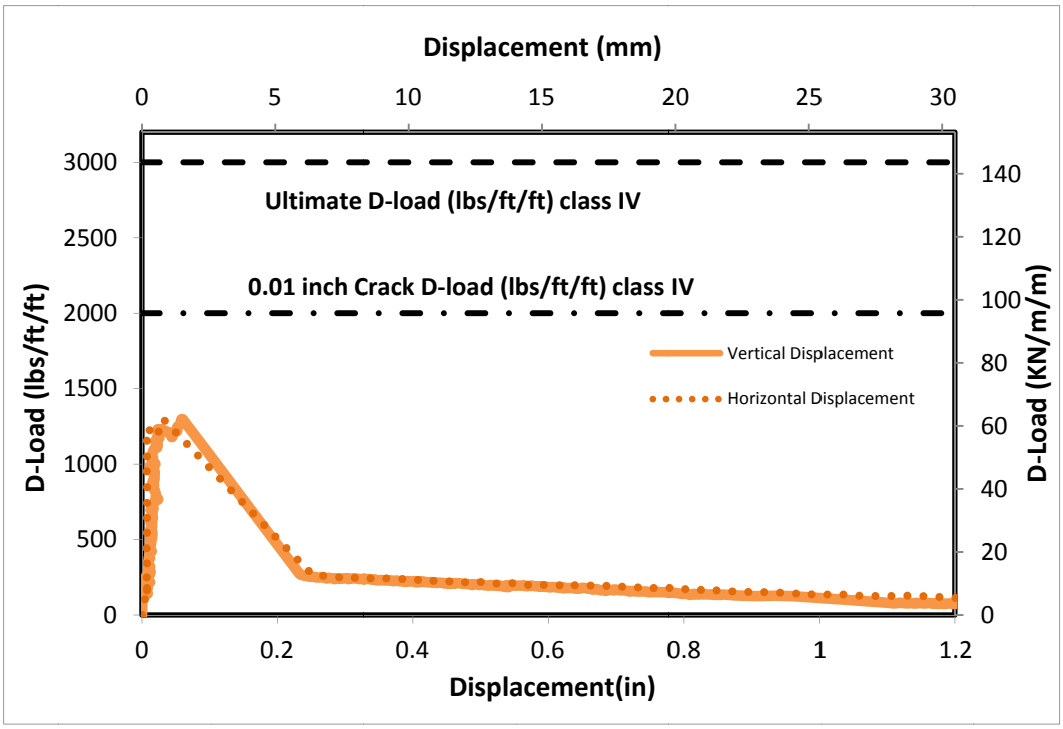

Figure B-41 Load-Deflection Plot for SFCP-24-6-B-10lbs steel

Figure B-42 Crack propagation for SFCP-24-6-B-10lbs steel

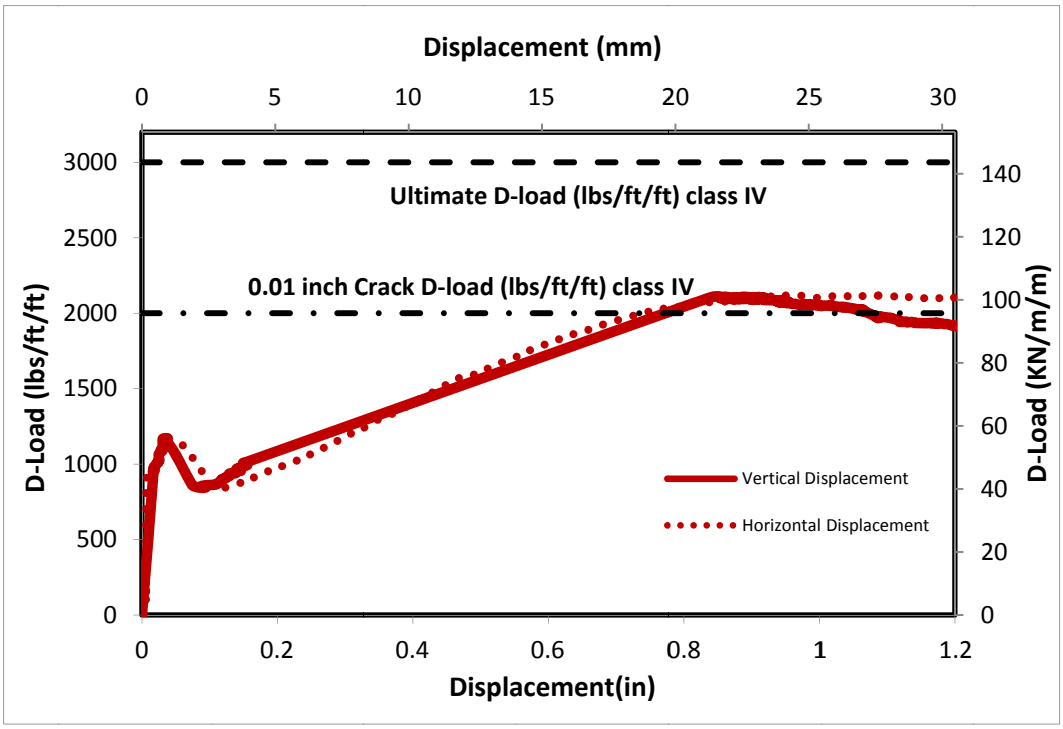

Figure B-43 Load-Deflection Plot for HYRCP-24-6-B-10lbs steel-8% rubber

Figure B-44 Crack propagation for HYRCP-24-6-B-10lbs steel-8% rubber

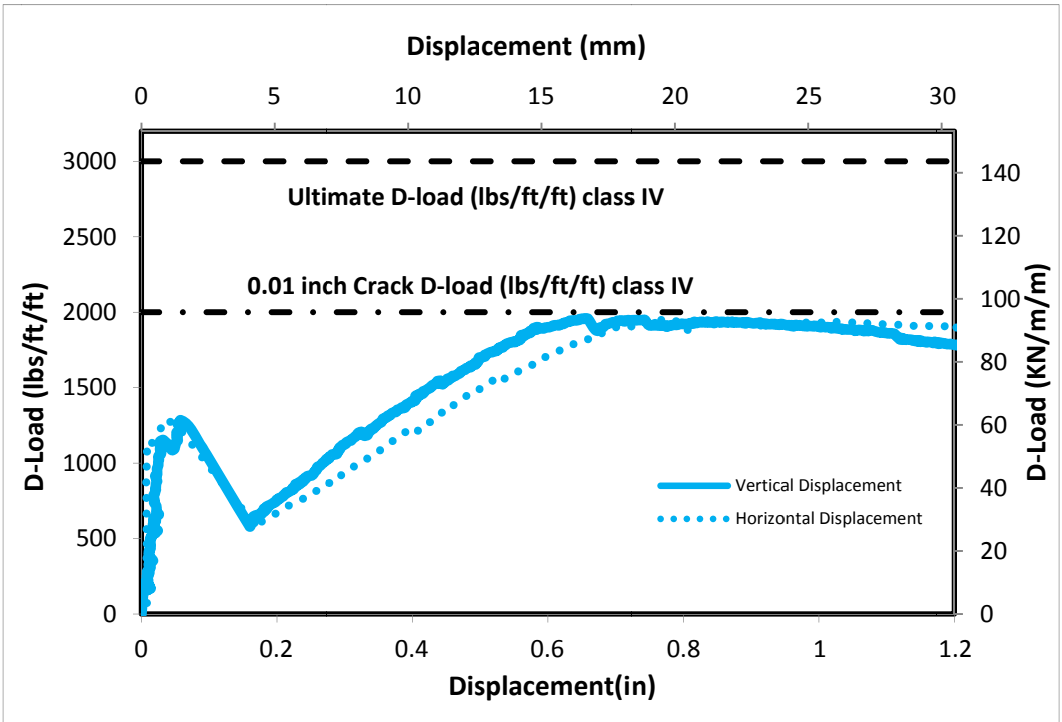

Figure B-45 Load-Deflection Plot for RCP-24-6-B

Figure B-46 Crack propagation for RCP-24-6-B

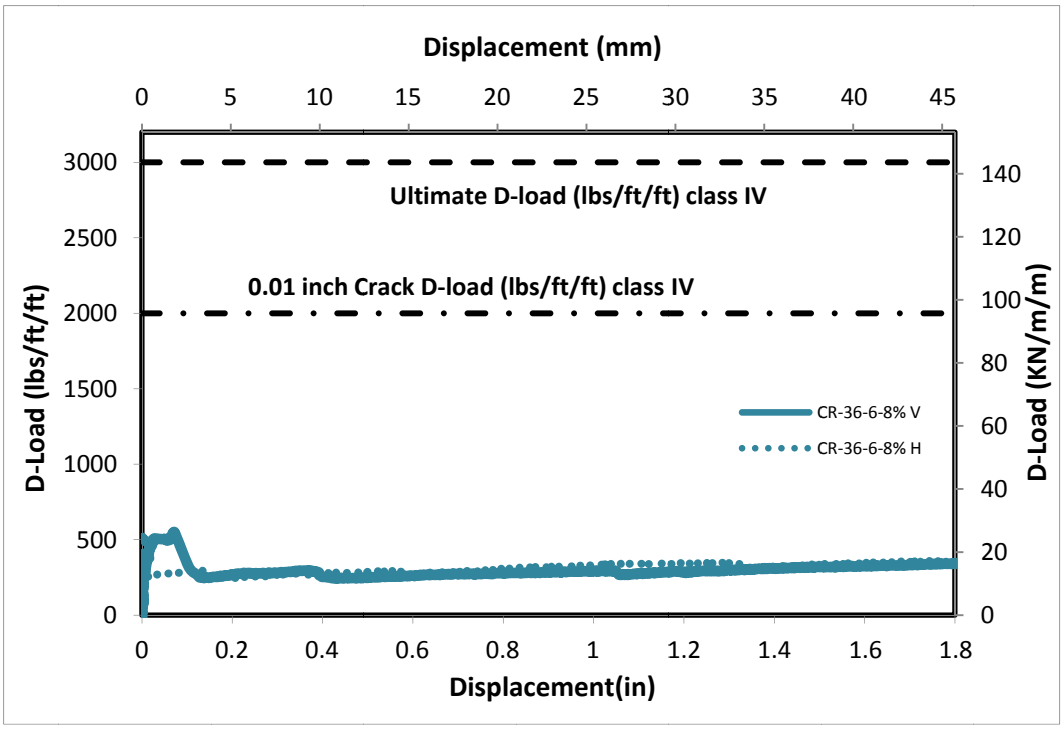

Figure B-47 Load-Deflection Plot for CRCP-36-6-8%rubber

Figure B-48 Crack propagation for CRCP-36-6-8%rubber

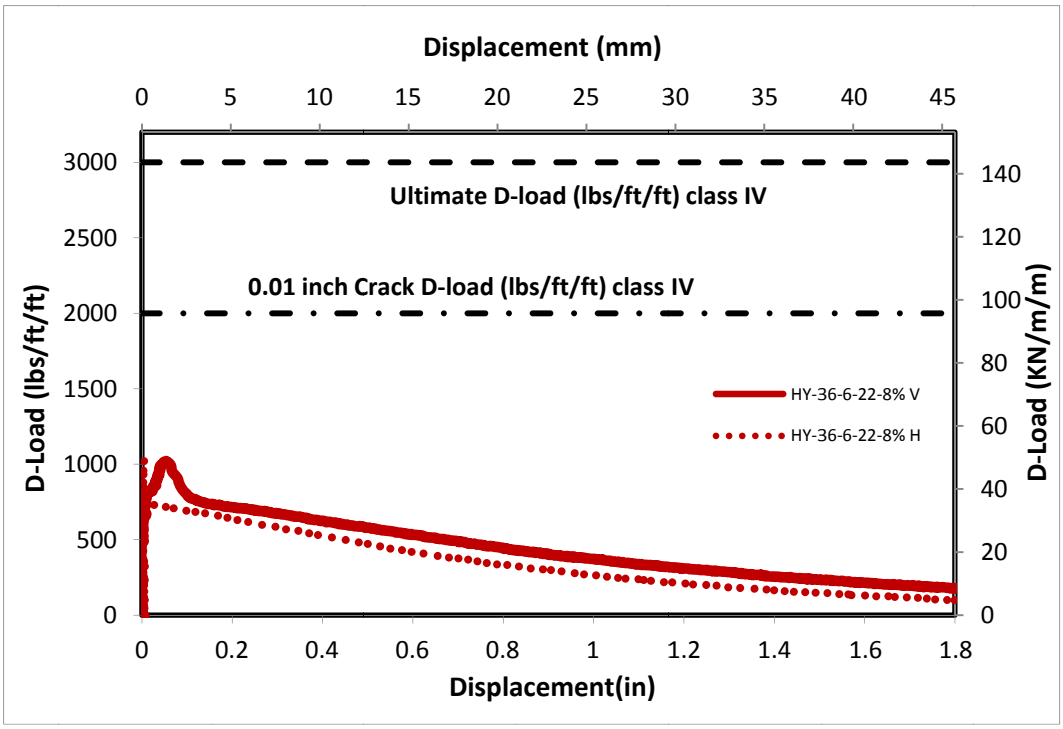

Figure B-49 Load-Deflection Plot for HYCP-36-6-22lbs steel-8%rubber

Figure B-50 Crack propagation for HYCP-36-6-22lbs steel-8%rubber

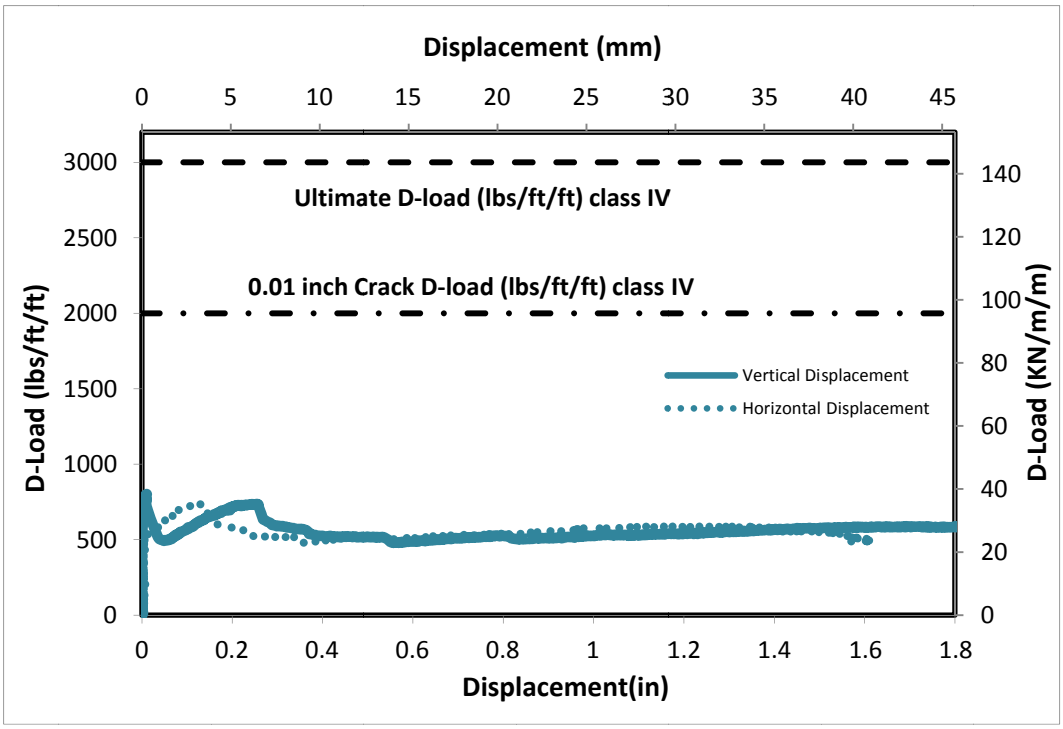

Figure B-51 Load-Deflection Plot for CRCP-36-6-8%rubber

Figure B-52 Crack propagation for CRCP-36-6-8%rubber

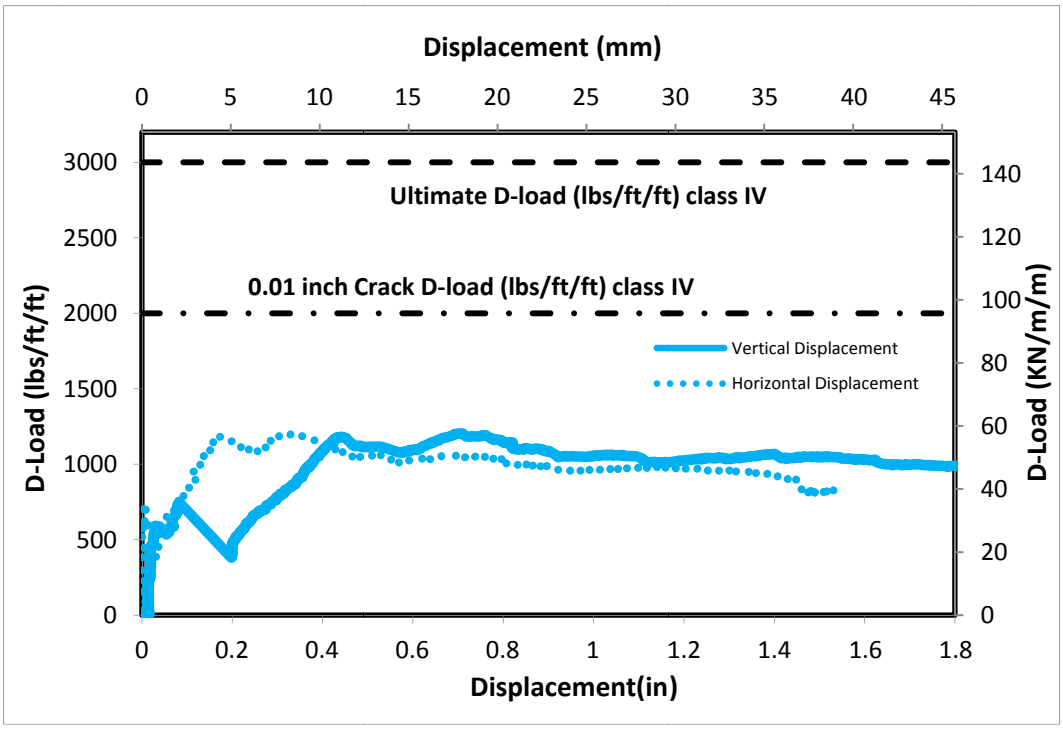

Figure B-53 Load-Deflection Plot for RCP-36-6-B

Figure B-54 Crack propagation for RCP-36-6-B

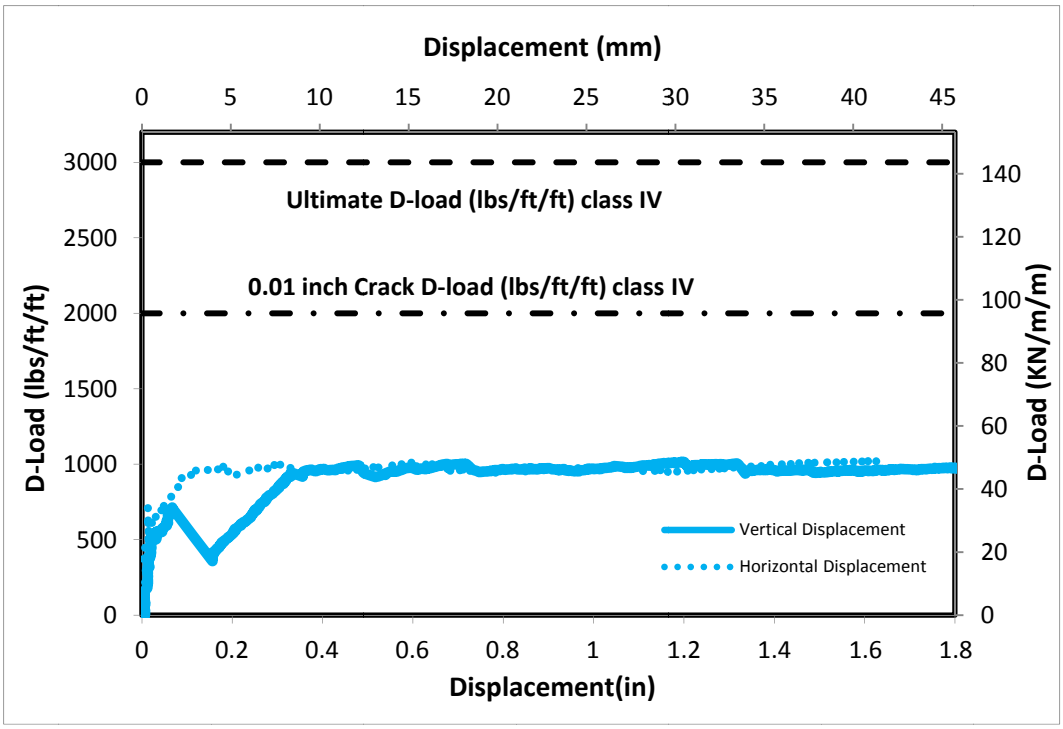

Figure B-55 Load-Deflection Plot for RCP-36-6-B

Figure B-56 Crack propagation for RCP-36-6-B

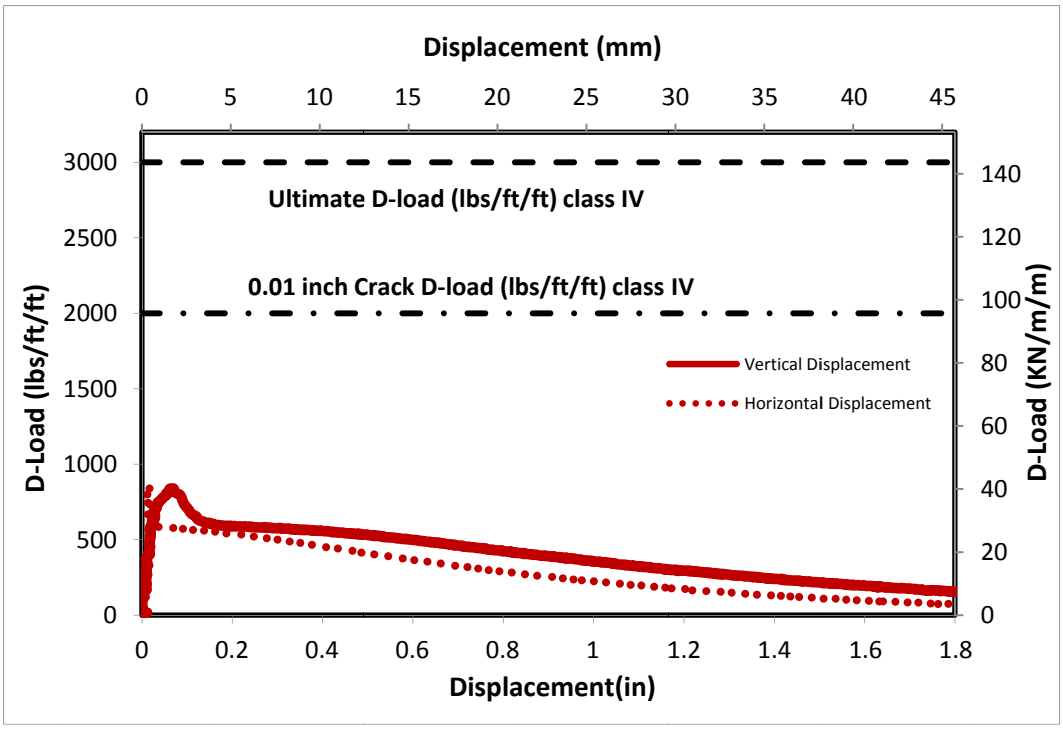

Figure B-57 Load-Deflection Plot for HYCP-36-6-22-8% rubber

Figure B-58 Crack propagation for HYCP-36-6-22-8% rubber

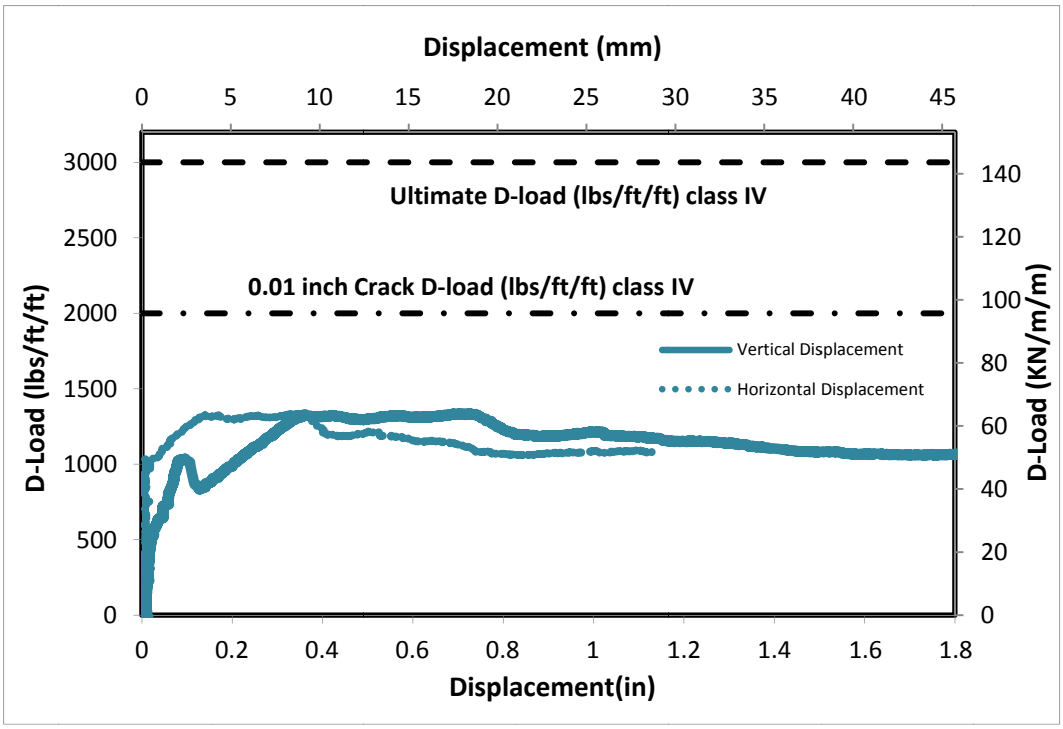

Figure B-59 Load-Deflection Plot for CRCP-36-6-B-10%rubber

Figure B-60 Crack propagation for CRCP-36-6-B-10%rubber

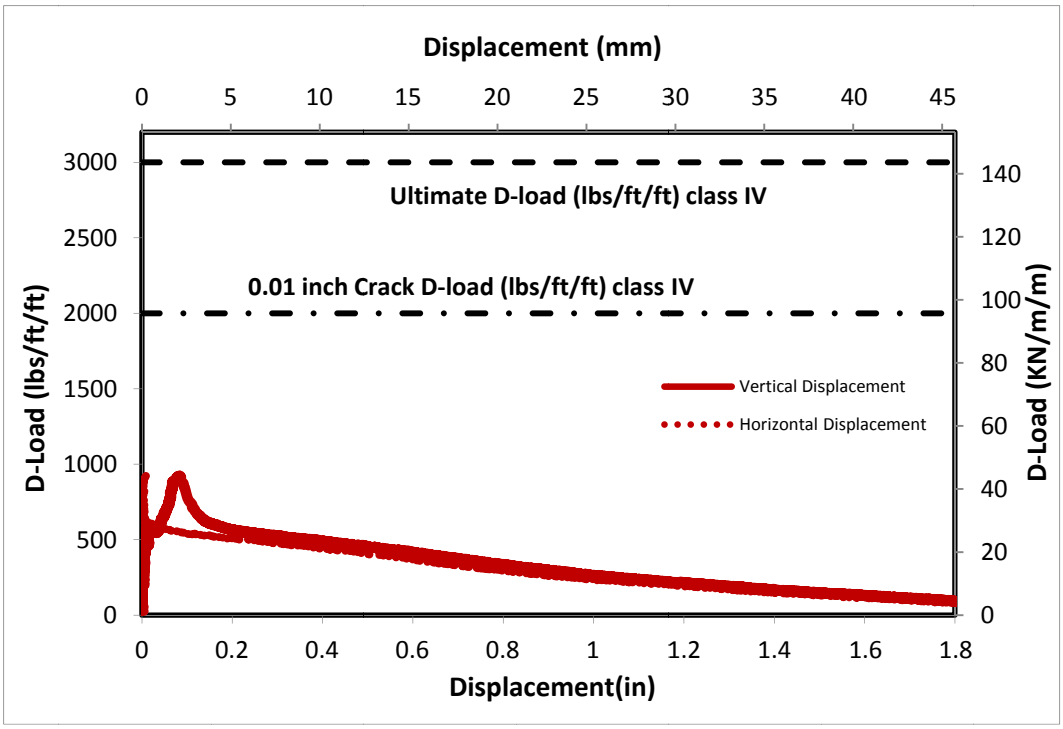

Figure B-61 Load-Deflection Plot for HYCP-36-6-B-22-10%rubber

Figure B-62 Crack propagation for HYCP-36-6-B-22-10%rubber

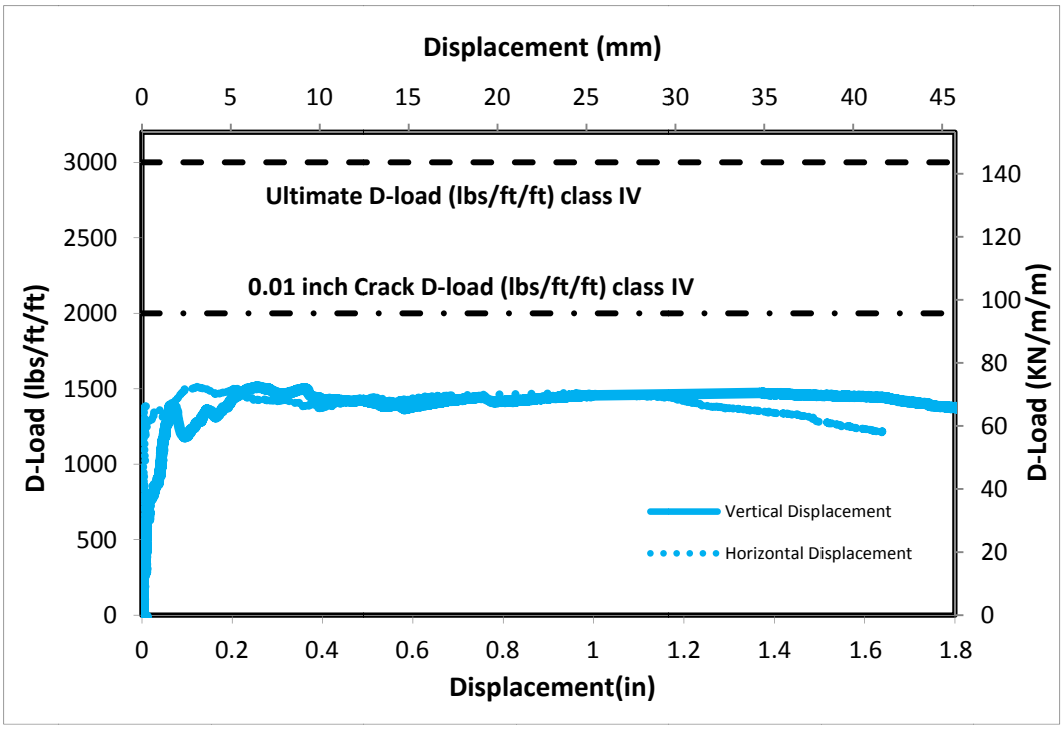

Figure B-63 Load-Deflection Plot for RCP-36-6-B

Figure B-64 Crack propagation for RCP-36-6-B

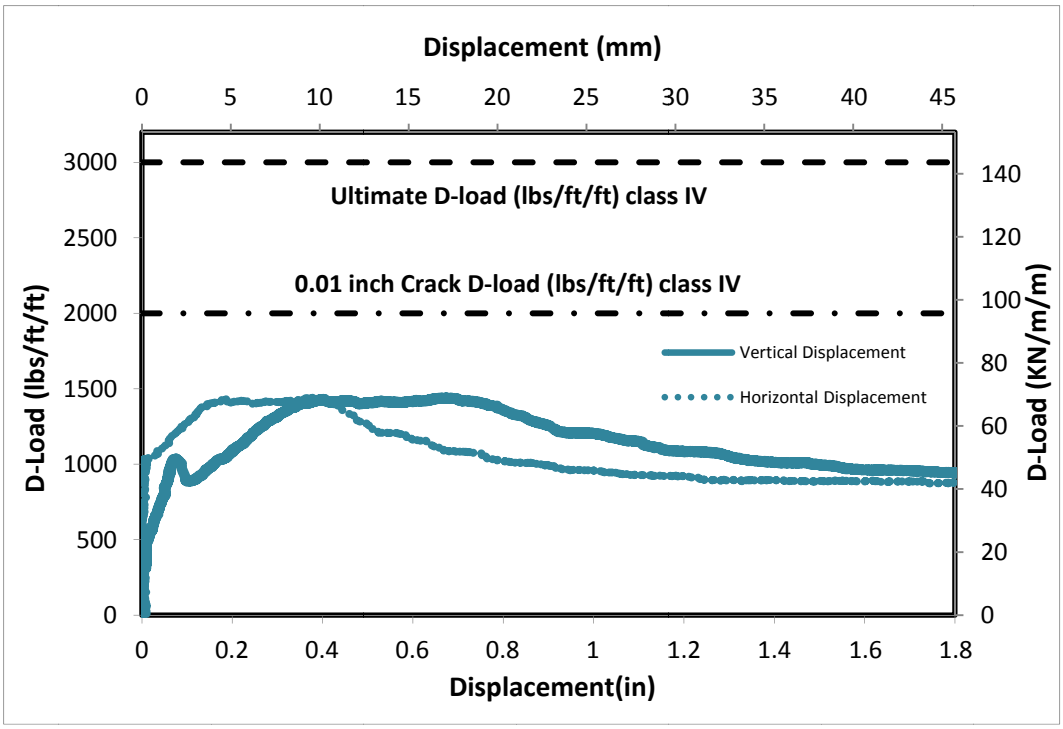

Figure B-65 Load-Deflection Plot for CRCP-36-6-B-10%rubber

Figure B-66 Crack propagation for CRCP-36-6-B-10%rubber

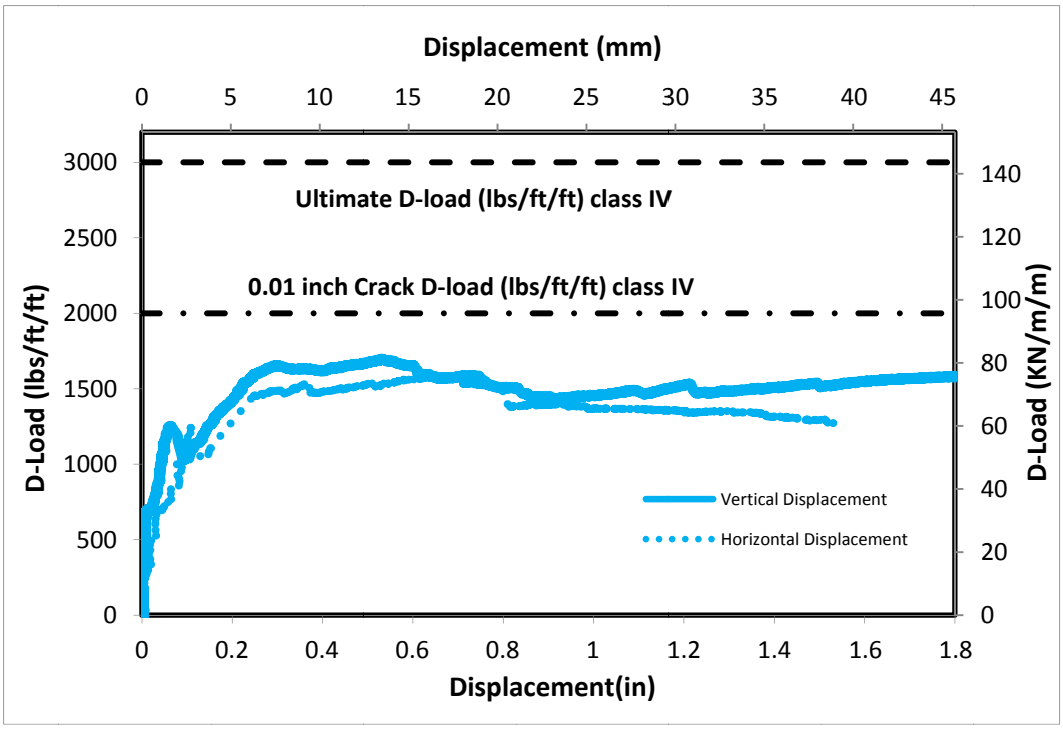

Figure B-67 Load-Deflection Plot for RCP-36-6-B

Figure B-68 Crack propagation for RCP-36-6-B

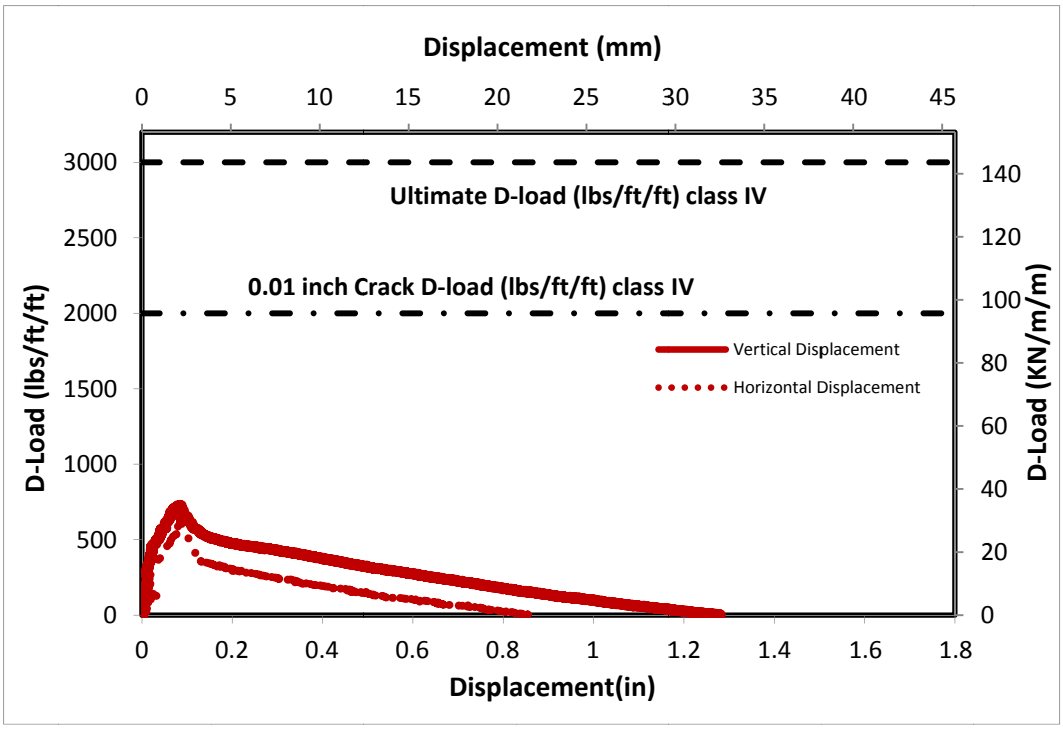

Figure B-69 Load-Deflection Plot for HYCP-36-6-B-22-10%rubber

Figure B-70 Crack propagation for HYCP-36-6-B-22-10%rubber

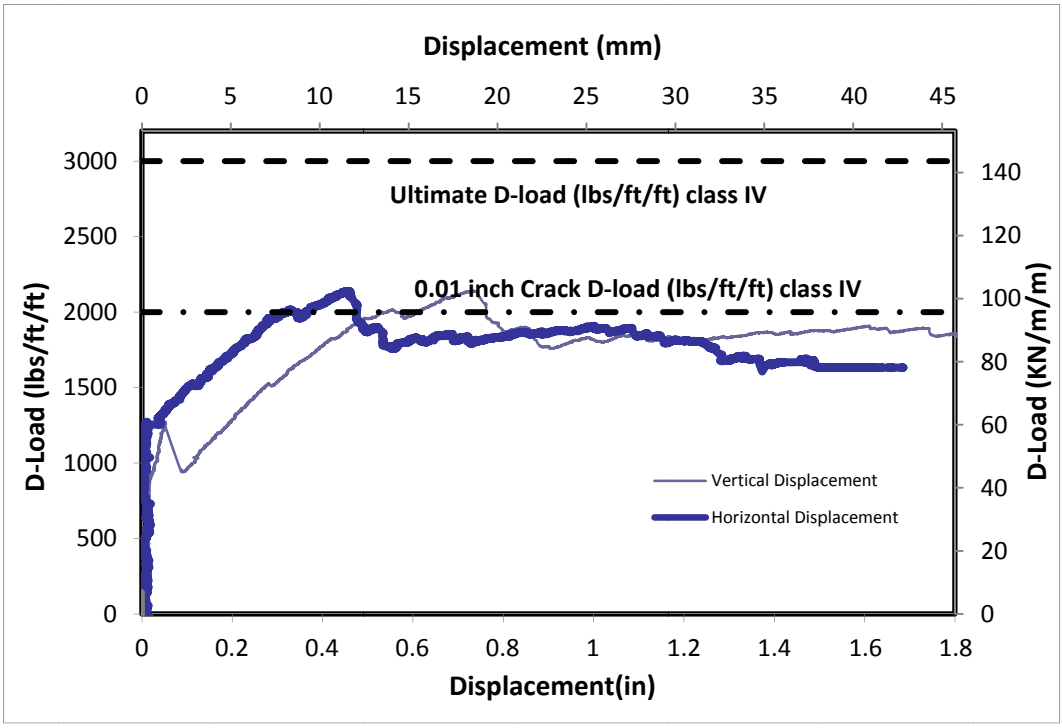

Figure B-71 Load-Deflection Plot for RCP-36-6-B

Figure B-72 Crack propagation for RCP-36-6-B

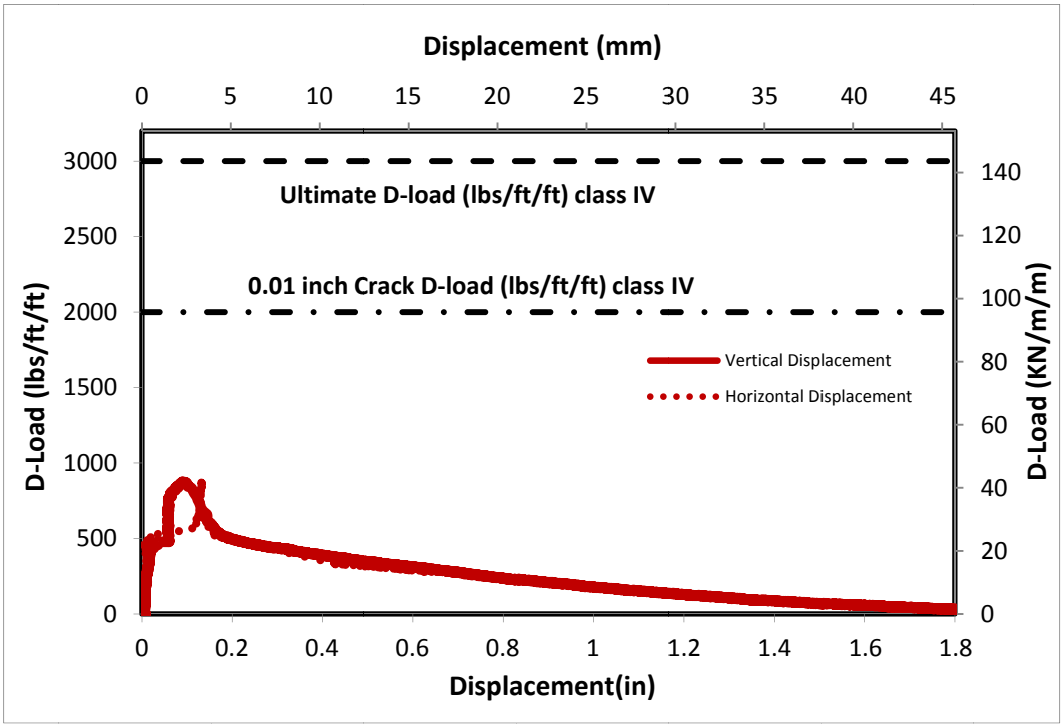

Figure B-73 Load-Deflection Plot for HYCP-36-6-B-44lbs steel-12%rubber

Figure B-74 Crack propagation for HYCP-36-6-B-44lbs steel-12%rubber

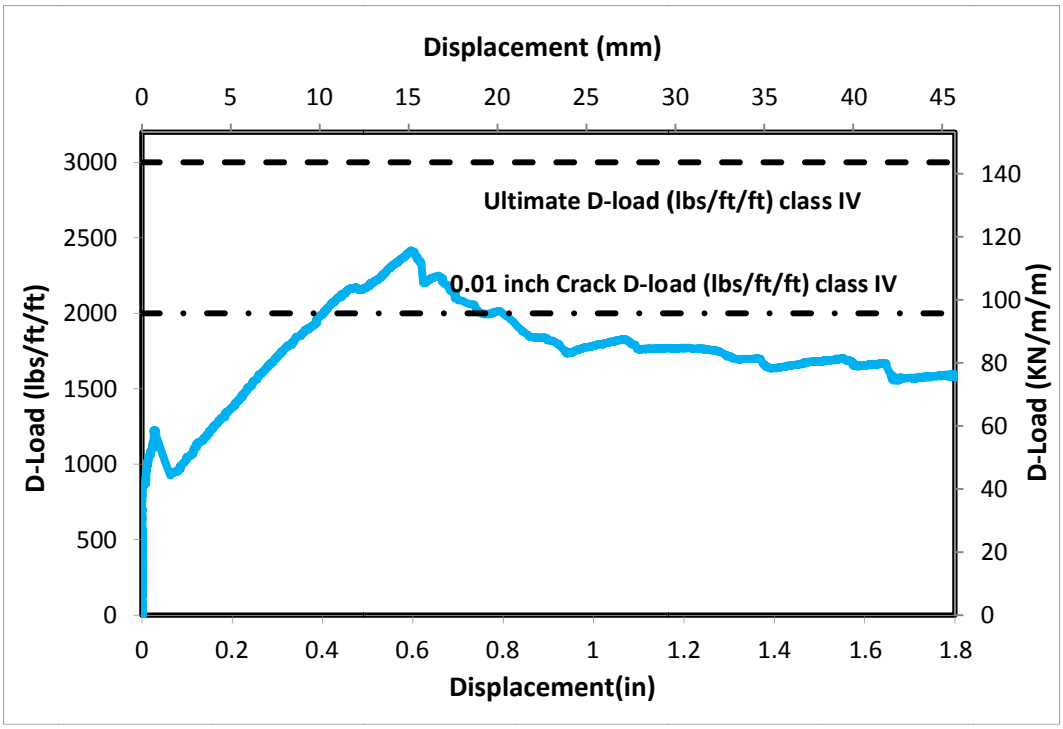

Figure B-75 Load-Deflection Plot for RCP-36-6-B

Figure B-76 Crack propagation for RCP-36-6-B

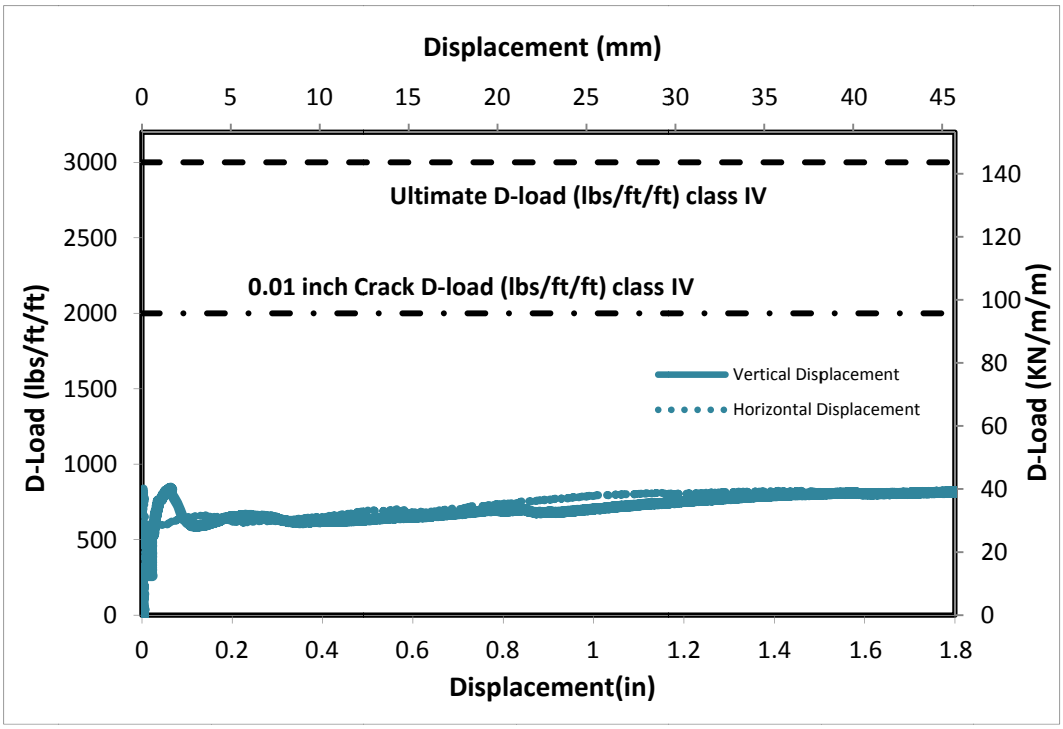

Figure B-77 Load-Deflection Plot for CRCP-36-6-B-12%rubber

Figure B-78 Crack propagation for CRCP-36-6-B-12%rubber

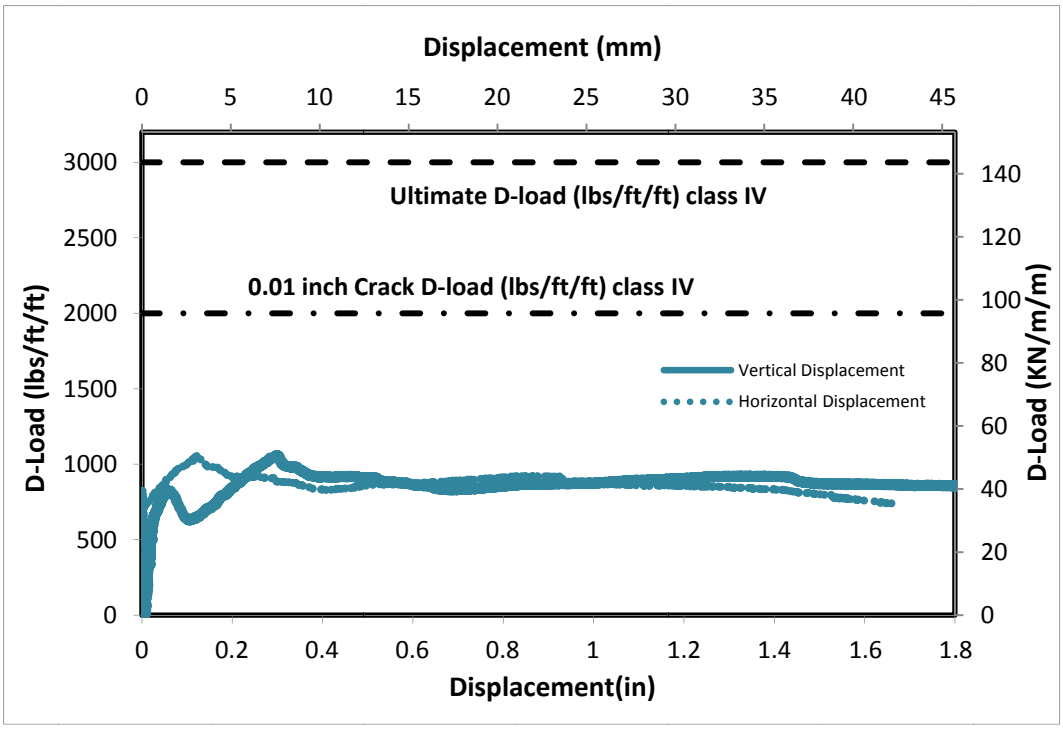

Figure B-79 Load-Deflection Plot for CRCP-36-6-B-12%rubber

Figure B-80 Crack propagation for CRCP-36-6-B-12%rubber

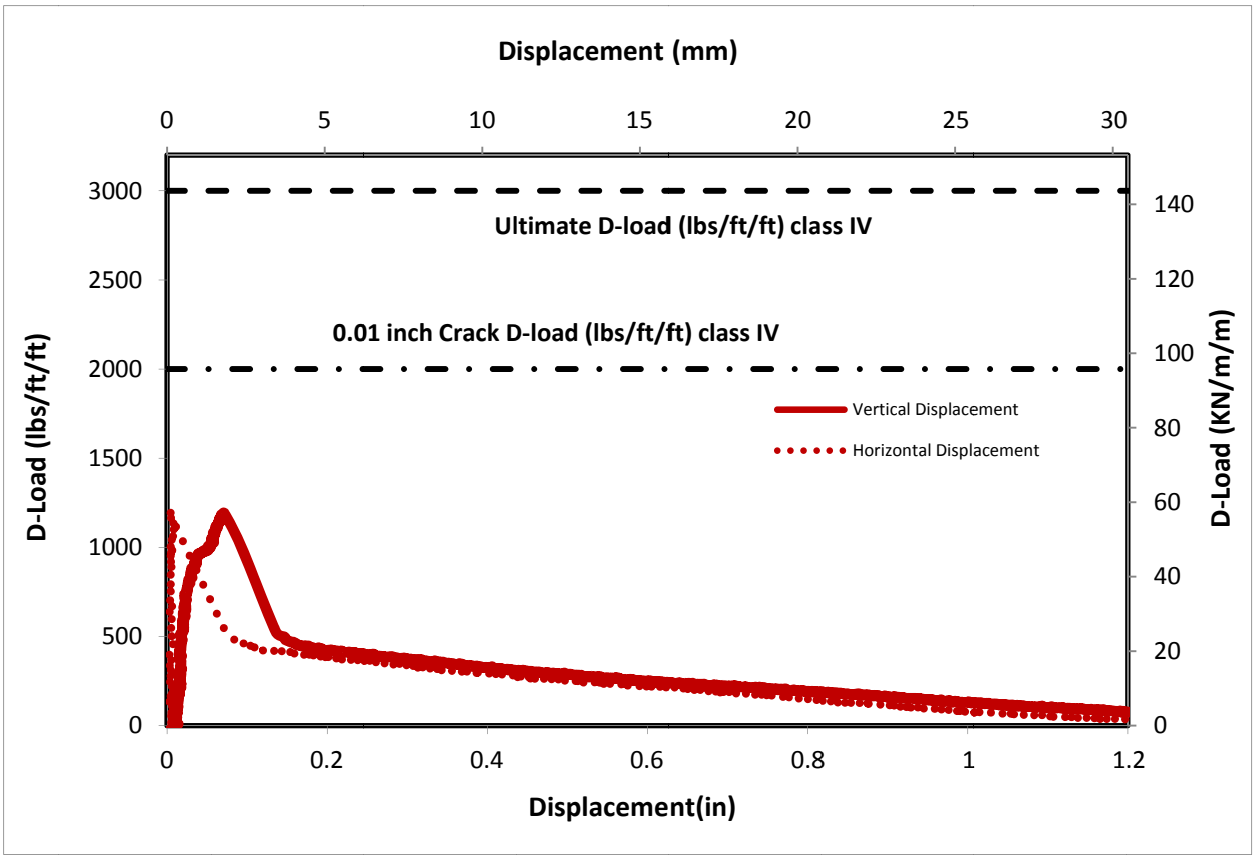

Figure B-81 Load-Deflection Plot for HYCP-24-6-B-44lbs steel-10%rubber

Figure B-82 Crack propagation for HYCP-24-6-B-44lbs steel-10%rubber

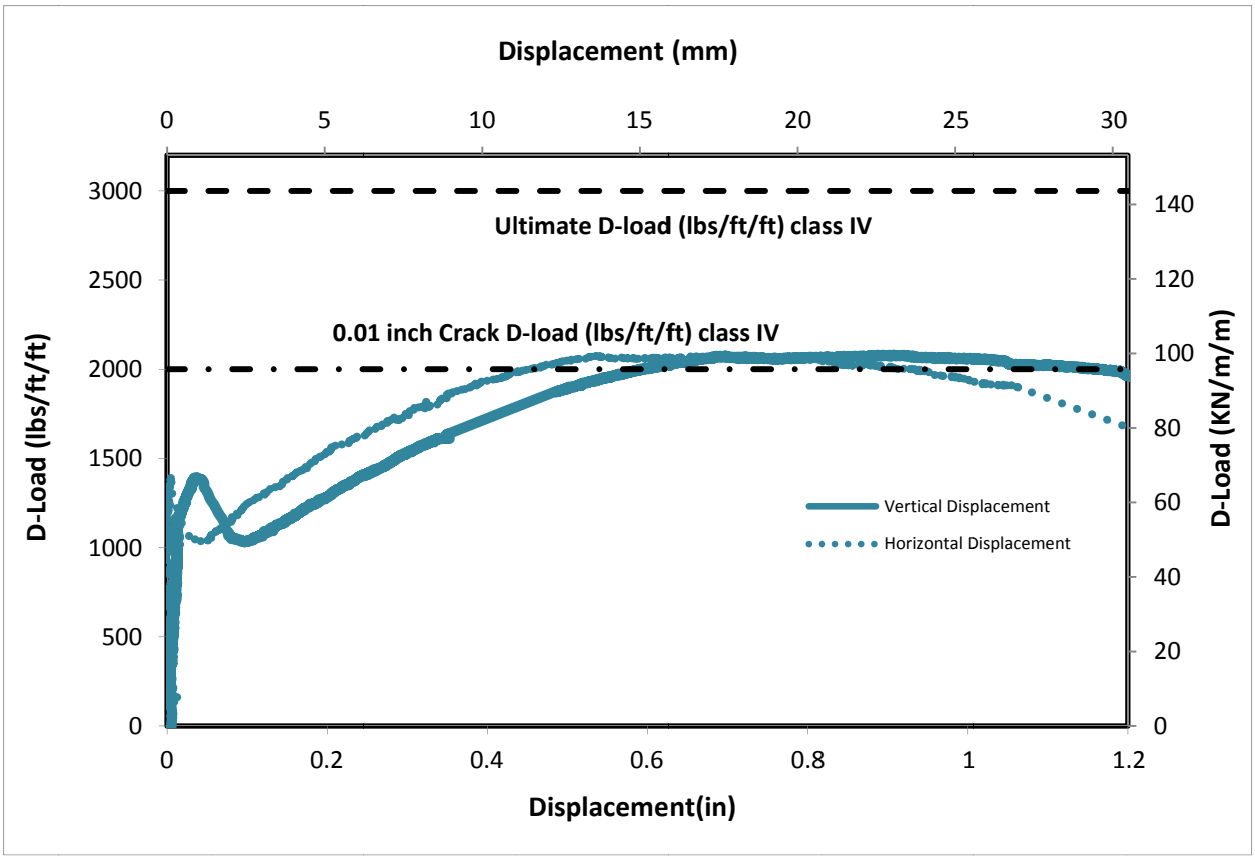

Figure B-83 Load-Deflection Plot for CRCP-24-6-B-10%rubber

Figure B-84 Crack propagation for CRCP-24-6-B-10%rubber

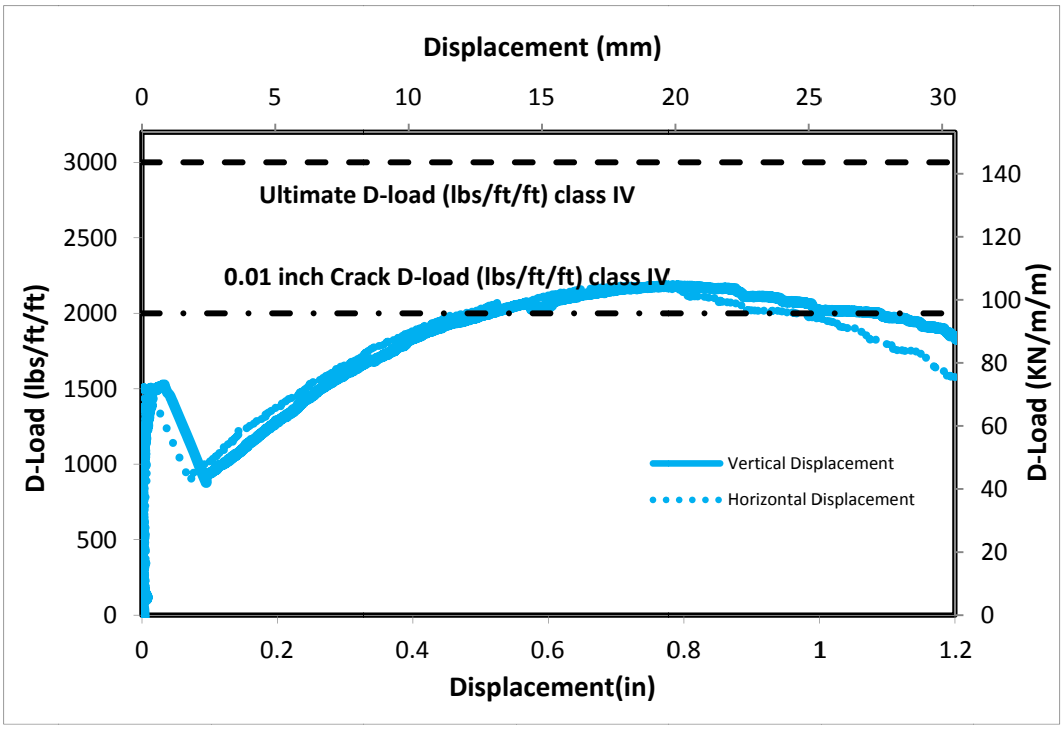

Figure B-85 Load-Deflection Plot for RCP-24-6-B

Figure B-86 Crack propagation for RCP-24-6-B

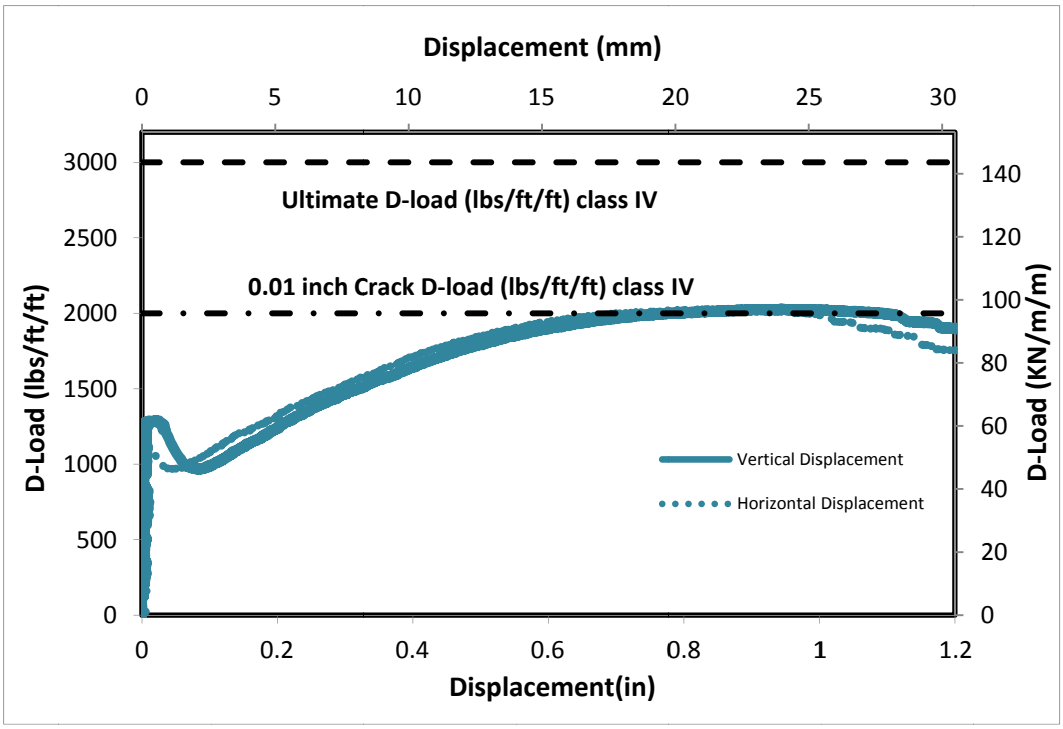

Figure B-87 Load-Deflection Plot for CRCP-24-6-B-10%rubber

Figure B-88 Crack propagation for CRCP-24-6-B-10%rubber

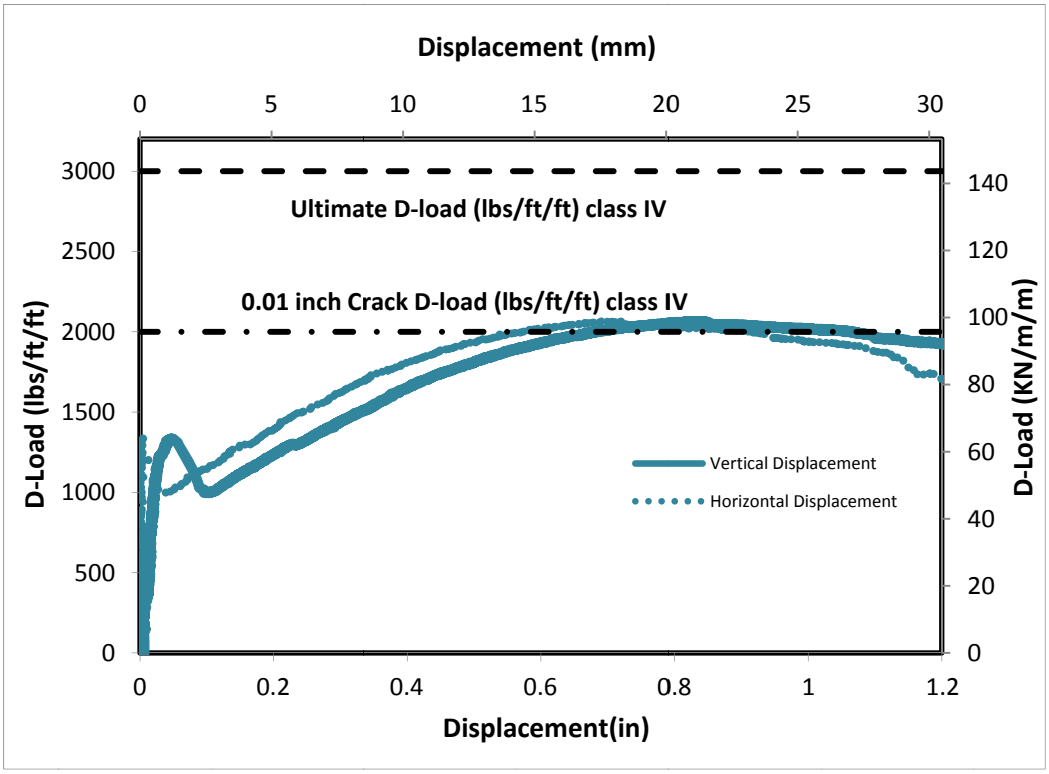

Figure B-89 Load-Deflection Plot for CRCP-24-6-B-10%rubber

Figure B-90 Crack propagation for CRCP-24-6-B-10%rubber

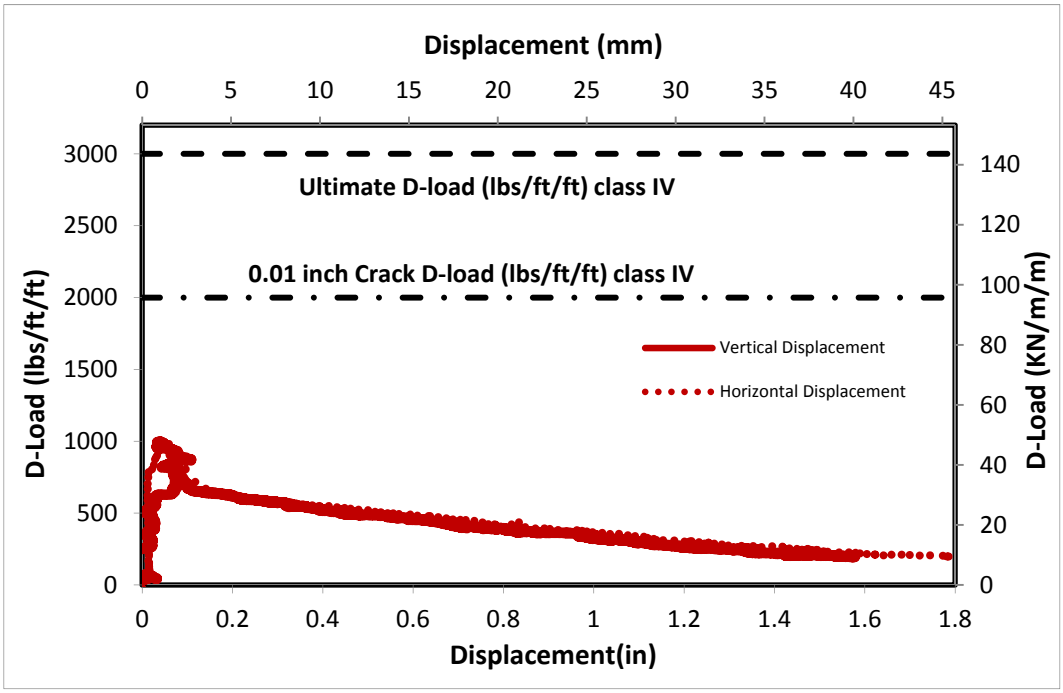

Figure B-91 Load-Deflection Plot for HYCP-36-6-B-44lbs steel-10%rubber

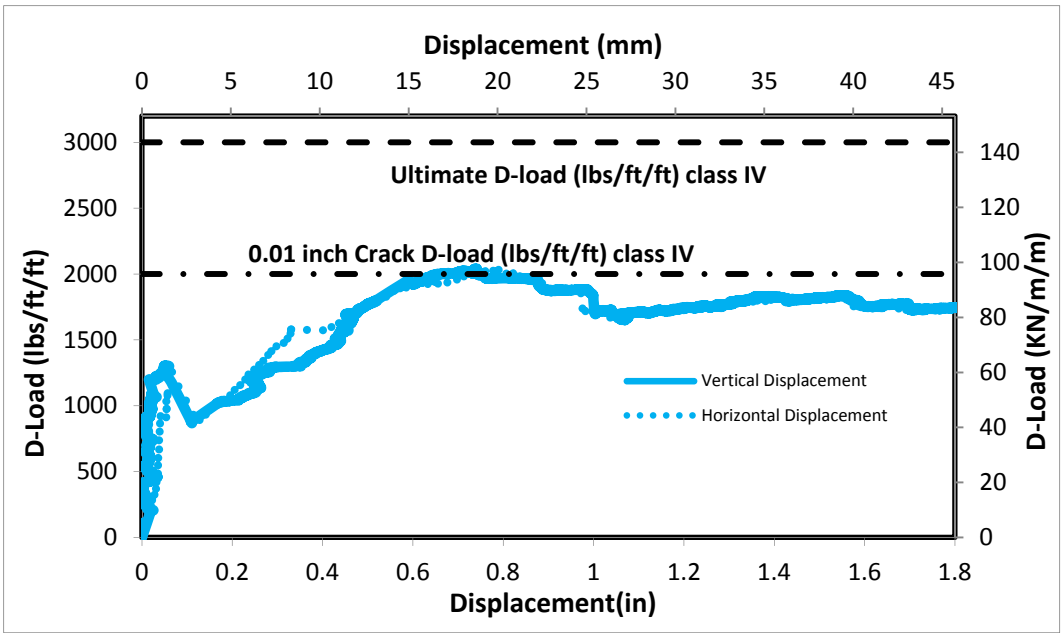

Figure B-92 Load-Deflection Plot for RCP-36-6-B

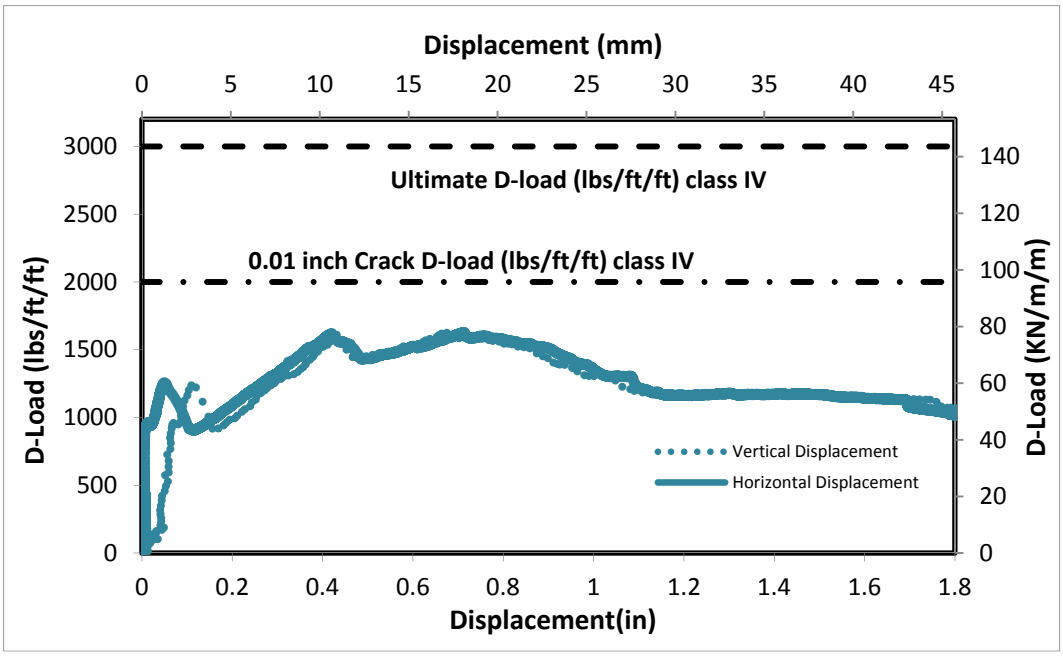

Figure B-93 Load-Deflection Plot for CRCP-36-6-B-10%rubber

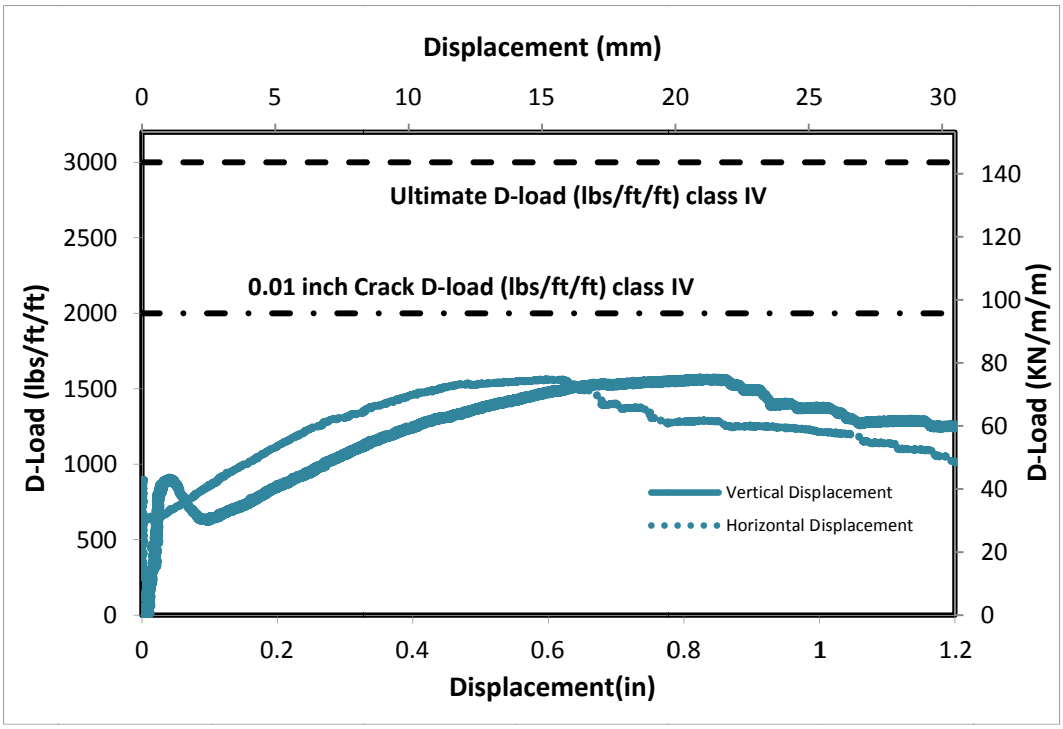

Figure B-94 Load-Deflection Plot for CRCP-24-6-B-15%rubber

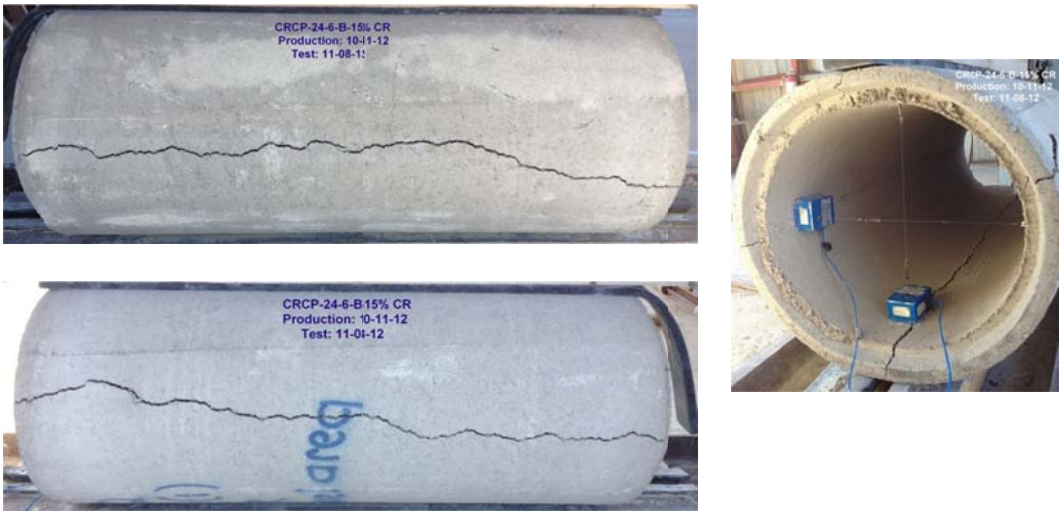

Figure B-95 Crack propagation for CRCP-24-6-B-15%rubber

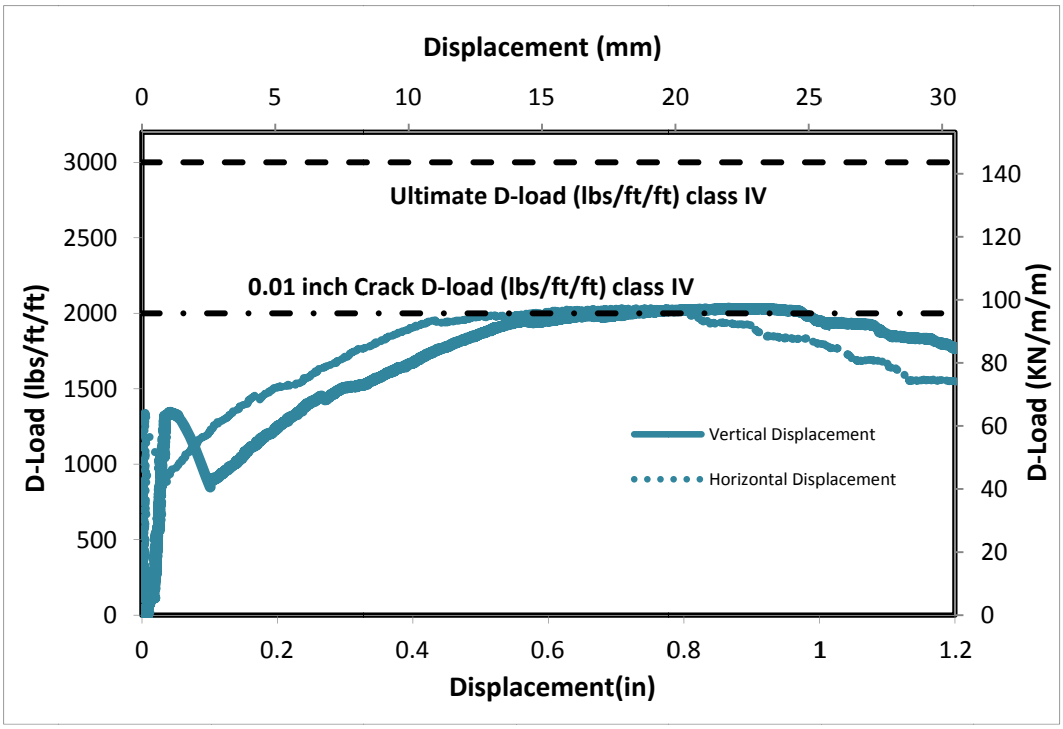

Figure B-96 Load-Deflection Plot for RCP-24-6-B

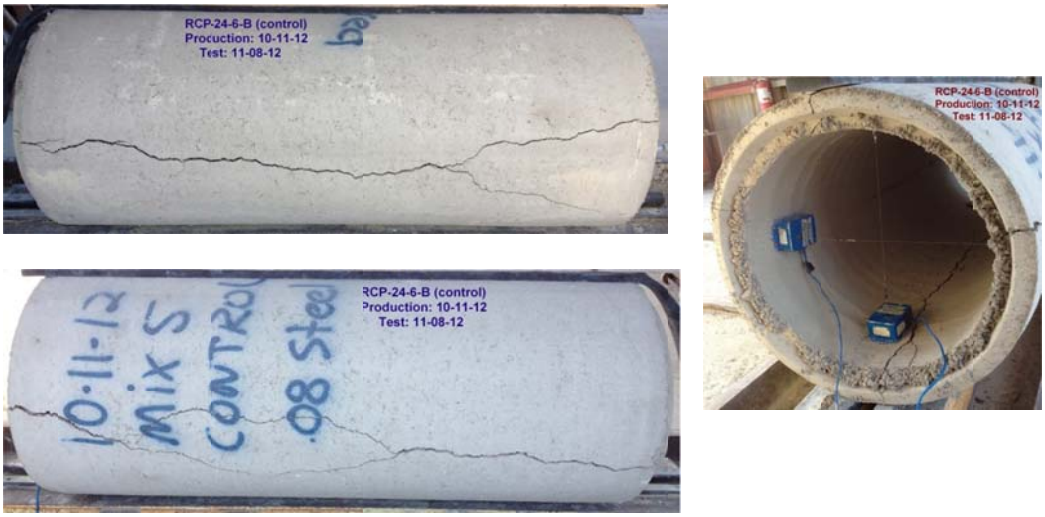

Figure B-97 Crack propagation for RCP-24-6-B

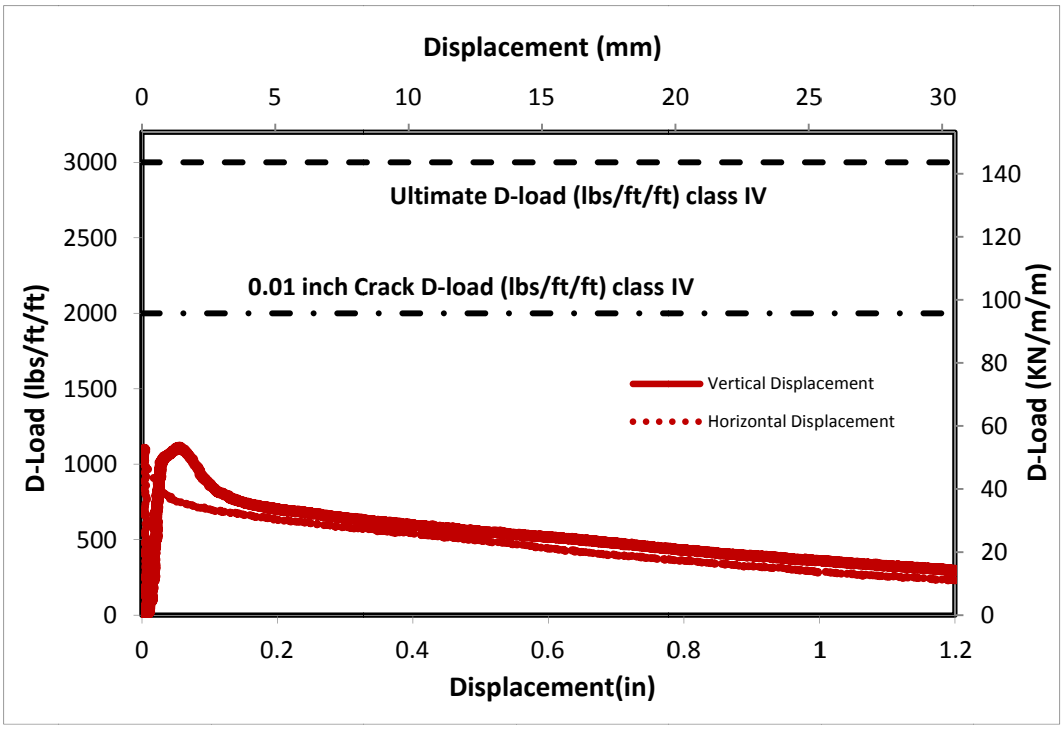

Figure B-98 Load-Deflection Plot for HYCP-24-6-B-44lbs steel-15%rubber

Figure B-99 Crack propagation for HYCP-24-6-B-44lbs steel-15%rubber

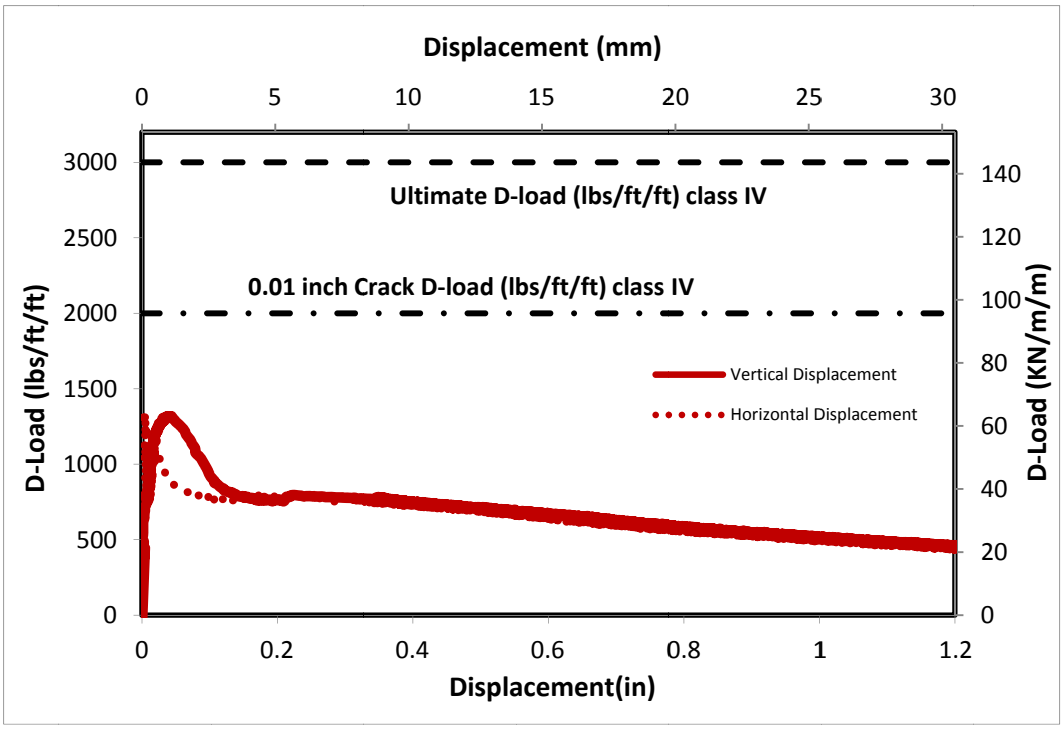

Figure B-100 Load-Deflection Plot for HYCP-24-6-B-44lbs steel-15%rubber

Figure B-101 Crack propagation for HYCP-24-6-B-44lbs steel-15%rubber

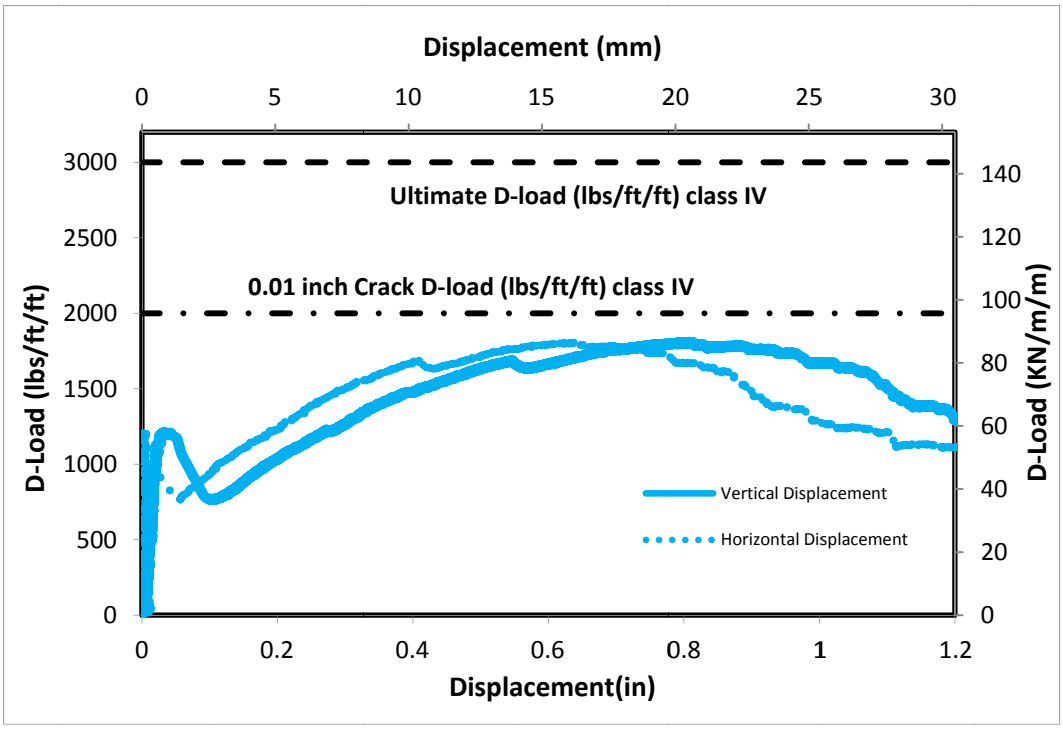

Figure B-102 Load-Deflection Plot for RCP-24-6-B

Figure B-103 Crack propagation for RCP-24-6-B

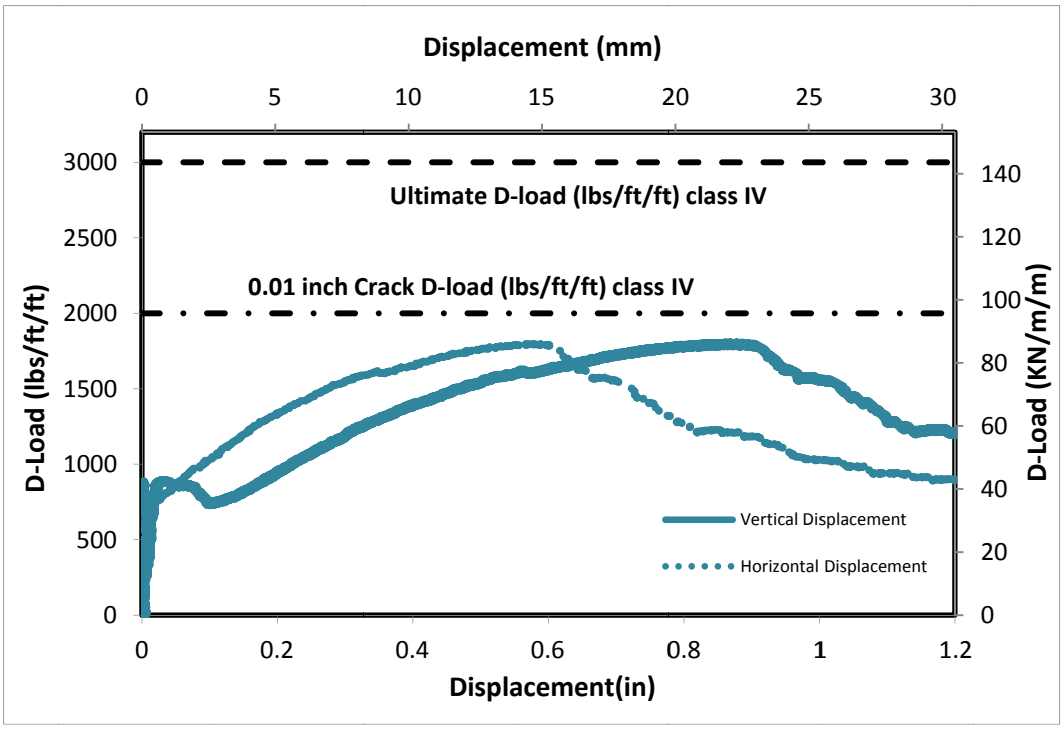

Figure B-104 Load-Deflection Plot for CRCP-24-6-B-15%rubber

Figure B-105 Crack propagation for CRCP-24-6-B-15%rubber

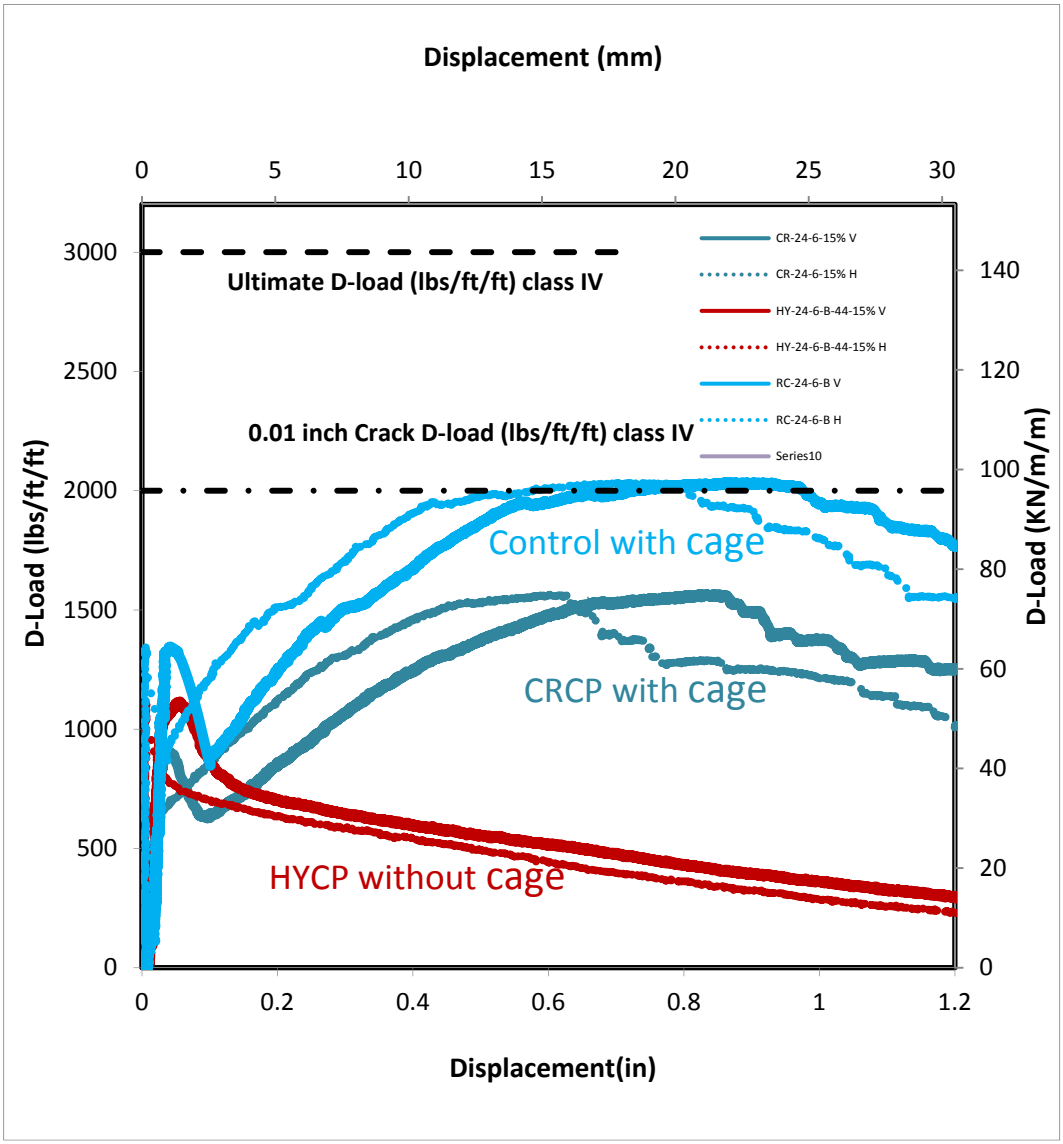

Figure B-106 Load-Deflection Plot for HYCP-24-6-B-44lbs steel-15%rubber, CRCP-24-6-15%rubber and RCP-24-6-B

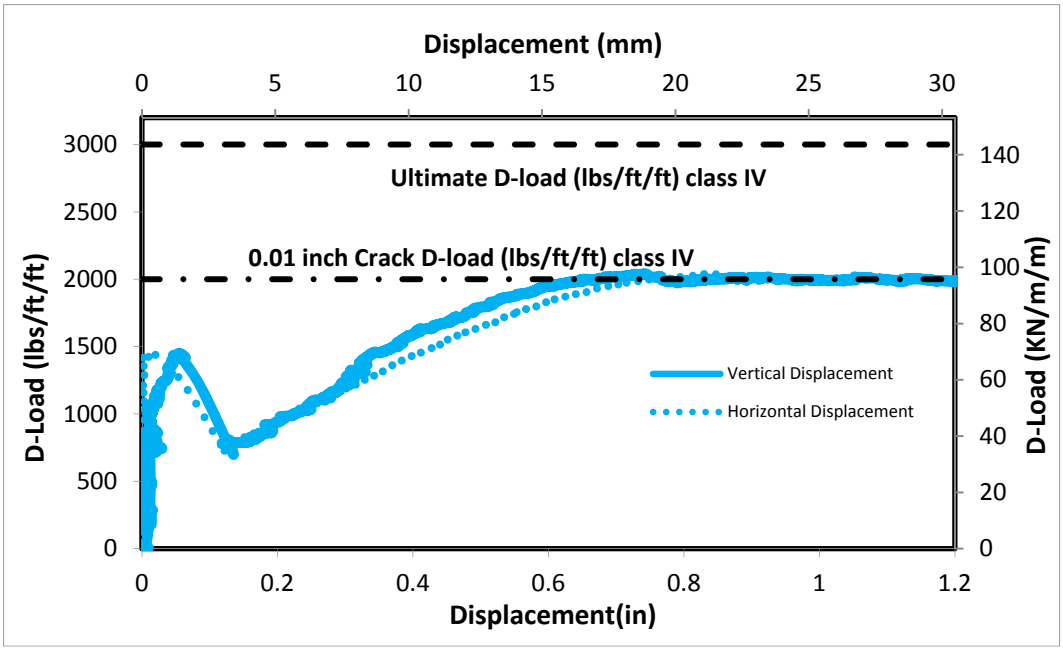

Figure B-107 Load-Deflection Plot for RCP-24-6-B-20%rubber

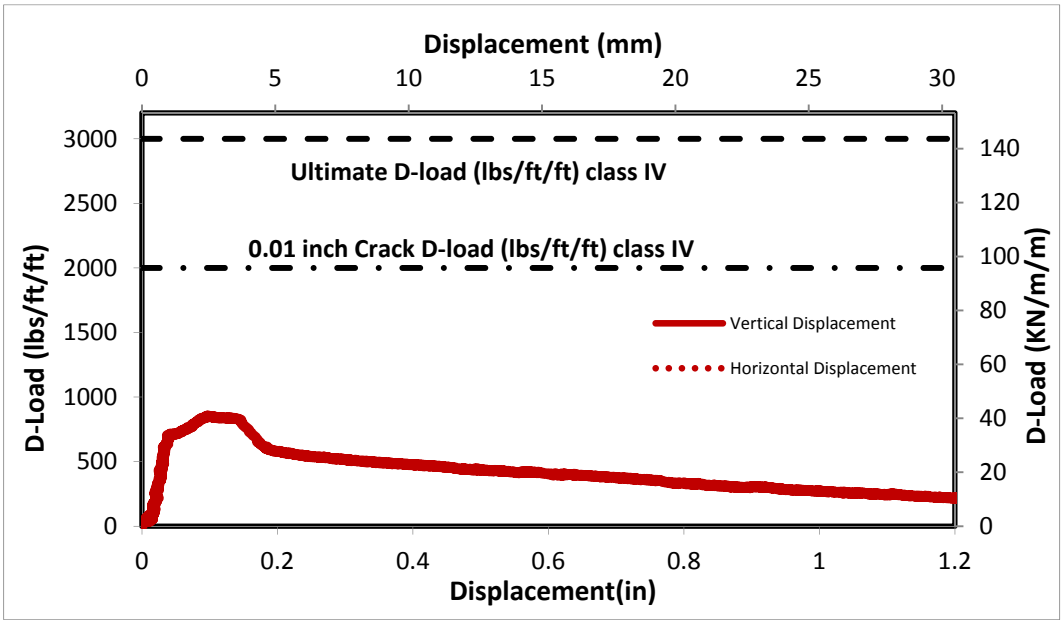

Figure B-108 Load-Deflection Plot for HYCP-24-6-B-44lbs steel-20%rubber

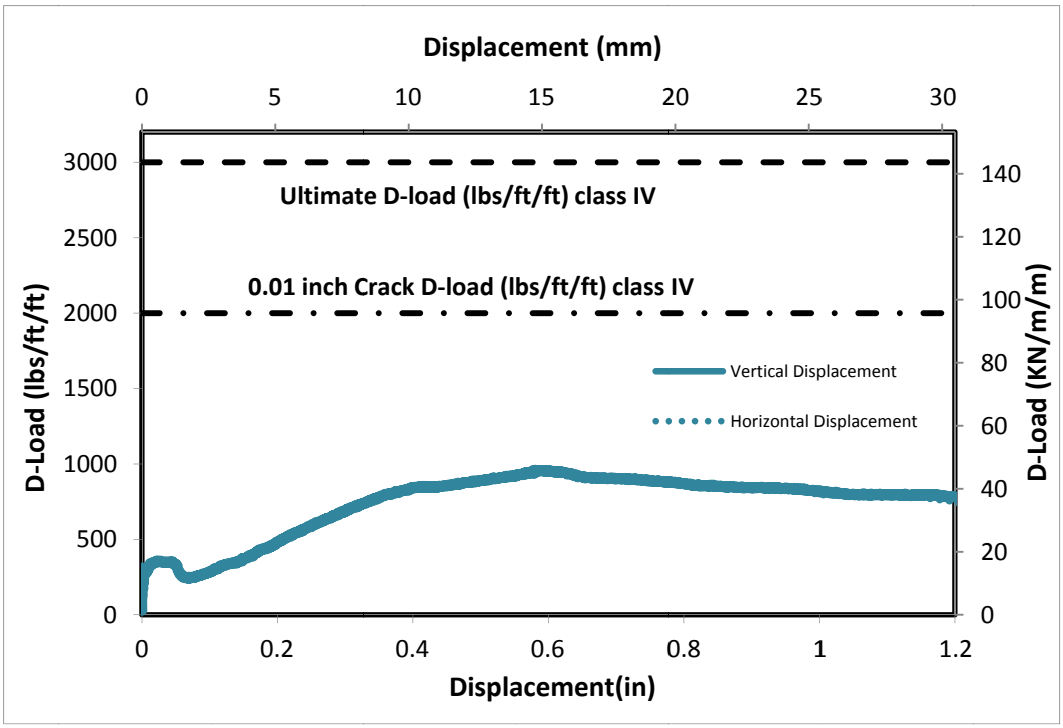

Figure B-109 Load-Deflection Plot for CRCP-24-6-B-20%rubber

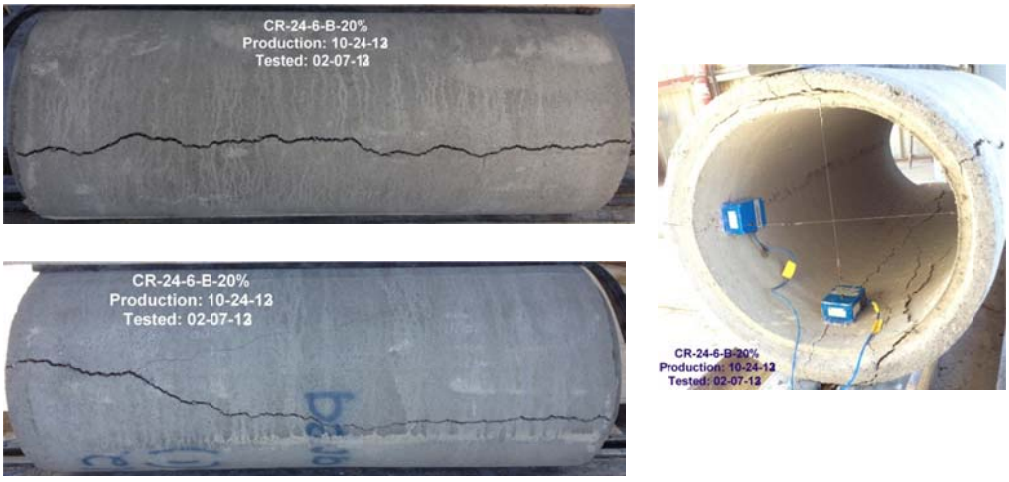

Figure B-110 Crack propagation for CRCP-24-6-B-20%rubber

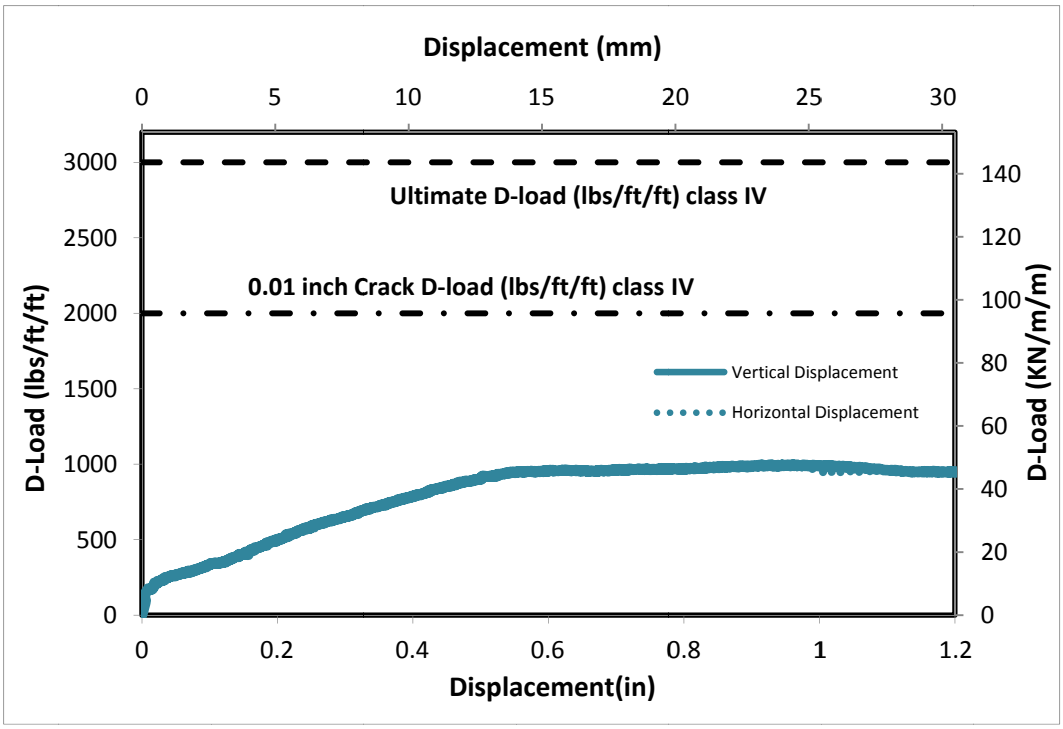

Figure B-111 Load-Deflection Plot for CRCP-24-6-B-20%rubber

Figure B-112 Crack propagation for CRCP-24-6-B-20%rubber

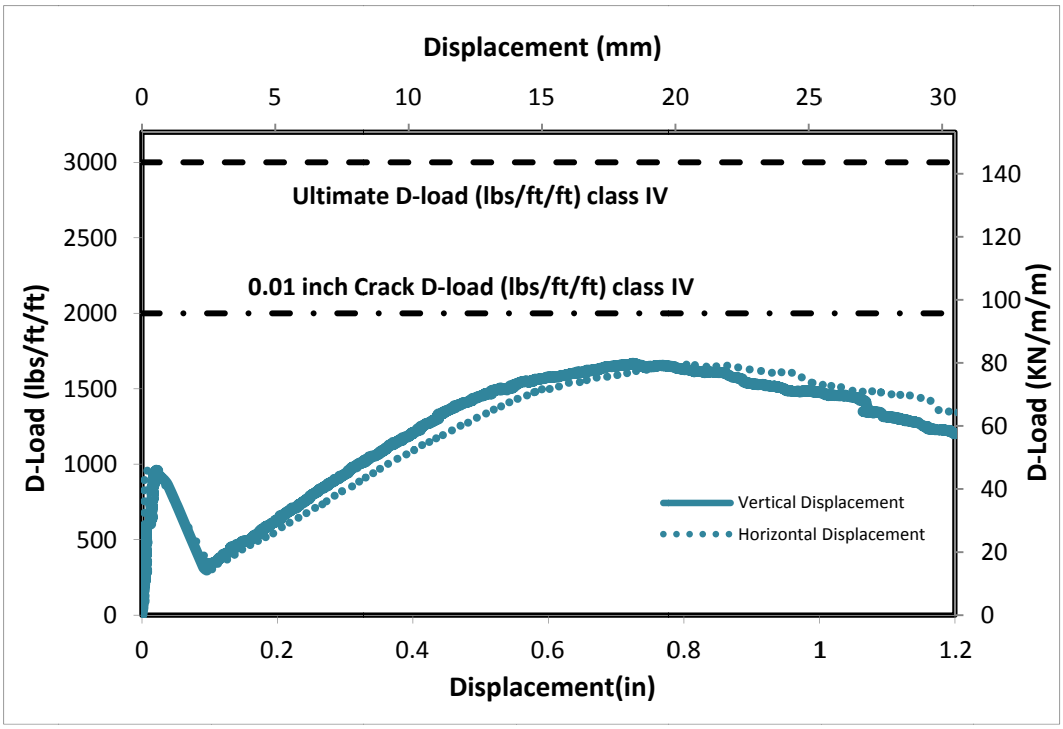

Figure B-113 Load-Deflection Plot for RCP-24-6-B

Figure B-114 Crack propagation for RCP-24-6-B

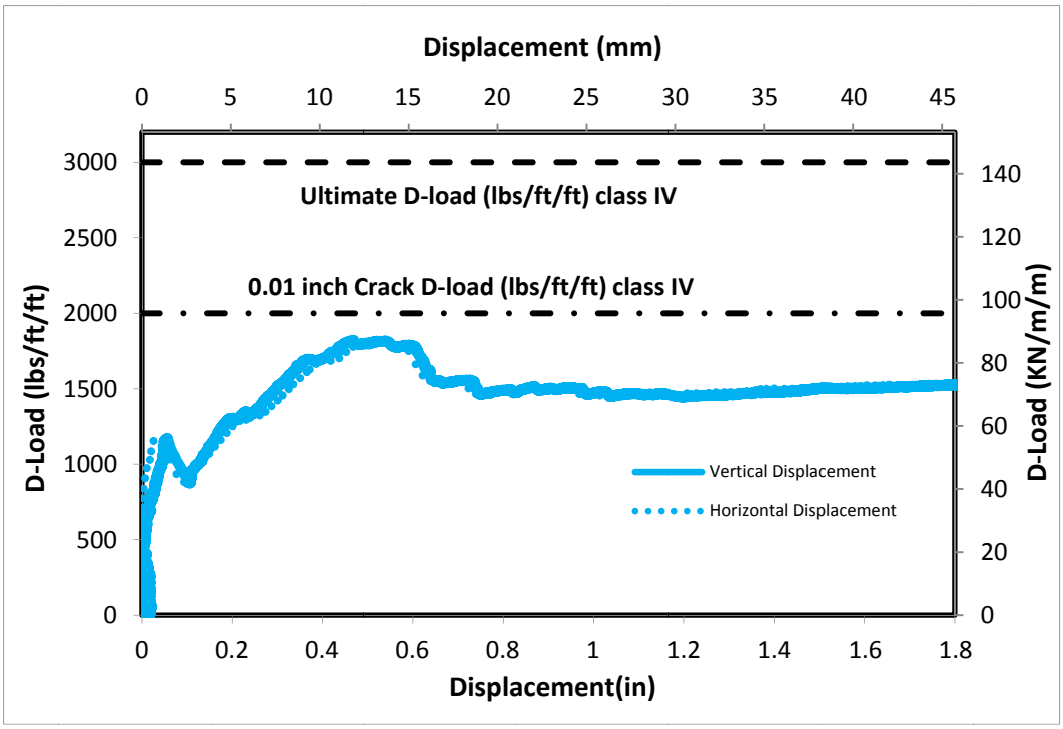

Figure B-115 Load-Deflection Plot for RCP-36-6-B

Figure B-116 Crack propagation for RCP-36-6-B

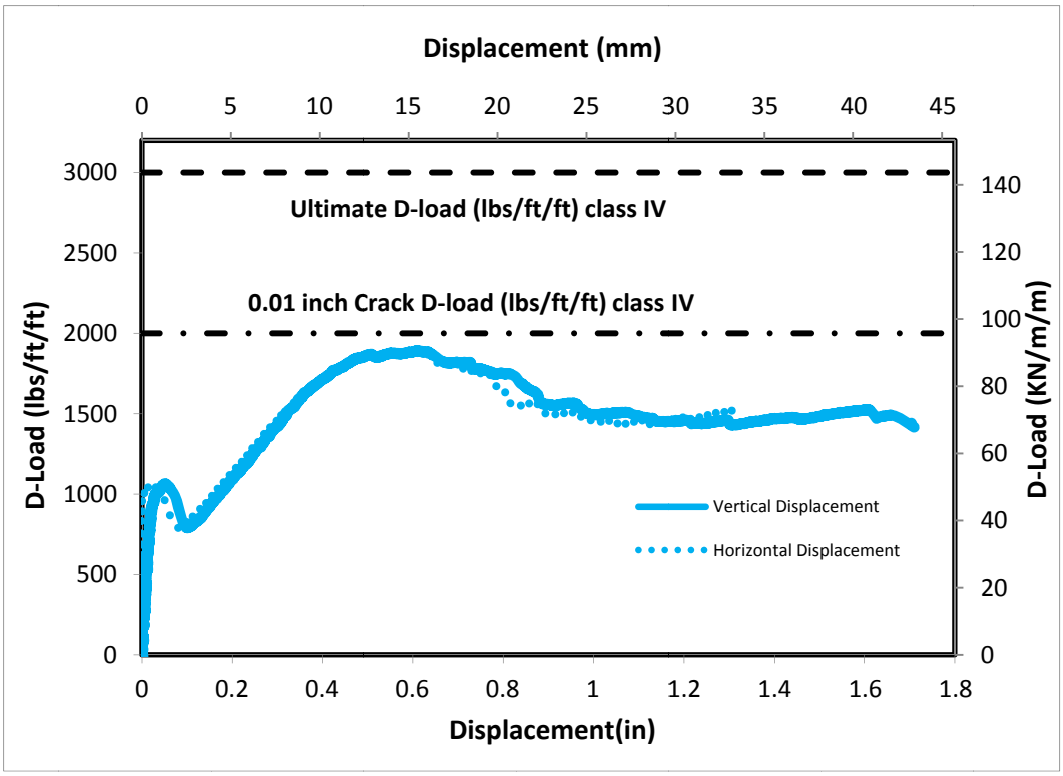

Figure B-117 Load-Deflection Plot for RCP-36-6-B

Figure B-118 Crack propagation for RCP-36-6-B

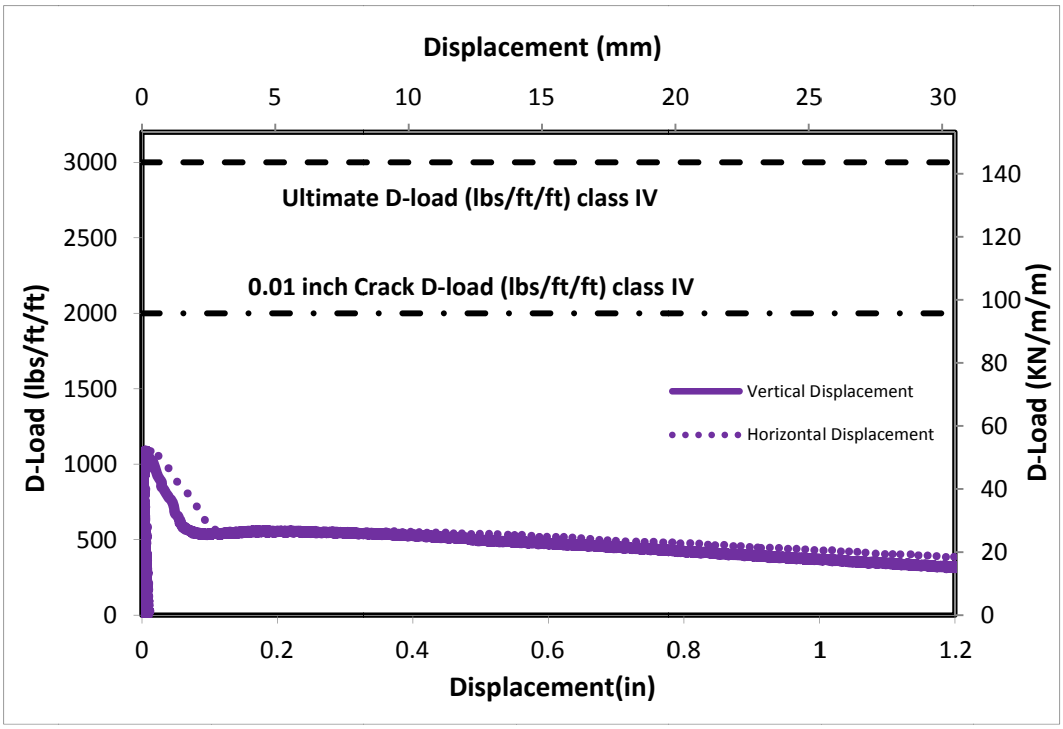

Figure B-119 Load-Deflection Plot for SNFCP-24-6-B-10%rubber-8lbs synth

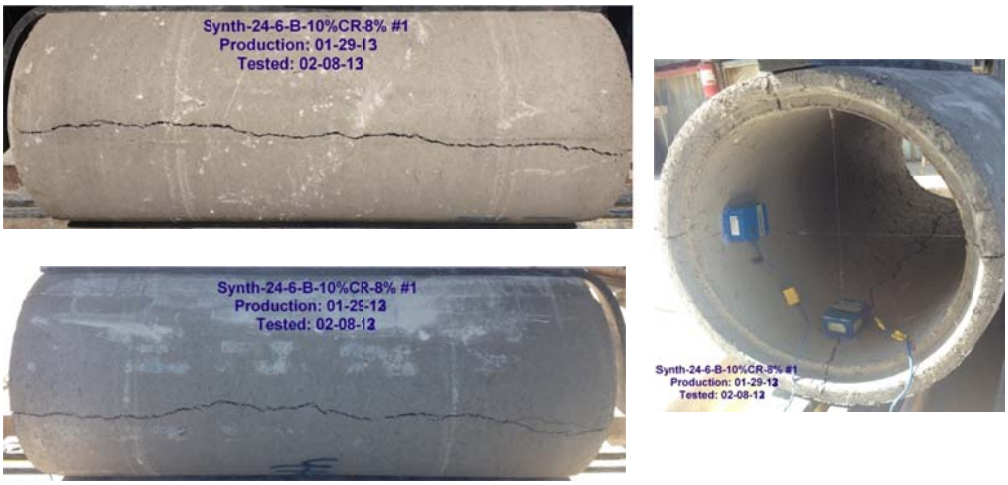

Figure B-120 Crack propagation for SNFCP-24-6-B-10%rubber-8lbs synth

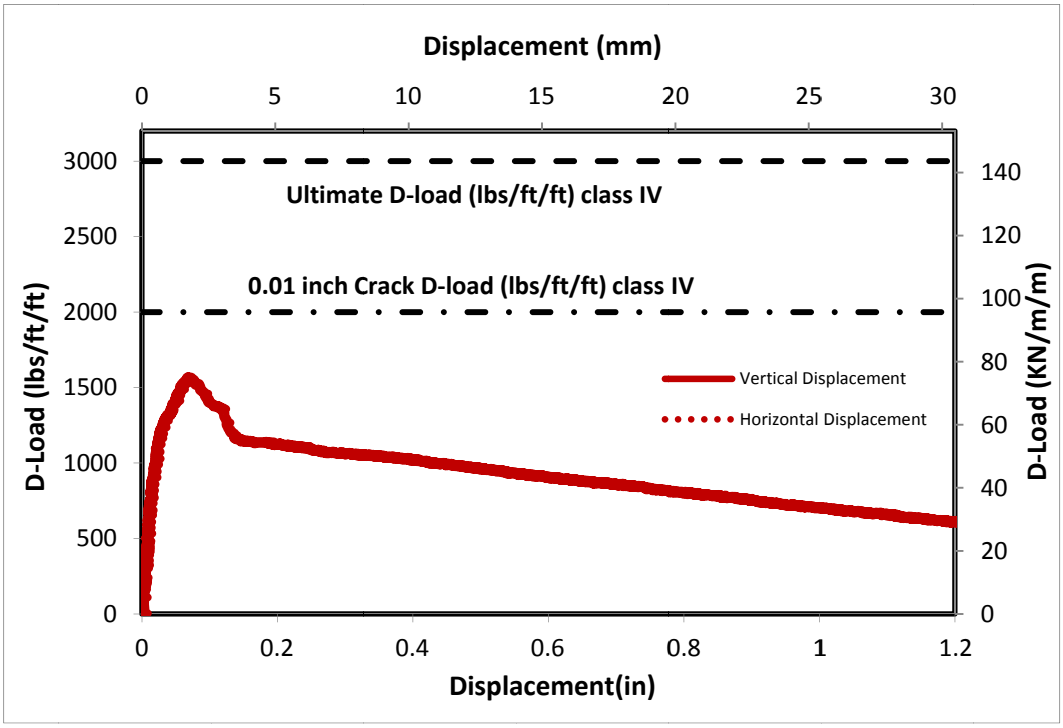

Figure B-121 Load-Deflection Plot for HYCP-24-6-B-44lbs steel-10%rubber

Figure B-122 Crack propagation for HYCP-24-6-B-44lbs steel-10%rubber

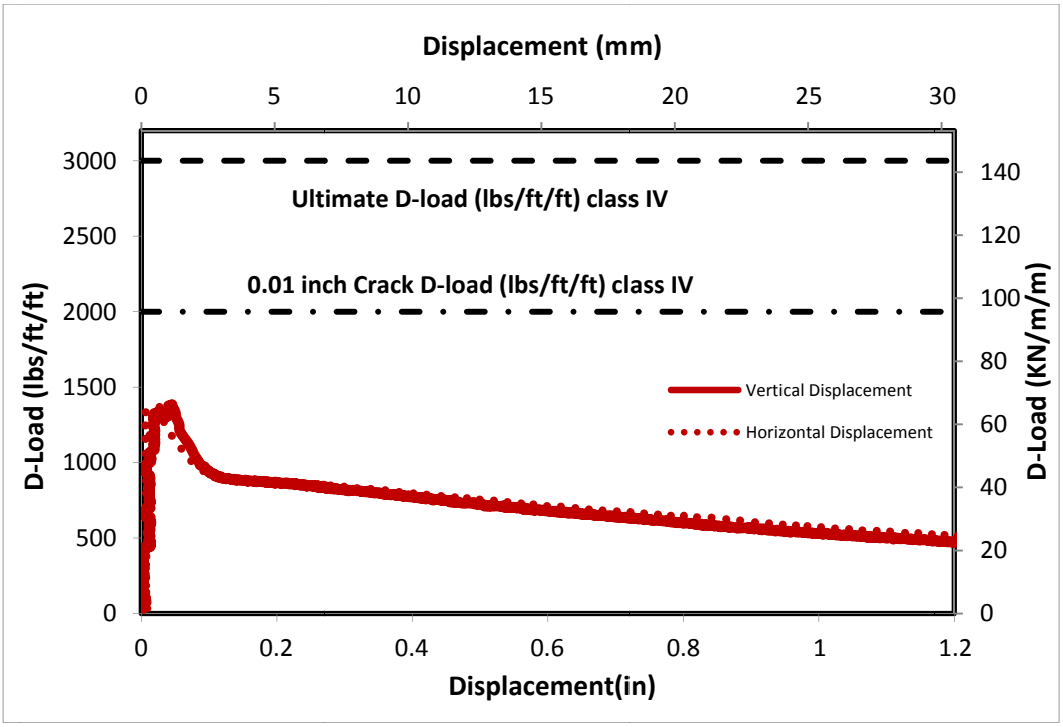

Figure B-123 Load-Deflection Plot for HYCP-24-6-B-44lbs steel-10%rubber

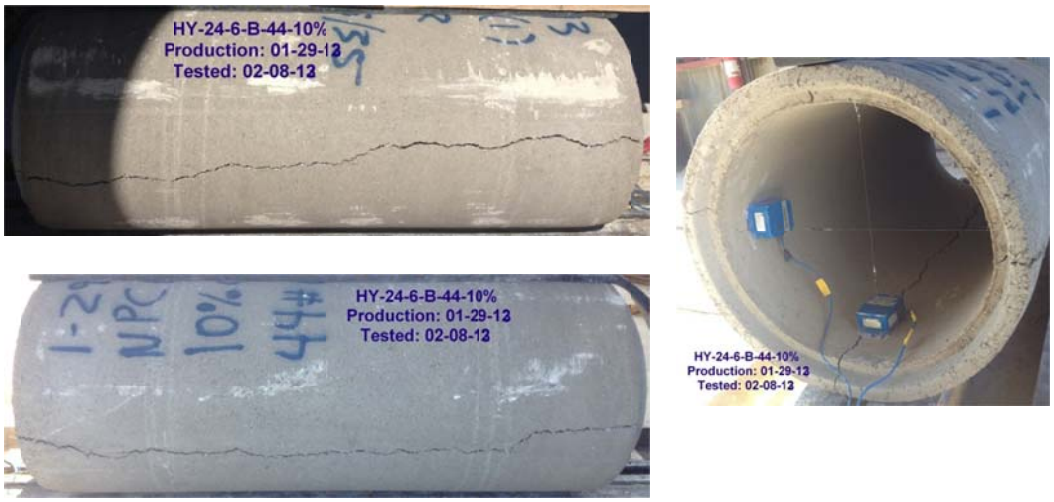

Figure B-124 Crack propagation for HYCP-24-6-B-44lbs steel-10%rubber

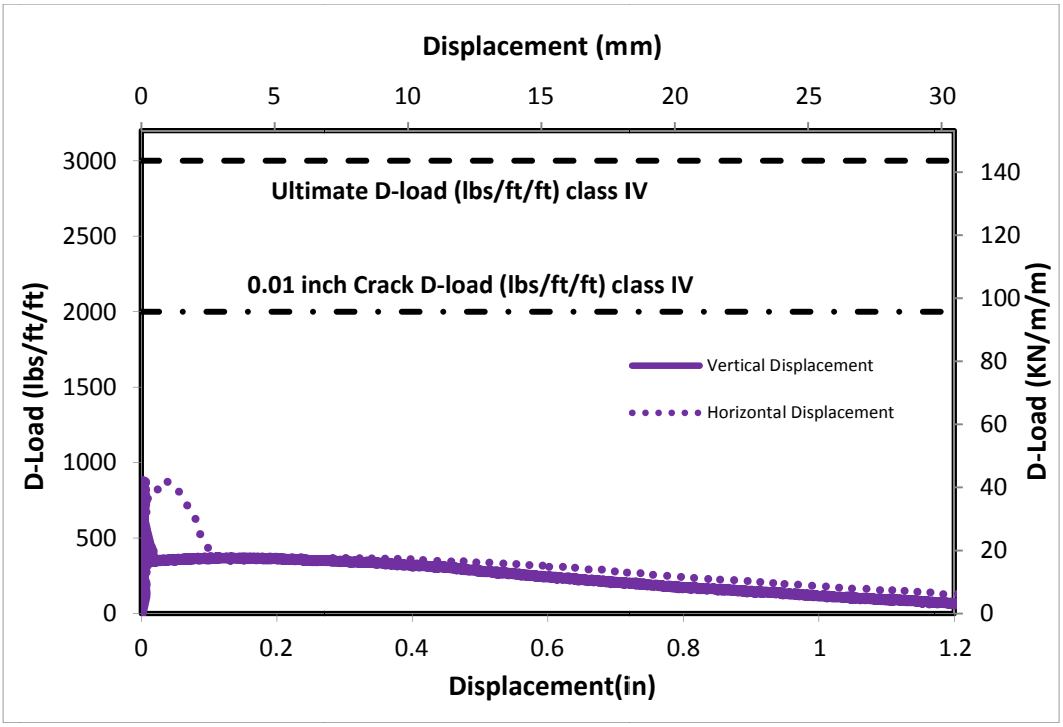

Figure B-125 Load-Deflection Plot for SNFCP-24-6-B-10%rubber-8lbs synth

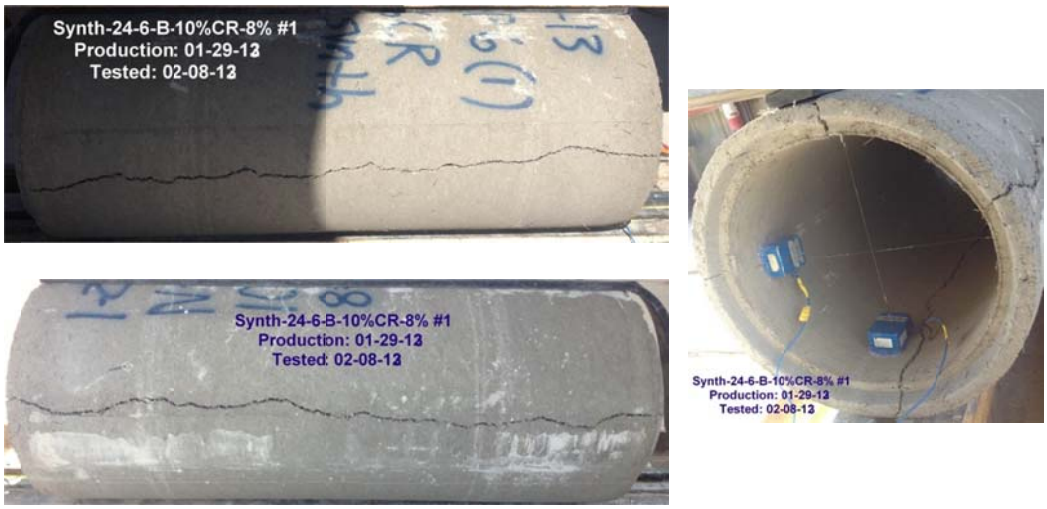

Figure B-126 Crack propagation for SNFCP-24-6-B-10%rubber-8lbs synth

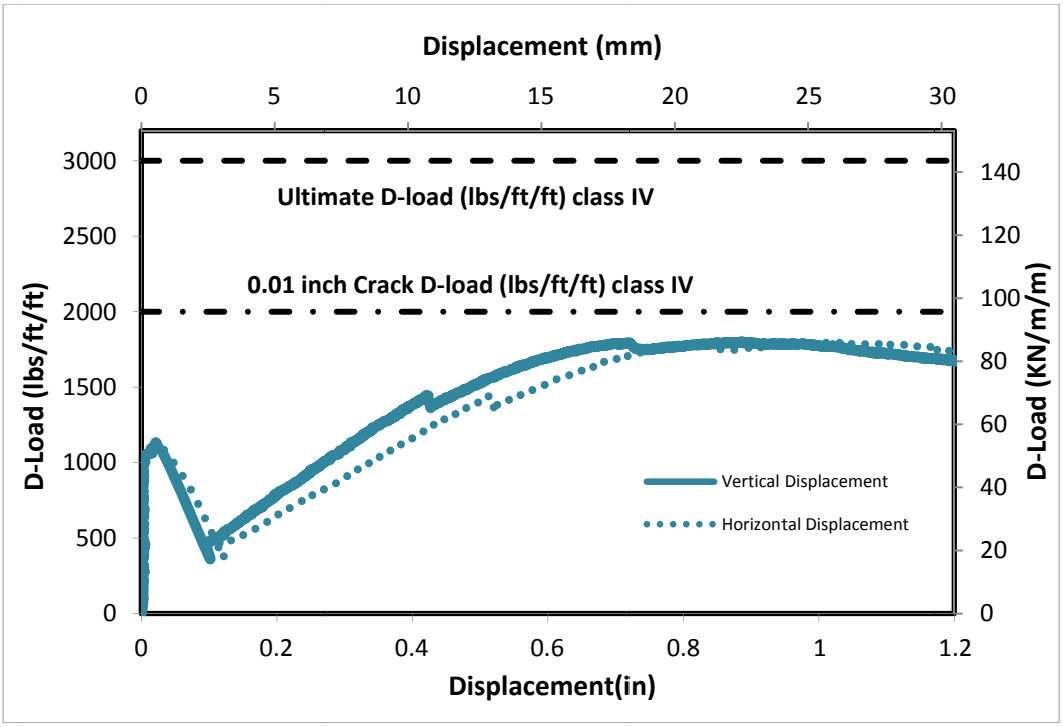

Figure B-127 Load-Deflection Plot for RCP-24-6-B

Figure B-128 Crack propagation for RCP-24-6-B

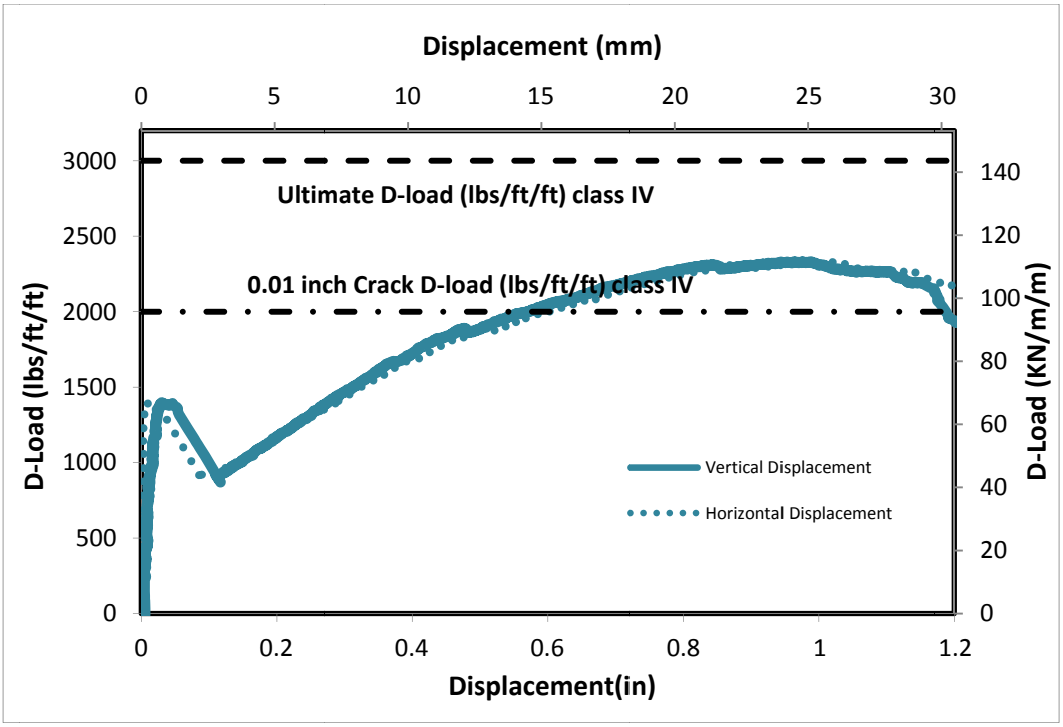

Figure B-129 Load-Deflection Plot for CRCP-24-6-10%rubber

Figure B-130 Crack propagation for CRCP-24-6-10%rubber

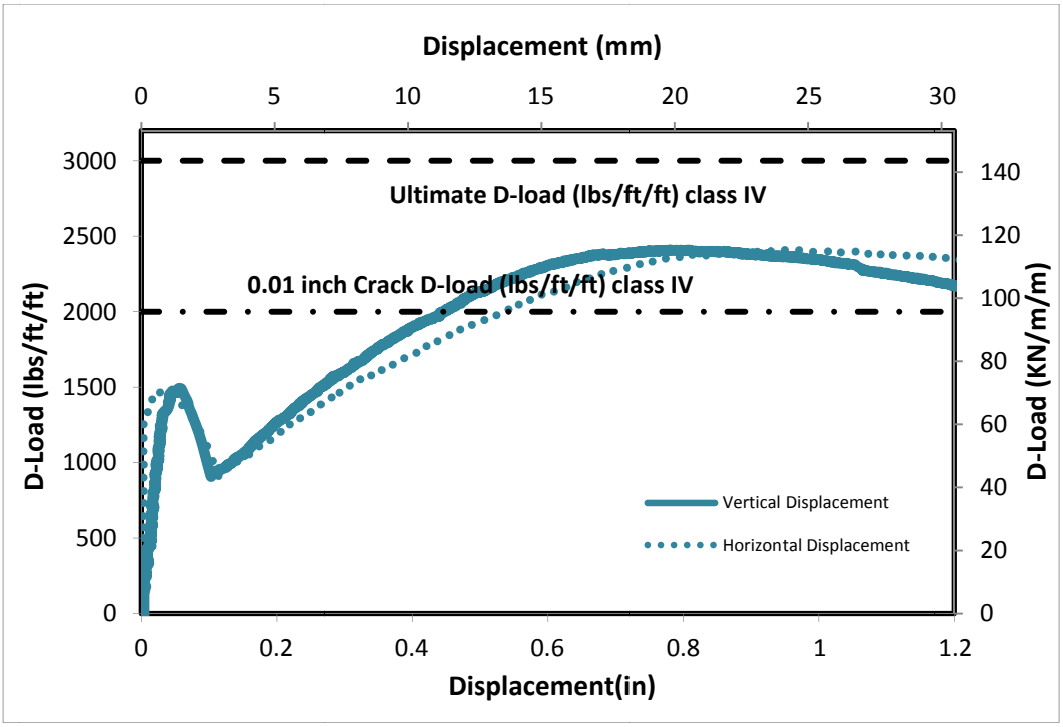

Figure B-131 Load-Deflection Plot for RCP-24-6-B

Figure B-132 Crack propagation for RCP-24-6-B

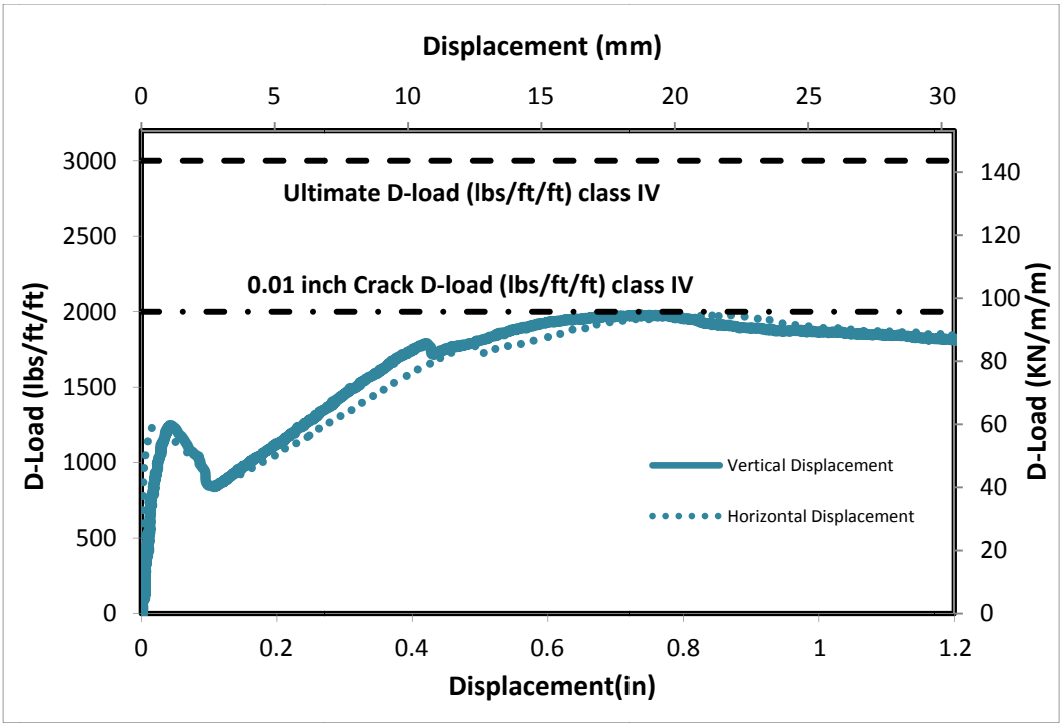

Figure B-133 Load-Deflection Plot for CRCP-24-6-10%rubber

Figure B-134 Crack propagation for CRCP-24-6-10%rubber

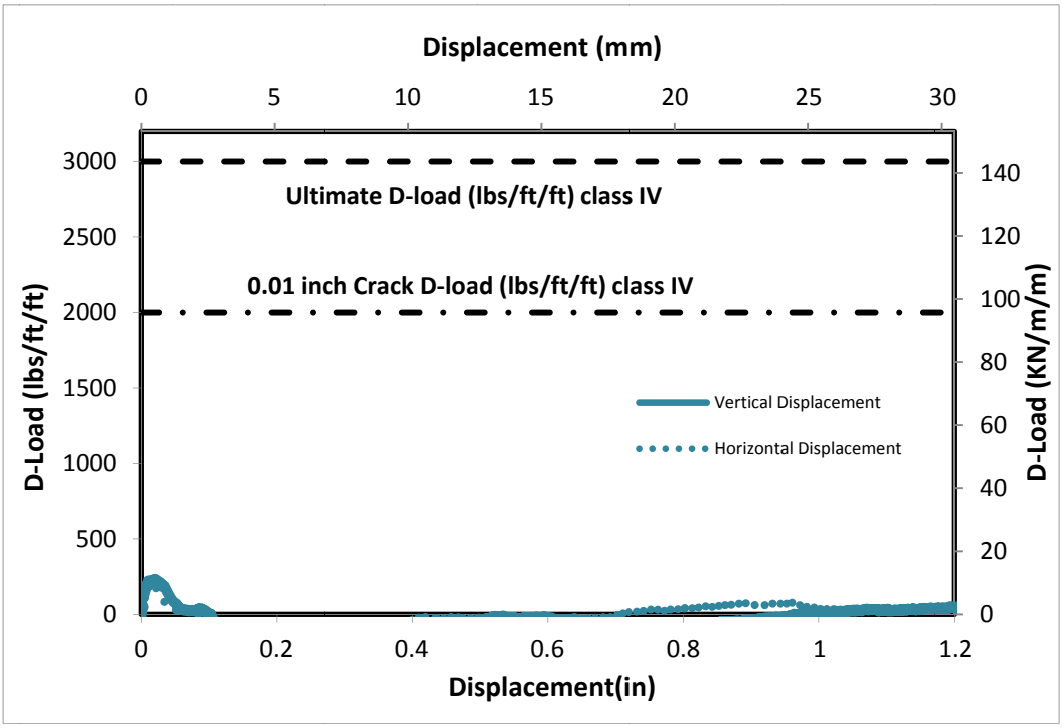

Figure B-135 Load-Deflection Plot for RCP-24-6-B

Figure B-136 Crack propagation for RCP-24-6-B

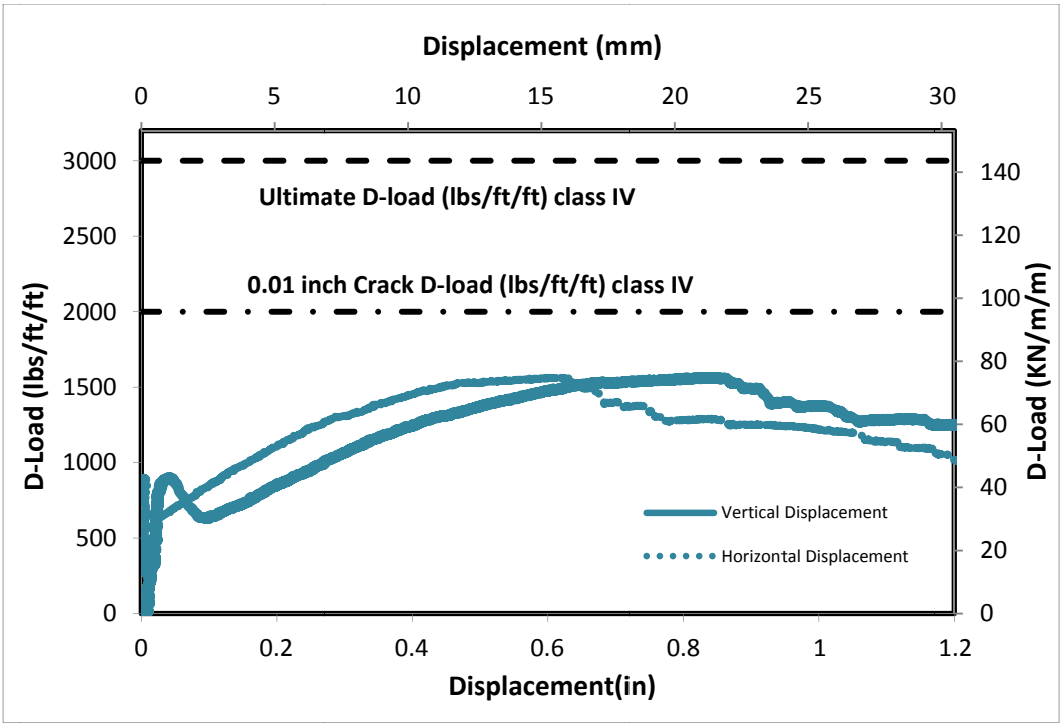

Figure B-137 Load-Deflection Plot for CRCP-24-6-B-20%rubber

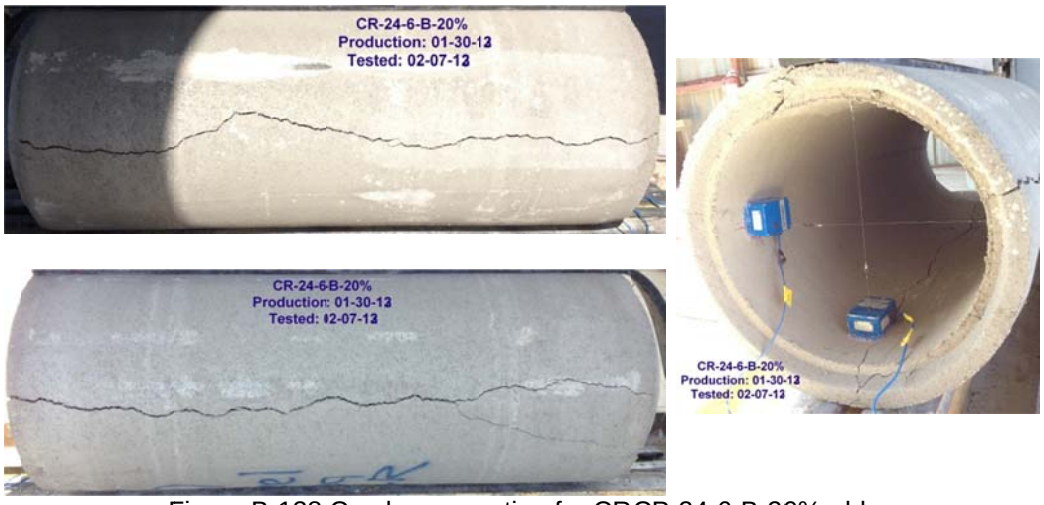

Figure B-138 Crack propagation for CRCP-24-6-B-20%rubber

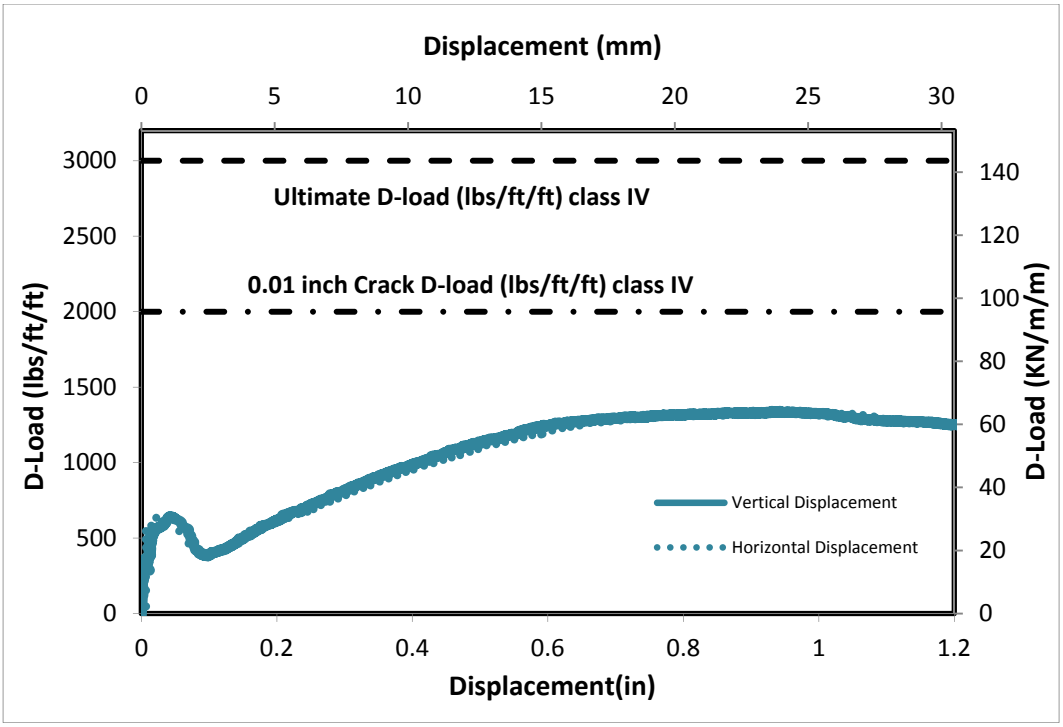

Figure B-139 Load-Deflection Plot for CRCP-24-6-B-20%rubber

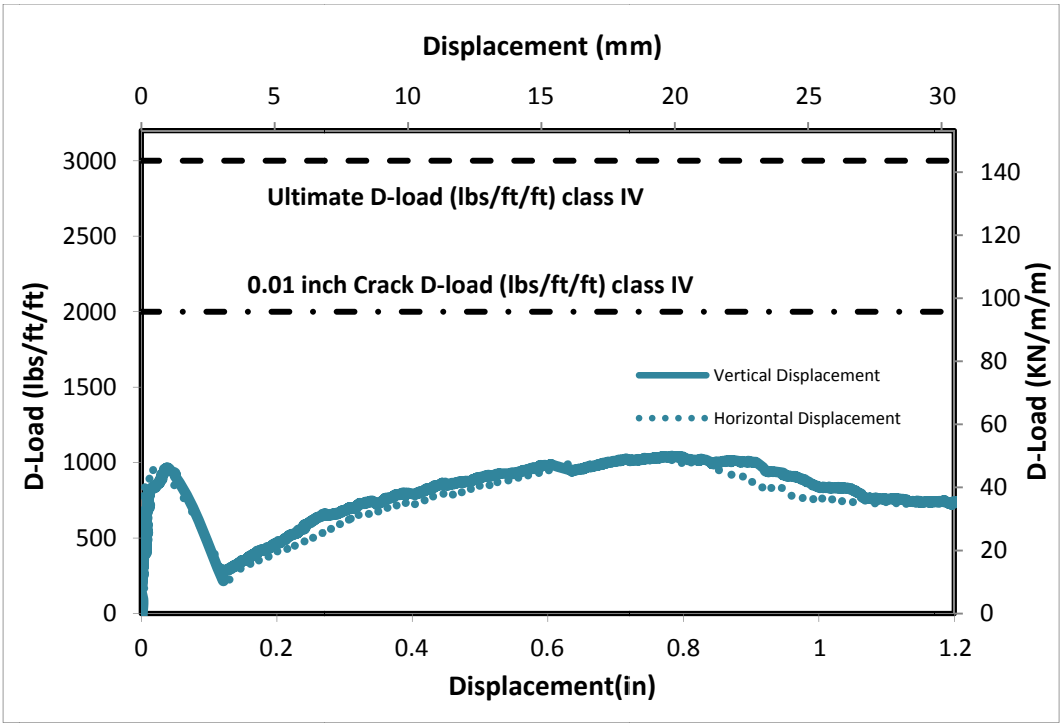

Figure B-140 Load-Deflection Plot for RCP-24-6-B

Figure B-141 Crack propagation for RCP-24-6-B

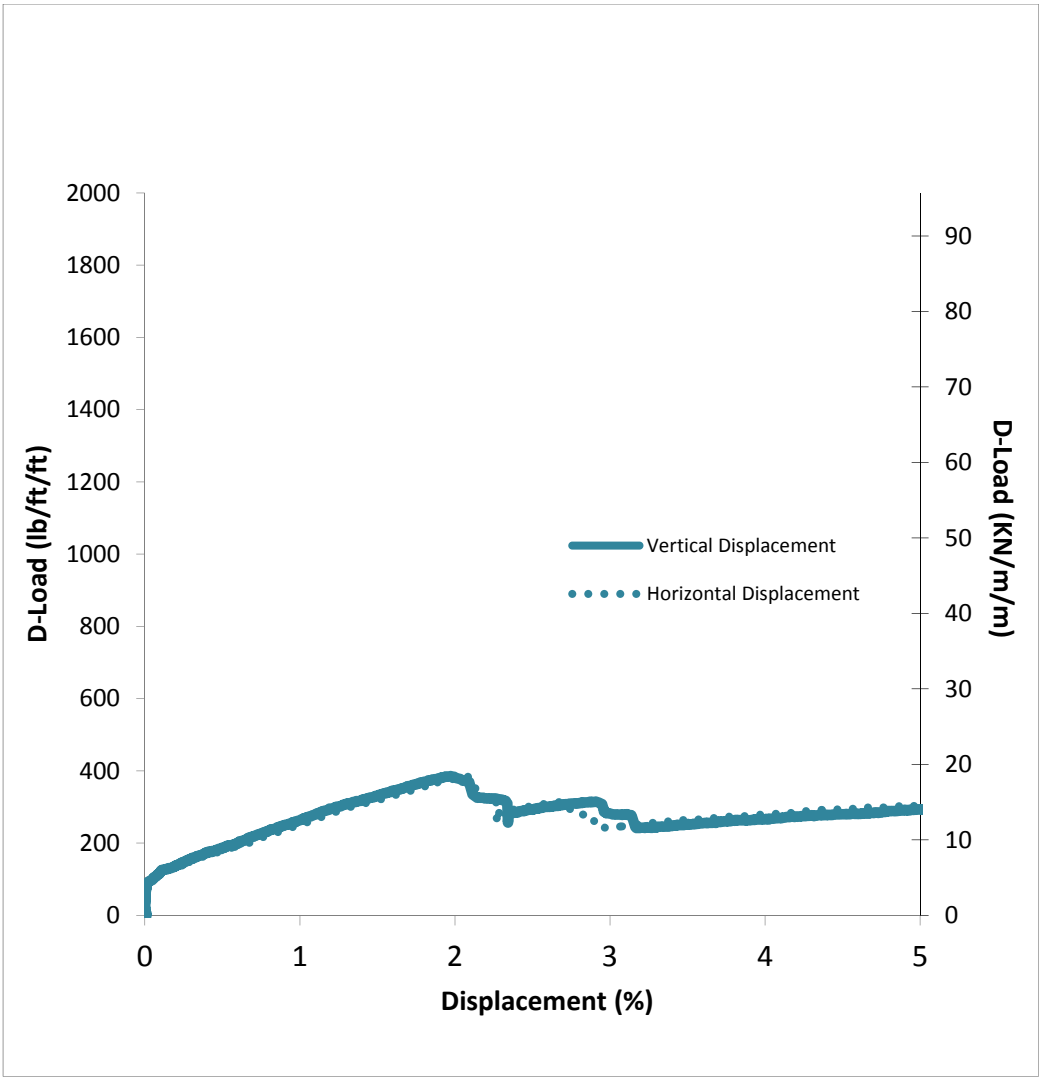

Figure B-142 Load-Deflection Plot for Thin wall- CR-60in-8ft-13%

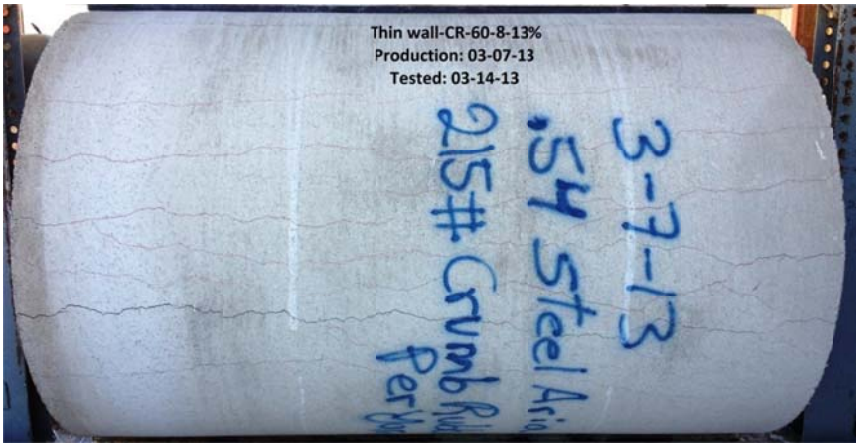

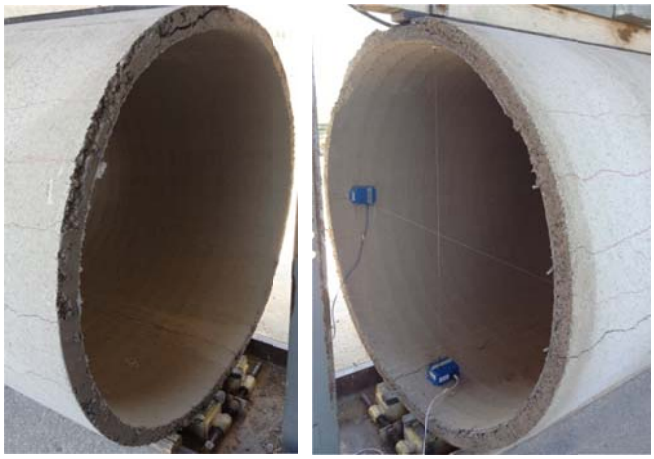

Figure B-143 Crack propagation for Thin wall-60-8-13%rubber

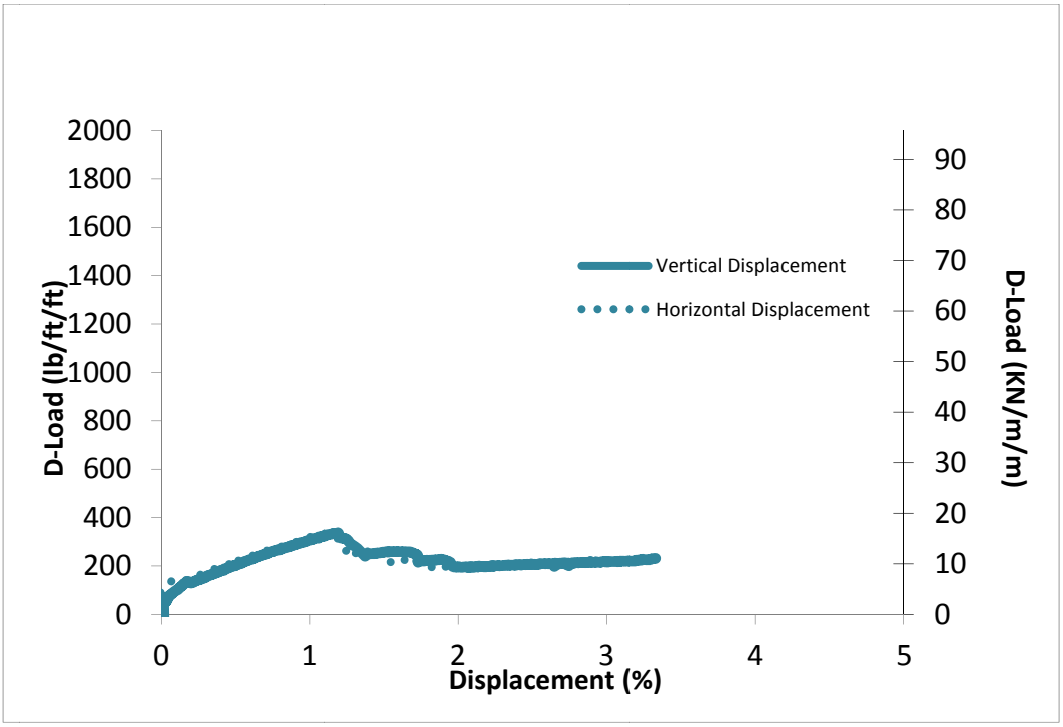

Figure B-144 Load-Deflection Plot for Thin wall-60"-20% rubber-8ft

Figure B-145 Crack propagation for Thin wall-60"-20% rubber-8ft

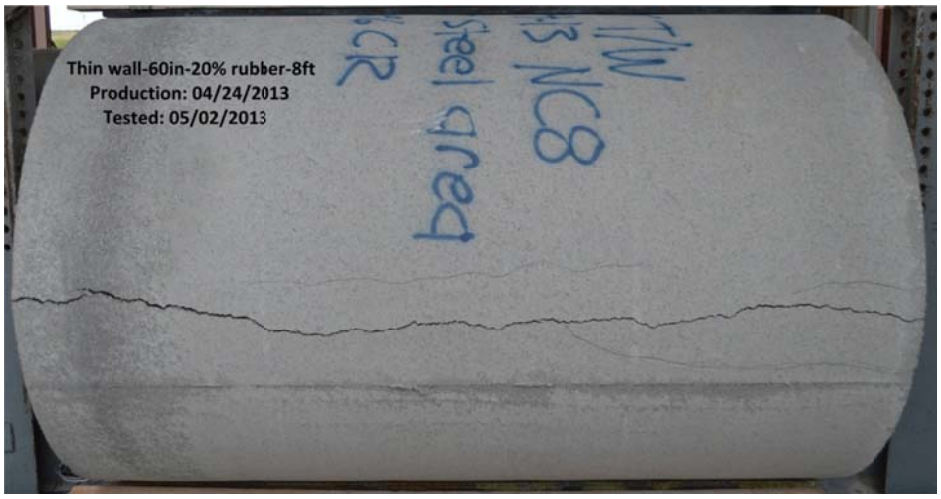

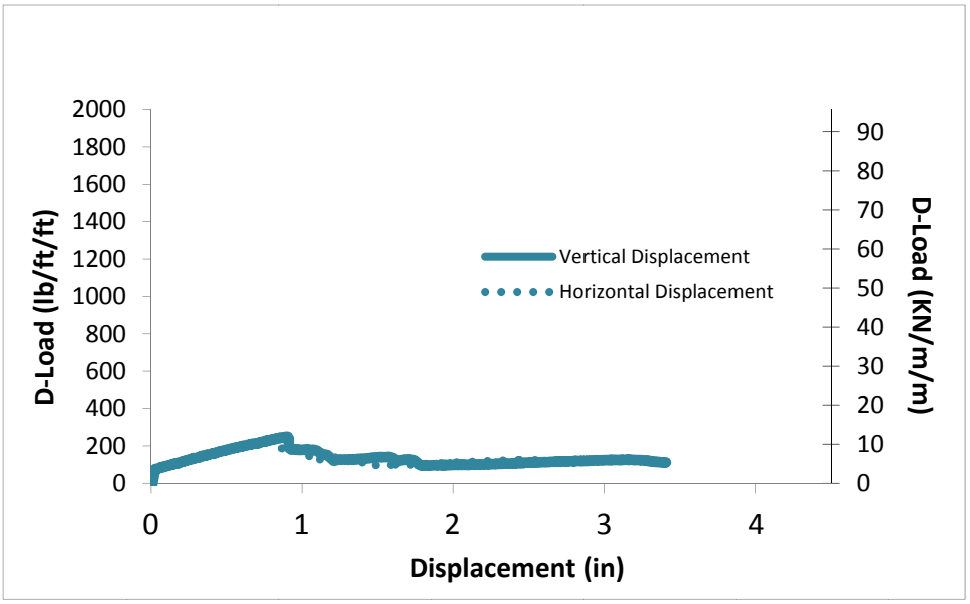

Figure B-146 Load-Deflection Plot for Thin wall-60"-20% rubber-8ft

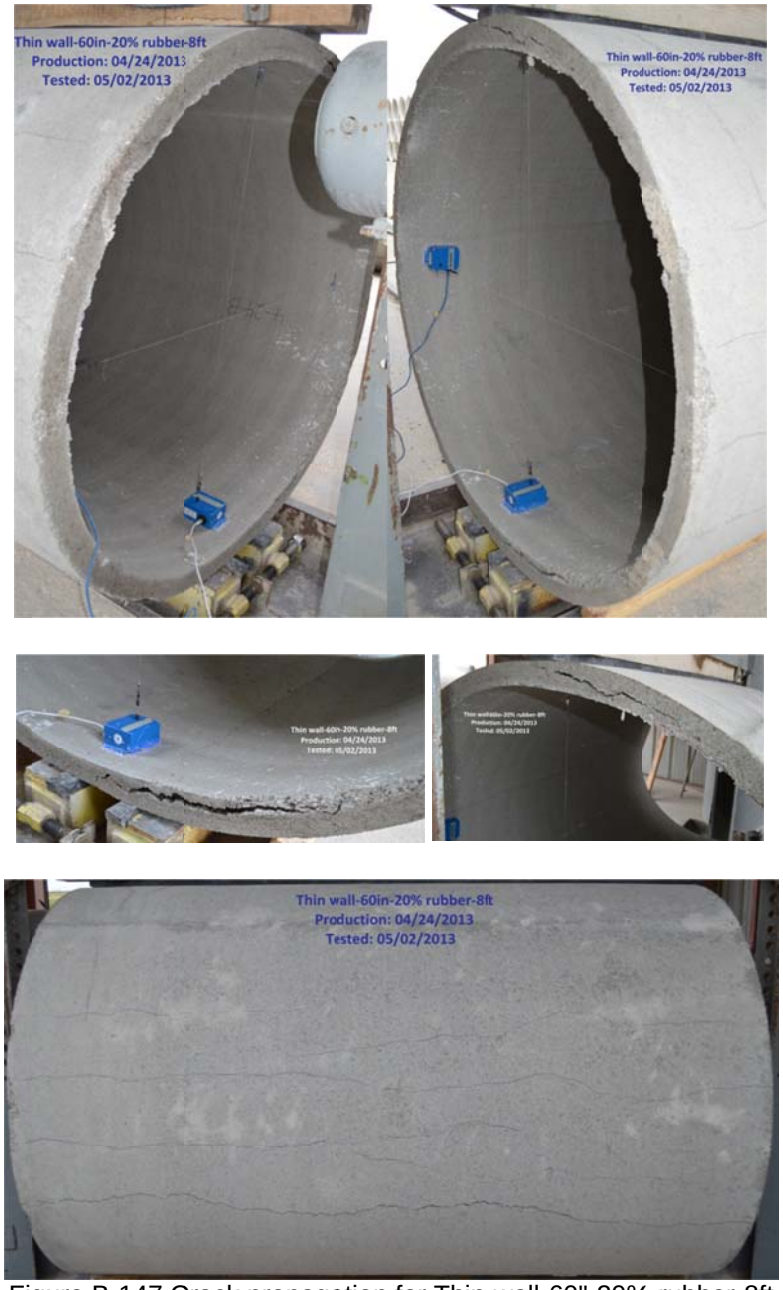

Figure B-147 Crack propagation for Thin wall-60"-20% rubber-8ft

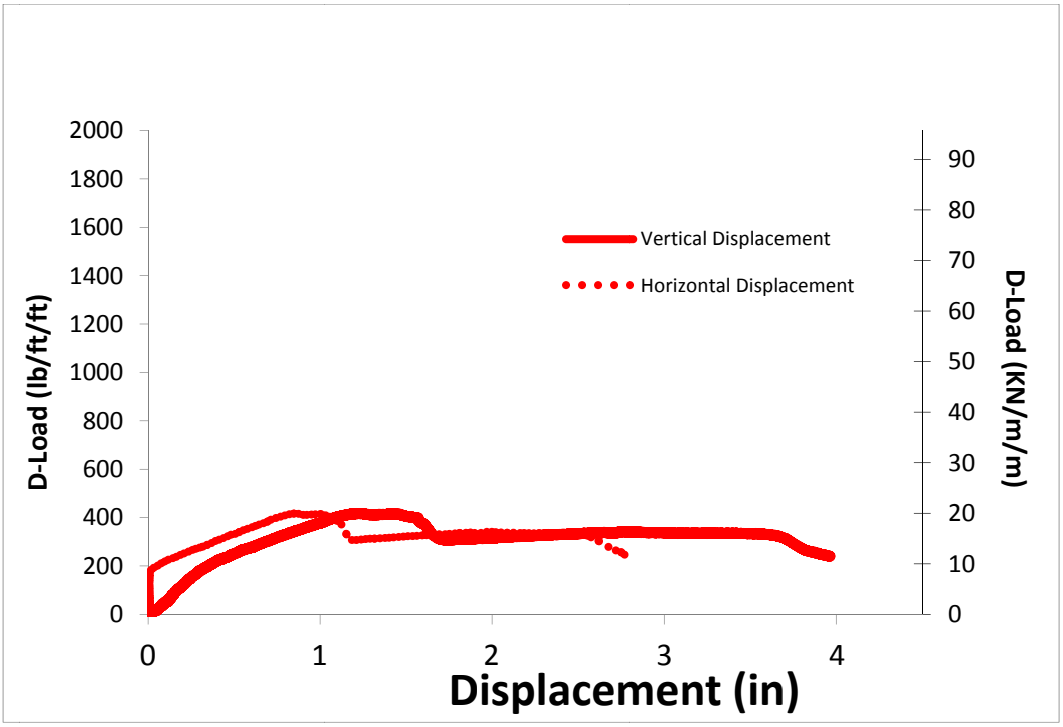

Figure B-148 Load-Deflection Plot for Thin wall-60"-11PCY SF-20% rubber-8ft

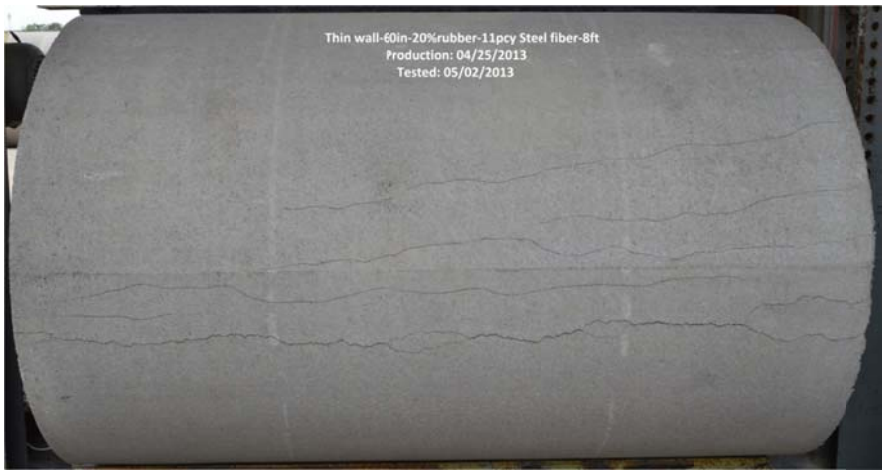

Figure B-149 Crack propagation for Thin wall-60"-11PCY SF-20% rubber-8ft

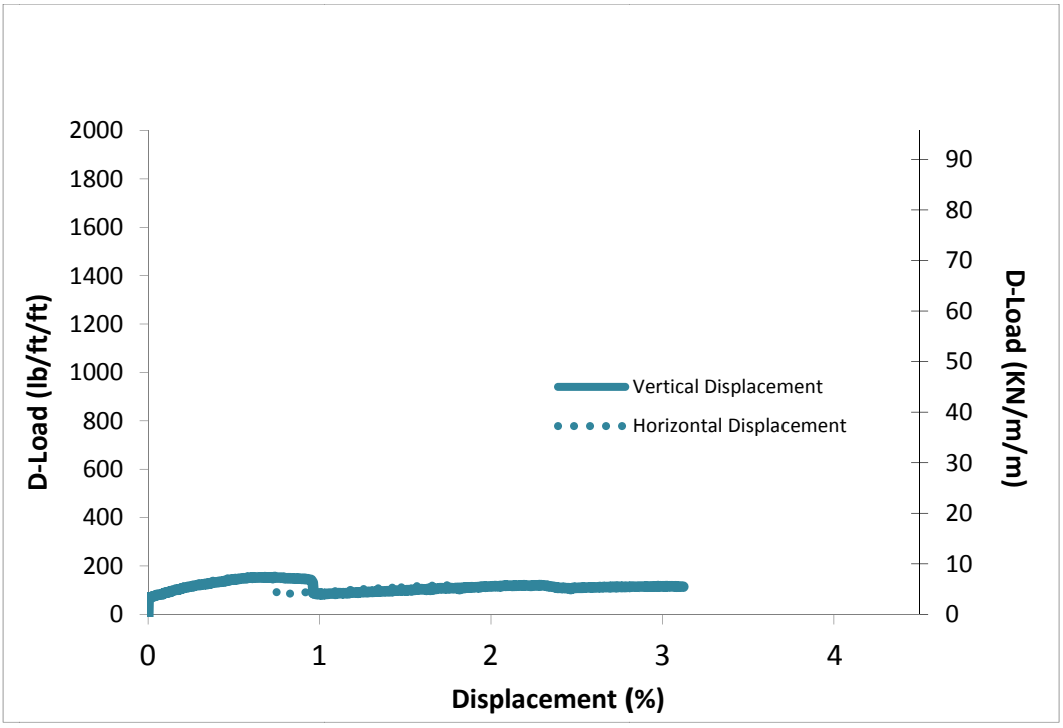

Figure B-150 Load-Deflection Plot for Thin wall-60"-4PCY Synth-20% rubber-8ft

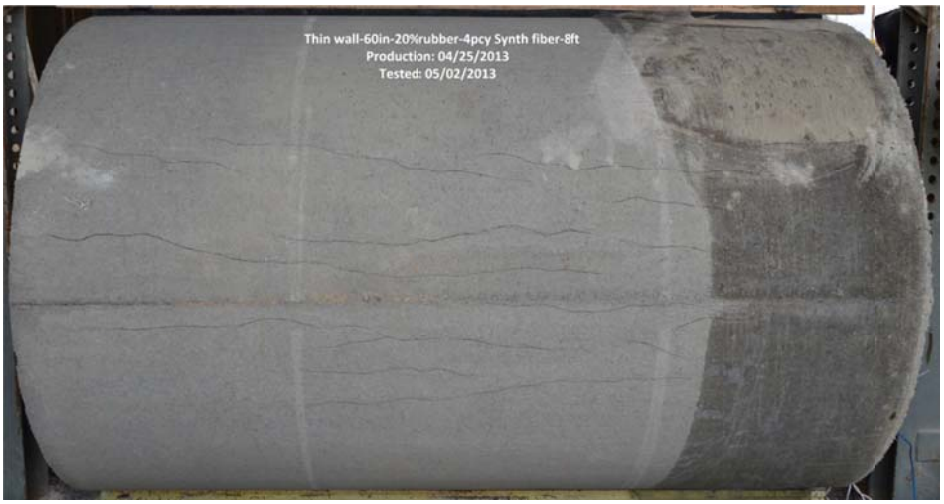

Figure B-151 Crack propagation for Thin wall-60"-4PCY Synth-20% rubber-8ft

Appendix C

Flexural Beam Test Results

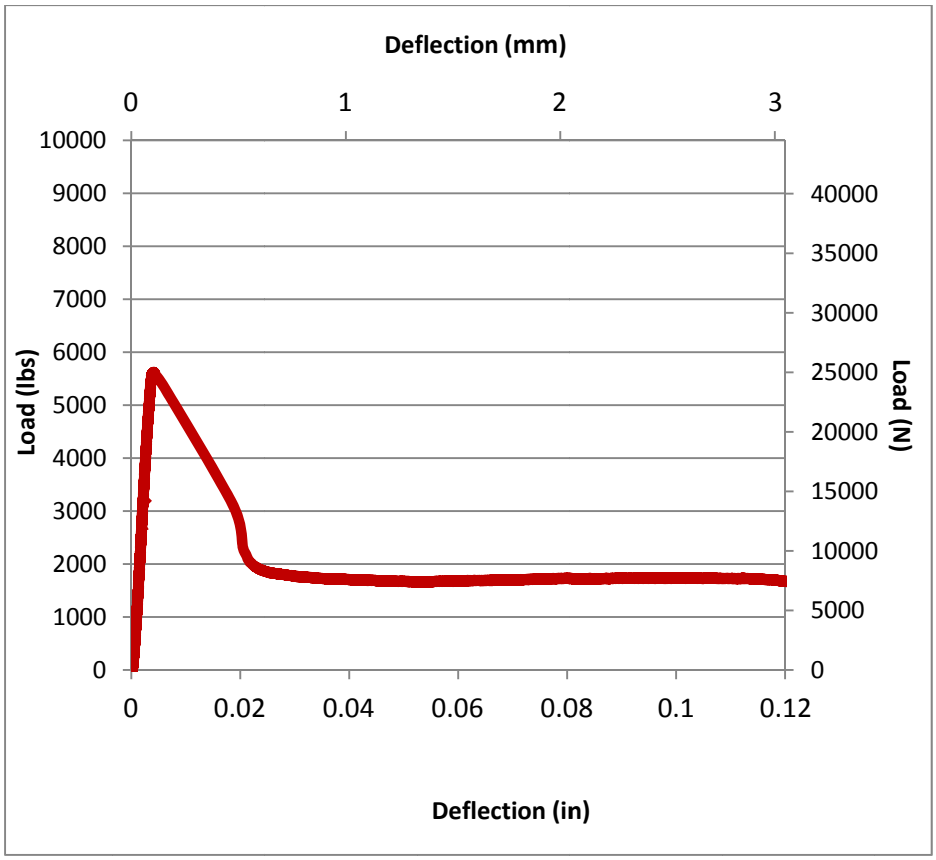

Figure C-1 Load-Deflection Plot for HY-24-6-BM-44lbs-8%

Figure C-2 Photograph of Crack for HY-24-6-BM-44lbs-8%

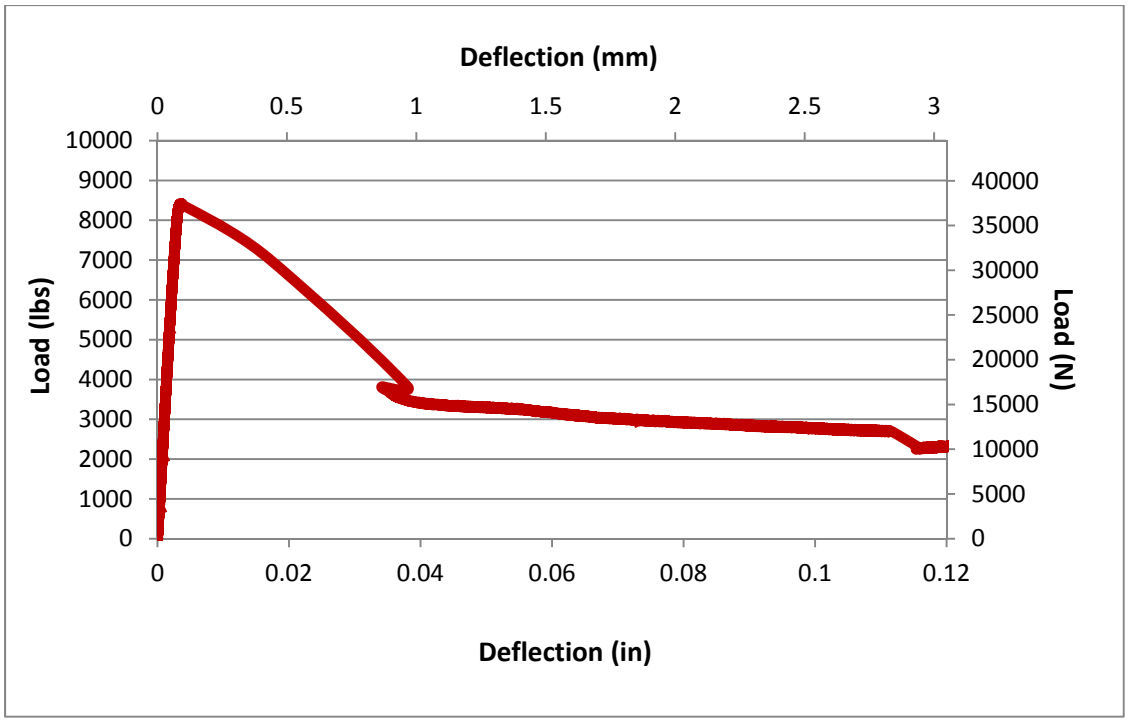

Figure C-3 Load-Deflection Plot for HY-24-6-BM-44lbs-10%

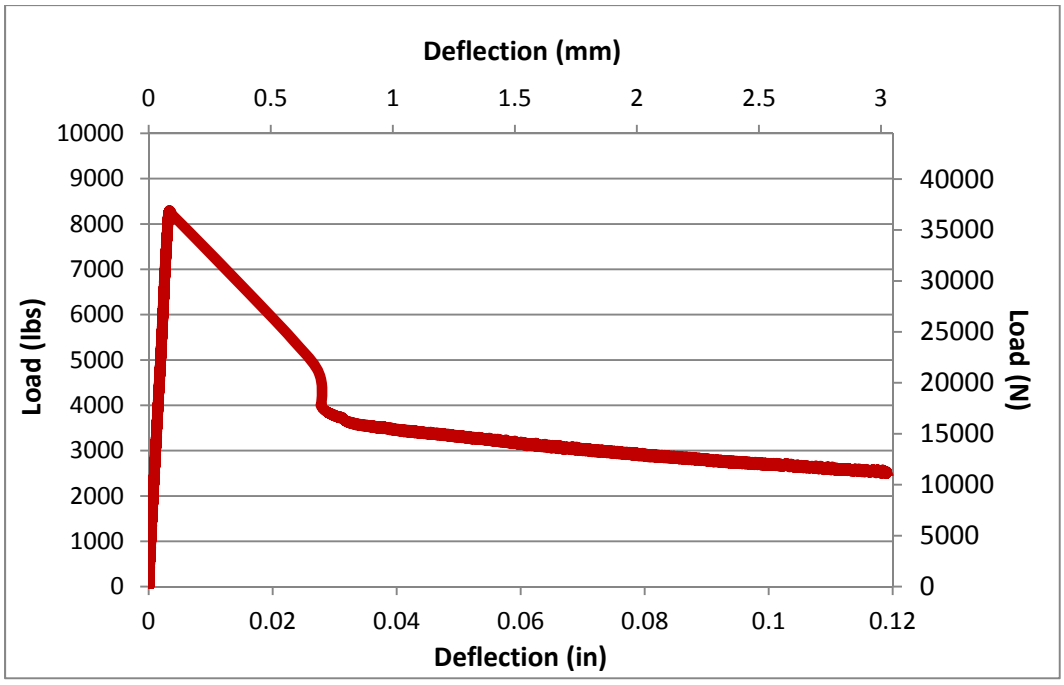

Figure C-4 Load-Deflection Plot for HY-24-6-BM-44lbs-8%

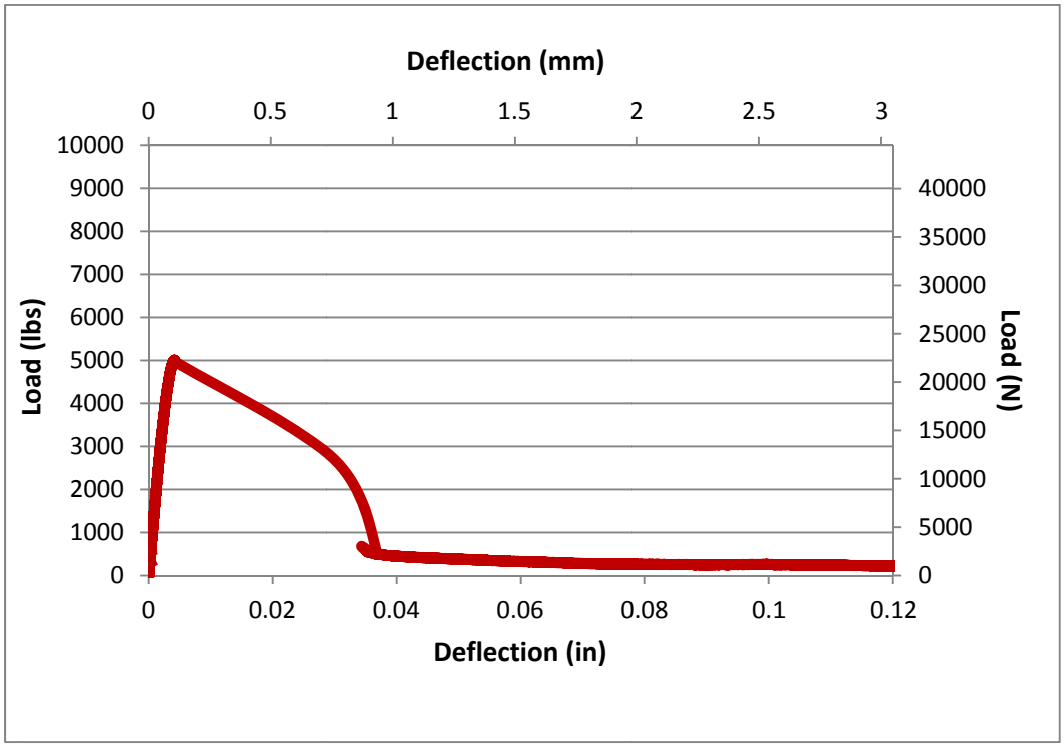

Figure C-5 Load-Deflection Plot for CR-24-6-BM-8%

Figure C-6 Photograph of Crack for HY-24-6-BM-44lbs-8%

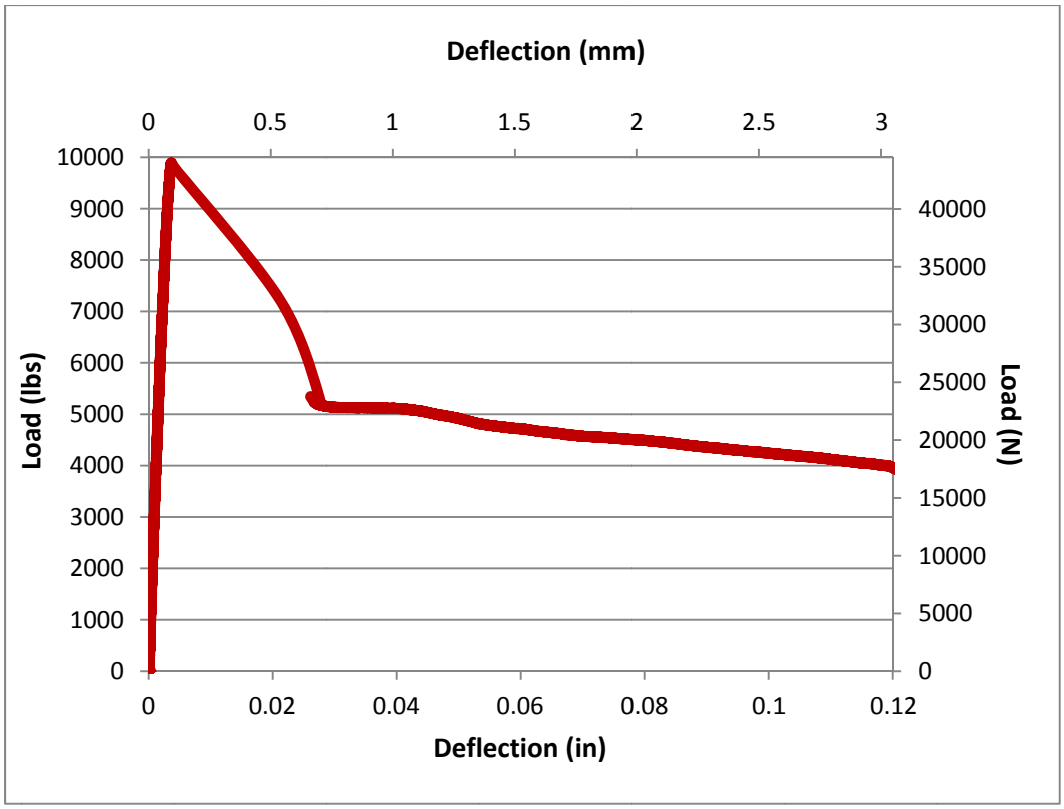

Figure C-7 Load-Deflection Plot for HY-24-6-BM-44lbs-6%

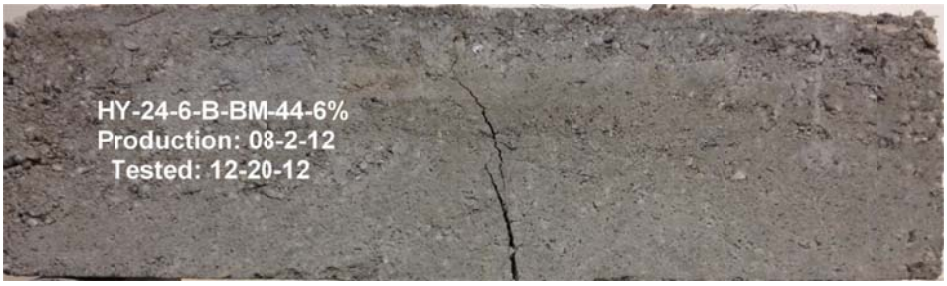

Figure C-8 Photograph of Crack for HY-24-6-BM-44lbs-6%

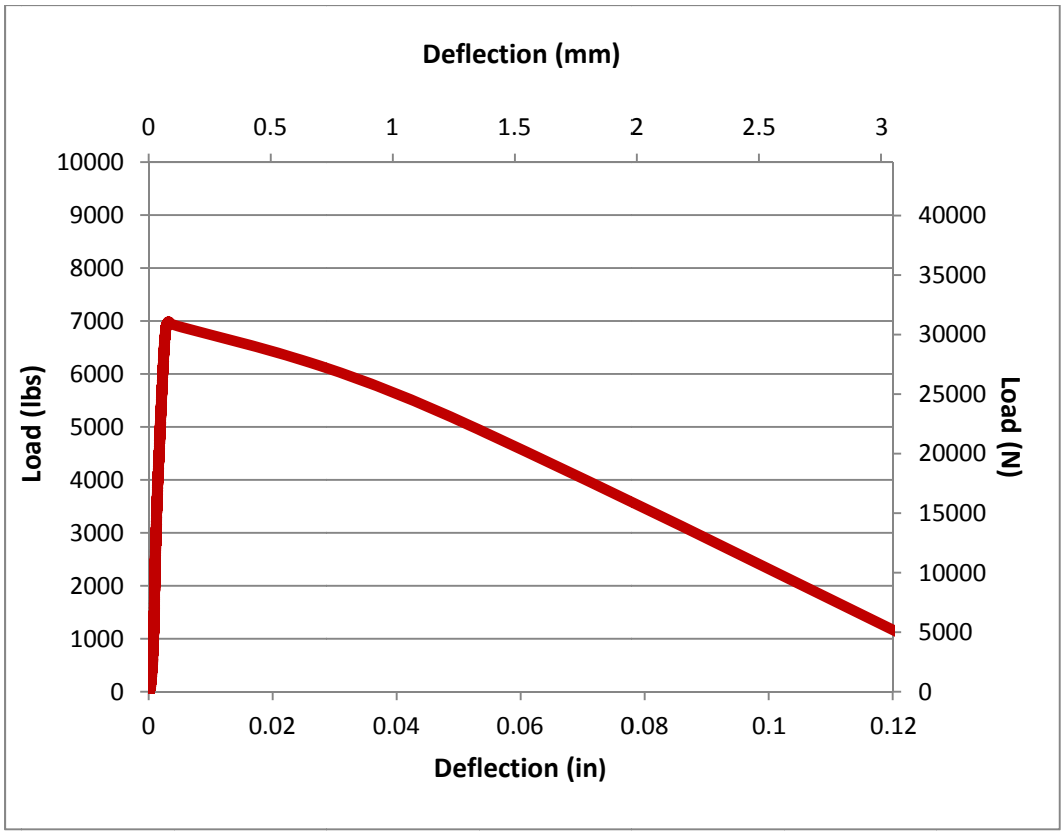

Figure C-9 Load-Deflection Plot for CR-24-6-BM-6%

Figure C-10 Photograph of Crack for CR-24-6-BM-6%

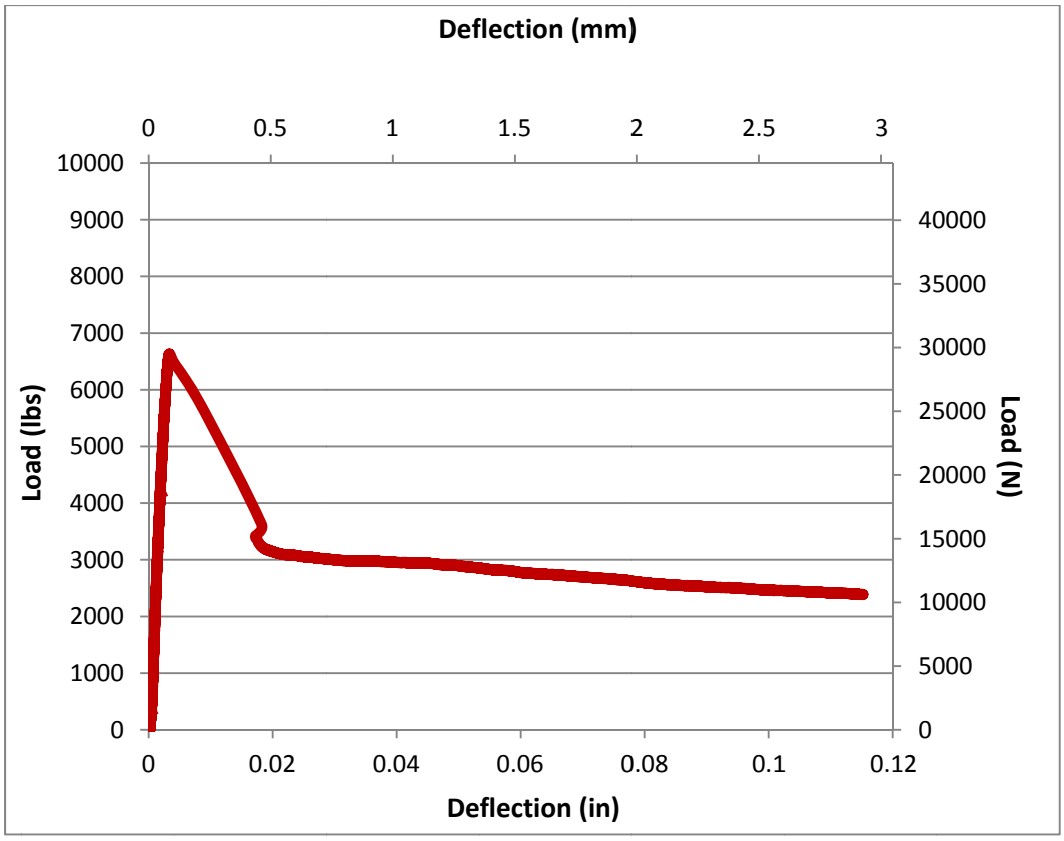

Figure C-11 Load-Deflection Plot for HY-24-6-BM-44-6%

Figure C-12 Photograph of Crack for HY-24-6-BM-44lbs-6%

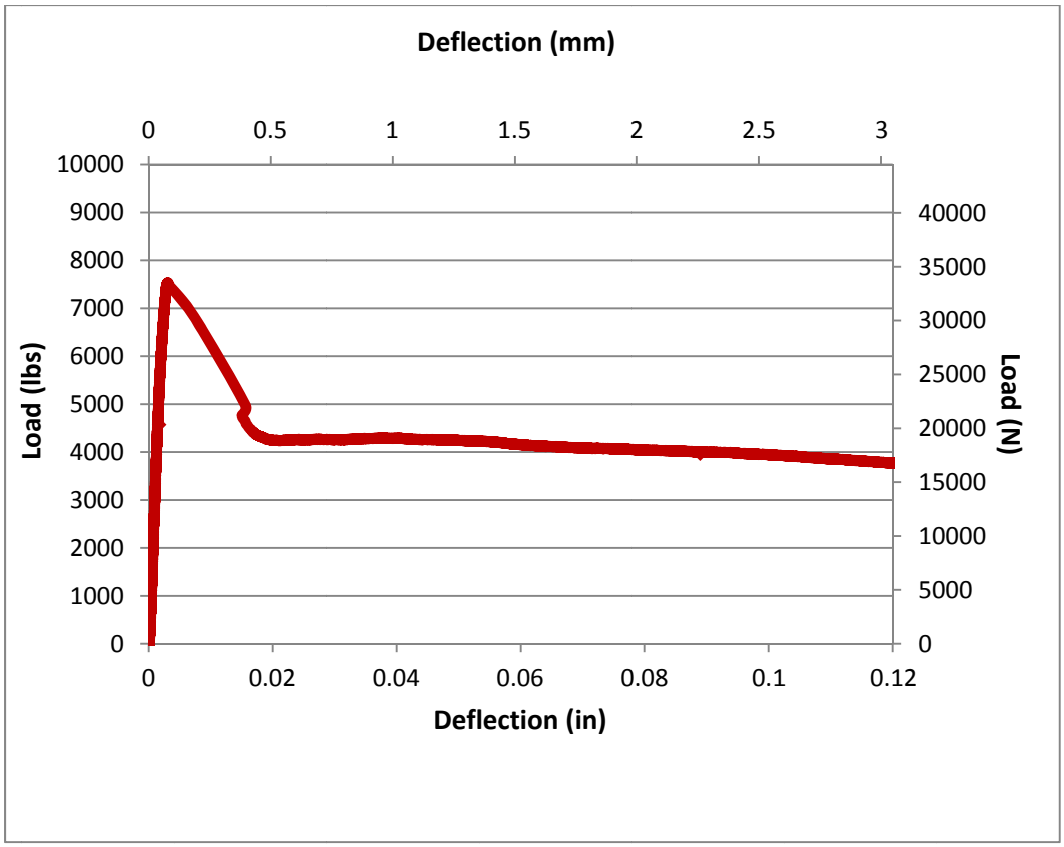

Figure C-13 Load-Deflection Plot for HY-24-6 -BM-44lbs-10%

Figure C-14 Photograph of HY-24-6-BM-44lbs-10%

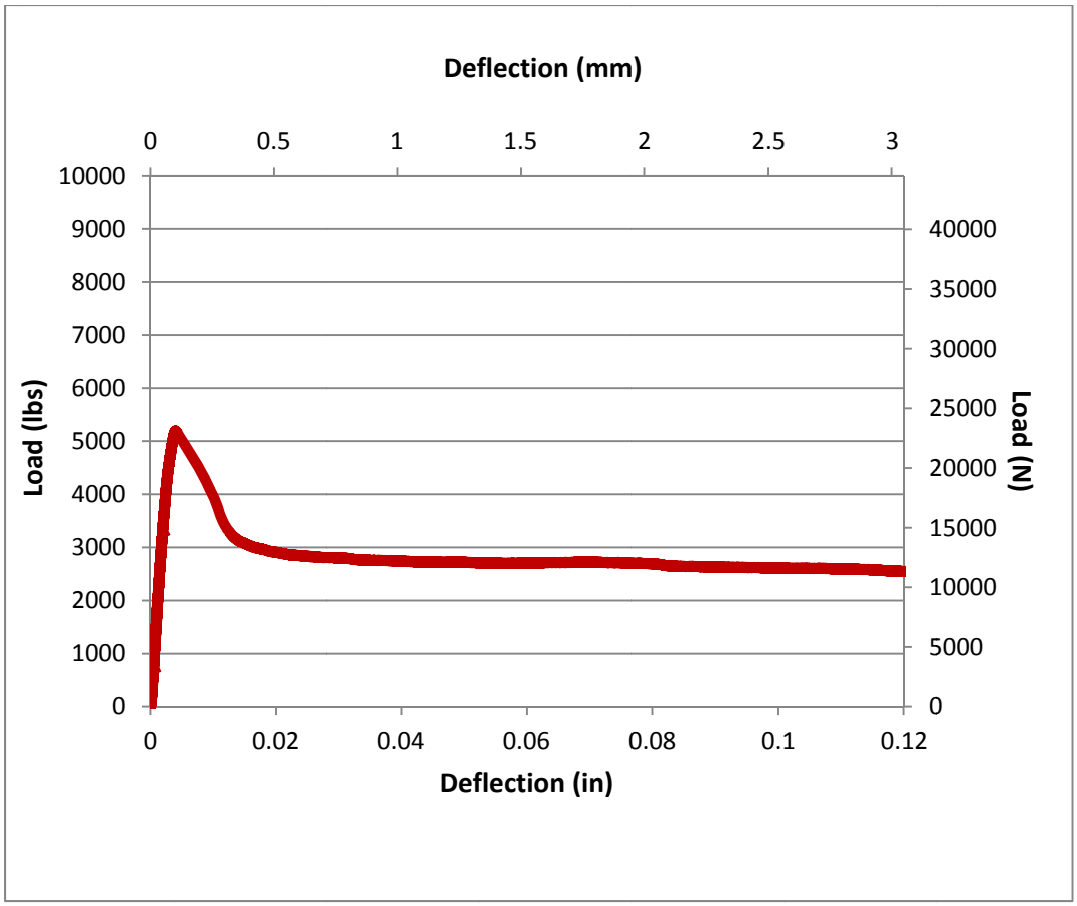

Figure C-15 Load-Deflection Plot for HY-24-6-BM-44lbs-10%

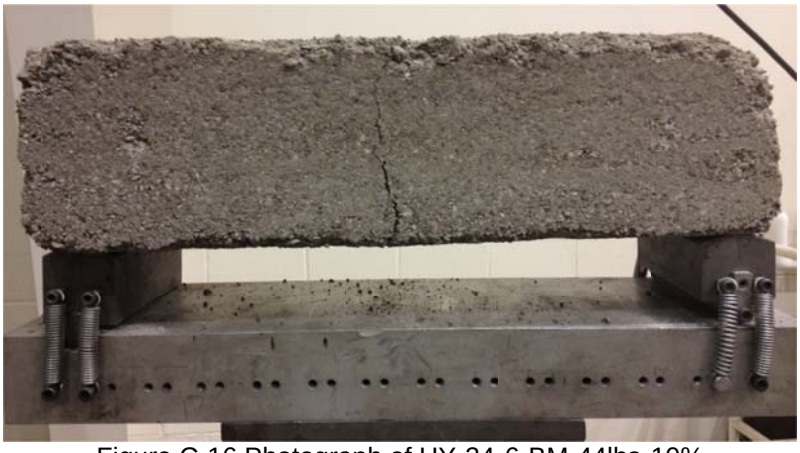

Figure C-16 Photograph of HY-24-6-BM-44lbs-10%

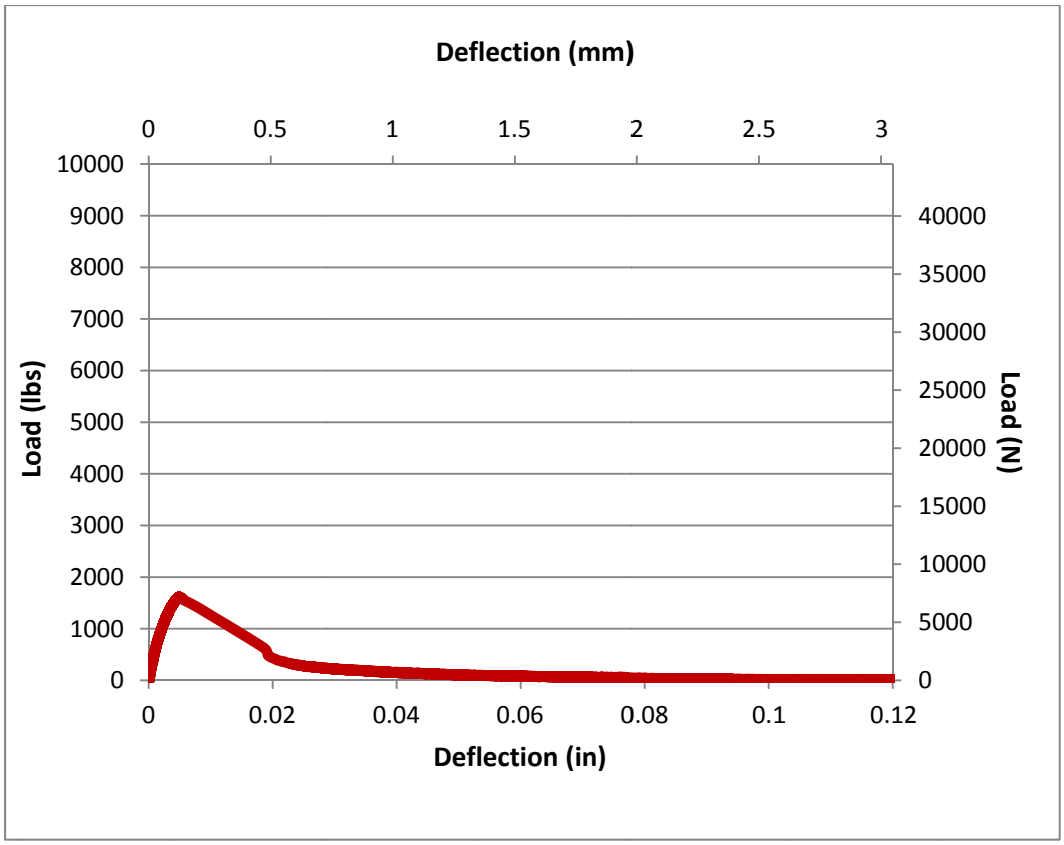

Figure C-17 Load-Deflection Plot for CR-24-6-BM-10%

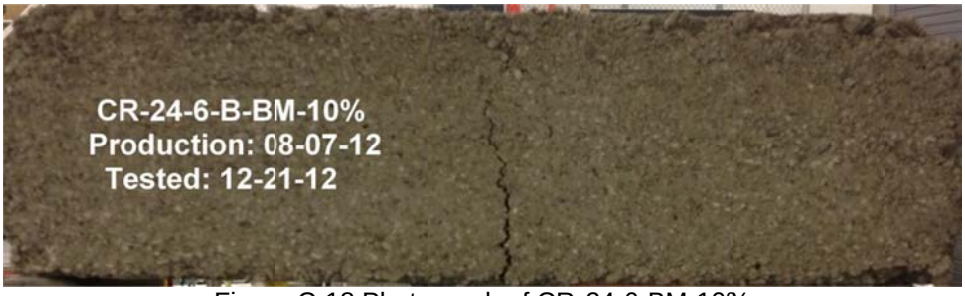

Figure C-18 Photograph of CR-24-6-BM-10%

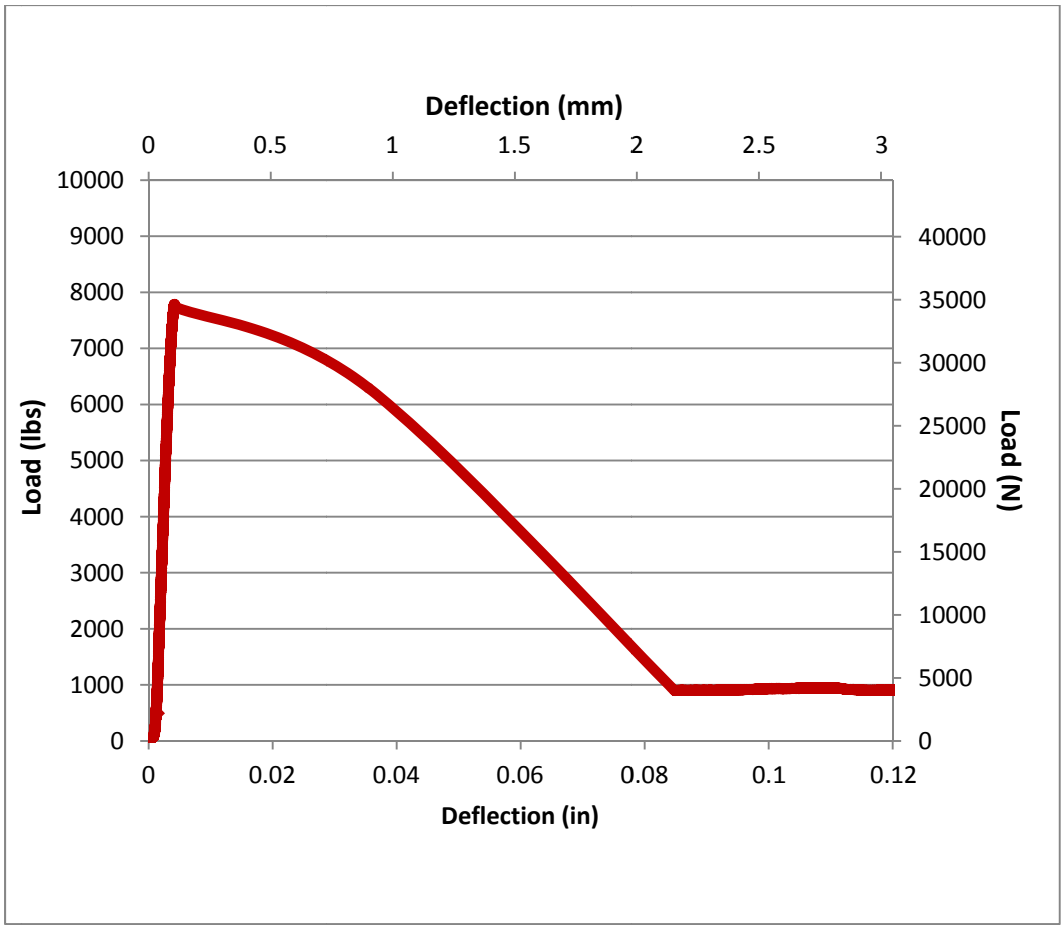

Figure C-19 Load-Deflection Plot for HY-24-6-BM-10lbs-8%

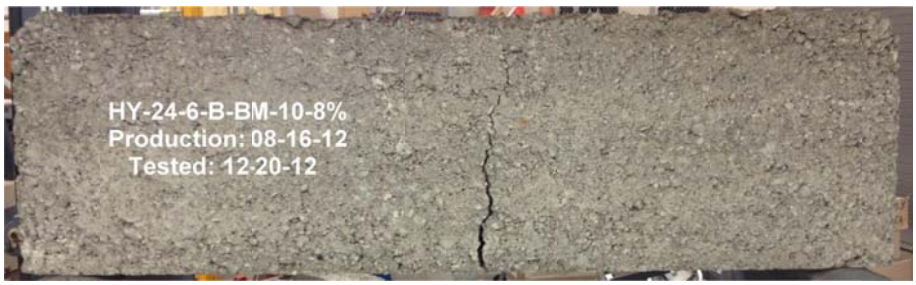

Figure C-20 Photograph of HY-24-6-BM-10lbs-8%

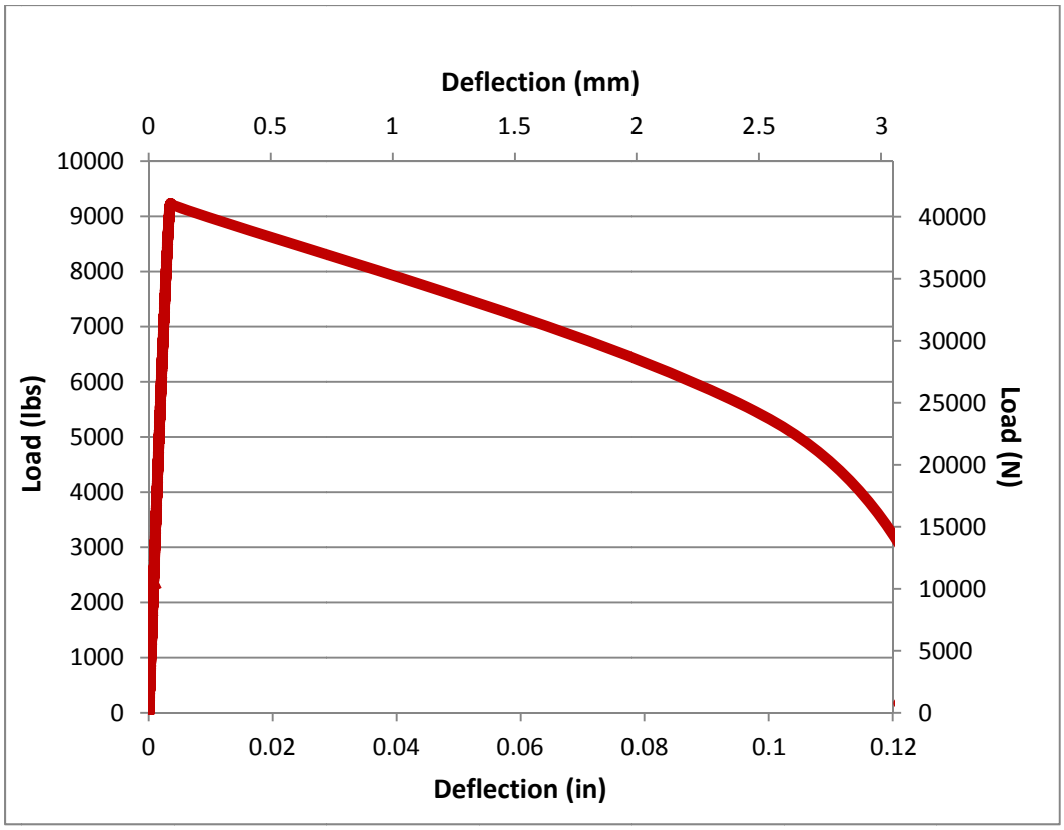

Figure C-21 Load-Deflection Plot for HY-24-6-BM-10lbs-8%

Figure C-22 Photograph of HY-24-6-BM-10lbs-8%

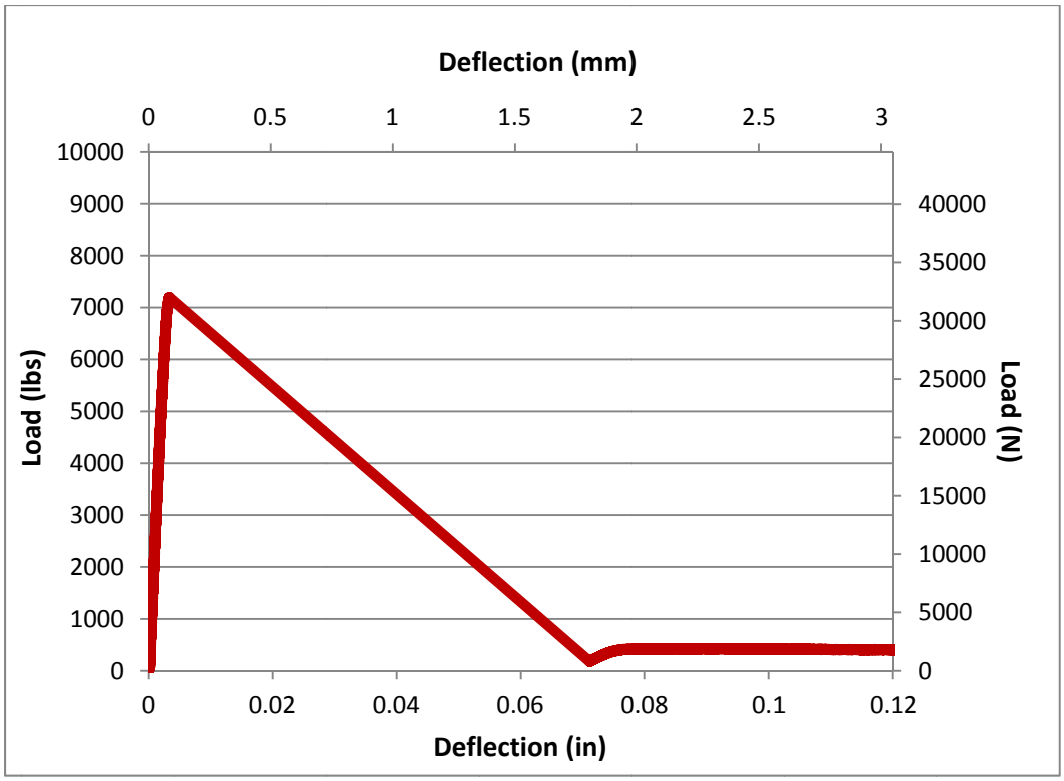

Figure C-23 Load-Deflection Plot for CR-24-6-BM-8%

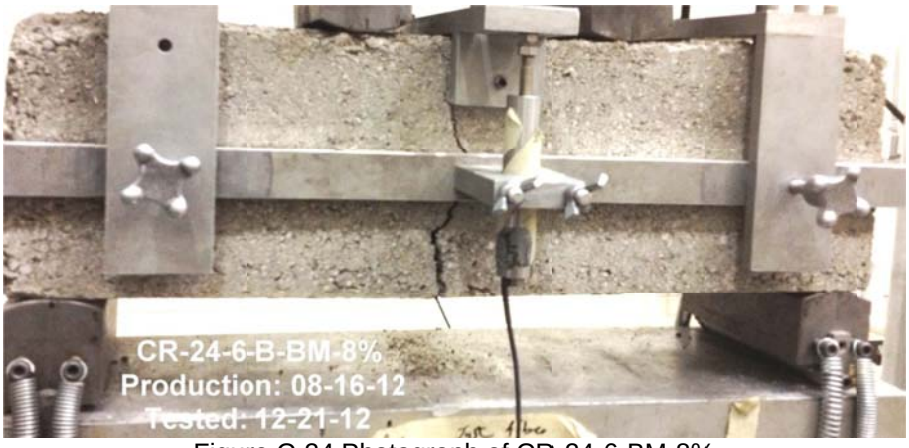

Figure C-24 Photograph of CR-24-6-BM-8%

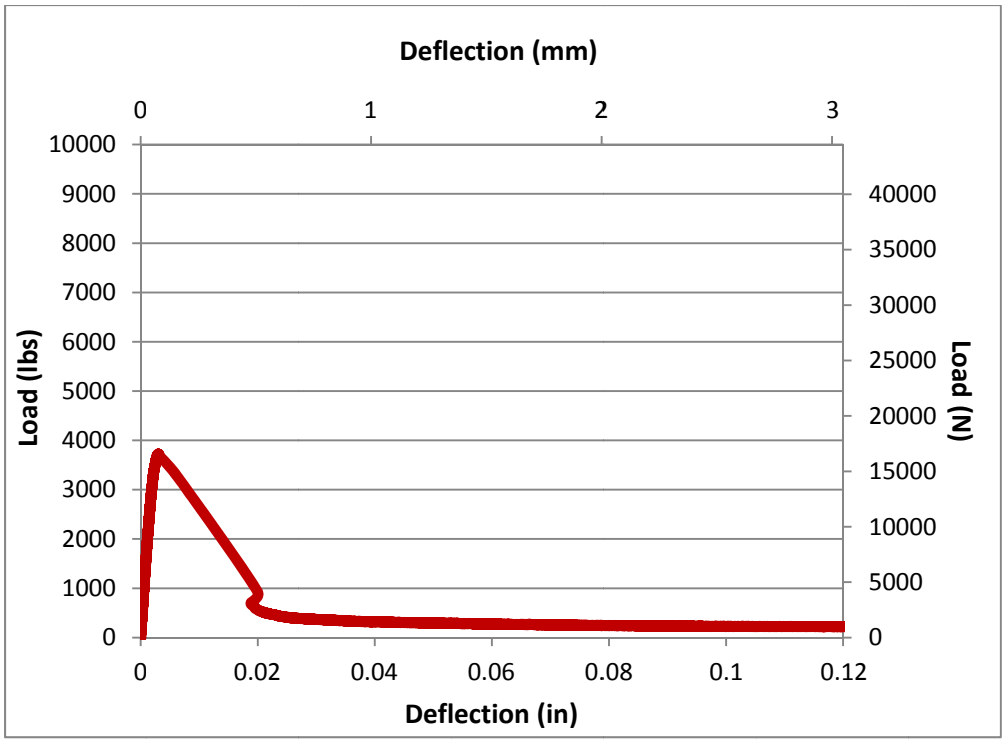

Figure C-25 Load-Deflection Plot for CR-36-6-BM-8%

Figure C-26 Photograph of CR-36-6-BM-8%

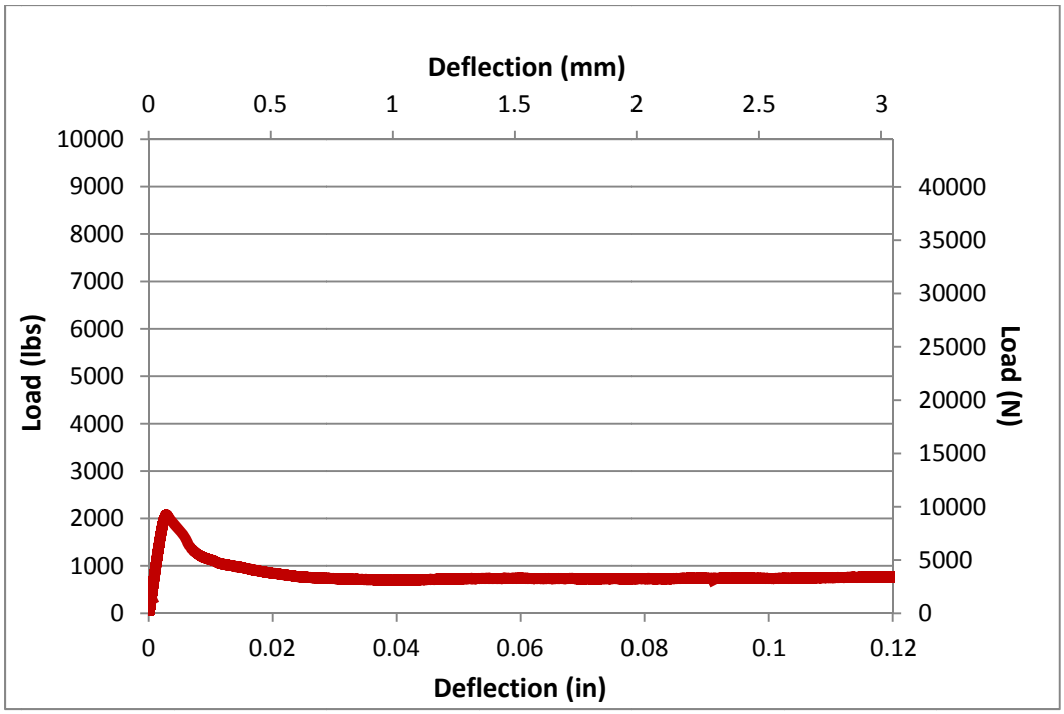

Figure C-27 Load-Deflection Plot for HY-36-6-BM-22lbs-8%

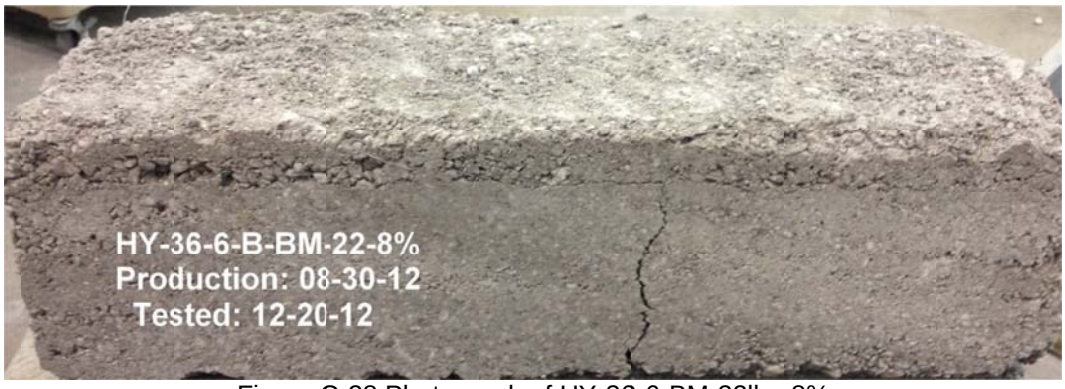

Figure C-28 Photograph of HY-36-6-BM-22lbs-8%

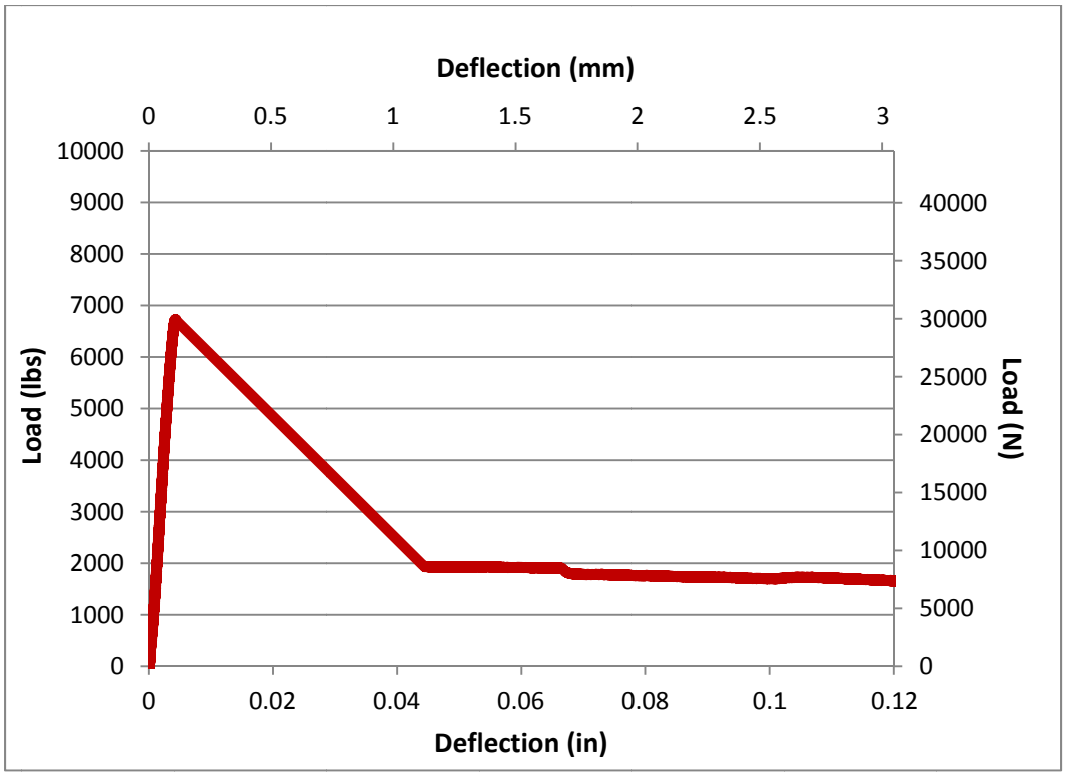

Figure C-29 Load-Deflection Plot for HY-36-6-BM-22lbs-8%

Figure C-30 Photograph of HY-36-6-BM-22lbs-8%

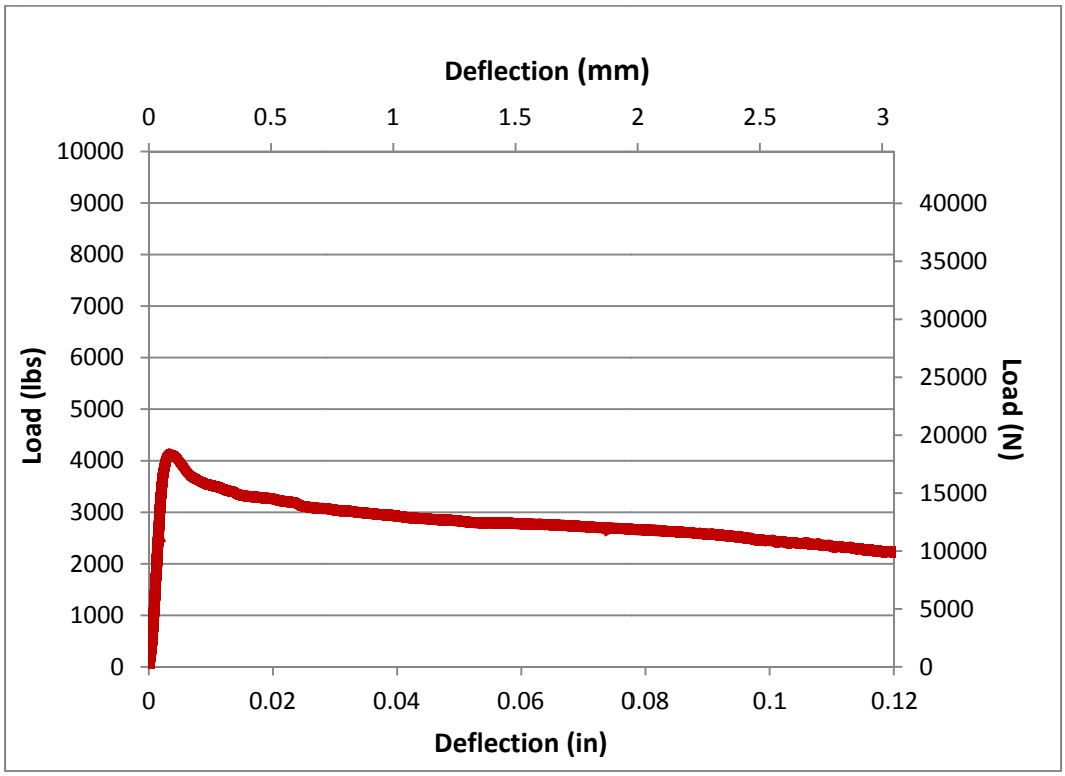

Figure C-31 Load-Deflection Plot for HY-36-6-BM-22lbs-10%

Figure C-32 Photograph of HY-36-6-BM-22lbs-10%

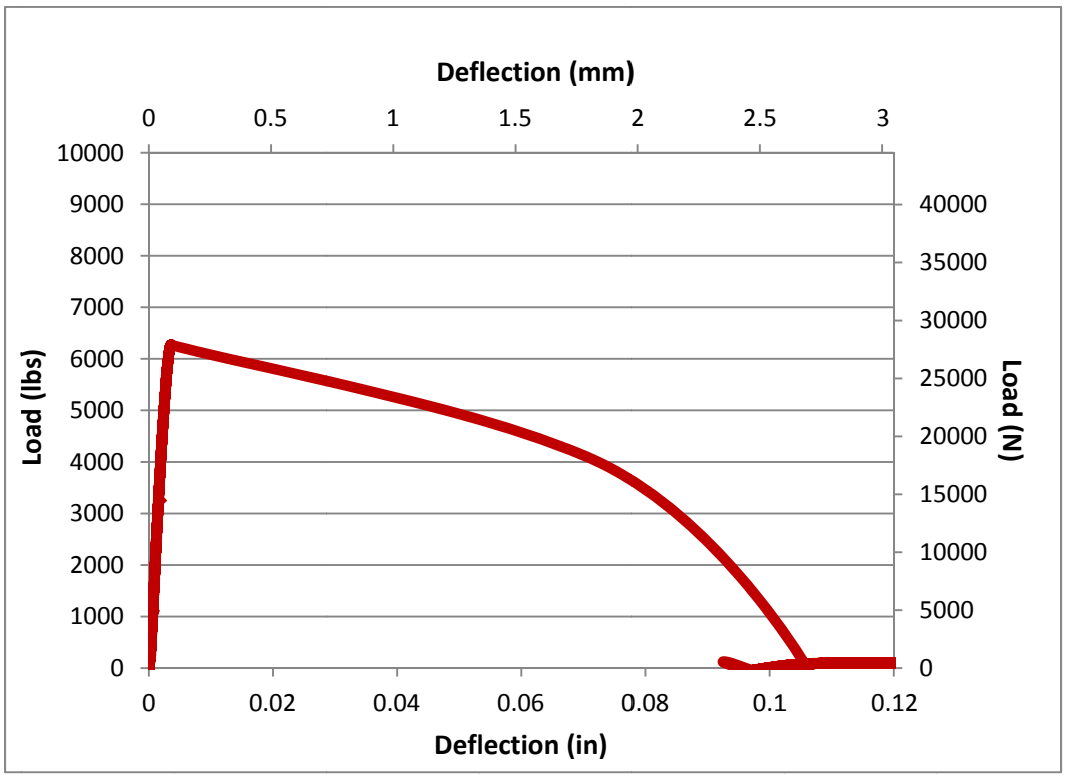

Figure C-33 Load-Deflection Plot for CR-36-6-BM-10%

Figure C-34 Photograph of CR-36-6-BM-10%

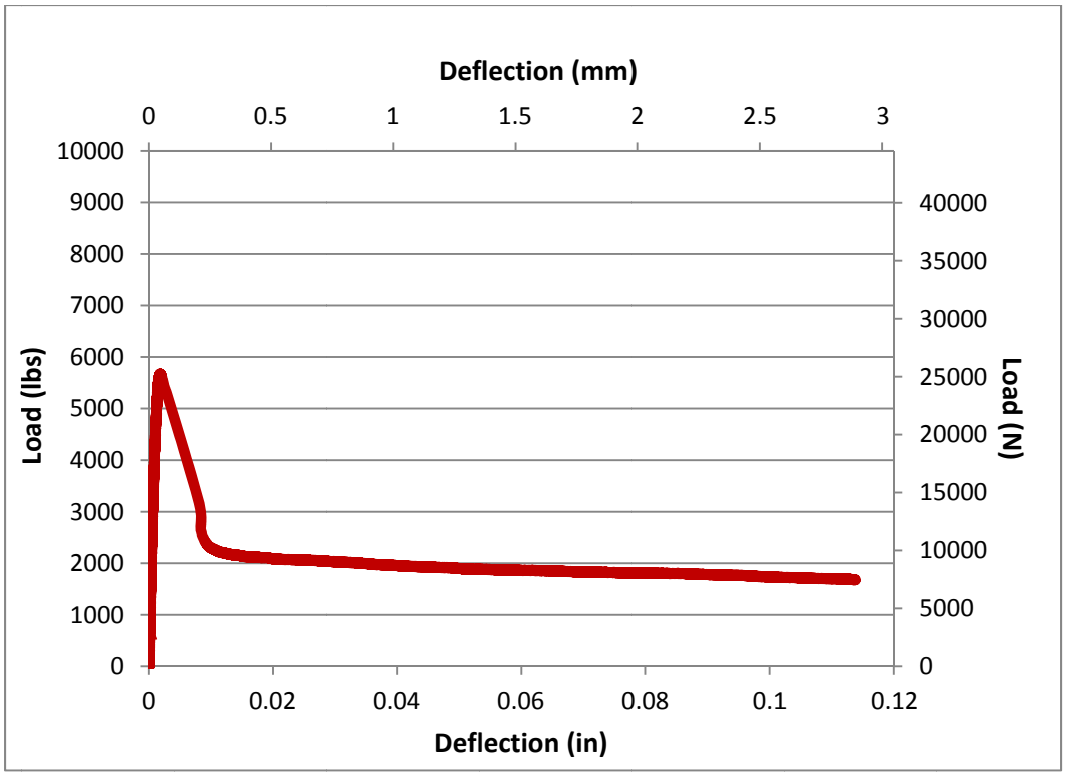

Figure C-35 Load-Deflection Plot for HY-36-6-BM-22lbs-10%

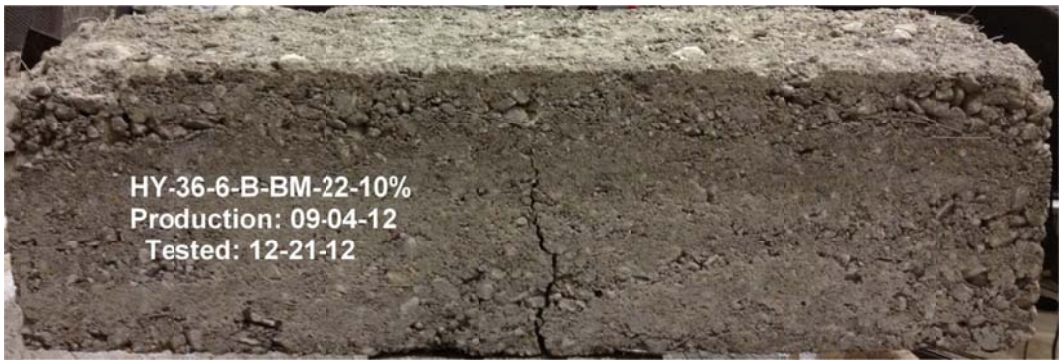

Figure C-36 Photograph of HY-36-6- BM-22lbs-10%

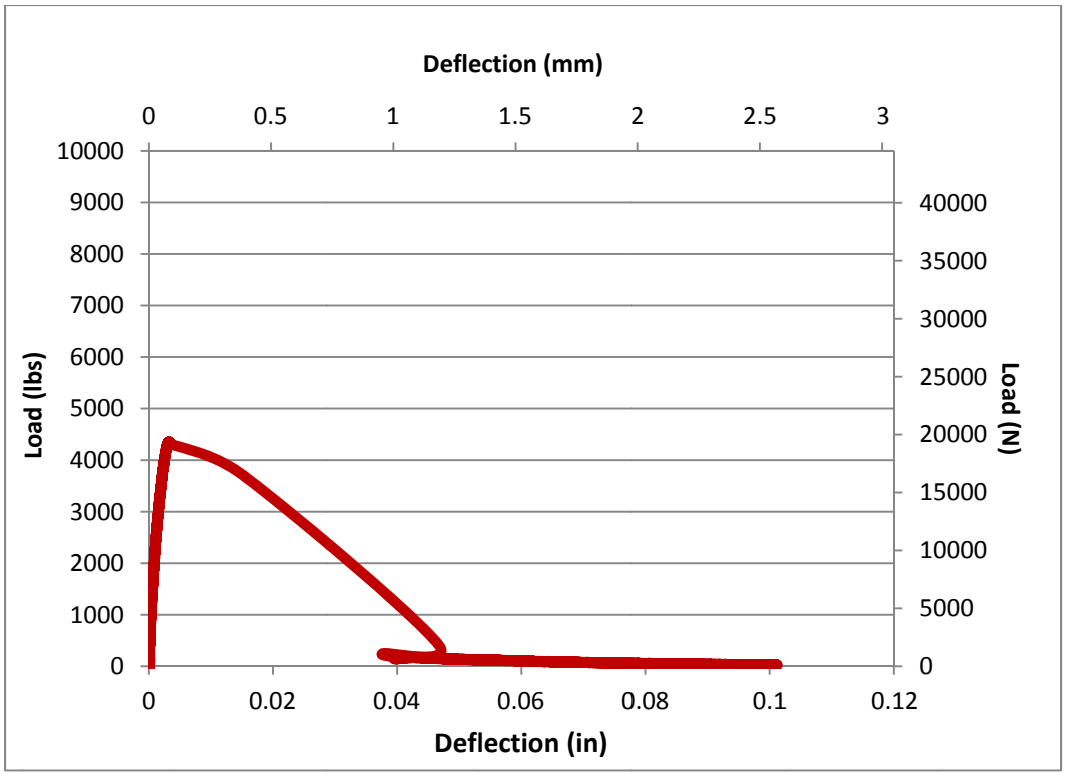

Figure C-37 Load-Deflection Plot for CR-36-6-BM-10%

Figure C-38 Photograph of CR-36-6-BM-10%

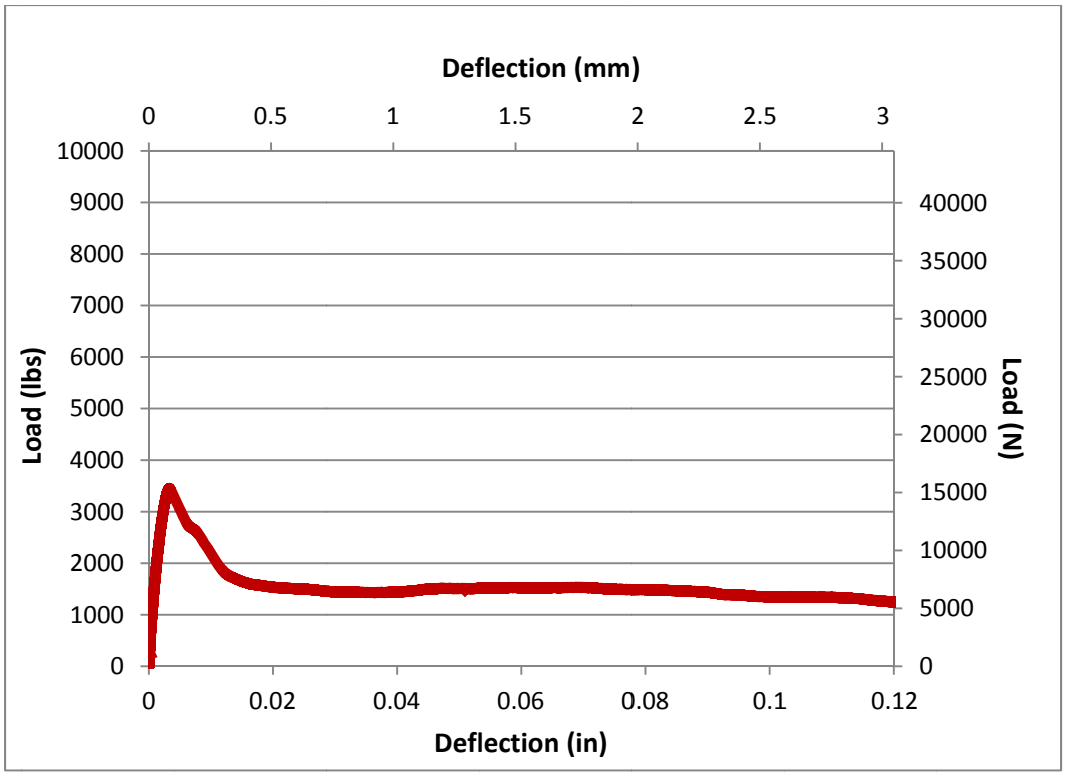

Figure C-39 Load-Deflection Plot for HY-36-6-BM-44lbs-12%

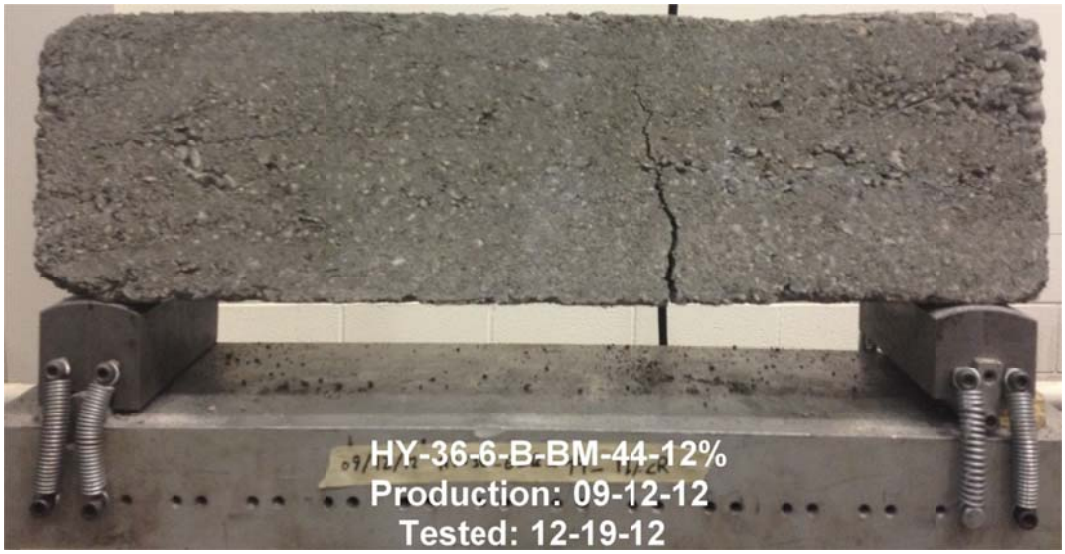

Figure C-40 Photograph of HY-36-6-BM-44lbs-12%

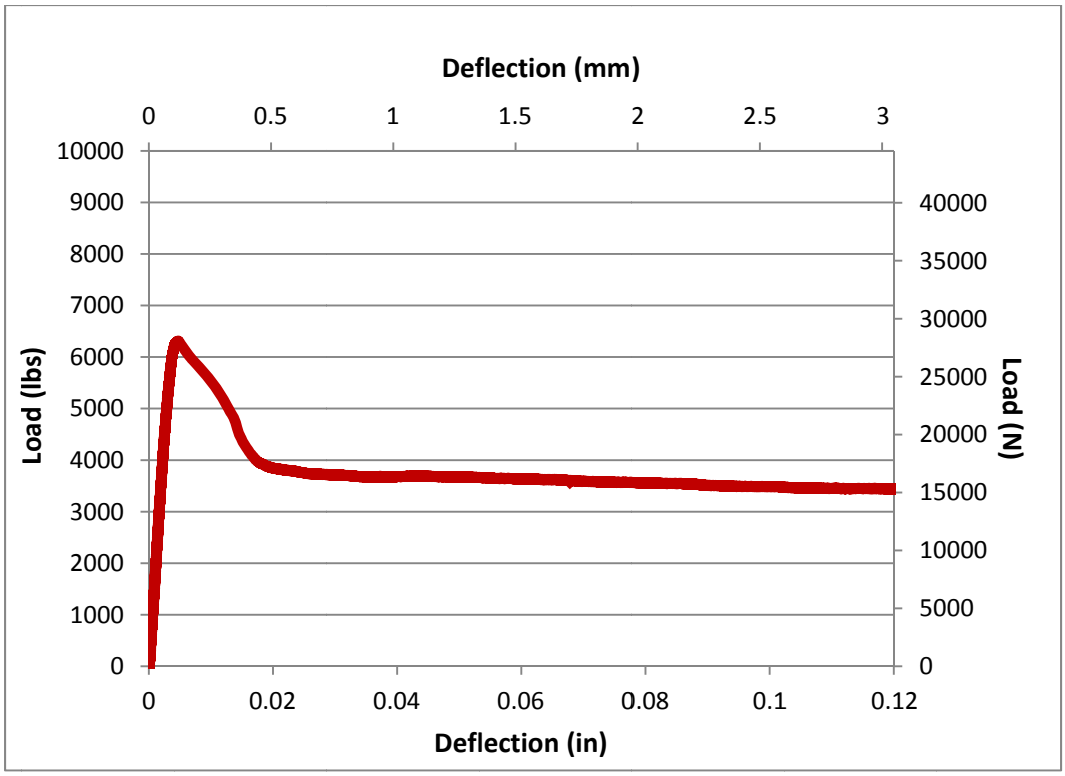

Figure C-41 Load-Deflection Plot for HY-36-6-BM-44lbs-12%

Figure C-42 Photograph of HY-36-6-BM-44lbs-12%

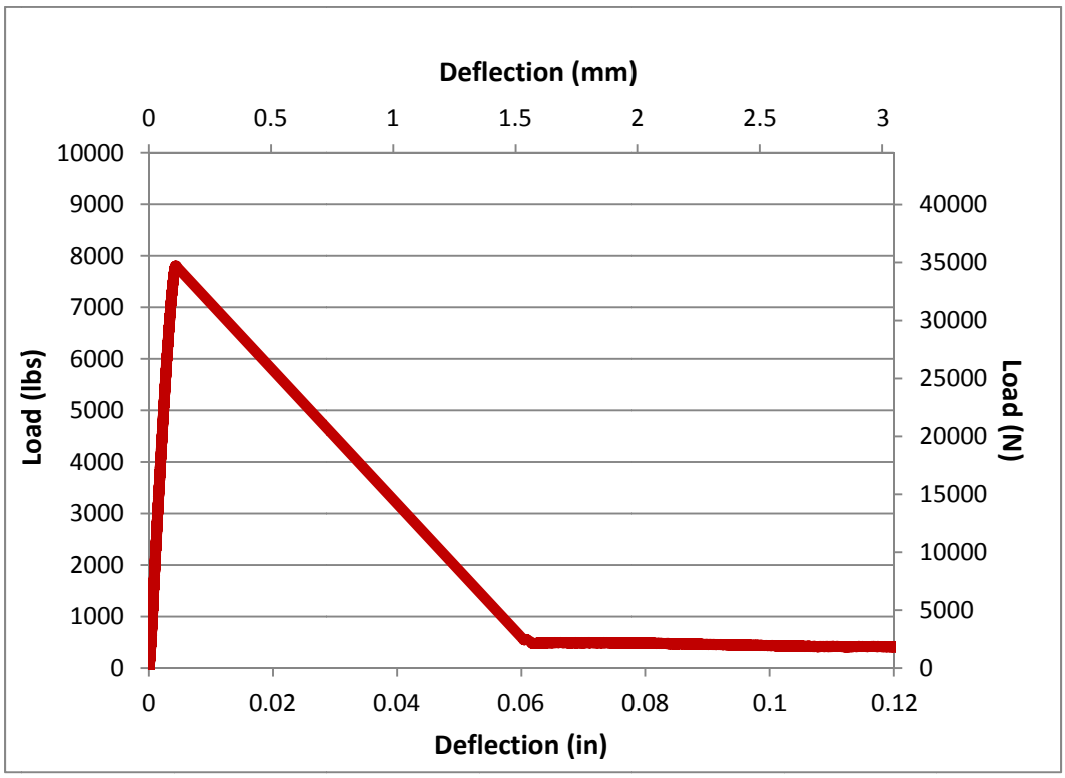

Figure C-43 Load-Deflection Plot for CR-36-6-BM-10%


Figure C-44 Photograph of CR-36-6-BM-10%

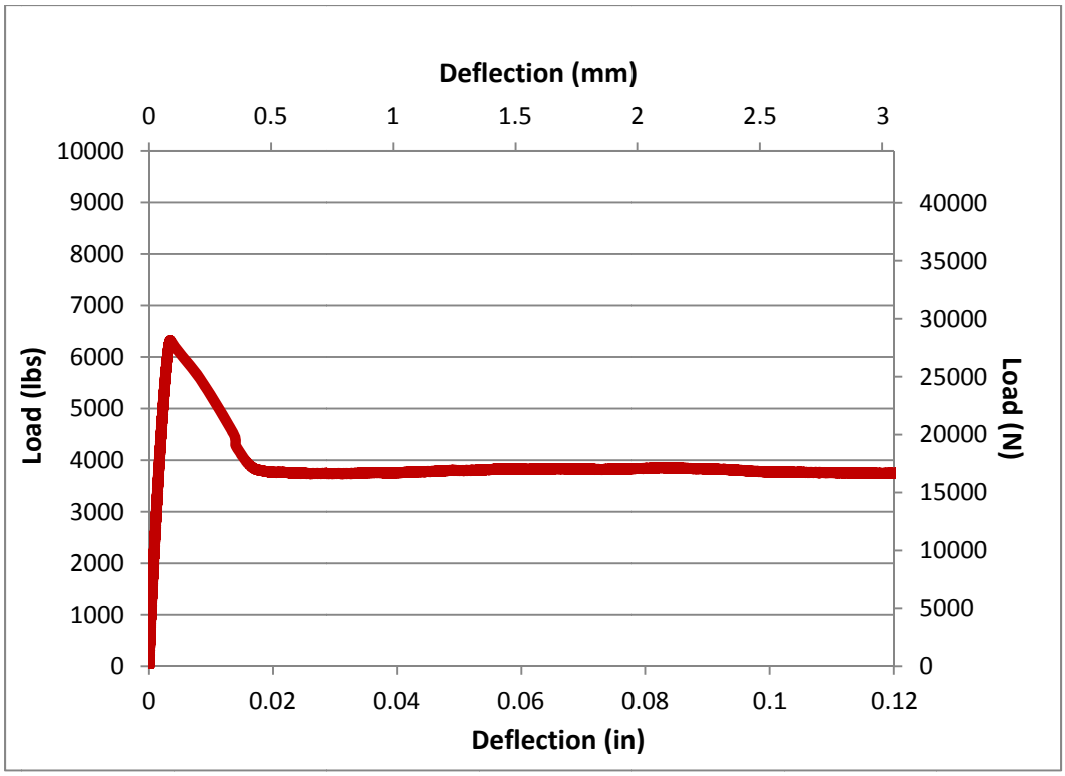

Figure C-45 Load-Deflection Plot for HY-24-6-BM-44lbs-10%

Figure C-46 Photograph of HY-24-6-BM-44lbs-10%

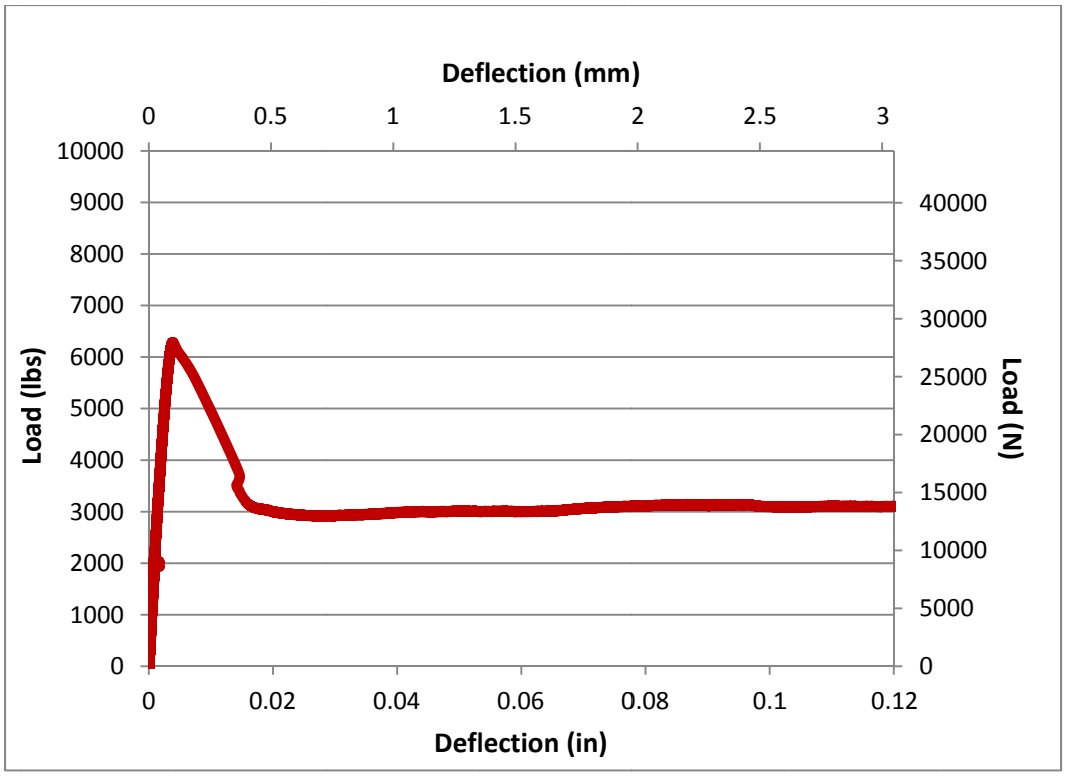

Figure C-47 Load-Deflection Plot for CR-36-6-BM-10%


Figure C-48 Photograph of CR-36-6-BM-10%

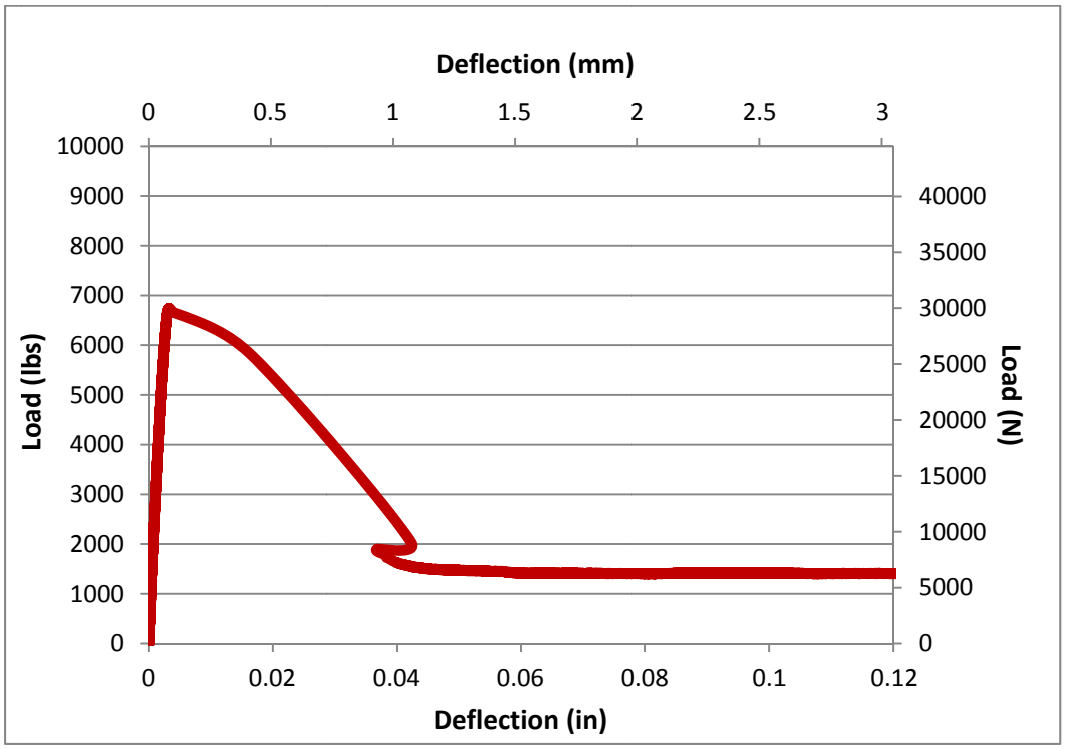

Figure C-49 Load-Deflection Plot for HY-24-6-BM-44lbs-10%

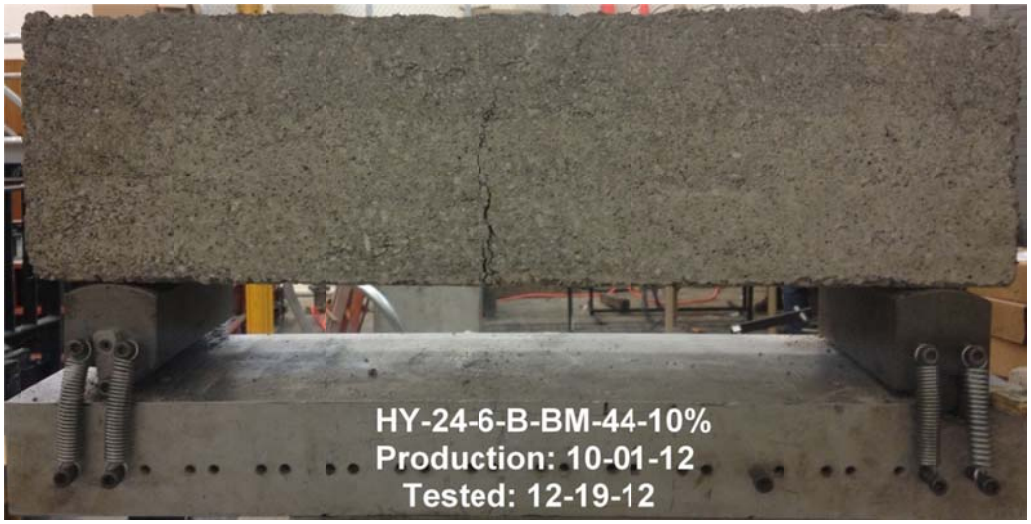

Figure C-50 Photograph of HY-24-6-BM-44lbs-10%

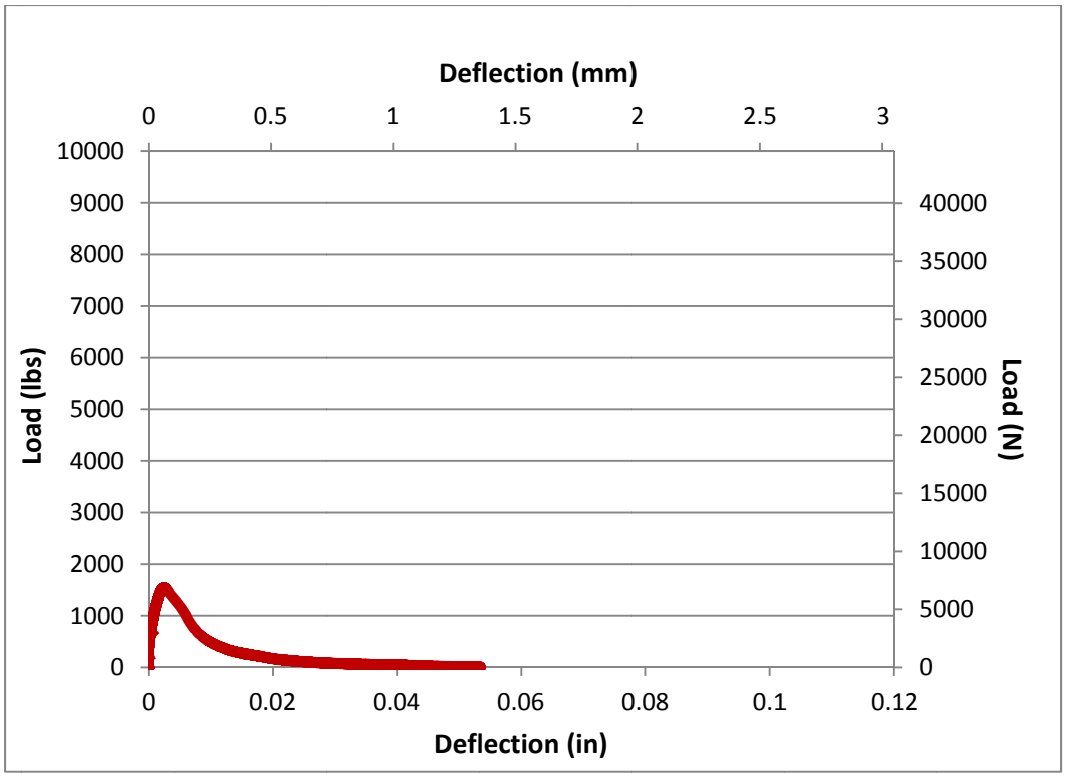

Figure C-51 Load-Deflection Plot for HY-36-44lbs-10%

Figure C-52 Photograph of HY-36-BM-44lbs-10%

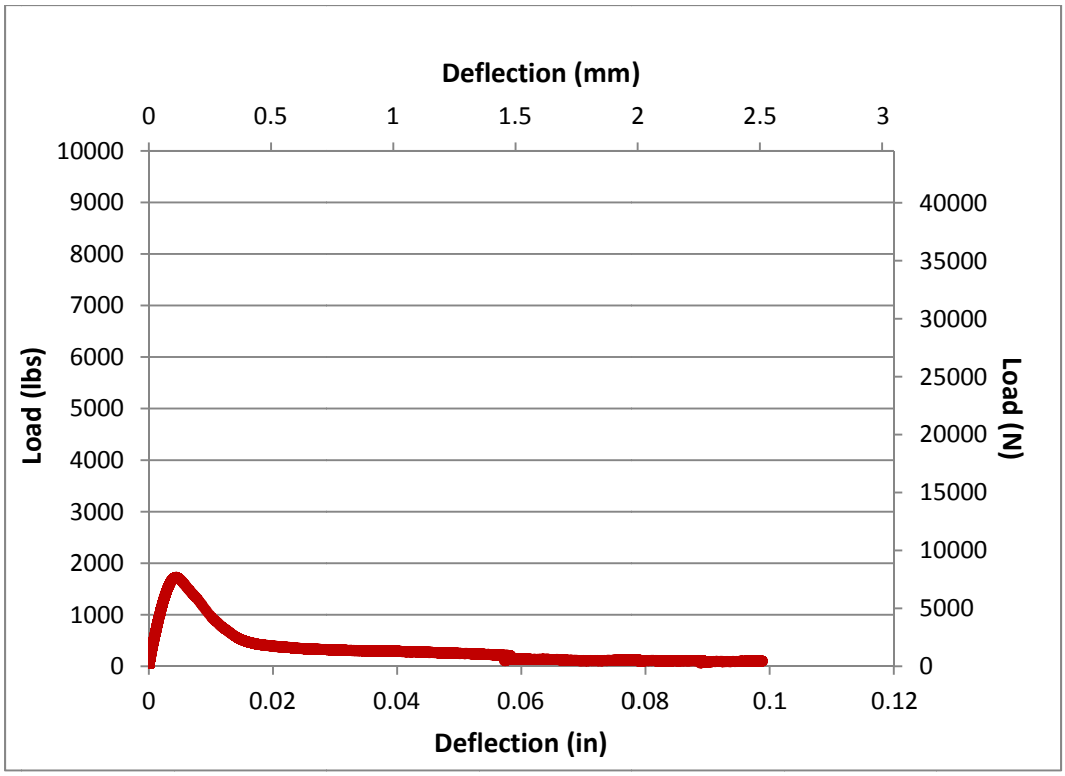

Figure C-53 Load-Deflection Plot for CR-36-6-B-BM-10%

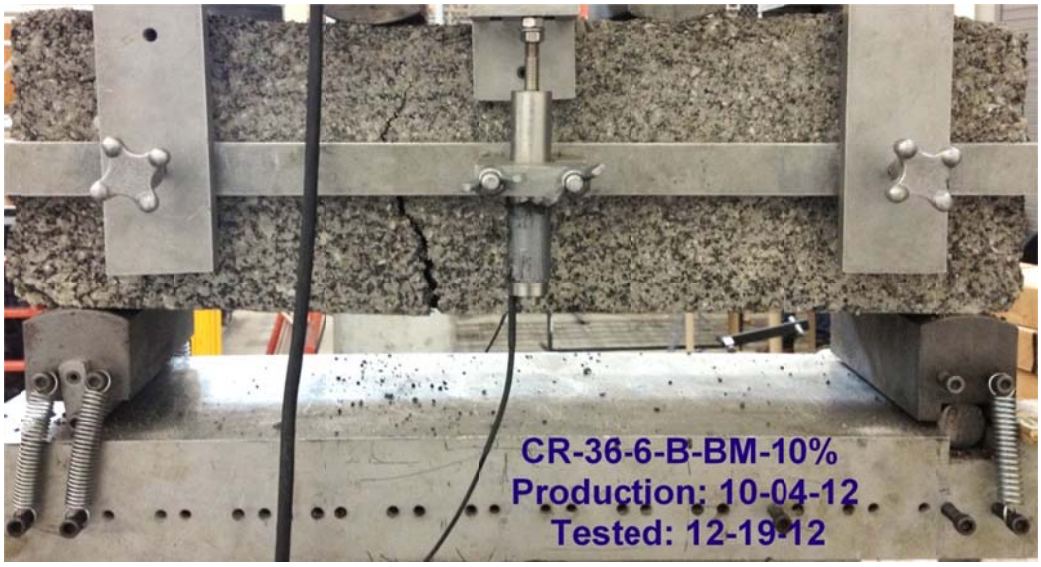

Figure C-54 Photograph of CR-36-6-BM-10%

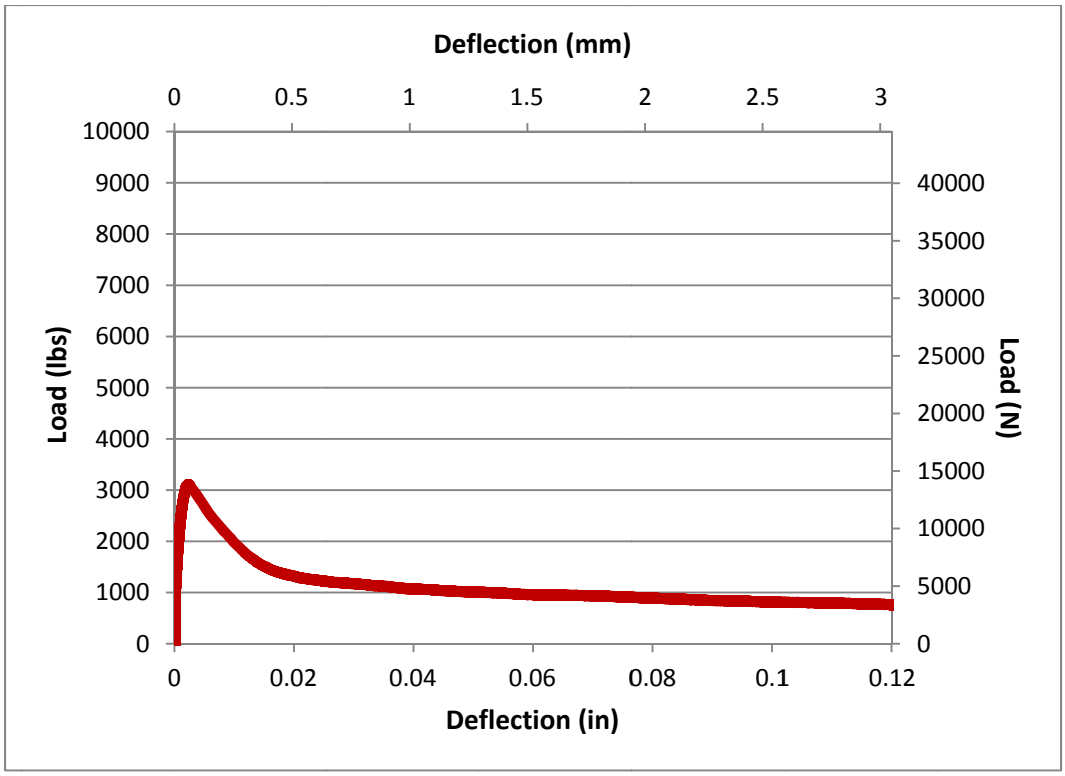

Figure C-55 Load-Deflection Plot for HY-24-6-B-BM-44lbs-15%

Figure C-56 Photograph of HY-24-6-BM-44lbs-15%

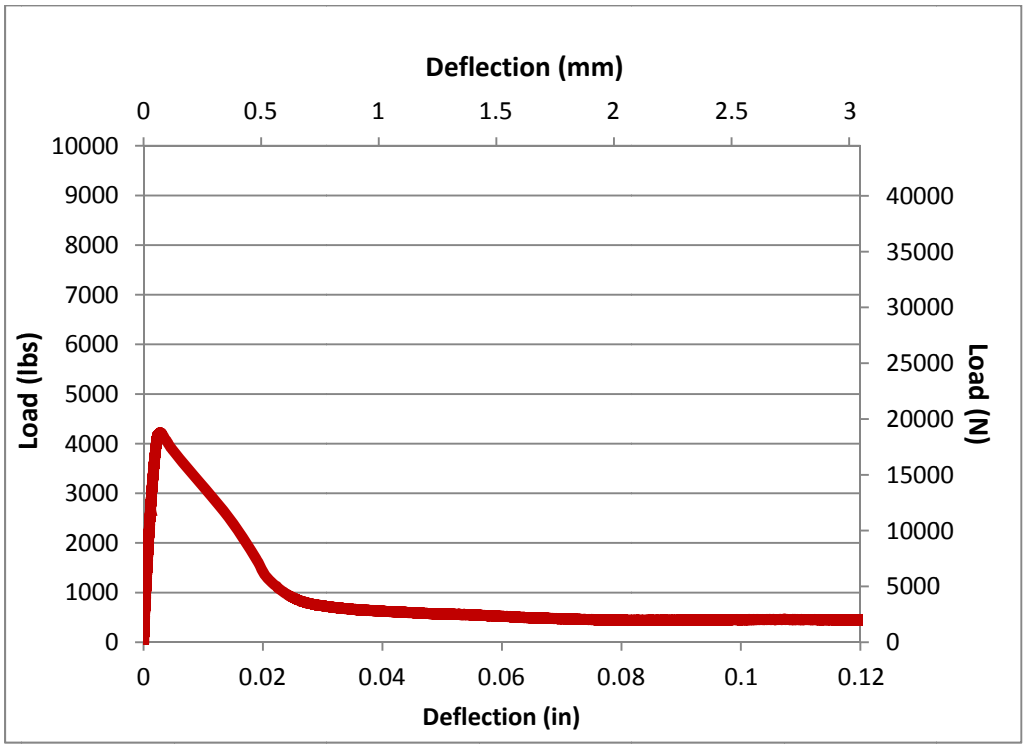

Figure C-57 Load-Deflection Plot for CR-24-6-B-BM-20%

Figure C-58 Photograph of CR-24-6-BM-20%

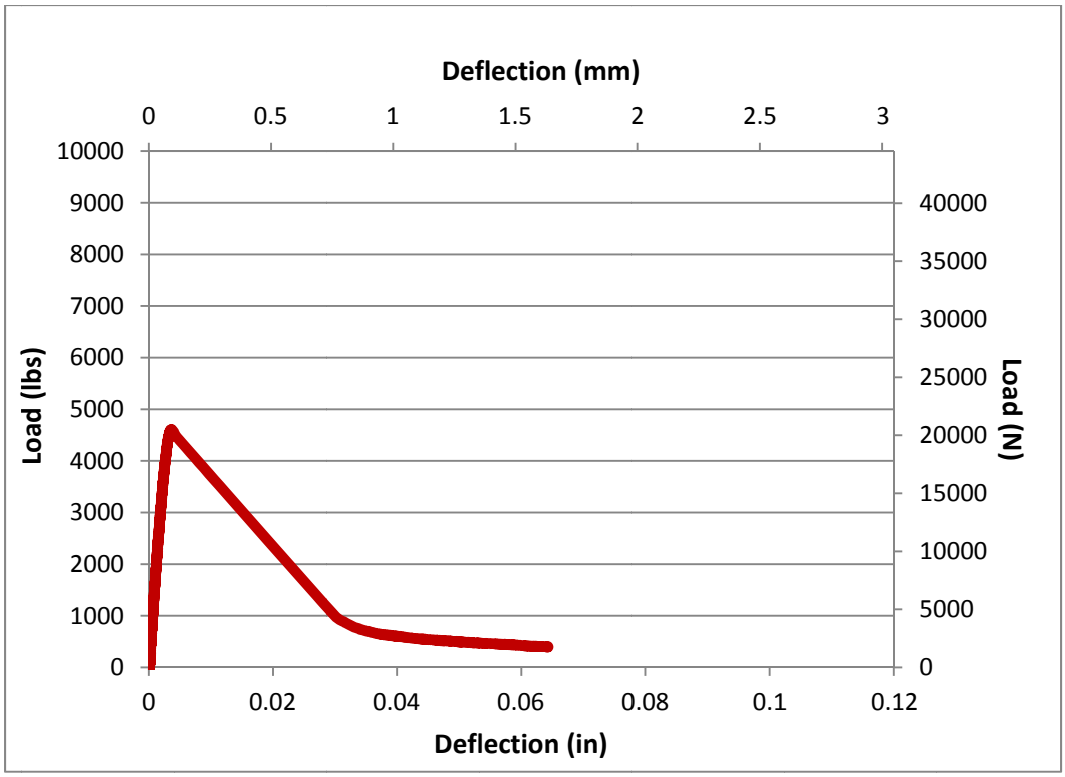

Figure C-59 Load-Deflection Plot for CR-24-6-B-BM-20%

Figure C-60 Photograph of CR-24-6-BM-20%

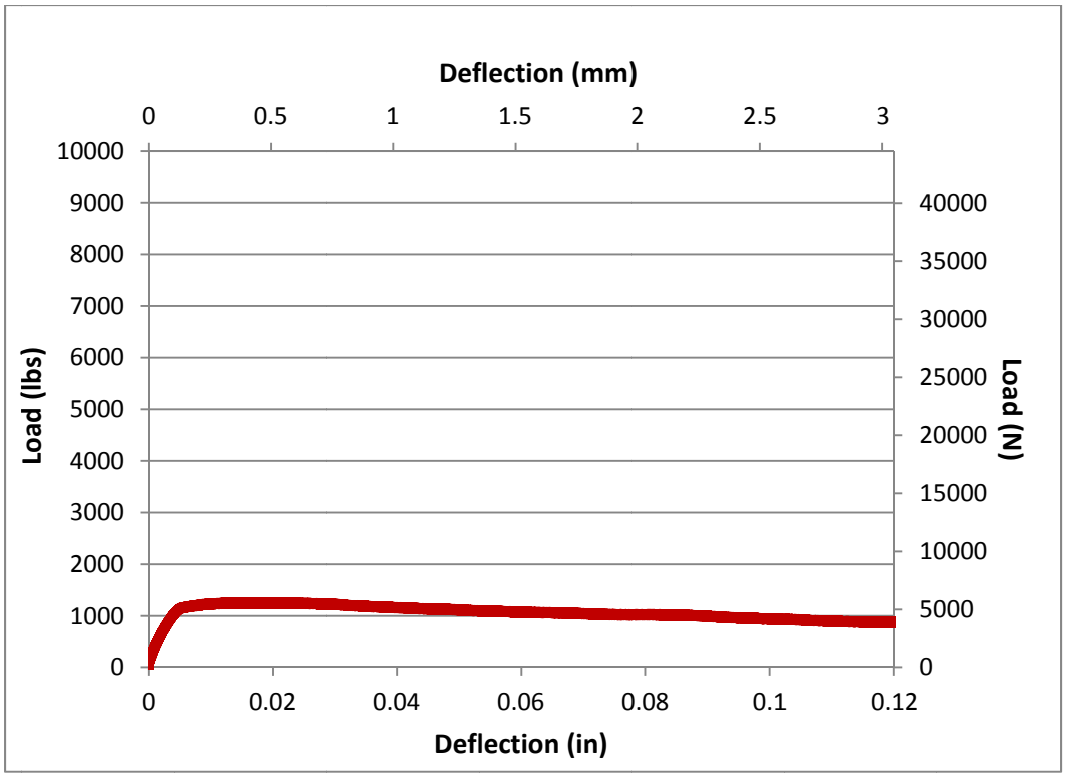

Figure C-61 Load-Deflection Plot for HY-24-6-BM-44lbs-20%

Figure C-62 Photograph of HY-24-6-BM-44lbs-20%

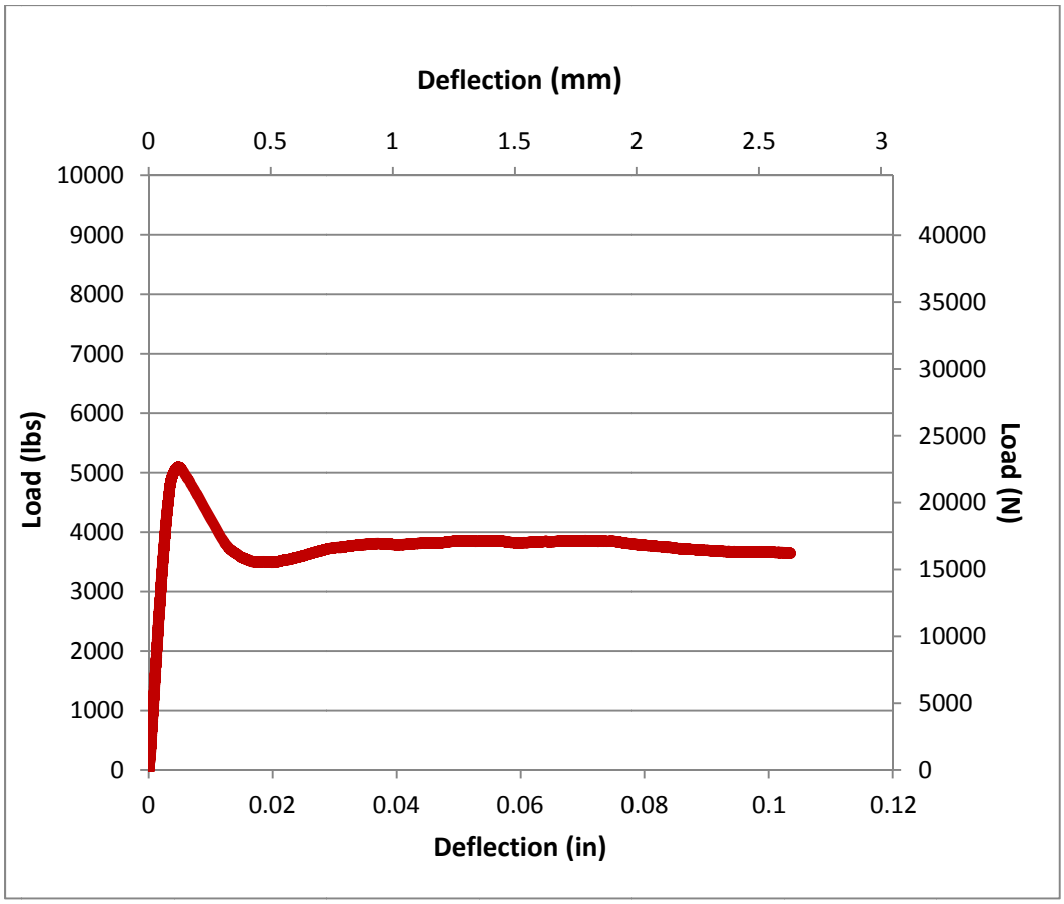

Figure C-63 Load-Deflection Plot for HY-44lbs steel-5lbs synth-3%

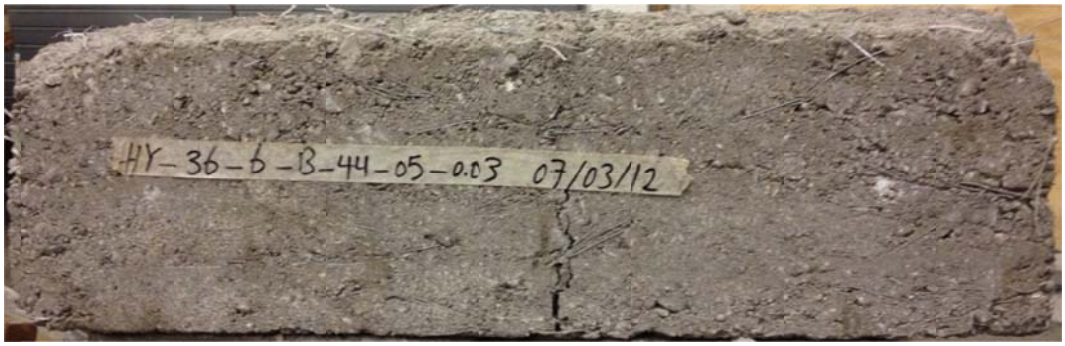

Figure C-64 Photograph of HY-44lbs steel-5lbs synth-3%

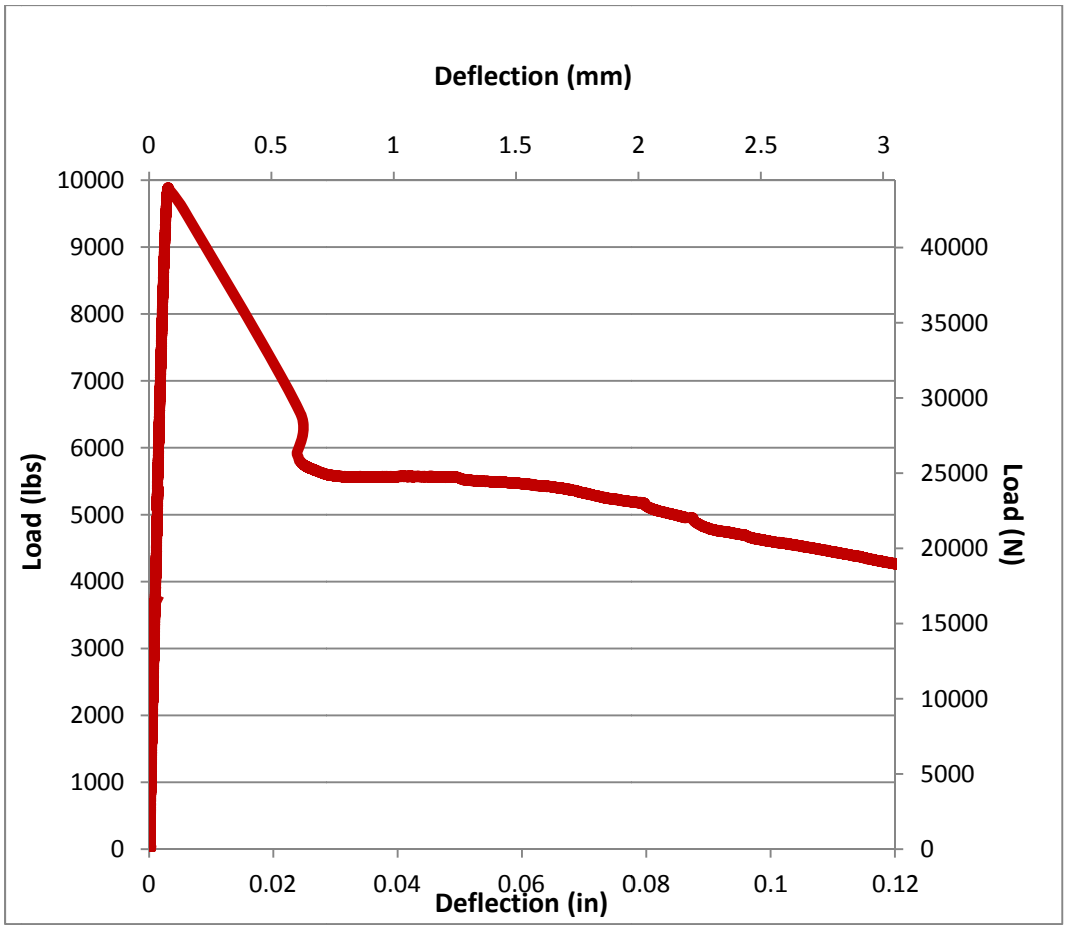

Figure C-65 Load-Deflection Plot for HY-24-6-B-BM-22lbs-5lbs-2%

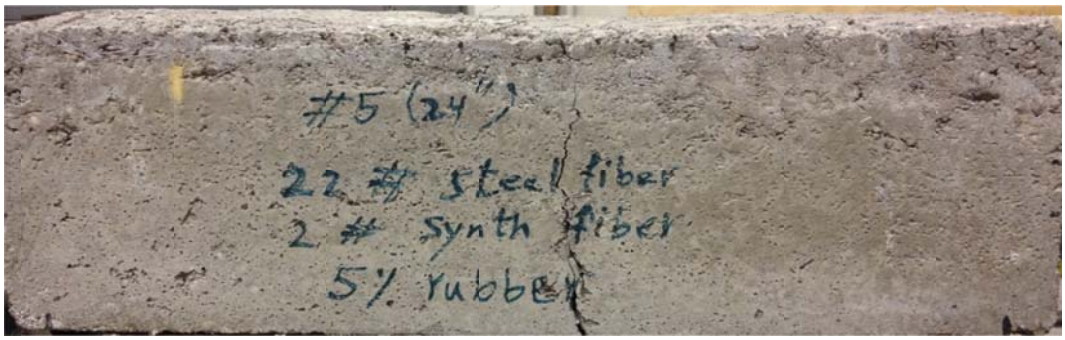

Figure C-66 Photograph of HY-24-6-B-BM-22lbs-5lbs-2%

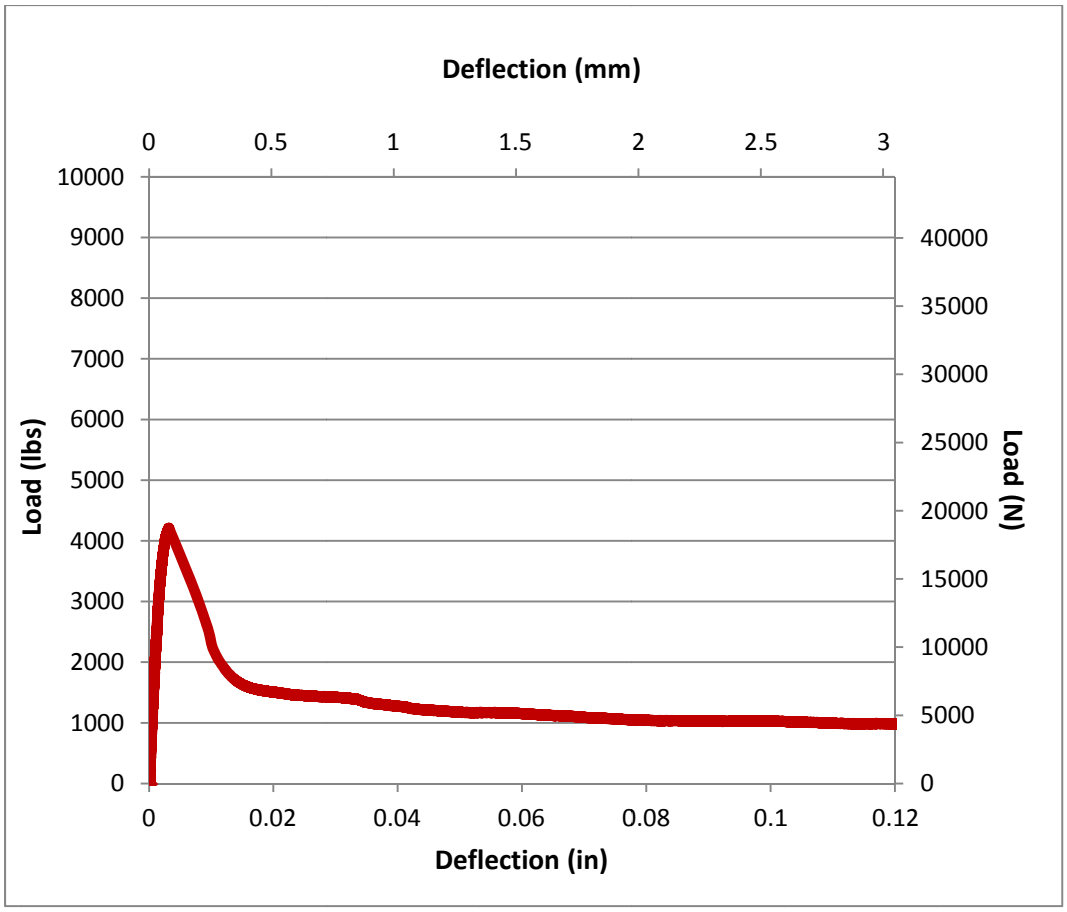

Figure C-67 Load-Deflection Plot for Control-36-6-B-BM

Figure C-68 Photograph of Control-36-6-B-BM

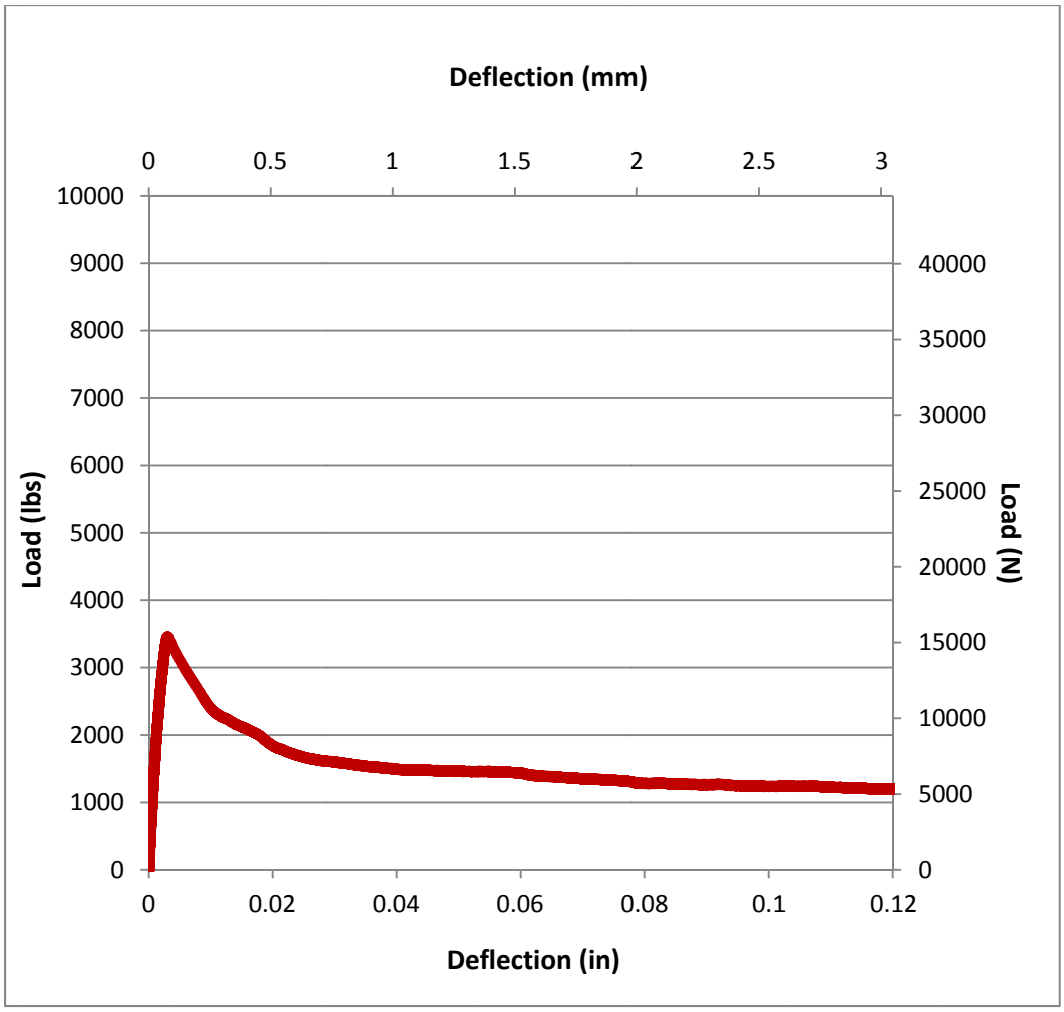

Figure C-69 HY-36-6-B-BM-44-10

Figure C-70 Photograph of HY-36-6-B-BM-44-10

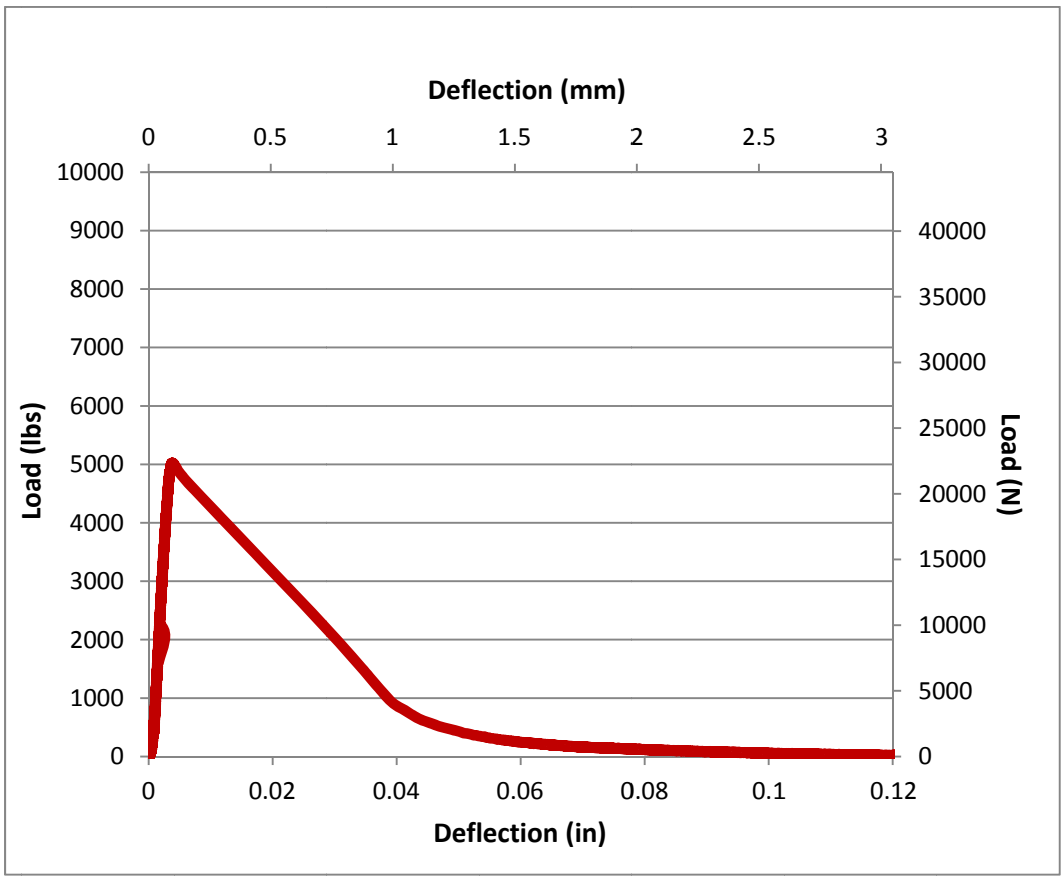

Figure C-71 Load-Deflection Plot for CR-36-6-B-BM-20%

Figure C-72 Photograph of CR-36-6-B-BM-20%

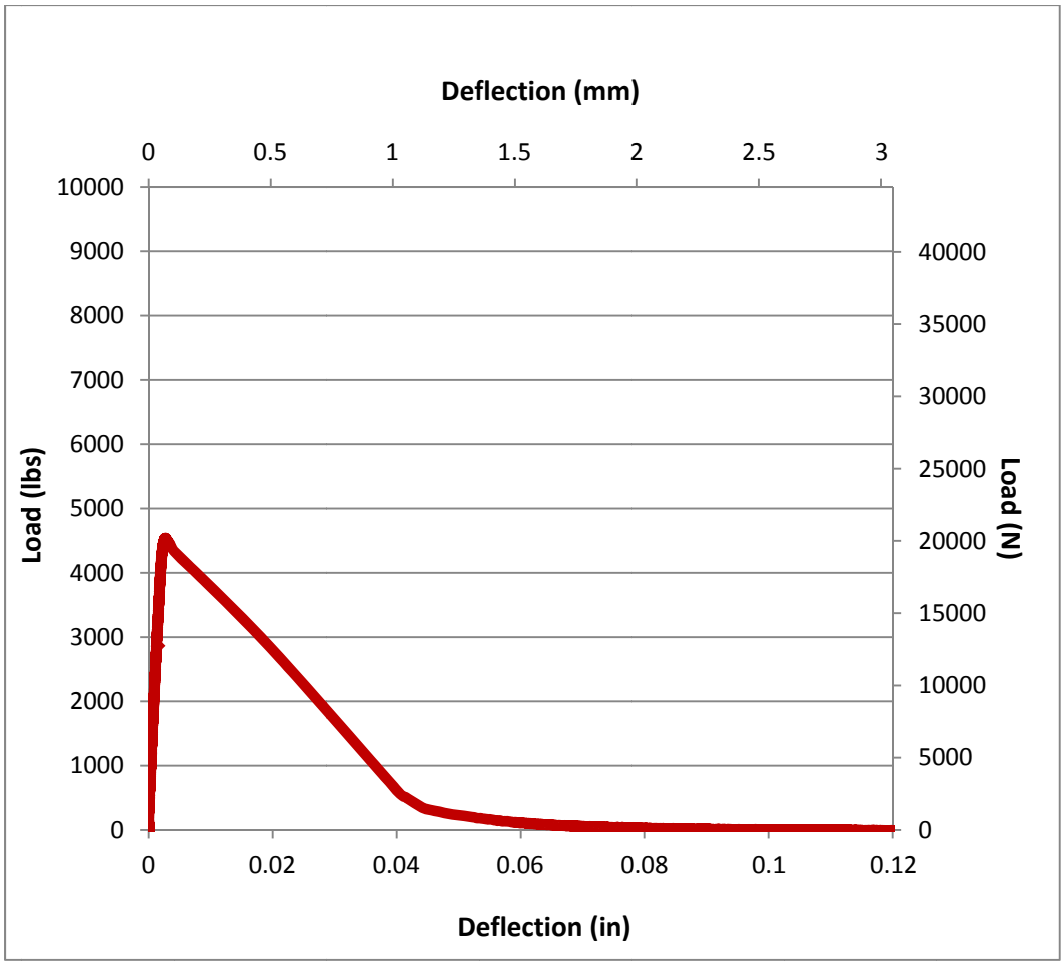

Figure C-73 Load-Deflection Plot for CR-36-6-B-BM-20%

Figure C-74 Photograph of for CR-36-6-B-BM-20%

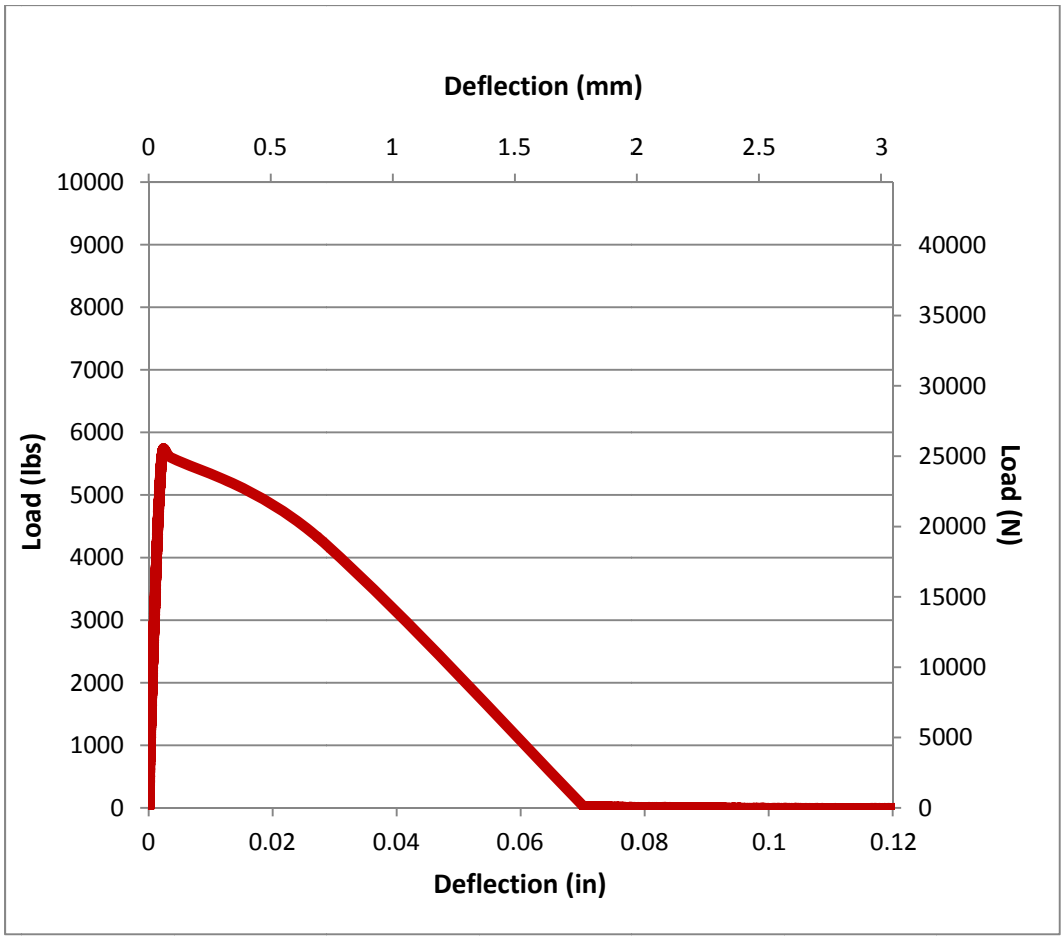

Figure C-75 Load-Deflection Plot for CR-36-6-B-BM-10%

Figure C-76 Photograph of CR-36-6-B-BM-10%

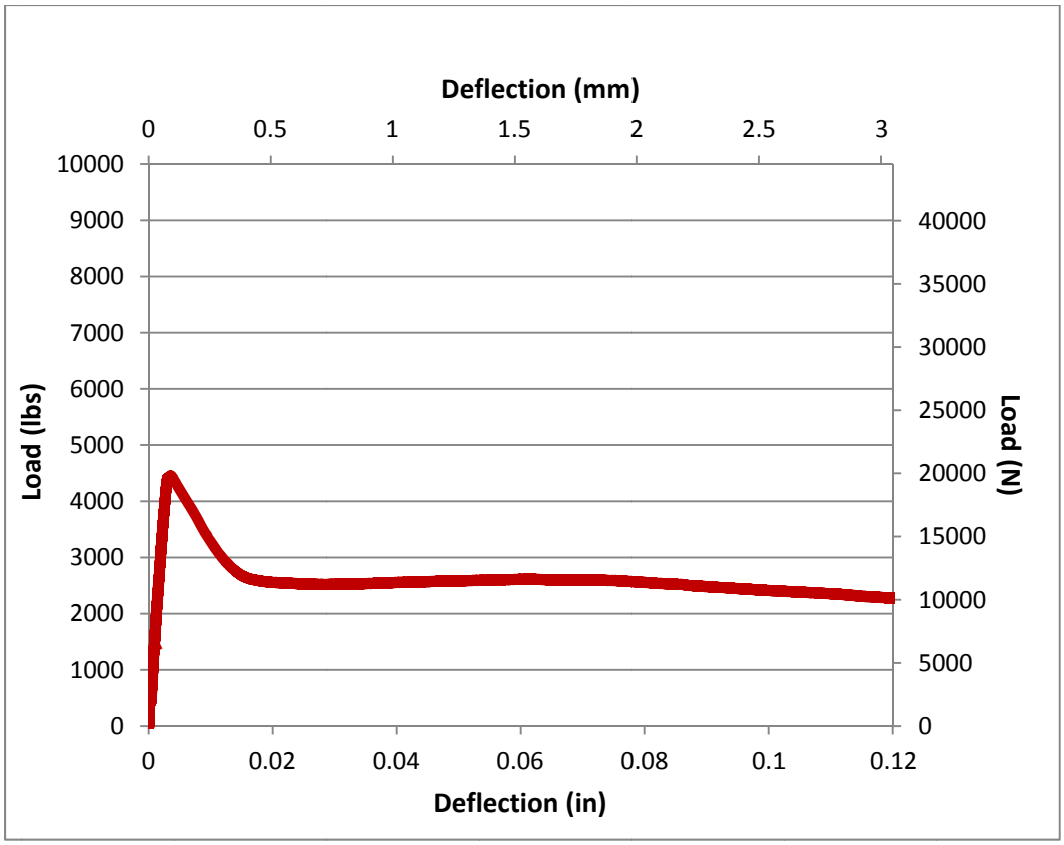

Figure C-77 Load-Deflection Plot for HY-36-6-B-BM-8% synth-20% rubber

Figure C-78 Photograph of HY-36-6-B-BM-8% synth-20% rubber

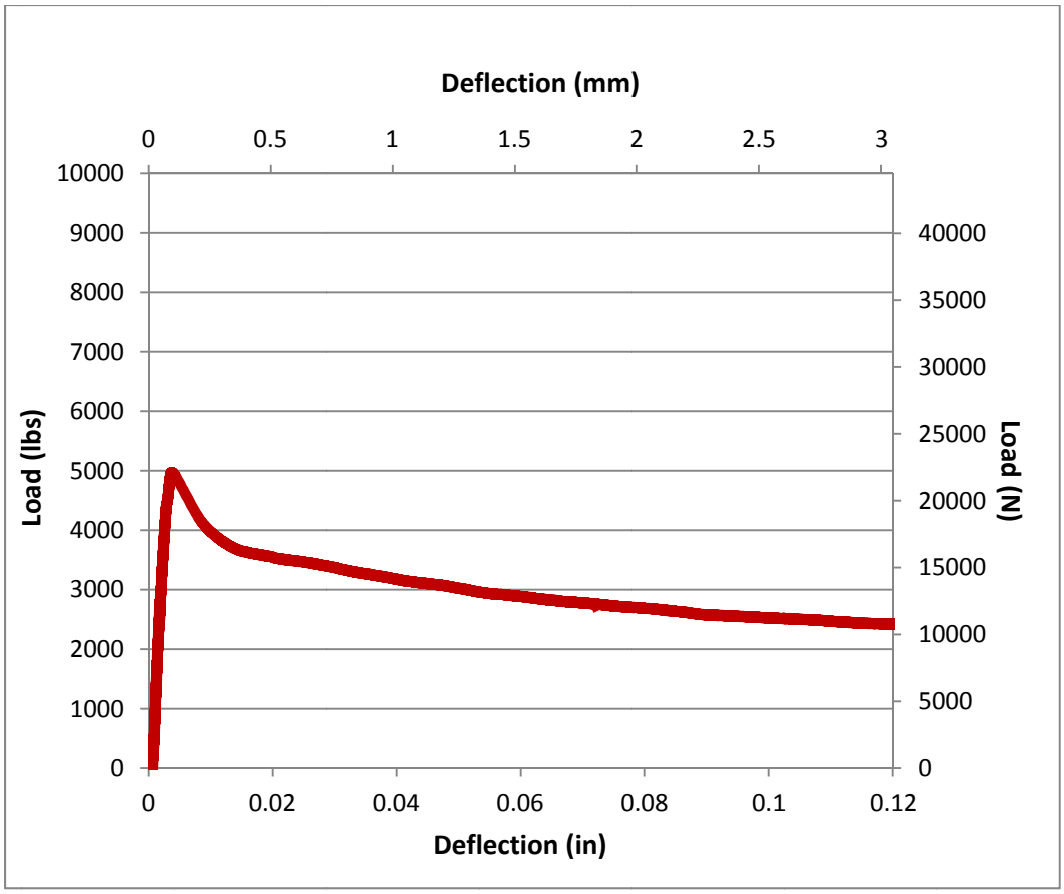

Figure C-79 Load-Deflection Plot for HY-36-6-B-BM-44lbs-20%

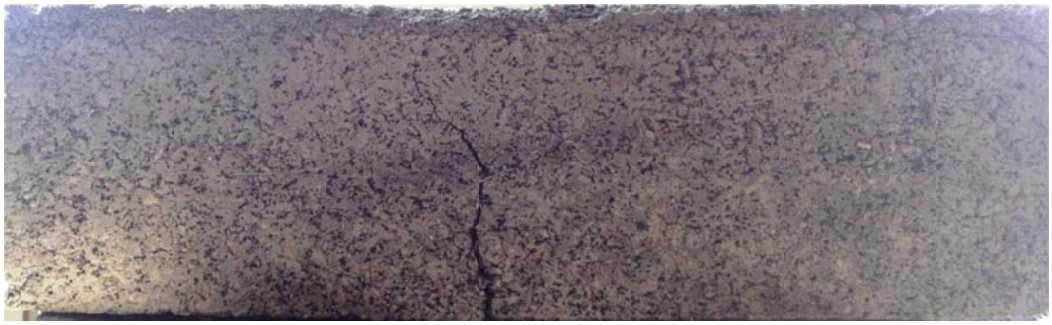

Figure C-80 Photograph of HY-36-6-B-BM-44lbs-20%

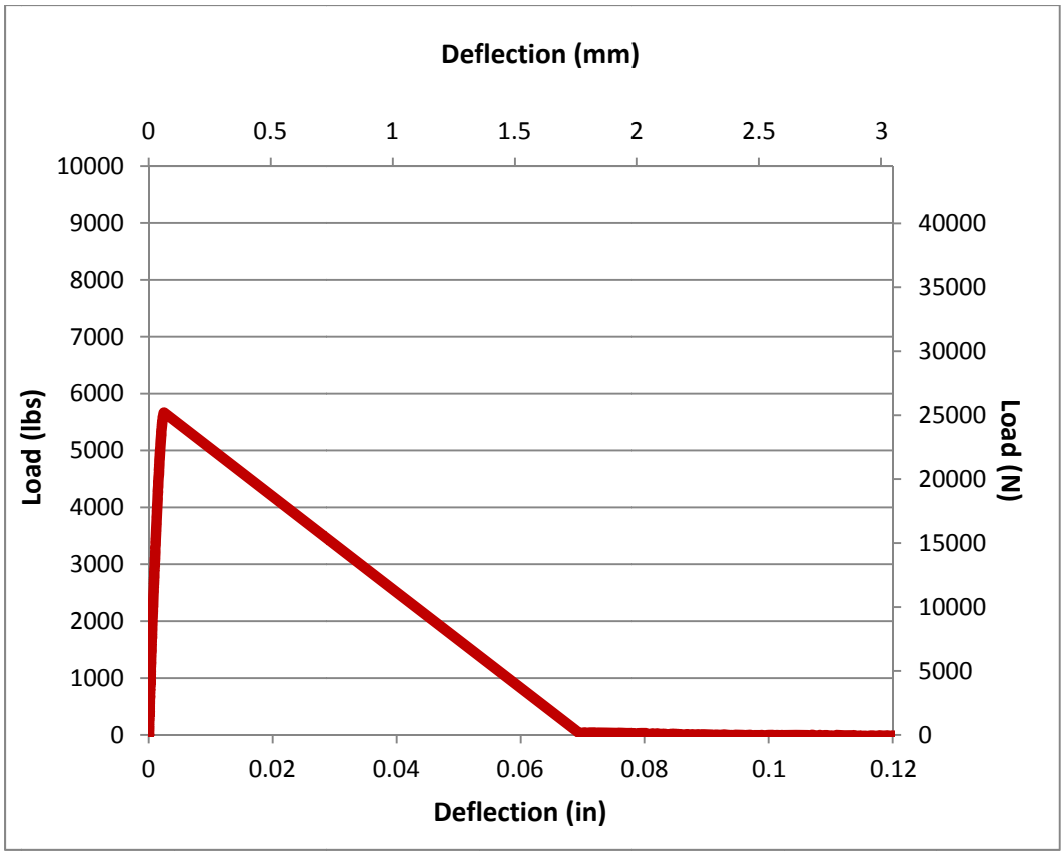

Figure C-81 Load-Deflection Plot for CR-36-6-B-BM-10%

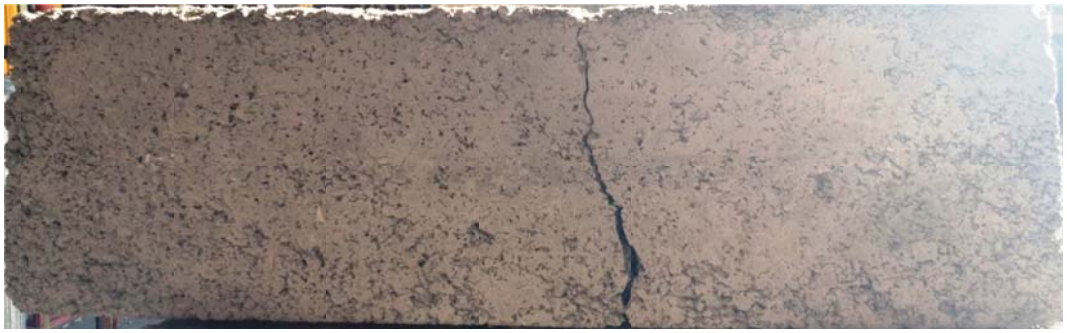

Figure C-82 Photograph of CR-36-6-B-BM-10%

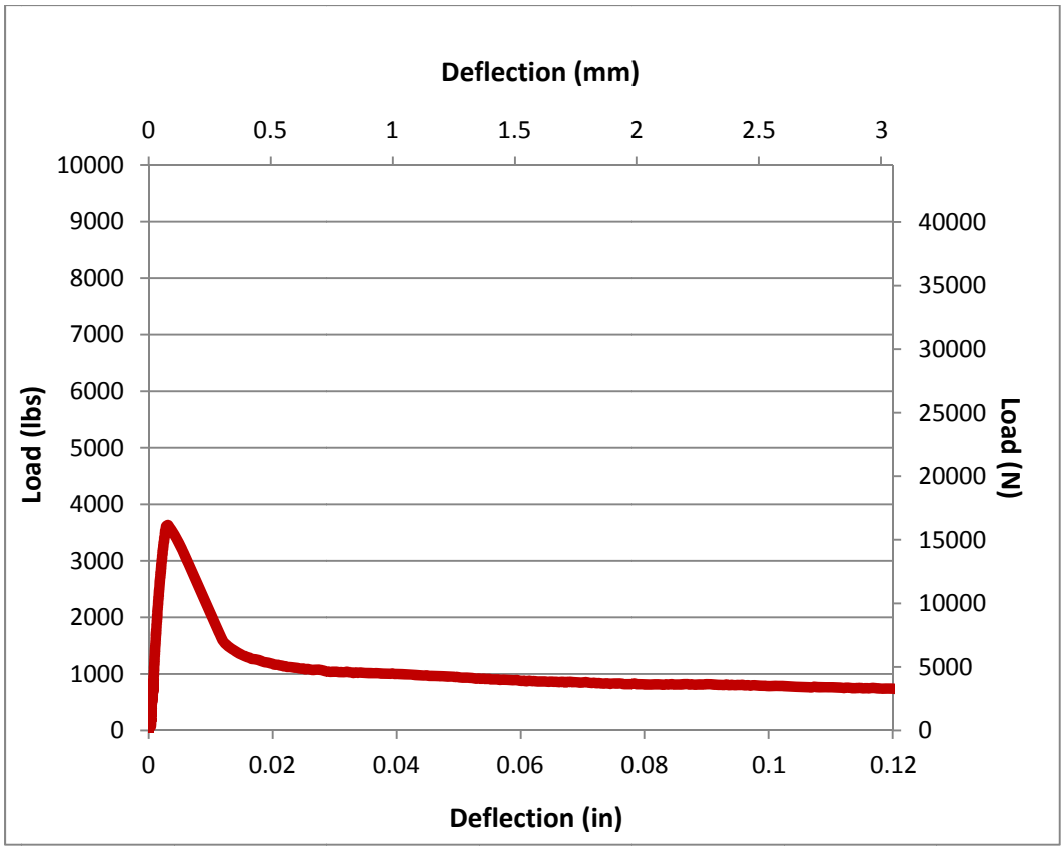

Figure C-83 Load-Deflection Plot for Control-36-6-B-BM

Figure C-84 Photograph of Control-36-6-B-BM

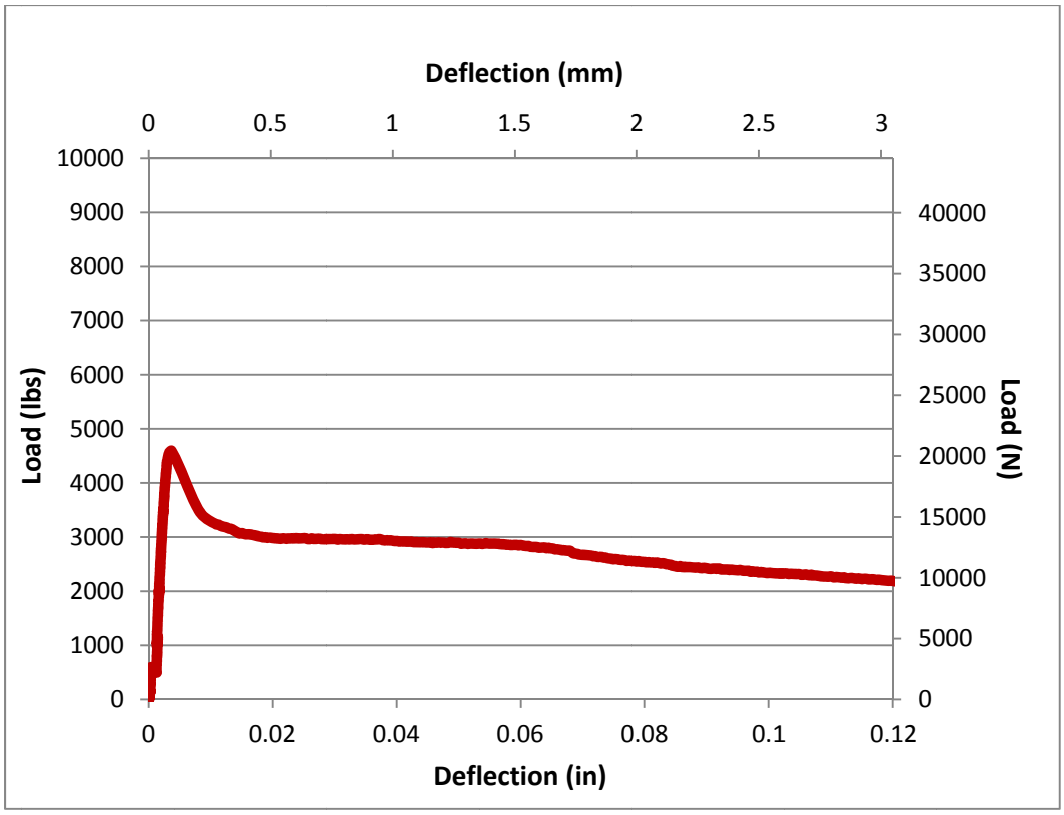

Figure C-85 Load-Deflection Plot for HY-36-6-B-BM-44lbs-10%

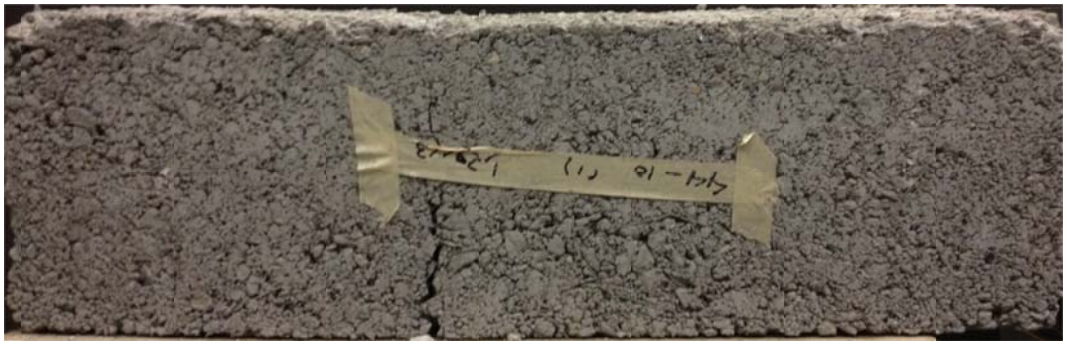

Figure C-86 Photograph of HY-36-6-B-BM-44lbs-10%

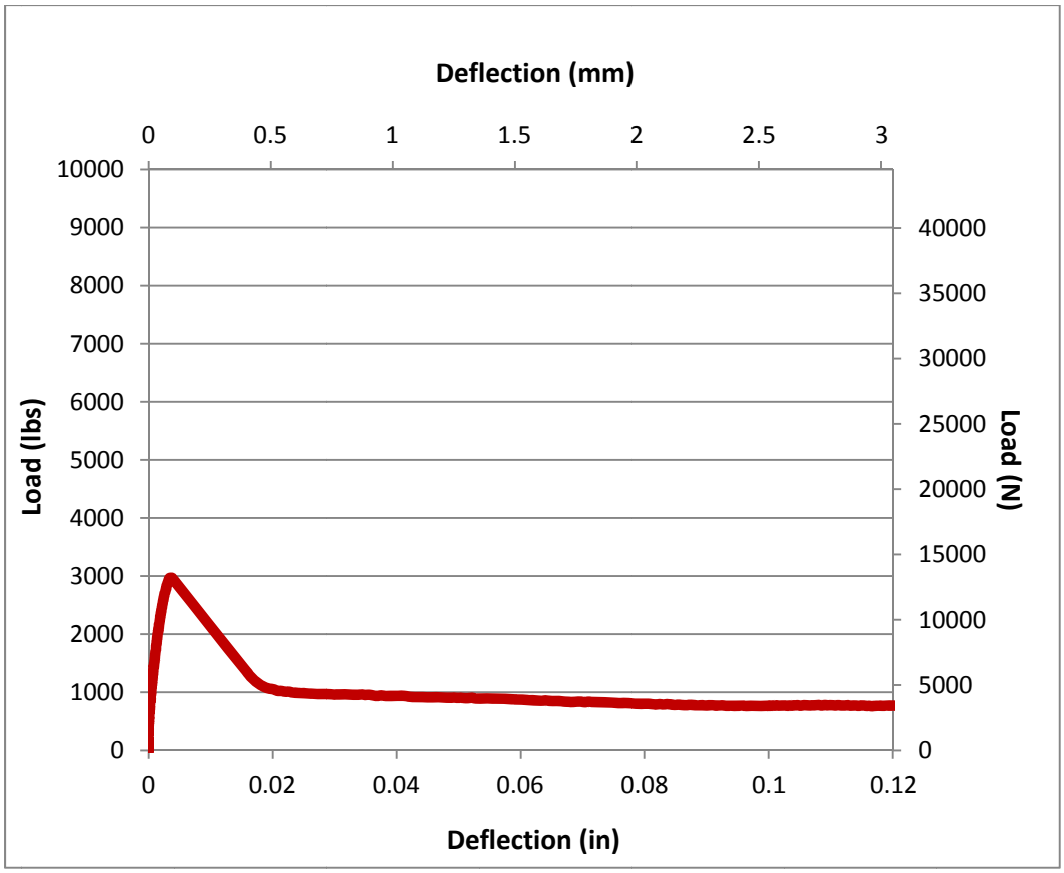

Figure C-87 Load-Deflection Plot for HY-36-6-B-BM-44-10%-8lbs Synth

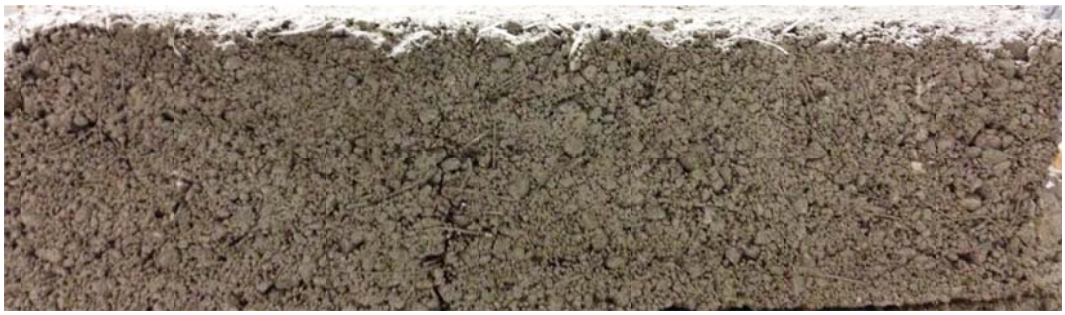

Figure C-88 Photograph of HY-36-6-B-BM-44-10%-8lbs Synth

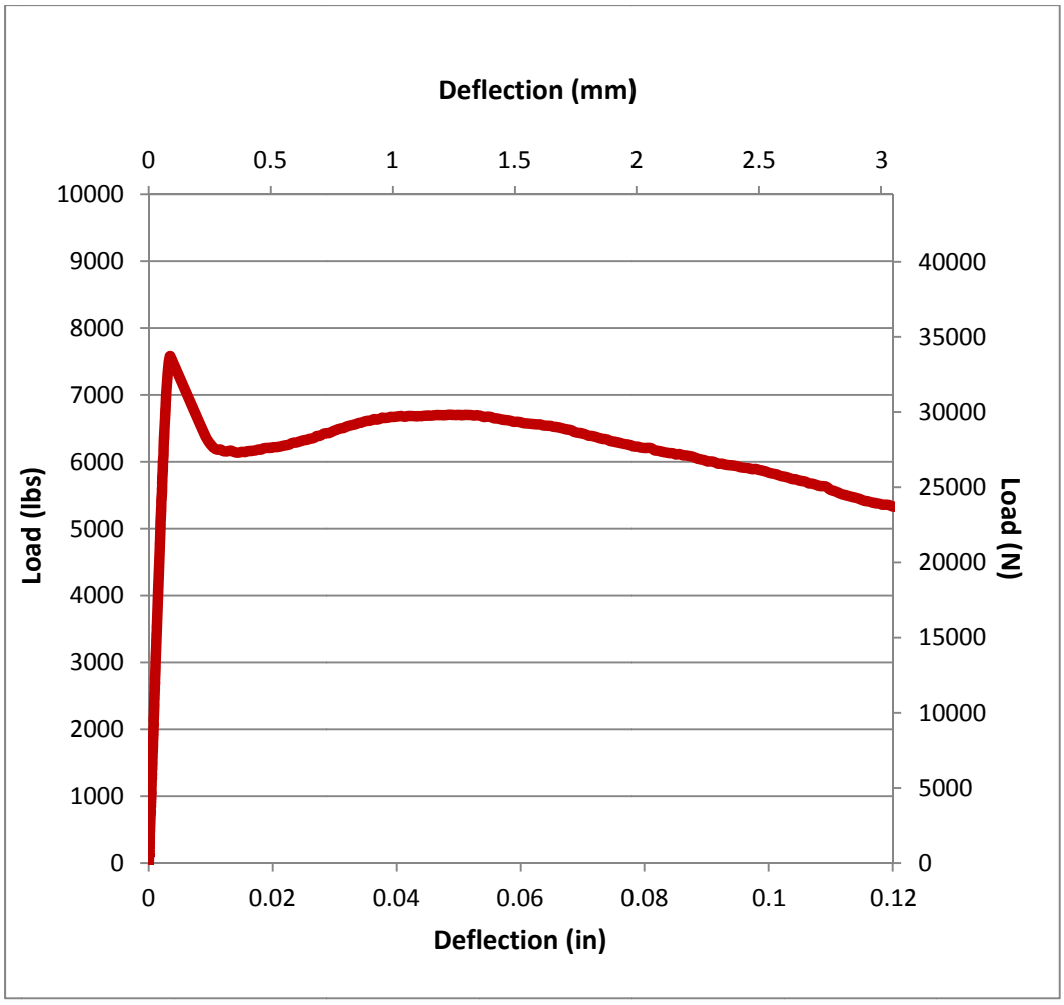

Figure C-89 Load-Deflection Plot for HY-44lbs steel-5lbs synth-3%

Figure C-90 Photograph of HY-44lbs steel-5lbs synth-3%

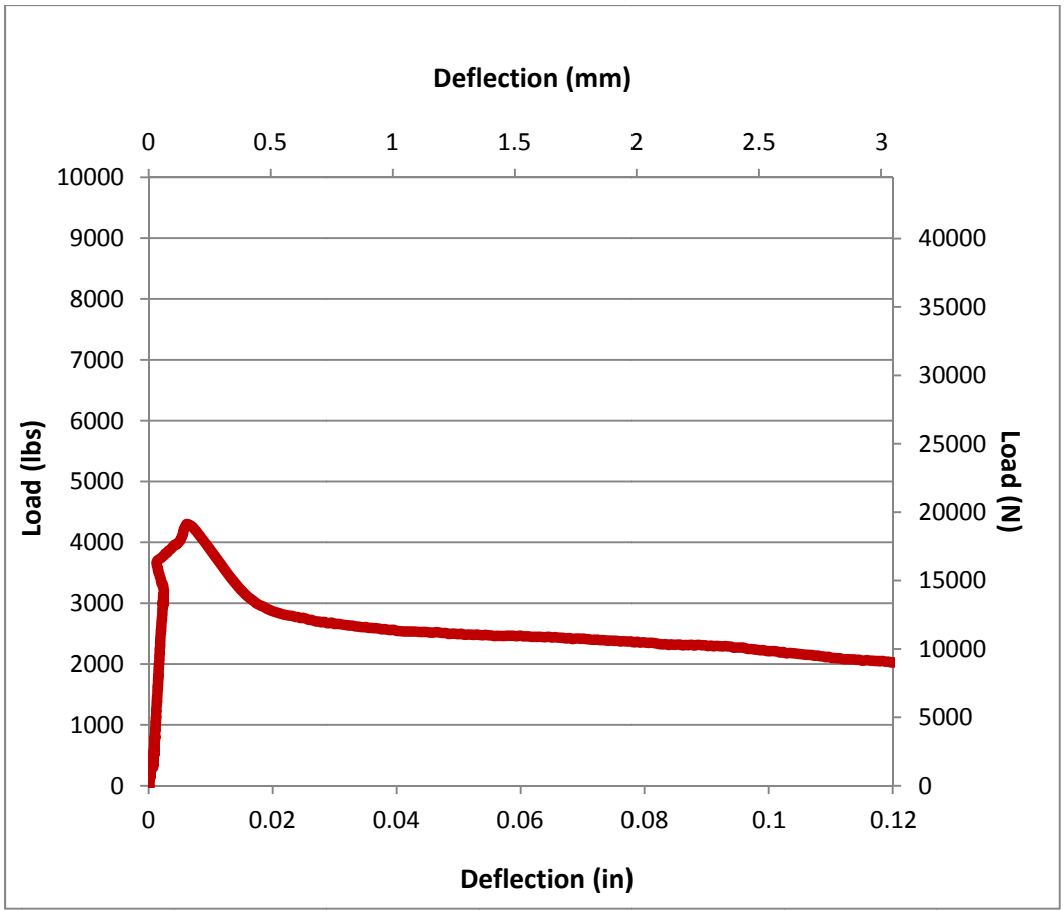

Figure C-91 Load-Deflection Plot for HY-36-6-B-BM-44lbs-20%

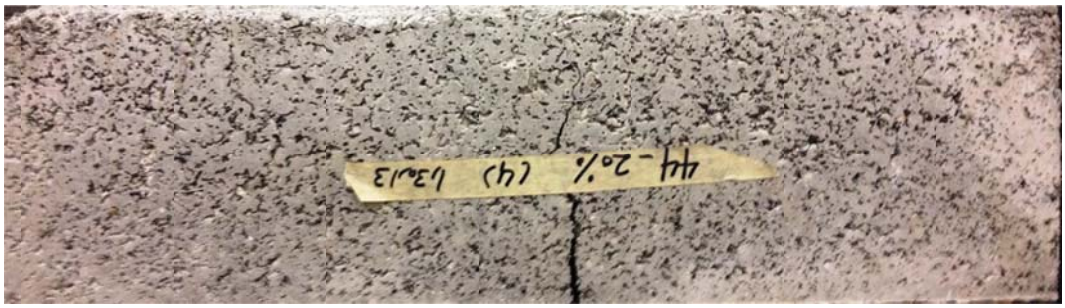

Figure C-92 Photograph of HY-36-6-B-BM-44lbs-20%

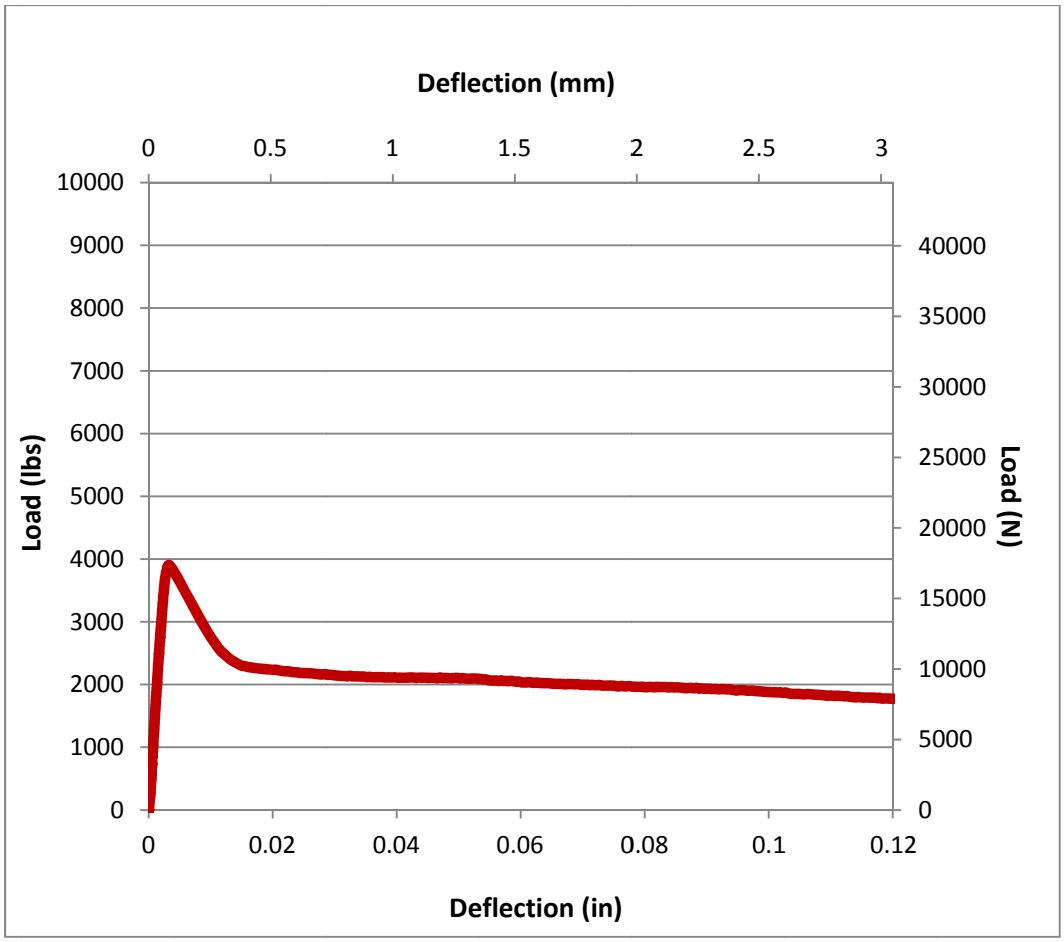

Figure C-93 Load-Deflection Plot for HY-36-6-B-BM-20%-8lbs synth

Figure C-94 Photograph of HY-36-6-B-BM-20%-8lbs synth

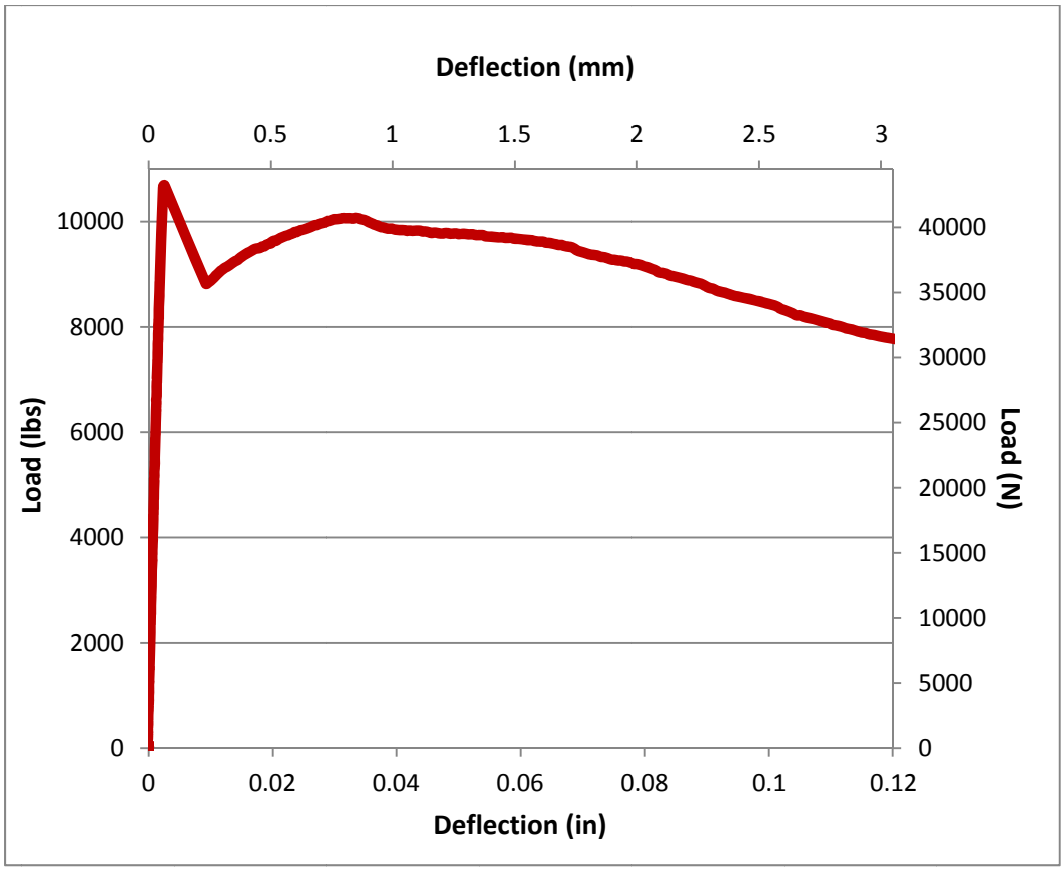

Figure C-95 Load-Deflection Plot for HY-36-6-B-BM-44lbs-5lbs synth-3%rubber

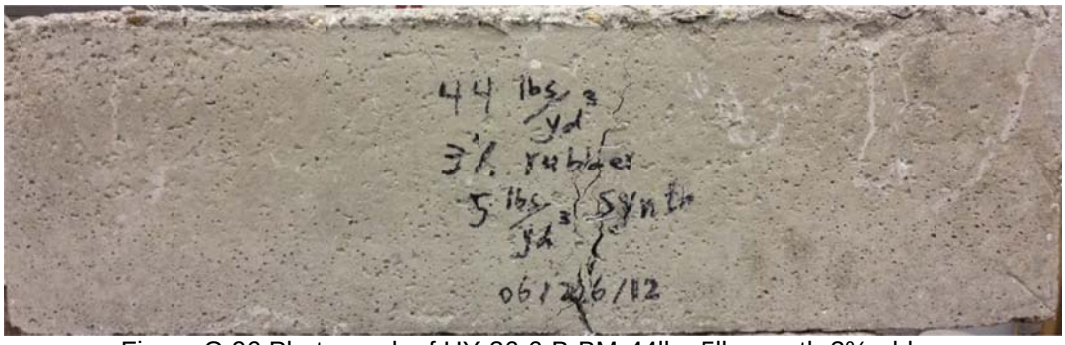

Figure C-96 Photograph of HY-36-6-B-BM-44lbs-5lbs synth-3%rubber

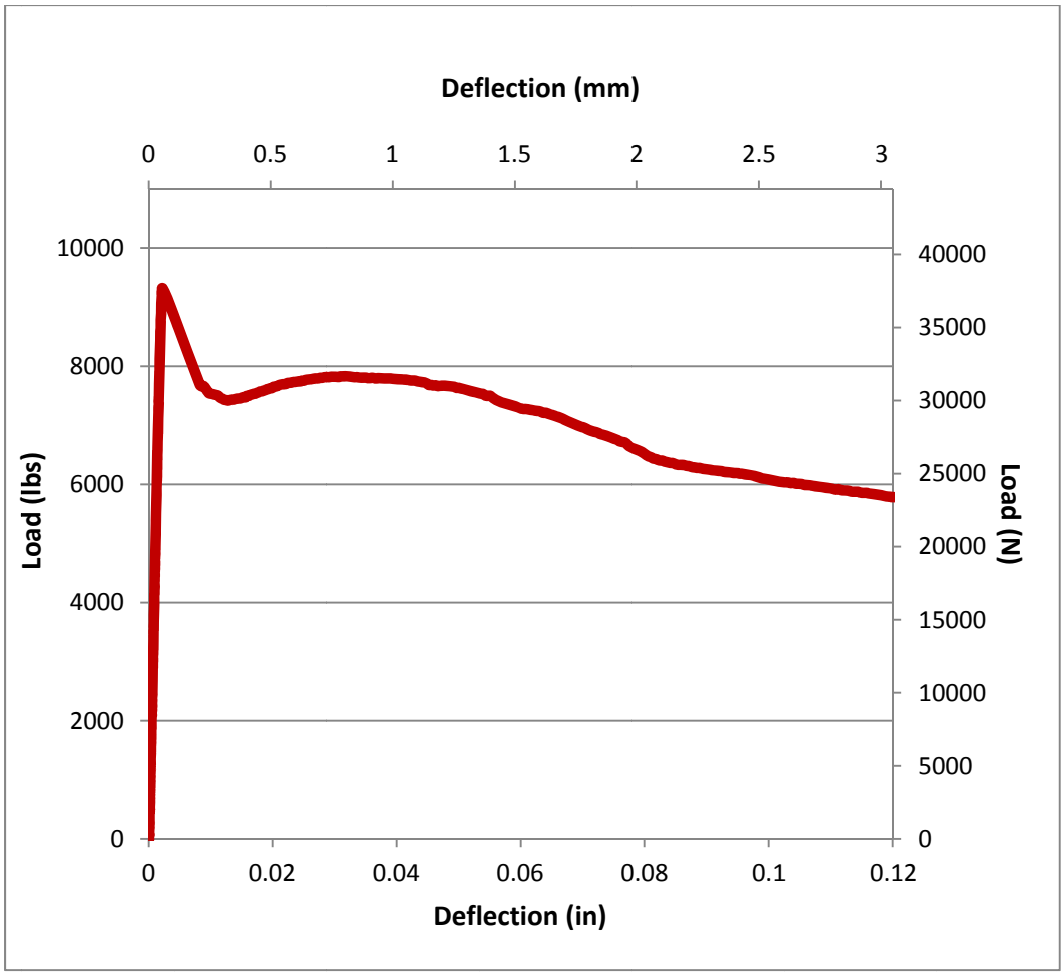

Figure C-97 Load-Deflection Plot for HY-36-6-B-BM-44lbs-8lbs synth-3%rubber

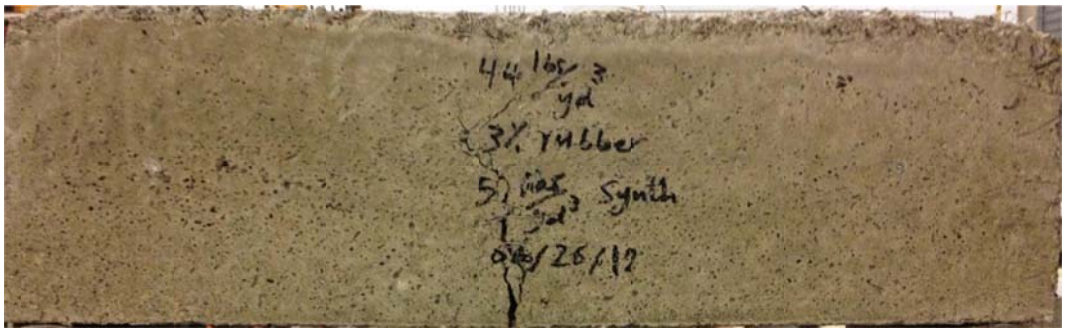

Figure C-98 Photograph of HY-36-6-B-BM-44lbs-8lbs synth-3%rubber

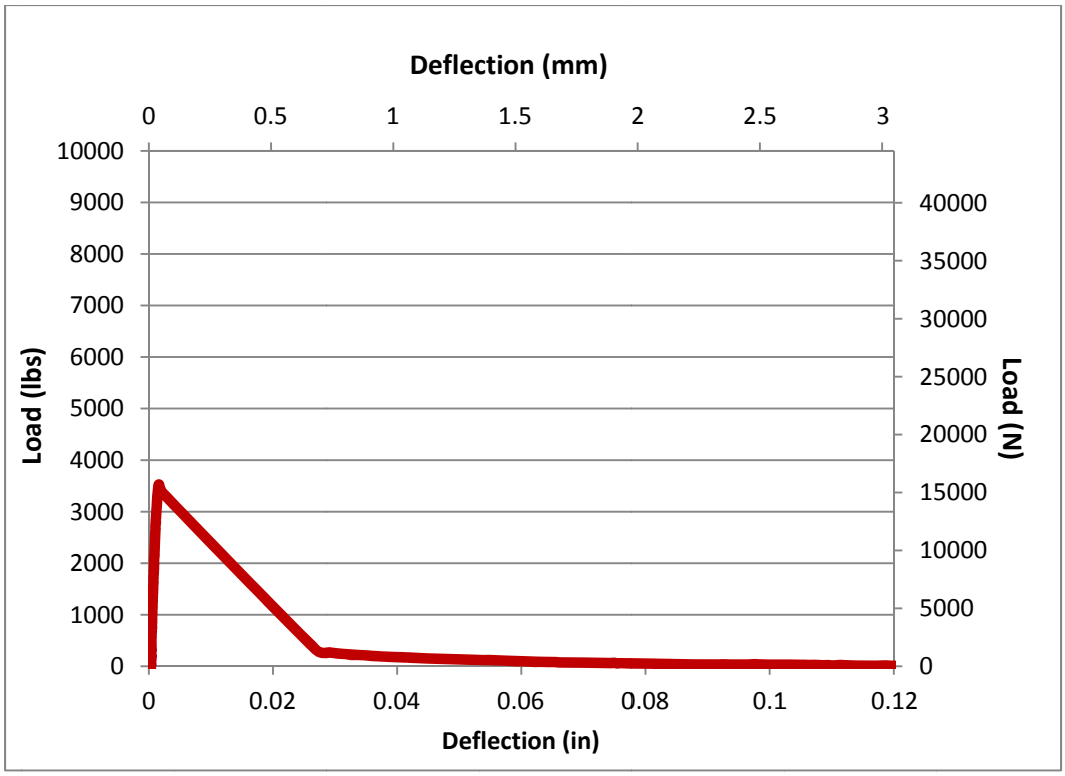

Figure C-99 Thin wall-60in-20% rubber-8ft

Figure C-100 Photograph of Thin wall-60in-20% rubber-8ft

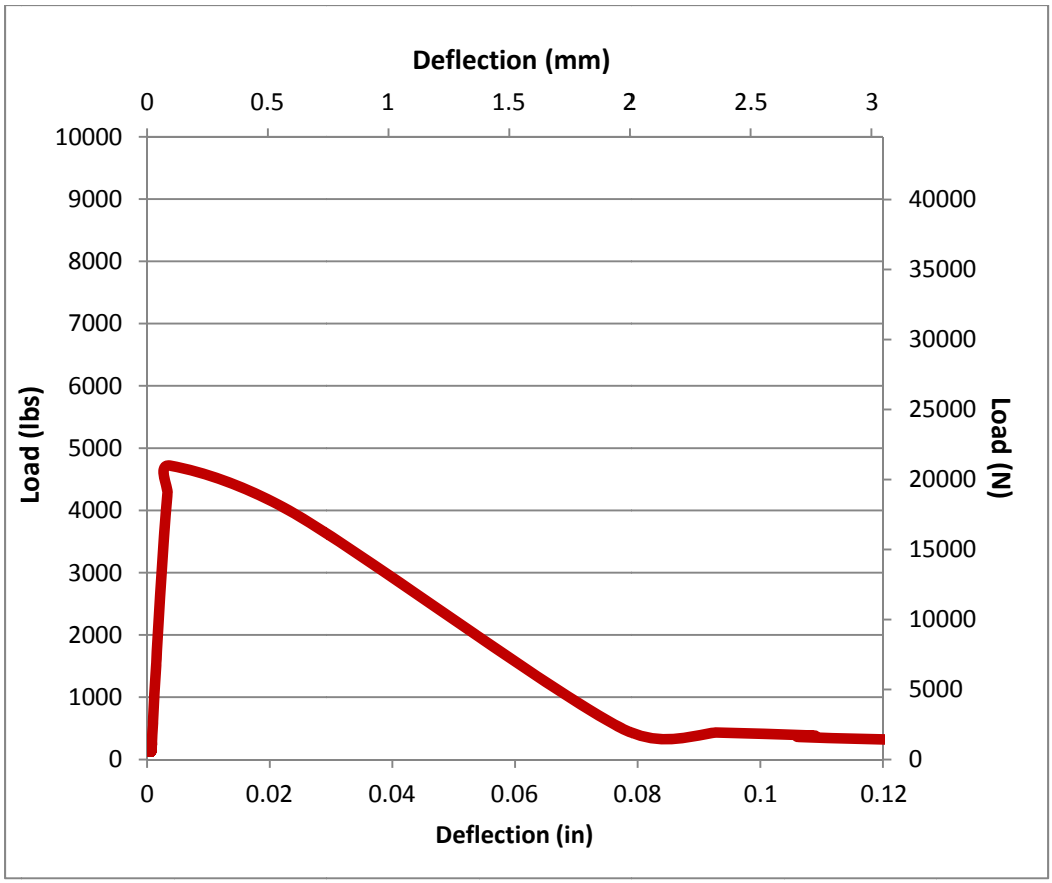

Figure C-101 Thin wall-60in-20% rubber-8ft

Figure C-102 Photograph of Thin wall-60in-20% rubber-8ft

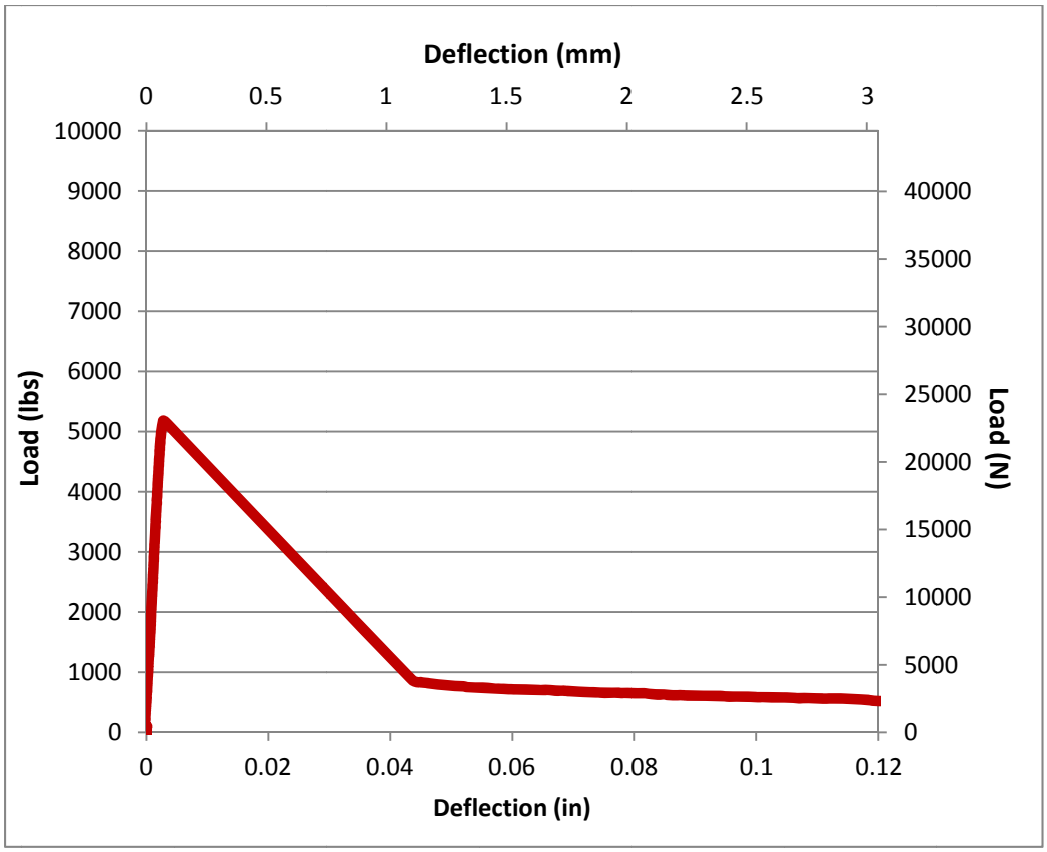

Figure C-103 Thin wall-60in-11PCY SF-20% rubber-8ft

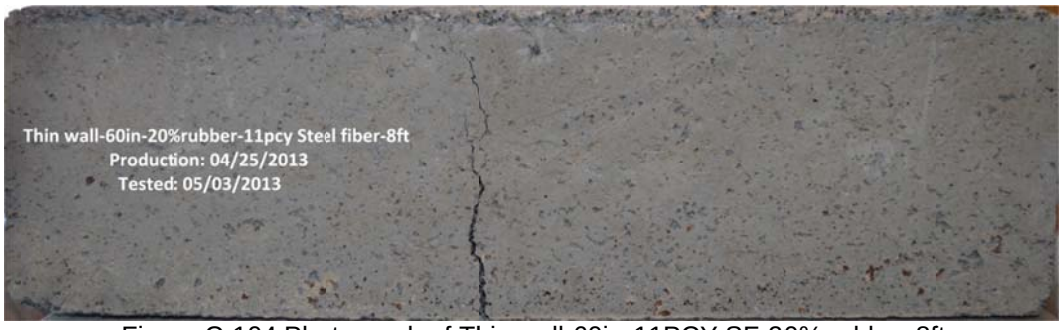

Figure C-104 Photograph of Thin wall-60in-11PCY SF-20% rubber-8ft

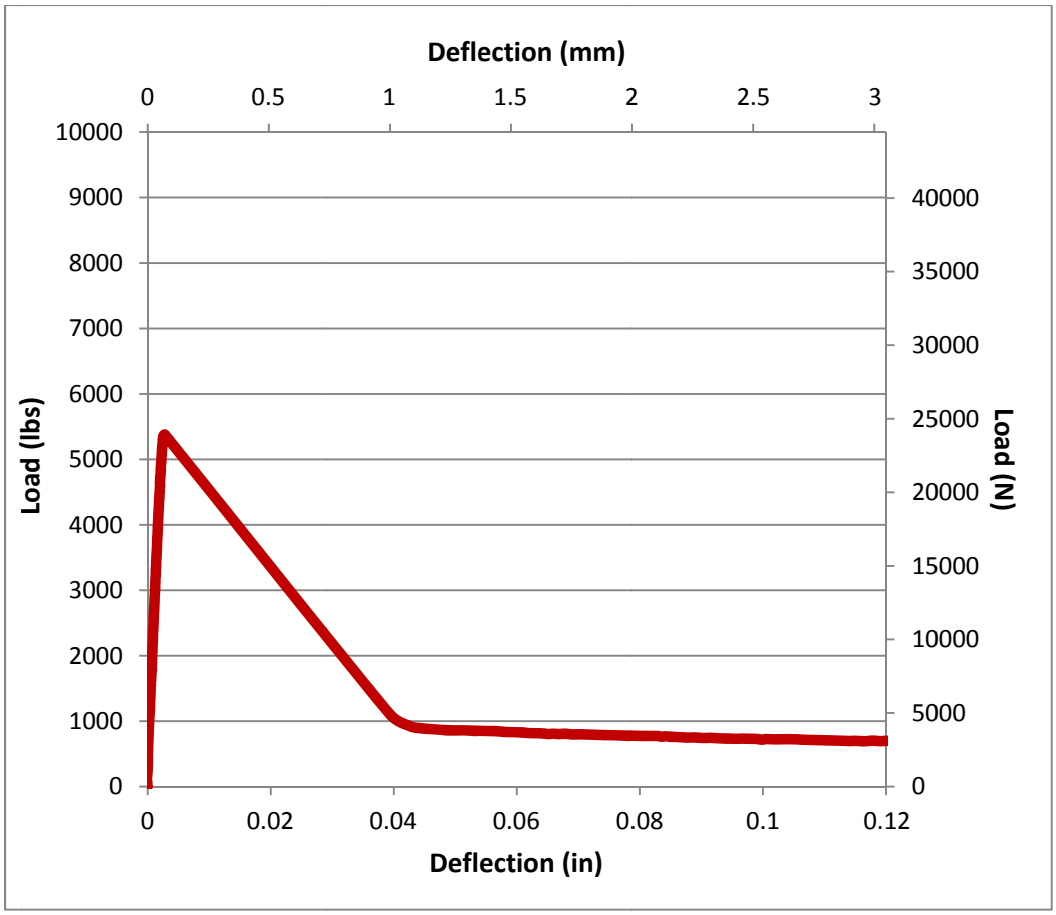

Figure C-105 Thin wall-60in-11PCY SF-20% rubber-8ft

Figure C-106 Photograph of Thin wall-60in-11PCY SF-20% rubber-8ft

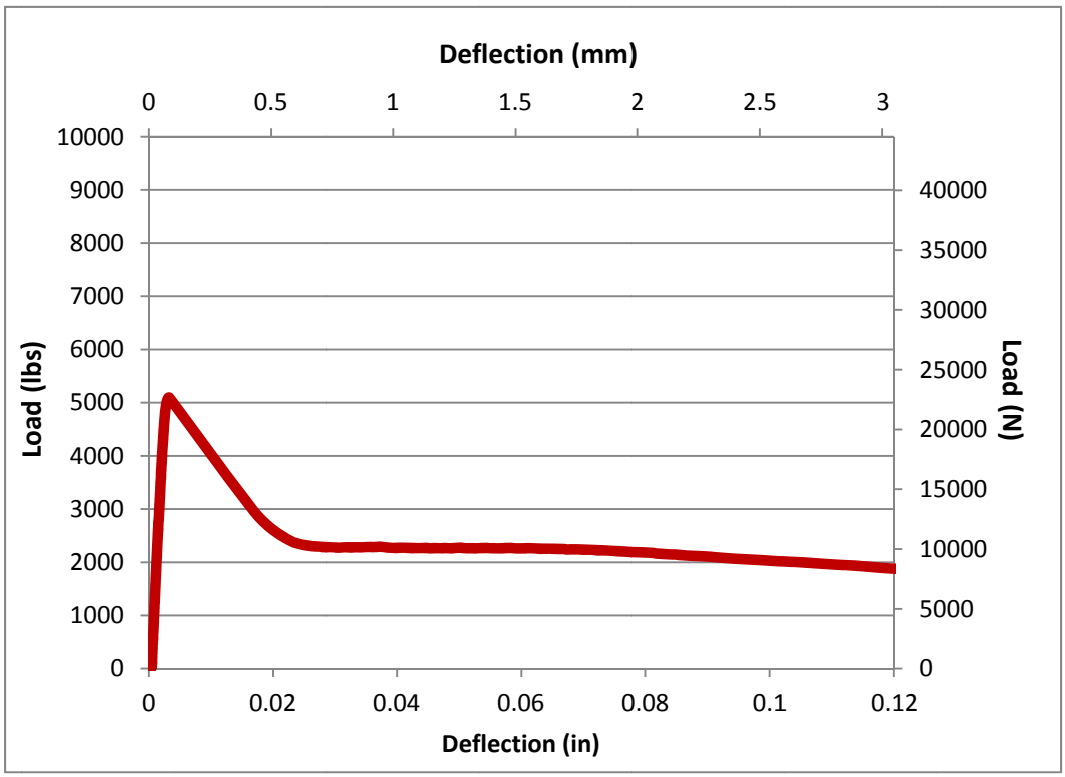

Figure C-107 Thin wall-60in-4PCY Synth-20% rubber-8ft

Figure C-108 Photograph of Thin wall-60in-4PCY Synth-20% rubber-8ft

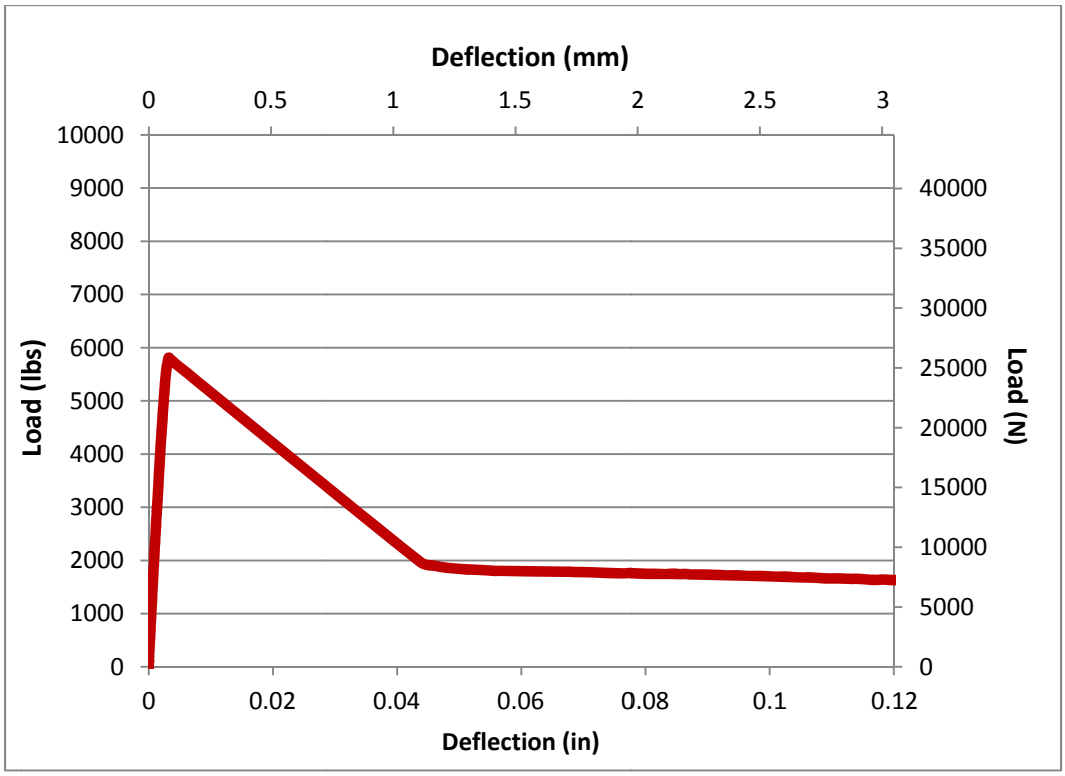

Figure C-109 Thin wall-60in-4PCY Synth-20% rubber-8ft

Figure C-110 Photograph of Thin wall-60in-4PCY Synth-20% rubber-8ft

References

1. Maidl, B.R. 1995. Steel Fibre Reinforced Concrete. Ernst & Sohn.
2. Katzer, Jacek. "Steel Fibers and Steel Fiber Reinforced Concrete in Civil Engineering." Pacific Journal of Science and Technology 7 (2006): 53ó58.
3. ACI Committee 544. "State-of-the-Art Report on Fiber Reinforced Concrete." ACI Journal Proceedings. Vol. 70. No. 11. ACI, 1973.
4. Hoff G. C. (1986), Use of Steel Fiber Reinforced Concrete in Bridge Decks and Pavements, Steel Fiber Concrete 1(1):67-108.
5. J. M. Doyle, J.M. and Fang, S.J. “Underground Pipe” Structural Engineering Handbook Ed. Chen Wai-Fah Boca Raton: CRC Press LLC, 1999 page 2
6. State-of-the-Art Report on Fiber Reinforced Concrete Reported by ACI Committee 544
7. (Ali O. Atahan, Ayhan Öner Yücel, Crumb rubber in concrete: Static and dynamic evaluation, Construction and Building Materials, Volume 36, November 2012, Pages 617-622)
8. Van Chanh, Nguyen. "Steel fiber reinforced concrete." Faculty of Civil Engineering Ho chi minh City university of Technology. Seminar Material. 2004
9. Concrete Pipe Technology Handbook. American Concrete Pipe Association, 1993
10. Rafat Siddique, Tarun R. Naik, Properties of concrete containing scrap-tire rubber – an overview, Waste Management, Volume 24, Issue 6, 2004, Pages 563-569, ISSN 0956-053X, 10.1016/j.wasman.2004.01.006.
11. Siringi, Gideon Momanyi. "Properties Of Concrete With Tire Derived Aggregate And Crumb Rubber As A Ligthweight Substitute For Mineral Aggregates In The Concrete Mix." (2012).

12. Ilker Bekir Topçu, The properties of rubberized concretes, Cement and Concrete Research, Volume 25, Issue 2, February 1995, Pages 304-310, ISSN 0008-8846, 10.1016/0008-8846(95)00014-3.
13. H.A. Toutanji, The use of rubber tire particles in concrete to replace mineral aggregates, Cement and Concrete Composites, Volume 18, Issue 2, 1996, Pages 135-139, ISSN 0958-9465, 10.1016/0958-9465(95)00010-0
14. Van Chanh, Nguyen. "Steel fiber reinforced concrete." Faculty of Civil Engineering Ho chi minh City university of Technology. Seminar Material. 2004.
15. Khaloo, Ali R., M. Dehestani, and P. Rahmatabadi. "Mechanical properties of concrete containing a high volume of tire–rubber particles." Waste management 28.12 (2008): 2472-2482.
16. M.N. Soutsos, T.T. Le, A.P. Lampropoulos, Flexural performance of fibre reinforced concrete made with steel and synthetic fibres, Construction and Building Materials, Volume 36, November 2012, Pages 704-710, ISSN 0950-0618, 10.1016/j.conbuildmat.2012.06.042.
17. Specimens, Compression Test. "ASTM C 31/C 31M. a." Cast and laboratory cure two sets of two standard cylinder specimens for each composite sample. b. Cast and field cure two sets of two standard cylinder specimens for each composite sample.
18. Cominoli, L., C. Failla, and G. A. Plizzari. "Steel and synthetic fibres for nhancing concrete toughness and shrinkage behaviour." Proc. Int. Conf.: Sustainable construction materials and technologies. 2007.
19. C497 Test Methods for Concrete Pipe, Manhole Sections, or Tile cite.

20. ASTM C1609 Standard Test Method for Flexural Performance of Fiber-Reinforced Concrete (Using Beam With Third-Point Loading). American Society for Testing and Materials, 2011

Biographical Information

Mohammadagha was born in Tehran, Iran, in January 1988. He graduated from Sharif University of Technology in the Fall of 2011. He received a Bachelor of Science Degree in Civil Engineering. In December 2011, he moved to Texas to pursue his Master of Science degree in Structural Engineering from the University of Texas at Arlington(UTA) under the supervision of Dr. Ali Abolmaali. Mohammadagha is currently working at Trinity Infrastructure, LLC in Dallas, TX.